Order Number 9209707

Nitrogen oxides in the Arctic troposphere

Honrath, Richard Edward, Jr., Ph.D.

University of Alaska Fairbanks, 1991

U·M·I
300 N. Zeeb Rd.
Ann Arbor, MI 48106

NITROGEN OXIDES IN THE ARCTIC TROPOSPHERE

A

THESIS

Presented to the Faculty

of the University of Alaska Fairbanks

in Partial Fulfillment of the Requirements

for the Degree of

DOCTOR OF PHILOSOPHY

By

Richard E. Honrath, Jr., B.S., M.S.

Fairbanks, Alaska

September 1991

NITROGEN OXIDES IN THE ARCTIC TROPOSPHERE

by

Richard E. Honrath, Jr.

RECOMMENDED:

Dr. Joan P. Gosink

Dr. Richard J. Stolzberg

Dr. Knut Stamnes

Dr. Glenn E. Shaw

Dr. Daniel A. Jaffe, Chairman, Advisory Committee

Dr. L. Claron Hoskins, Head, Chemistry Department

APPROVED:

Dr. Paul Reichardt, Dean, College of Natural Sciences

Dr. Luis Proenza, Dean of the Graduate School

8/1/91

Date

Abstract

Nitrogen oxides play a critical role in tropospheric photochemistry. In order to characterize these compounds in the arctic troposphere, ground-level concentrations of total reactive nitrogen (NO_y) and NO were determined over an extended period at a site near Barrow, Alaska. A high-sensitivity instrument developed for this purpose was used in three measurement campaigns: summer 1988, spring 1989, and March–December 1990. During the 1990 campaign, the detection limit for NO was 3–10 pptv (depending on averaging period), and the NO_y uncertainty was ±26%. A screening algorithm was applied to the data to eliminate effects from local (Barrow) sources, and the remaining data were divided into "background periods" (unaffected by local or regional NO_x sources), and "events" (periods when emissions from a regional NO_x source—the Prudhoe Bay oil-producing region—apparently impacted Barrow).

These measurements revealed a sharp seasonal cycle of background NO_y concentrations, with high values in early spring (median 560–620 pptv) and ~70 pptv (median) during summer. This cycle is similar to that of other compounds in arctic haze but is partially attributed to a reduction in NO_y lifetime due to organic nitrate decomposition as temperatures and insolation increased.

Evidence indicates that the springtime arctic NO_y reservoir was primarily composed of stable removal-resistant species, including PAN and other organic nitrates. PAN decomposition as temperatures rose in late spring likely caused an observed pulse of NO to ~35 pptv (maximum hourly average); hourly-average NO concentrations were otherwise generally <8 pptv. NO_x production from PAN decomposition due to the onset of spring or southward advection may affect springtime O_3 levels both in the Arctic and in the northern mid-latitudes.

NO_y and O_3 concentrations were positively correlated during summer, possibly indicating long-range transport of both and/or the presence of a mid-tropospheric

NO_y reservoir combined with a stratospheric O_3 source.

A number of events with substantially elevated NO_y concentrations (to 16 ppbv) were observed in air not impacted by emissions from the town of Barrow. Substantial evidence indicates that these events were a result of NO_x emissions from the Prudhoe Bay region (~300 km to the ESE), which is also expected to affect measurements of other compounds at the Barrow site.

Acknowledgments

I would like to thank my wife, Ms. Lori Mills Honrath, for the support and inspiration she has given me over my years as a graduate student and for the limitations she accepted so that I could complete this work.

I would also like to thank my graduate advisor, Dr. Daniel Jaffe, who helped me clarify the goals and scientific objectives of this research, as well as the other members of my graduate advisory committee—Dr. Glenn Shaw, Dr. Richard Stolzberg, Dr. Knut Stamnes, and Dr. Joan Gosink.

I collaborated with a number of other researchers in this work, in addition to Dr. Jaffe. Mr. John Herring (University of Alaska) helped develop the molybdenum NO_y converter used in Barrow during 1989. Dr. Shao-Meng Li (National Center for Atmospheric Research), Dr. Gary Herbert (National Oceanic and Atmospheric Administration Climate Monitoring and Diagnostics Laboratory—NOAA CMDL), and Dr. Samuel Oltmans (NOAA CMDL) provided the results of their measurements at Barrow, which were used in the analysis presented here. In addition, Dr. Joyce Harris (NOAA CMDL) provided the results of back-trajectory calculations and Dr. Jonathon Kahl (University of Wisconsin) provided meteorological expertise that was very helpful in the meteorological analysis of the NO_y events presented in Chapter 4.

The results and analyses presented in chapters 3 and 4 are based on work previously published in collaboration with some of the researchers noted above. The work in chapter 3 was originally published as: Honrath, R. E. and D. A. Jaffe, Measurements of nitrogen oxides in the Arctic, *Geophys. Res. Lett., 11*, 425–428, 1990. The work presented in chapter 4 was originally published as: Jaffe, D. J., R. E. Honrath, J. A. Herring, S.-M. Li, and J. D. Kahl, Measurements of nitrogen oxides at Barrow, Alaska during spring: evidence for regional and northern hemispheric sources of pollution, *J. Geophys. Res., 96*, 7395–74-5, 1991.

Contents

List of Figures

List of Tables

Chapter 1

Introduction

The reactive nitrogen oxides play a critical role in tropospheric photochemistry. By controlling the rate of ozone production, NO_x, which includes nitric oxide (NO) and nitrogen dioxide (NO_2), has a direct impact on the concentration of tropospheric ozone, a radiatively-active "greenhouse" gas. In addition, NO_x affects the concentration of the hydroxyl radical (OH), which determines the tropospheric lifetimes of many other compounds. Nitric acid (HNO_3) is a major component of acidic precipitation. Finally, peroxyacetyl nitrate (PAN) plays an important role in the redistribution of nitrogen oxides from polluted environments to remote regions. The reactive nitrogen oxides, or NO_y, include NO_x, HNO_3, and PAN, as well as all other reactive nitrogen-containing species that act as sources or sinks of these compounds in the troposphere. Thus, $NO_y \equiv NO + NO_2 + HNO_3 + PAN + NO_3 + 2N_2O_5 + \cdots$.

In the remote troposphere, photochemical ozone formation may occur as a result of reactions involving carbon monoxide (CO), methane (CH_4), or other hydrocarbons [e.g. *Crutzen,* 1979; *Fishman et al.,* 1979]. In the case of CO, ozone is produced through the following reactions:

$$CO + OH \longrightarrow CO_2 + H \tag{1.1}$$

$$H + O_2 + M \longrightarrow HO_2 + M \tag{1.2}$$

$$HO_2 + NO \longrightarrow OH + NO_2 \tag{1.3}$$

$$NO_2 + h\nu \longrightarrow NO + O \qquad \lambda \leq\sim 400\text{nm} \tag{1.4}$$

$$O + O_2 + M \longrightarrow O_3 + M \tag{1.5}$$

$$\text{Net: } CO + 2O_2 \longrightarrow CO_2 + O_3, \tag{1.6}$$

where M represents any molecule that absorbs the excess energy of the reacting species, allowing the product to form. Through this mechanism, NO_x is a catalyst in the oxidation of CO by molecular oxygen, with concomitant formation of ozone. In this scheme, one O_3 molecule is produced per CO molecule; the corresponding reaction sequences for CH_4 and non-methane hydrocarbons result in the formation of greater than one O_3 molecule per carbon atom. Net O_3 production is dependent upon the presence of NO above a critical level, however, as a result of competing ozone loss reaction sequences such as

$$CO + OH \longrightarrow CO_2 + H \tag{1.1}$$

$$H + O_2 + M \longrightarrow HO_2 + M \tag{1.2}$$

$$HO_2 + O_3 \longrightarrow OH + 2O_2 \tag{1.7}$$

$$\text{Net: } CO + O_3 \longrightarrow CO_2 + O_2. \tag{1.8}$$

Whether net O_3 production or loss occurs is determined by the relative rates of reactions 1.3 and 1.7. By comparing the rate constants for these two reactions, a critical NO concentration can be calculated, above which reaction 1.3 dominates (approximately 10 pptv under typical tropospheric conditions; *Fishman et al.,* [1979a]). At higher NO concentrations, net O_3 production is expected to occur, while net O_3

destruction occurs at lower NO concentrations. However, even at lower NO concentrations an increase in NO concentration would result in reduced O_3 destruction, and therefore an increase in the O_3 concentration.

Through its control of tropospheric O_3 production, NO also has a direct impact on the concentration of the hydroxyl radical (OH), which is formed as a result of O_3 photolysis in the presence of water vapor:

$$O_3 + h\nu \longrightarrow O(^1D) + O_2 \qquad \lambda \leq\sim 310\text{nm} \tag{1.9}$$

$$O(^1D) + H_2O \longrightarrow 2OH. \tag{1.10}$$

The hydroxyl radical is the primary determinant of the lifetime of many tropospheric gases, such as CO, hydrocarbons, and chlorinated hydrocarbons [*Levy,* 1971; *Crutzen,* 1979].

NO is rapidly oxidized to NO_2 in the presence of ozone. However, under sunlit conditions NO_2 photolyses to NO through the following reactions, referred to as the photostationary-state reaction sequence

$$NO + O_3 \longrightarrow NO_2 + O_2 \tag{1.11}$$

$$NO_2 + h\nu \longrightarrow NO + O \qquad \lambda \leq\sim 400\text{nm} \tag{1.4}$$

$$O + O_2 + M \longrightarrow O_3 + M. \tag{1.6}$$

This interconversion is rapid, with a time constant of minutes under mid-day, mid-latitude conditions. As a result of this rapid interconversion, NO and NO_2 are linked and the sum $(NO + NO_2)$ is often referred to as a single entity, NO_x.

NO_2 may also react with hydroxyl to form nitric acid:

$$NO_2 + OH + M \longrightarrow HNO_3 + M. \tag{1.13}$$

This reaction, followed by rainout or surface deposition of HNO_3, results in estimated NO_x lifetimes of ~1–2 days in the remote mid-latitude troposphere in summer and

~10 days in winter [*Logan et al.,* 1981]. As a result, HNO_3 is a major component of acidic precipitation [*Galloway and Likens,* 1981].

The presence of nitrogen oxides in the troposphere is primarily a result of NO_x emissions from combustion sources, lightning, and biogenic emissions from soil [*Logan,* 1983]. NO_x emissions from anthropogenically-controlled sources—fossil fuel combustion and biomass burning—account for about two-thirds of the global NO_x emissions [*Logan,* 1983] and are a result of NO formation from N_2 and O_2 during high-temperature combustion [*Seinfeld,* 1975]. Anthropogenic emissions of NO_x have increased substantially in recent decades. For example, *Hameed and Dignon* [1988] have estimated that global NO_x emissions from fossil-fuel combustion increased by almost a factor of 2 from 1960 to 1980.

Anthropogenic emissions are concentrated in populated areas, and the short lifetime of NO_x limits the impact these emissions can have on concentrations in remote regions. However, NO_x may still be transported to remote regions in the form of relatively stable reservoir species such as peroxyacetyl nitrate (PAN) [*Singh and Hanst,* 1981; *Singh et al.,* 1986]. PAN is formed from photochemical reactions of NO_x and hydrocarbons, and is a major product of photochemistry in urban smog [*Stephens,* 1969]. PAN is thermally unstable, but at the low temperatures of the middle and upper troposphere it is highly stable and can be transported over long distances. The lifetime of PAN in the boundary layer is not expected to exceed 1–2 days under typical mid-latitude conditions, while lifetimes to three months are expected in the mid-troposphere [*Singh,* 1987]. Thus mixing of polluted air into the free troposphere is a potential mechanism for the long-range transport of nitrogen oxides in the form of PAN. When heated to typical lower-tropospheric temperatures, PAN decomposes, releasing NO_x, and this process has been proposed as a mechanism for the transfer of NO_x from polluted areas to the remote troposphere [*Singh and Hanst,* 1981].

There is substantial evidence that increasing anthropogenic NO_x emissions are

indeed affecting O_3 and HNO_3 in remote regions. For example, O_3 measurements at baseline stations in Mauna Loa, Hawaii, and Barrow, Alaska, indicate increases in annual-average surface O_3 concentrations of ~1%/year since 1973 [*Oltmans and Komhyr,* 1986]. In addition, samples from an ice core in Greenland indicate a substantial increase in NO_3^- deposition to the Greenland ice sheet, beginning around 1955 [*Mayewski et al.,* 1986]. The transport of anthropogenic NO_x emissions to remote regions may be particularly important because the dispersal of NO_x over a wide area may lead to increased total O_3 production [*Liu et al.,* 1987]. This results from a reduced O_3 production efficiency in urban areas, where high NO_x concentrations cause reduced lifetimes of the ozone precursors (NO_x and the peroxy radicals) [*Liu et al.,* 1987; *Lin et al.,* 1988].

This discussion demonstrates the importance of an understanding of the global budget of nitrogen oxides. However, the current understanding of this budget is limited by gaps in our knowledge of concentrations of the nitrogen oxides in remote regions. In addition, some measurements have indicated that a significant fraction of the total NO_y reservoir in remote regions is composed of unknown and/or unmeasured compounds [*Fahey et al.,* 1986; *Singh,* 1987; *Jacob and Wofsy,* 1990; *Singh et al.,* 1991b].

In the Arctic, the paucity of data is particularly evident. It is known that the arctic troposphere is highly polluted during winter and spring (relative to other remote regions), based on measurements of a number of anthropogenic pollutants [e.g. *Shaw,* 1982; *Barrie,* 1986]. This phenomena is known as "arctic haze" and is a result of less efficient pollutant removal and more efficient transport from pollutant source regions during winter–spring, relative to summer. However, there have been few nitrogen oxide measurements in the Arctic. Prior to the work reported here, NO_y in the Arctic had been measured only once, during a series of springtime aircraft flights [*Dickerson,* 1985]. Those measurements indicated that NO_y levels in the Arctic are also elevated during spring. Concentrations of 1000–1600 pptv were

found in arctic haze layers, and NO_y levels outside of haze layers were also enhanced (300–400 pptv). These measurements may be compared to NO_y concentrations in other regions remote from anthropogenic sources, which have been reported to be in the range of 100 to 250 pptv [*Galbally and Roy,* 1981; *Helas and Warneck,* 1981; *Stedman and McEwan,* 1983; *Hübler et al.,* 1989].

The only previous measurements in the Arctic of individual nitrogen oxide species were springtime measurements of PAN made at Alert, Canada, by *Bottenheim et al.* [1986], *Barrie et al.* [1989], and *Bottenheim and Gallant* [1989]. Springtime PAN concentrations at ground-level at Alert were 200–600 pptv, indicating that PAN is an important NO_y compound in the Arctic during spring.

The factors controlling ozone in the arctic troposphere are also poorly understood. Measurements of tropospheric ozone at the surface at Barrow, Alaska, have indicated an increase in summertime concentrations of ~2%/year since 1973 [*Oltmans and Komhyr,* 1986; *National Oceanic and Atmospheric Administration (NOAA),* 1989]. However, due to a paucity of data it is not possible to determine whether the increase is due to meteorological effects, in-situ photochemical production from increasing anthropogenic NO_x emissions, or long-range transport of ozone [*Oltmans and Komhyr,* 1986]. An understanding of ozone in the arctic troposphere is further complicated by the occurrence of ozone depletion events, which are observed in the Arctic during spring [*Oltmans,* 1981; *Bottenheim et al.,* 1986, 1990; *Barrie et al.,* 1988; *Barrie et al.,* 1989]. During these ozone depletion events, the ozone concentration measured at ground-level was observed to drop from ~30–40 ppbv to near 0 ppbv over a period of hours to a few days. The cause of the sharp drop in O_3 concentration is poorly understood, but has been attributed to catalytic O_3-destroying reactions involving BrO_x radicals, combined with a strong temperature inversion which prevents free-tropospheric ozone from reaching the boundary layer [*Barrie et al.,* 1988]. $CHBr_3$, which is apparently produced biologically in the Arctic Ocean, has been proposed as a source of BrO_x [*Barrie et al.,* 1988]. However, mod-

eling analyses by *Barrie et al.* [1988] indicated that the proposed mechanism was insufficient to explain the rate of the observed ozone depletion. An alternative catalytic cycle, involving photolysis of nitrosyl bromide ($BrNO_2$), formed from reaction of N_2O_5 with NaBr in sea salt, has also been proposed [*Finlayson-Pitts et al.*, 1990]. This mechanism requires the presence of significant concentrations of N_2O_5 in the early springtime arctic troposphere. (*Finlayson-Pitts et al.* [1990] assumed an N_2O_5 concentration or ~50 pptv, based on assumed NO_2 concentration of ~25 pptv.) Since N_2O_5 concentrations in the Arctic are not known, measurements are needed to determine whether this mechanism is feasible.

1.1 Goals of This Research

In light of the inadequacy of the current understanding of nitrogen oxides in the arctic troposphere, measurements of NO_y and NO were made at a site near Barrow, Alaska. These measurements were made with the following goals:

1. To determine the seasonal and diurnal cycles of NO_y and NO in the background arctic troposphere at Barrow (i.e., the concentrations in air unaffected by local sources and representative of the arctic troposphere in the region of Barrow).

2. To identify the relationship of NO_y and NO to O_3 in order to determine whether there is evidence that the summertime surface O_3 increase observed at Barrow may be a result of increasing anthropogenic NO_x emissions.

3. To determine NO concentrations during springtime O_3 depletion events to gain information on the importance of NO_x in arctic springtime O_3 destruction chemistry.

4. To assess the impacts of NO_x emissions from a major regional source—the Prudhoe Bay oil-producing region—to determine whether emissions from

Prudhoe Bay have an impact on regional tropospheric photochemistry or may affect the measurements of other compounds monitored at the Barrow monitoring site.

Measurements of NO_y and NO were made during three campaigns that took place during the summer of 1988, the spring of 1989, and March–December, 1990. The following chapters present discussions of the instrument developed to make these measurements and the results of the three measurement campaigns.

Chapter 2

Experimental

The theory, development, and operation of the UAF NO/NO_y instrument are described in this chapter. A theoretical overview of NO chemiluminescence detection is presented first, followed by a review of typical NO detector and NO_y converter designs used in previous studies. The remaining sections of this chapter pertain specifically to the instrument and measurements of this study. They include descriptions of the main components making up the instrument and a discussion of the operation of the instrument, including the instrument cycle, data reduction procedures, and estimated uncertainties. These discussions are followed by a description of the measurement site at Barrow. The final section of this chapter describes an intercomparison study, in which measurements with this instrument were compared with those of an independent research group.

2.1 Overview of NO/NO_y Chemiluminescence Detection

Determination of NO by chemiluminescent reaction with ozone was first described by *Fontijn et al.* [1970]. That first instrument had a detection limit of 4 ppbv (parts

in 10^9 by volume) and was reported to be interference-free. A variety of commercial instruments with detection limits of 2–5 ppbv were soon available [*Stevens and Hodgeson,* 1973], and were widely used for measurement of urban NO and NO_x (after conversion to NO—see discussion of NO_y measurement below). Instruments with much lower detection limits, suitable for use in the rural or remote troposphere and stratosphere, were soon developed [*Ridley and Howlett,* 1974; *Kley and McFarland,* 1980; *Delany et al.,* 1982; *Dickerson et al.,* 1984]. These improved instruments have detection limits in the range of 1 pptv–100 pptv (parts per 10^{12} by volume). Some of these instruments have been used to measure total reactive nitrogen—NO_y—by first reducing the other nitrogen oxides (e.g. NO_2, HNO_3 and PAN) to NO, using one of the techniques described in section 2.1.2. In the following sections, the theory and operation of NO chemiluminescence detectors is presented, followed by a brief discussion of systems for measurement of NO_y by reduction to NO (and subsequent chemiluminescence determination of NO).

2.1.1 NO Chemiluminescence Detectors

A schematic diagram of a typical high-sensitivity NO chemiluminescence detector is shown in Figure 2.1. The theory of operation and components of this instrument are described in detail in the following sections. However, the main instrument components and calibration parameters are presented here, for the simplified instrument shown in Figure 2.1. In this instrument, a flow of ambient air is mixed with a high concentration (several percent v/v) of ozone (O_3) in a low pressure (~5–20 torr) reaction chamber. NO in the sample flow reacts with O_3 to form the chemiluminescent excited-state NO_2 (NO_2^*). Light emitted from NO_2^* decay is detected by an adjacent photomultiplier tube (PMT). Instrument sensitivity is determined using standard addition of NO in N_2 from a high-pressure tank. The instrument's response to NO

in units of photon counts per second (cps) is then

$$\text{Instrument Response} = S_{NO}[NO], \tag{2.1}$$

where [NO] is the ambient NO mixing ratio in pptv and S_{NO} (cps/pptv) is the instrument sensitivity. However, additional PMT pulses due to thermal noise and other sources necessitate the measurement of an instrument zero level. In the instrument shown in Figure 2.1, the zero level is determined by redirecting the O_3 flow into the sample line upstream of a "zeroing volume," as shown by the dotted line in Figure 2.1. The NO/O_3 reaction and photoemission then occurs in the zeroing volume, out of view of the PMT.

In operation, the instrument is cycled through a number of modes which allow the measurement of the sensitivity (S_{NO}) and the photon count rate during a zero (Z) and a measure (M) mode. The ambient NO concentration is then given by

$$[NO] = \frac{M - Z}{S_{NO}}. \tag{2.2}$$

Thus, accurate and precise determination of M, Z, and S_{NO} is a necessary condition for accurate and precise NO measurement. Measurement of S_{NO} depends on the sample and calibration gas mass flow rates determined by the mass flow controllers (MFCs) (shown in Figure 2.1) and on the NO concentration in the calibration gas cylinder. In addition, linearity of the instrument is implicitly assumed in equation 2.2. The precision of the M and Z measurements is limited by random variability in the PMT pulse rate, and thus depends on the averaging period of the measurements. The ultimate accuracy of NO measurements at very low concentrations is limited by the accuracy of the Z measurement. Errors in Z can lead to errors in [NO], referred to as "fake NO" or NO measurement artifacts. This NO artifact can be minimized or measured and corrected for, as described below. However, uncertainty in the NO artifact correction limits the minimum NO accuracy to approximately ± 2 pptv.

In the following section, the theory of operation of the NO chemiluminescence instrument is discussed. This discussion is followed by a brief description of the components making up the typical instrument shown in Figure 2.1 and a discussion of the primary limitations on the accuracy and precision of pptv-level NO measurements.

2.1.1.1 Kinetics of Chemiluminescence Detection

The kinetics of chemiluminescence NO detection have been described extensively by *Ridley and Howlett* [1974], *Kley and McFarland* [1980], *Bollinger* [1982], and *Drummond et al.* [1985]. This technique is based on the measurement of light emitted from a continuous flow reactor in which an air sample is mixed with a high concentration of ozone. The basic reactions are

$$NO + O_3 \longrightarrow NO_2 + O_2 \tag{2.3}$$

$$NO + O_3 \longrightarrow NO_2^* + O_2 \tag{2.4}$$

$$NO_2^* \longrightarrow h\nu + NO_2 \tag{2.5}$$

$$NO_2^* + M \longrightarrow NO_2 + M, \tag{2.6}$$

where $k_{2.3} = 2.3 \times 10^{-12}\exp(-1475/T)$, $k_{2.4} = 2.9 \times 10^{-12}\exp(-1951/T)$, and $k_{2.5}/k_{2.6} \sim 1.3 \times 10^{14}$ molec/cm^3 [*Drummond et al.*, 1985]. These reactions take place in a reflective reaction chamber, and the resulting photons, which are in the red to infrared region ($\lambda \sim$ 700–2600 nm [*Clough and Thrush*, 1967], are detected by a red-sensitive photomultiplier tube. The photon production intensity in a well-mixed reaction chamber, I, is thus

$$I = \frac{k_{2.4}}{(k_{2.3} + k_{2.4})} \cdot \frac{k_{2.5}}{(k_{2.5} + k_{2.6}M)} \cdot N_{NO} F \cdot [1 - \exp(-(k_{2.3} + k_{2.4})[O_3]_R t_R)] \tag{2.7}$$

[*Kley and McFarland*, 1980], where N_{NO} and M are the number density (molecules/cm^3) for NO and air, respectively, F is the pumping speed (cm^3/s),

$[O_3]_R$ is the O_3 concentration in the reaction chamber, and t_R is the reaction chamber residence time. The PMT output in counts per second (cps) is equal to I times a proportionality factor α, which includes reaction chamber geometry and reflectivity as well as the product of PMT sensitivity, optical filter transmittance, and relative intensity of the NO_2^* photoemission integrated over this wavelength region. This factor is on the order of 2×10^{-5} for a typical reaction chamber and PMT, assuming the reaction chamber reflects only 1–5% of the produced photons to the filter window [*Bollinger,* 1982].

At pressures above about 5 torr, $k_{2.6}\mathrm{M} \gg k_{2.5}$, so the PMT signal due to NO (in cps) is

$$\begin{aligned} \text{Signal} &= S_{NO}[NO] = \alpha I \\ &= \alpha \cdot \frac{k_{2.4}}{k_{2.3}+k_{2.4}} \cdot \frac{k_{2.5}}{k_{2.6}} \cdot \frac{N_{NO}}{\mathrm{M}} \cdot \mathrm{F} \cdot [1-\exp(-(k_{2.3}+k_{2.4})[O_3]_R t_R)] \end{aligned} \quad (2.8)$$

[*Drummond et al.,* 1985], where [NO] is the NO mixing ratio in pptv ([NO] $\equiv 10^{12} N_{NO}/\mathrm{M}$ and S_{NO} is the sensitivity [cps/pptv]). Equation 2.8 indicates that the signal is directly proportional to NO mixing ratio, as desired. In addition, the theoretical signal is proportional to the volume flow rate in the reaction chamber, but is not related to the total mass flow rate, as a result of the competing effects of increased NO throughput and quenching due to increased reaction chamber pressure. In operation, however, the instrument sensitivity is determined by standard addition of a known NO concentration, rather than by relying on theoretical calculations.

The total PMT signal is larger than $S_{NO}[NO]$, however. The additional signal is due (following *Drummond et al.* [1985]) to PMT dark pulses (S_D) and chemiluminescence of other reactions (S_I), giving a total signal (Sm) of

$$S_m = S_{NO}[NO] + S_D + S_I \quad (2.9)$$

[*Drummond et al.,* 1985]. The PMT dark pulse rate (S_D) is dependent on PMT temperature, while S_I depends on poorly characterized factors (discussed in section 2.1.1.3 below). To determine $S_{NO}[NO]$, (S_D+S_I) is estimated in a "zero mode,"

in which NO is removed from the sample flow by mixing with ozone out of view of the PMT. However, this technique will only be successful if the concentration of interfering compounds is not significantly changed during the zero mode. Thus, it is necessary that

$$\exp(-[O_3]_z(k_{2.3} + k_{2.4})t_z) \ll \exp(-[O_3]_z k_{int} t_z) \tag{2.10}$$

where $[O_3]_z$ and t_z are the ozone concentration and residence time during zeroing, respectively, and k_{int} is the reaction rate of O_3 with the interfering compound.

That this is indeed the case has been demonstrated through tests of individual compounds that could potentially interfere with the measurement. *Bollinger* [1982] found discrimination factors (concentration of potentially interfering compound/absolute value of apparent NO concentration due to interfering compound) of 1,000–10,000 in tests of benzene, toluene, ethylene, C_1–C_4 alkanes, terpenes, CFC-11, methanol, and trichloroethylene. Nevertheless, many NO detectors exhibit an artifact signal (or "fake NO") during periods when NO is known to be absent, an indication that unknown interferences may be important (see discussion in section 2.1.1.3 below). The artifact signal is determined either by sampling air at night, away from sources (when reaction with ambient O_3 should drive the NO concentration to zero) or by sampling ultra-zero high purity synthetic air.

In order to minimize potential interferences, a red filter is used to screen out photons not from reaction 2.5. In addition, use of a minimum value of $([O_3]_z t_z)$ has been recommended, so that any difference between k_{int} and $(k_{2.3} + k_{2.4})$ can be exploited to the maximum degree [*Bollinger,* 1982; *Drummond et al.,* 1985). *Drummond et al.* [1985] recommend an O_3 concentration low enough that only ~85% of the NO is lost in the zeroing and reaction chambers. At such low O_3 concentrations, the NO sensitivity can vary significantly with small changes in $[O_3]_R$, so a more stable O_3 source would be required to operate under such conditions [*Drummond et al.,* 1985].

2.1.1.2 Components of Typical High-Sensitivity NO Detectors

The components of a typical high-sensitivity NO detector are shown schematically in Figure 2.1. The reagent O_3 is most commonly generated from oxygen using a high-voltage discharge. Ozone and the sample air are added to the reaction chamber at a location near the red filter. Reaction chamber designs vary greatly, and are discussed further in section 2.2.3. Typical sizes are 250 ml–1000 ml. In many cases, the reaction chamber temperature is controlled to minimize variations in k_2 and resulting sensitivity changes (e.g., *Bollinger* [1982], *Parrish et al.* [1990]). Resulting photons are detected by a red-sensitive PMT after passing through a red filter (wavelength cutoff $\sim$ 620 nm). The signal can be measured using pulse-counting or analog techniques. A variety of reflective coatings have been tested for use in the reaction chamber, including gold, silver, magnesium oxide, and barium sulfate [*Ridley and Howlett,* 1974; *Fontijn et al.,* 1970]. In most instruments, however, gold is used because it is highly reflective in the region of the NO_2 chemiluminescence [*Kley and McFarland,* 1980].

Zeroing. Zeroing is accomplished by allowing the $NO + O_3$ reaction to occur out of sight of the PMT. This is usually done with the zeroing volume located in the sample line, as shown in Figure 2.1, but in some designs the zeroing volume is located in the ozone line [*Delany et al.,* 1982; *Dickerson et al.,* 1984]. In some instruments, the sample and O_3 flows are mixed prior to the reaction chamber, and the zeroing volume is in-line only during zeroing [*Drummond et al.,* 1985, 1988]. Other methods of zeroing use a separate source of O_3. Stedman and *McEwan* [1983] used ambient O_3 in a 200 l reaction chamber. *Kaplan et al.* [1988] and *Bakwin et al.* [1990] generated O_3 ($\sim$5 ppmv) from ambient O_2 in the sample flow using a small mercury lamp.

A variety of materials have been used for the zeroing reaction chamber, including glass, teflon, and stainless steel (e.g., *Parrish et al.* [1990]; *Drummond et al.*

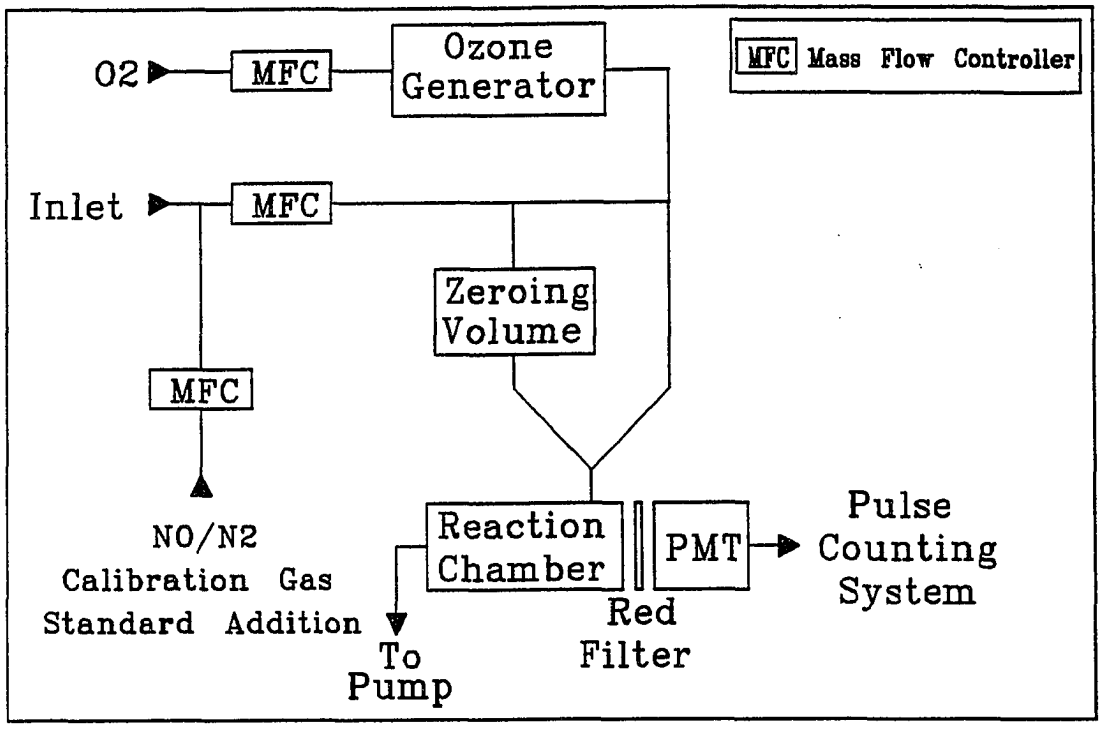

Figure 2.1 Schematic diagram of a typical high-sensitivity NO detector. The path of sample air during zeroing is shown by the dashed line.

[1988]; *Dickerson et al.* [1984]). *Bollinger* [1982] recommended that stainless steel not be used due to transient effects he observed as a result of changes in relative humidity in stainless steel inlet lines. In many cases, the zeroing reaction chamber is thermostatted (e.g. *Bollinger* [1982]; *McFarland et al.* [1986]; *Drummond et al.* [1988]).

Calibration. High-sensitivity NO instruments are calibrated using ppmv-level cylinder standards of NO in N_2. The calibration is accomplished by standard addition, as shown in Figure 2.1, at a dilution of ~1000. In most cases, mass flow controllers are used to control the calibration gas and sample flows to ensure accurate calibration.

In systems with thermostatted reaction chambers, variation in sensitivity is on the order of 10% over a period of months, and that amount of variation is largely

attributable to variations in ambient ozone levels, which result in varying inlet losses of NO (due to NO oxidation by O_3) [*Parrish et al.*, 1990].

2.1.1.3 Limitations on Low-Level NO Detection

In chemiluminescence NO detectors utilizing photon counting, the detection limit is theoretically determined by counting statistics. The number of PMT pulses observed in a given period follows a Poisson distribution such that $\sigma_c = \sqrt{c}$, where c is the total number of accumulated counts in a given time interval and σ_c is the standard deviation of c [*Malmstadt et al.*, 1972]. Due to the necessary zero correction, the NO concentration is calculated as

$$[\mathrm{NO}] = \frac{\mathrm{M} - \mathrm{Z}}{\mathrm{S_{NO}}}, \tag{2.11}$$

where [NO] is the NO mixing ratio (pptv), M and Z are the counting rates (cps) in M and Z modes, respectively, and S_{NO} is the sensitivity, in cps/pptv NO. Near the detection limit, M $\sim$ Z, and the standard deviation of (M-Z) is expected to be approximately $\sqrt{\sigma_M{}^2 + \sigma_Z{}^2} \sim \sqrt{2Z}$, by error propagation. Uncertainty in S_{NO} is usually negligible compared to (M-Z) uncertainty. Thus, if the M and Z signals are each averaged over N seconds the detection limit (2σ) is

$$\mathrm{DL}_{2\sigma} = \frac{2}{\mathrm{S_{NO}}}\sqrt{\frac{2\mathrm{Z}}{\mathrm{N}}} \tag{2.12}$$

Values of S_{NO} reported for high-sensitivity NO detectors range from 0.2 to 7 cps/pptv [*Ridley and Howlett*, 1974; *Schiff et al.*, 1979; *McFarland et al.*, 1979; *Kley and McFarland*, 1980; *Bollinger*, 1982; *Carroll et al.*, 1985; *McFarland et al.*, 1986; *Ridley et al.*, 1987; *Parrish et al.*, 1990; *Kelly et al.*, 1980; *Torres*, 1985, *Torres and Buchan*, 1988; *Helas and Warneck*, 1981; *Helas et al.*, 1981; *Drummond et al.*, 1985; *Ridley and Grahek*, 1990]. Values of the zero signal (Z) range from as low as 10 cps to 1000 cps [*Schiff et al.*, 1979; *McFarland et al.*, 1986], but most are 200–600 cps, with PMT dark counts contributing ~100–200 cps [*Kley and McFarland*, 1980; *Kley*

et al., 1981; *Bollinger*, 1982; *Ridley et al.*, 1987; *Parrish et al.*, 1990; *Kelly et al.*, 1980; *Stedman and McEwan*, 1983; *Torres*, 1985; *Drummond et al.*, 1985]. These values result in detection limits (2σ) of 12-300 pptv for N = 1 s. Longer averaging periods (to 3 minutes) are actually used, resulting in lower detection limits for the averaged data.

Since a one-point calibration is typically conducted at a concentration ~1000 times the detection limit, linearity is a necessary condition for accuracy at low levels. Theory suggests that the response of NO chemiluminescence detectors should be linear (equation 2.8). Several investigators have tested this expectation, over various concentrations ranging from 7 pptv to 10,000 ppmv, and no deviation from linearity has been found [*Stevens and Hodgeson*, 1973; *Fontijn et al.*, 1970; *Helas et al.*, 1981; *Kelly et al.*, 1980; *Carroll et al.*, 1985; *Bollinger*, 1982].

As discussed above, many NO detectors exhibit an artifact signal, or "fake NO" under conditions when NO is known to be absent. This artifact is essentially an indication of the difficulty in obtaining accurate measurements of the Z signal and can result in erroneous NO concentration estimates under low-[NO] conditions.

Reported artifacts (determined by sampling ambient air at night or using ultra-high purity synthetic air) range from -30 to >50 pptv, with most in the ±2 to 10 pptv range [*McFarland et al.*, 1979; *Kley and McFarland*, 1980; *Kley et al.*, 1981, *Bollinger*, 1982; *Bollinger et al.*, 1983; *Carroll et al.*, 1985; *McFarland et al.*, 1986; *Ridley et al.*, 1987, *Ridley et al.*, 1988; *Parrish et al.*, 1990, *Carroll et al.*, 1990; *Torres*, 1985; *Torres and Buchan*, 1988; *Bakwin et al.*, 1990, *Drummond et al.*, 1988; *Drummond et al.*, 1985; *Kondo et al.*, 1988a, 1988b]. The source of the artifact is not known. Suspected causes include: chemiluminescent reactions of O_3 and reaction chamber wall contaminants that vary in intensity between the zero and measure mode, due to variations in the ozone distribution; interference from other compounds, such as alkenes; and decomposition of O_3 on the reaction chamber walls [*Kley and McFarland*, 1980; *Bollinger*, 1982; *Bollinger et al.*, 1983;

Cox, 1977; *Drummond et al.,* 1988; *Drummond et al.,* 1985]. The artifact has been noted to be reaction chamber-specific, in at least one case in which more than one reaction chamber were available for comparison in the same instrument [*Torres and Buchan,* 1988]. A variety of measures have been undertaken in attempts to reduce or remove the artifact. Water is frequently added to the O_3 or sample flow, in order to displace adsorbed molecules from the reaction chamber wall [*Drummond et al.,* 1985). This method has resulted in a reduced zero signal and reduced artifact in many cases, but is not always successful [*Parrish et al.,* 1990]. Reduction of the O_3 amount and reaction volume used in zeroing [*Drummond et al.,* 1985] have been used to reduce effects of compounds that may interfere with the NO measurement, as described above. Finally, since differences in the sample and O_3 flows into the reaction chamber during the M and Z modes have been proposed as a cause of the artifact [*Bollinger et al.,* 1984] such differences have been minimized [*Drummond et al.,* 1985]. Nevertheless, all chemiluminescence NO instruments appear to be affected by this problem to some degree. However, careful instrument design and monitoring of artifact levels can be used to reduce the uncertainty resulting from NO artifacts as low as ± 2 pptv [*Torres,* 1985; *Drummond et al.,* 1985; *Bakwin et al.,* 1991].

The artifact is thus a primary limitation to low-level NO measurement. Regular artifact measurements, using synthetic zero air or nighttime air, have been used in an attempt to correct for the artifact [e.g., *McFarland et al.,* 1986]. However, variations in the artifact are often of the same order as the artifact itself. In addition, the use of zero air for artifact measurements is appropriate only if the artifact is not due to interference in the measurement from compounds present in ambient air.

2.1.2 Measurement of NO_y

NO_y can be measured as NO, after first reducing NO_y compounds to NO in a converter. Early NO detectors were designed to measure NO_x, and a variety of methods

to reduce NO_2 to NO were used, including heated stainless steel, gold wool, carbon, or molybdenum [*Stevens and Hodgeson,* 1973; *Winer et al.,* 1974]. However, it was discovered that these converters reduced a variety of NO_y compounds to NO, in addition to NO_2. As a result, similar converters have been used to measure NO_y. The most common converter types utilize reduction on molybdenum or gold-catalyzed reduction with CO. A variety of converter types have been used, including commercially-available molybdenum mesh converters, research-grade molybdenum converters (using lesser amounts of molybdenum mesh), and tubular gold/CO converters. Both molybdenum and gold/CO converters were used at different times for the measurements described in this thesis.

2.1.2.1 Molybdenum Converters

Molybdenum converters are commercially available (e.g. Thermo Environmental Instruments, Inc., Franklin, MA), and consist of a fine molybdenum mesh in a stainless steel container, which is heated to ~375°–525°C. Molybdenum converters have also been produced in the laboratory, using as little as 8 g molybdenum mesh [*Fehsenfeld et al.,* 1987]. The conversion efficiencies for a variety of NO_y species in heated (350°–450°C) molybdenum converters have been tested. Conversions above 90% were found for NO_2, HNO_3, PAN, ethyl nitrate, ethyl nitrite, methyl nitrate, and n-propyl nitrate (NPN) [*Fehsenfeld et al.,* 1987; *Winer et al.,* 1974; *Nunnermacker et al.,* 1988; *Grosjean and Harrison,* 1985]. In one test with a low-mass molybdenum mesh converter, however, a conversion efficiency of only 68% for NPN was observed [*Fehsenfeld et al.,* 1987].

Molybdenum converters are limited in their application to low-level NO_y measurements as a result of a "memory effect" [*Dickerson et al.,* 1984; *Fehsenfeld et al.,* 1987]. After exposure to high NO_y levels, an increased background signal persists for hours to days. After exposure to 100 ppbv NO_y, this background signal can be as high as 200 pptv and last several hours [*Dickerson et al.,* 1984]. Theoretically, this

NO_y artifact could be corrected for by regularly sampling NO_y-free synthetic air. Unfortunately, it is difficult to effectively remove NO_y from high-purity synthetic air to levels below 50–100 pptv [*Fahey et al.*, 1985] and no procedure to produce NO_y-free synthetic air has been reported.

While in operation and during high-temperature bakeouts, the surface of molybdenum converters is oxidized to MoO_2 and MoO_3. The surface may be regenerated using hydrogen. In addition, it is necessary to periodically remove contaminants from the converter to maintain a high conversion efficiency, and this is commonly done using high-temperature (500–600°C) bakeouts [*Fehsenfeld et al.*, 1987]. However, migration of MoO_3 powder from a molybdenum converter has been observed following such a bakeout [*Fehsenfeld et al.*, 1987]. In that case, the MoO_3 powder migrated into an NO detector, where it apparently caused the reduction of NO_y compounds to NO and resulted in erroneous NO measurements. Therefore it has been recommended that a filter always be used downstream of molybdenum converters [*Fehsenfeld et al.*, 1987].

2.1.2.2 Gold/CO Converters

The use of gold to catalyze the reduction of NO_y compounds to NO, using added CO as a reducing agent, was first reported by *Bollinger* [1982], and extensive tests of the converter were described by *Bollinger et al.* [1983] and *Fahey et al.* [1985]. This system consists of a 35 cm by 0.4 cm i.d. gold tube, heated to 300°C, through which the sample air flows at 1 slpm (liter per minute at standard conditions of 760 torr and 0°C), with CO added to 0.3% (v/v). This type of converter reduces NO_2 to NO with >99% efficiency, in accord with theoretical predictions based on diffusion-limited conversion [*Fahey et al.*, 1985; *Bollinger et al.*, 1983; *Murphy and Fahey*, 1987]. Tests by *Fehsenfeld et al.* [1987] and *Fahey et al.* [1985] indicate that NO_2, HNO_3, and N_2O_5 are converted with $\geq$ 95% efficiency. PAN conversion was ~93% [*Fahey et al.*, 1985], although a conversion efficiency as low as 89% for PAN has

been reported for this type of converter [*Fehsenfeld et al.*, 1987]. NPN conversion appears to generally be somewhat lower than that of the other compounds, at 67–76% [*Bollinger et al.*, 1983; *Fehsenfeld et al.*, 1987]. These conversion efficiencies are temperature-dependent, and ~100% conversion of all tested compounds was achieved at a temperature of 500°C. However, at that temperature oxidation of NH_3 and HCN to NO may become significant, possibly depending on humidity, resulting in an unwanted interference in the NO_y measurement, since NO_y is defined to exclude N_2O and ammonia and other reduced nitrogen compounds [*Fahey et al.*, 1985].

2.2 The NO/NO_y Instrument Used in This Work

The development and operation of the UAF NO/NO_y instrument is described in this section. The design and development discussed in this section were conducted with the goal of producing an instrument that could make accurate and precise NO and NO_y measurements at the levels expected at Barrow (i.e., NO levels to a few pptv and NO_y to below 100 pptv). In addition, a primary goal was that the instrument be able to run for extended periods at a remote site with a minimum amount of maintenance. Since the instrument was to be used at a stationary site where changes in the background NO and NO_y concentrations were expected to be slow, measurements averaged over periods of ~1–2 min were considered acceptable.

The following section presents an overview of the separate versions of the NO/NO_y instrument used for the three measurement campaigns—summer 1988, spring 1989, and March–December, 1990. This is followed by descriptions of the separate components of the NO/NO_y monitor and discussions of experiments used to develop the final designs. The component descriptions are followed by a discussion of the instrument cycle and the data reduction procedure and a summary of calibration parameter measurements during the three campaigns. Finally, uncer-

tainty estimates based on these discussions are presented in section 2.2.11 for each measurement campaign.

2.2.1 Summary of Instrument Configurations

The NO/NO_y detector, first used during the summer 1988 campaign, was significantly modified between the 1988 and 1989 campaigns, and again before the 1990 measurements. In each case, the modifications resulted in improvements in precision and/or detection limit as well as increased instrument complexity. Schematic diagrams of the instruments used for the three measurement campaigns are shown in Figures 2.2 (1988), 2.3 (1989), and 2.4 (1990); the individual components shown in the schematic diagrams are described in the following sections. Sample flow rates, reaction chamber pressures, and NO sensitivities are displayed in Table 2.1. The basic instrument operation was the same for the three instrument designs. As described in section 2.1.1, the instrument cycled between calibration measurements and ambient measurement and zero modes. This was accomplished using computer-controlled solenoid valves. The solenoid valves determined whether the instrument zero or ambient concentration was being measured, whether or not the sample flow passed through the NO_y converter, and controlled the standard addition of the calibration gas. Photon count rates were monitored and stored by the dedicated microcomputer.

The separate components that make up the instrument are described in detail in the following sections, which cover the initial materials and optical components, reaction chamber, ozone generator, zeroing system, calibration system, NO_y converter, and other components. The experiments used to develop the final designs are discussed, and some experimental results that did not lead to design improvements are also included, so that they will not be unnecessarily duplicated in the future.

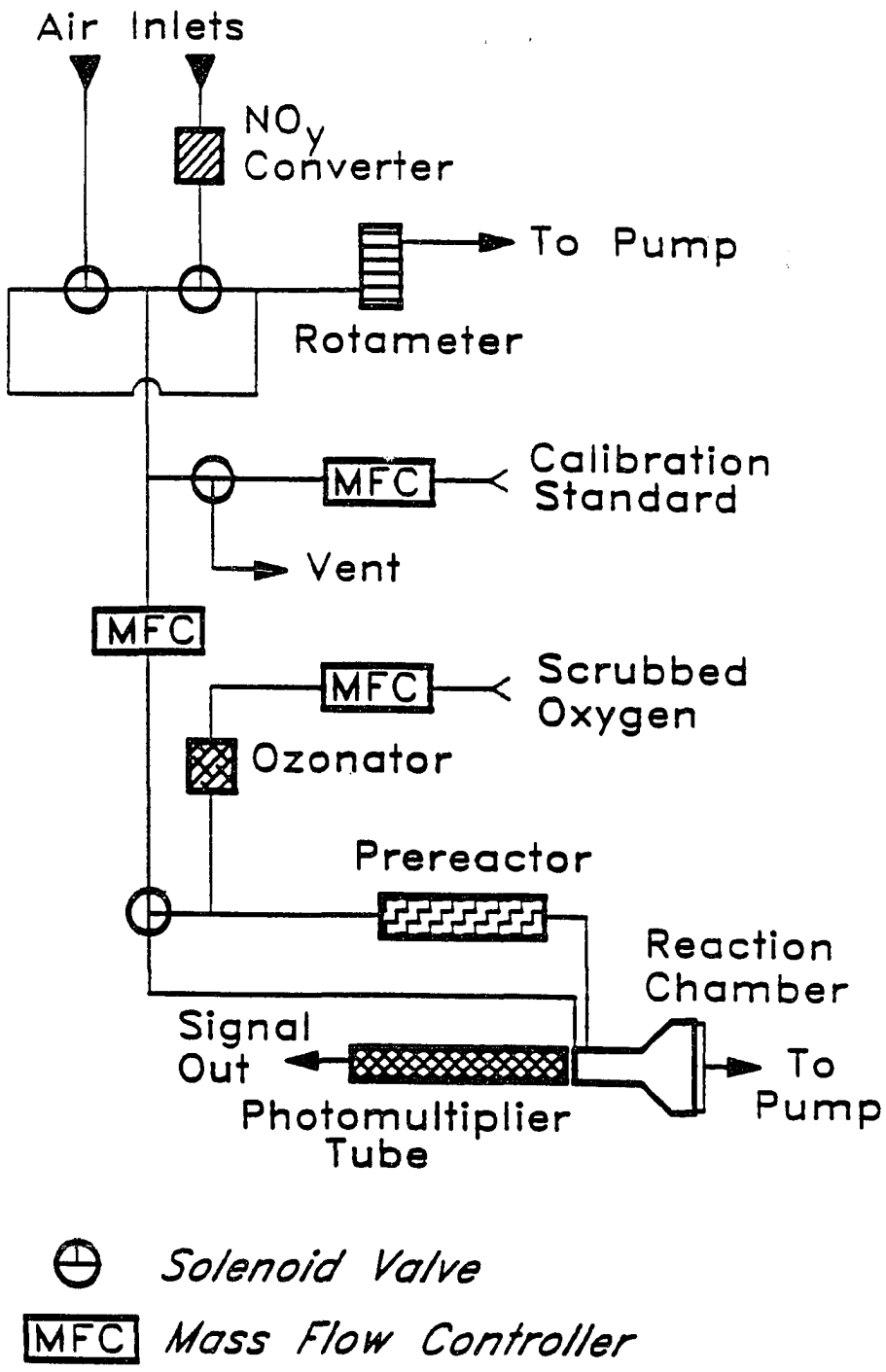

Figure 2.2 Schematic diagram of the NO/NO_y instrument used during the summer 1988 measurements.

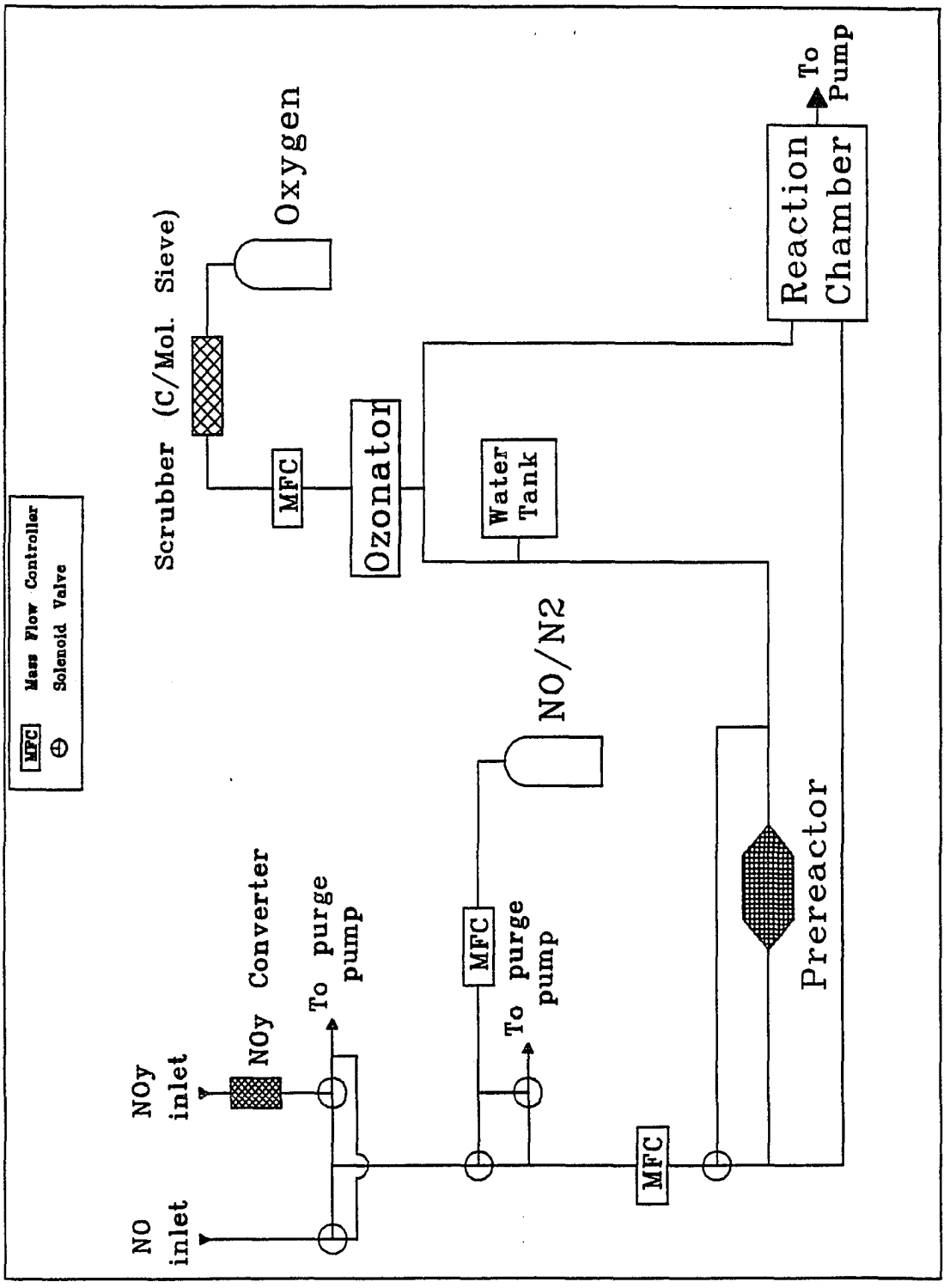

Figure 2.3 Schematic diagram of the NO/NO_y instrument used during the spring 1989 measurements.

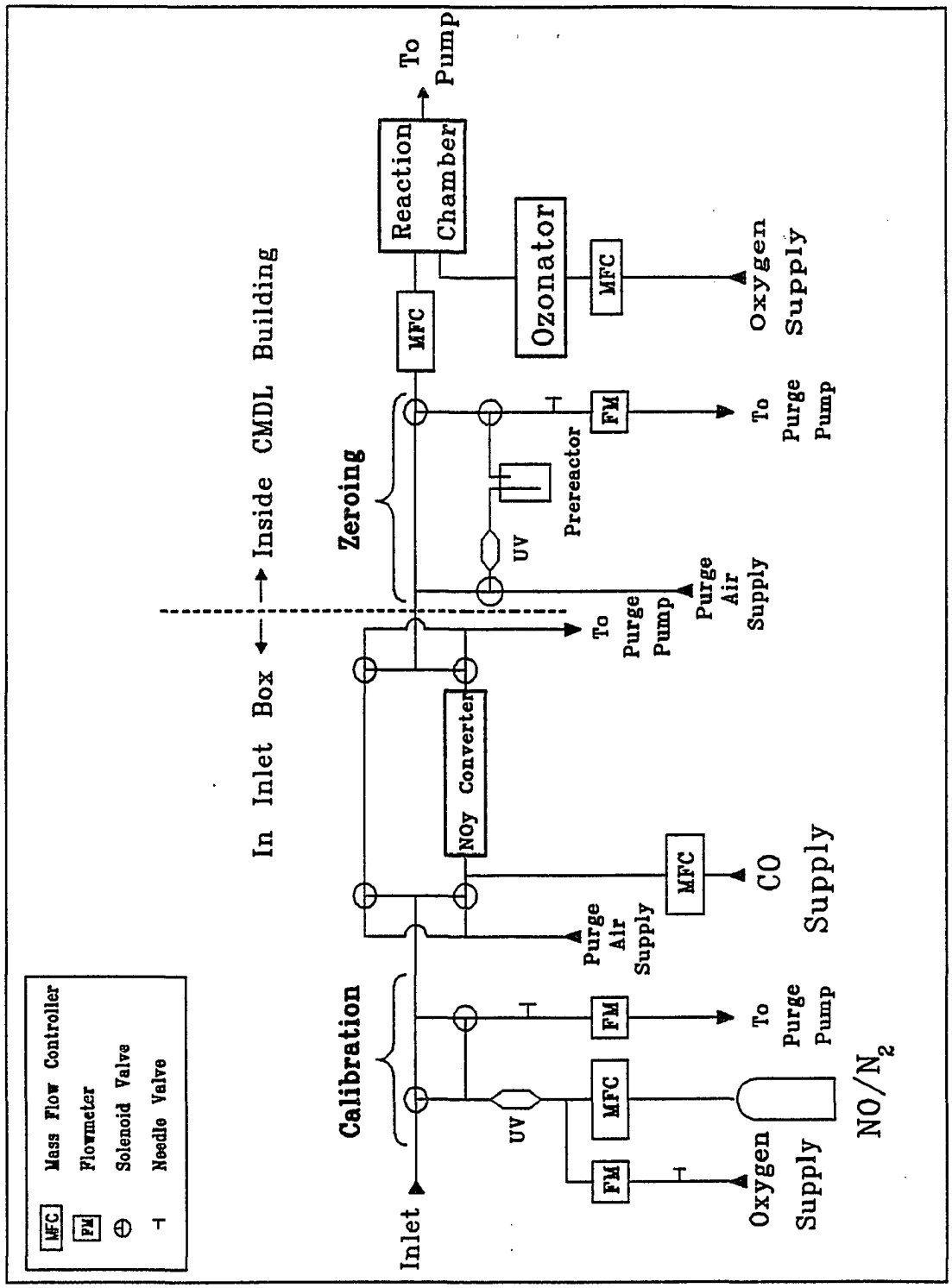

Figure 2.4 Schematic diagram of the NO/NO_y instrument used during the 1990 measurements.

Table 2.1 Sample Flow, Reaction Chamber Pressure, and Sensitivity for the Three Instrument Configurations.

	Sample Flow (slpm)	Reaction Chamber pressure (torr)	NO Sensitivity (cps/pptv)
1988	2.0	$\geq$50	0.4–0.7
1989	2.0	~20	0.9–1.2
1990	1.0	5–7	1.0–1.4

2.2.2 Initial Materials

The optical components of an existing Thermo Electron Co. (TECO) Model 14T NO_x analyzer (Thermo Environmental Instruments, Incorporated, Franklin, MA) were used for this instrument. The TECO instrument had a specified detection limit of 4 ppbv. In order to improve the detection limit by approximately three orders of magnitude, most parts of the TECO instrument were removed and replaced by improved components. The primary limitations on the detection limit of commercial NO detectors like that in the TECO instrument include the use of a small reaction chamber ($\leq$10 cm^3) that is not reflectively coated, and a weak pump. However, the entire instrument was modified in order to improve both the accuracy and precision at low NO levels. As a result, the only parts of the TECO instrument that were used are the photomultiplier tube (PMT), PMT cooler, PMT preamplifier, and the power supply.

Use of these components resulted in reduced development time and costs, relative to the fabrication of an entirely new instrument. However, these components also limited the performance of the final NO detector. The peltier cooler from the TECO instrument was not thermally controlled. In its original configuration, it is able to maintain a PMT temperature ~35°C below ambient [*Dickerson et al.,* 1984]. However, with the addition of an enlarged reaction chamber close to the PMT (see below), the cooler was able to cool the PMT to only ~20°C below ambient. As a result, the PMT temperature and dark count varied significantly with room temperature and were higher than the levels reported by some other investigators.

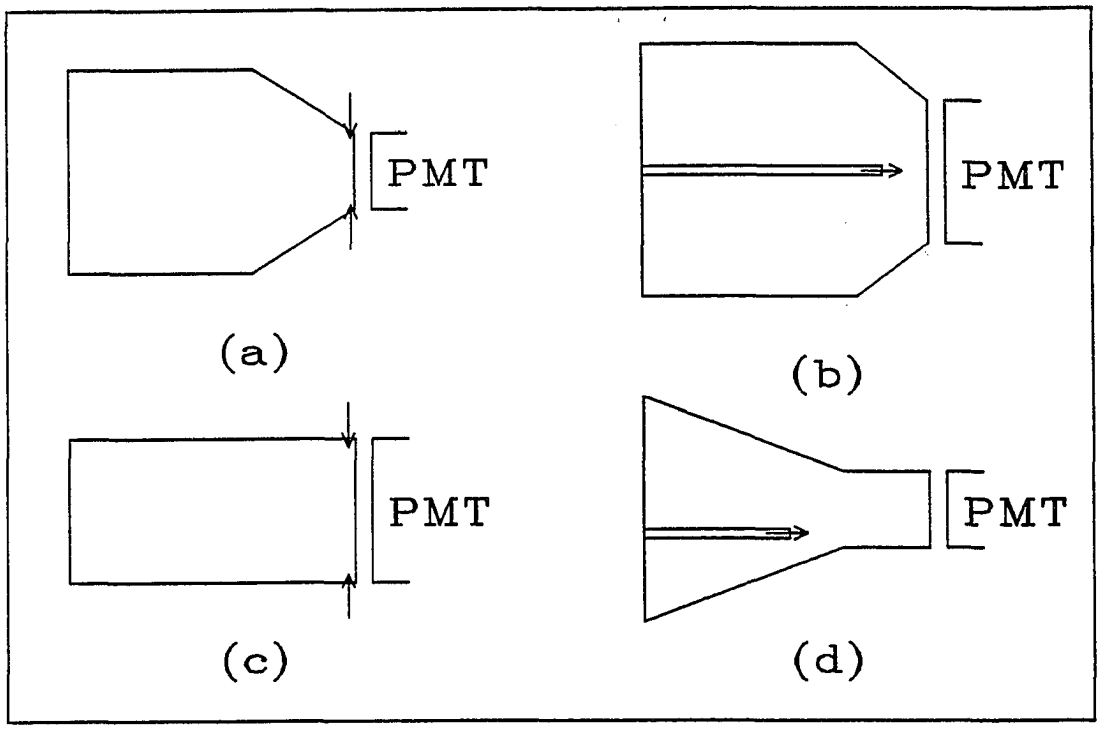

Figure 2.5 Reaction chamber designs used in previous NO detectors. (a) *Kley and McFarland* [1980]; (b) *Drummond et al.* [1985]; (c) *Ridley and Grahek* [1990]; and (d) *Dickerson et al.* [1984].

In addition, use of the existing PMT cooler severely constrained the design of an improved reaction chamber (described in the next section).

2.2.3 Reaction Chamber Design

A new reaction chamber was designed in order to increase the sensitivity through operation at lower pressure (which requires a larger reaction chamber and/or higher ozone concentration) and increased photon capture efficiency. The design was based on a review of previous designs [*Kley and McFarland,* 1980; *Delany et al.,* 1982; *Dickerson et al.,* 1984; *Ridley and Grahek,* 1990], within the constraints imposed by use of the TECO PMT cooler. The reaction chamber designs used by these previous investigators are shown schematically in Figure 2.5.

There are several factors that must be considered to produce a good reaction

chamber—one that will enhance the sensitivity of the NO detector. These include the following:

1. Location of the $NO+O_3$ reaction. It is desirable that most of the photon emissions occur near the PMT, to minimize loss due to wall reflections. All four designs shown in Figure 2.5 introduce the sample/O_3 mixture near the PMT for this reason.

2. Mixing. It is important that the sample and O_3 flows be well-mixed, to maximize the overall reaction rate. In the designs from Kley and McFarland and from Ridley and Grahek, the sample and O_3 flows are introduced into separate annular rings and are mixed as they flow toward the reaction chamber along a thin circumferential gap.

3. Shape and reflectivity. The reaction chamber should be designed so that photons emitted in any direction are efficiently reflected toward the PMT. The reaction chambers shown in Figure 2.5 are polished and reflectively plated to reduce reflection losses. However, the variety of shapes that have been chosen indicates a lack of agreement on the optimal shape for efficient reflection.

4. Size. The reaction chamber must be large enough that the $NO + O_3$ reaction has time to reach near-completion within the chamber. The necessary size is determined by the flow rate in the reaction chamber (determined by the pump chosen) and the rate of production of reagent ozone.

The relative importance of these factors is not well known, because no study of the effect of reaction chamber design on sensitivity has been reported.

The reaction chamber designed for this study is shown in Figure 2.6. The design has a volume of 500 ml and incorporates an annular flow injection system similar to that of *Kley and McFarland* [1980]. However, due to the limited diameter of the PMT cooler into which the reaction chamber was to fit, a single annular ring was

used. The sample and O_3 flows were introduced into the annular ring at adjacent points (rather than separate rings for the two flows as in the *Kley and McFarland* [1980] design). A thin annular groove allowed the gases to flow radially into the reaction chamber. The flow out of the annulus was blocked within 60° of the point at which the air and O_3 flows were injected, in order to improve circumferential mixing.

The shape of the reaction chamber was chosen based on a ray-tracing analysis. In this analysis, the paths of rays emanating from within the reaction chamber were modeled, assuming specular reflection off the reaction chamber walls. The rays were followed until they exited the reaction chamber through the exit filter, and at each reflection the intensity of the rays was reduced to account for non-unity reflectivity. This analysis considered rays emanating from two locations axially: (a) 1/2 inch above the exit filter; and (b) 2/3 of the distance from the filter toward the mirror. The rays were assumed to originate from the axis of the reaction chamber or from a point 1/8 inch from the reaction chamber wall. Rays emanating in all integral directions (in degrees) from these four points were modeled.

These calculations considered two shapes: a flared shape (similar to that used by *Dickerson et al.* [1984] and shown in Figure 2.5d), and a cylindrical shape (similar to that used by *Ridley and Grahek* [1990] and shown in Figure 2.5c). The PMT cooler size combined with machining constraints limited the reaction chamber diameter within the PMT cooler to 1.25 inches, which precluded use of a reaction chamber shaped like that used by *Kley and McFarland* [1980] (see Figure 2.5a). Both modeled designs were 500 ml in volume.

The results of the ray-tracing analysis indicated that the flared shape would be significantly more efficient at funnelling light to the exit filter. The reaction chamber design chosen for fabrication was flared and is shown in Figure 2.6. The fractional intensities passing through the exit filter (averaged over all light emission directions), assuming a 95% reflectivity, are shown in Table 2.2 for the chosen flared

design and for a cylinder of the same volume. The efficiency (fractional intensity passing through the exit) of the chosen design is significantly greater than that of the cylinder in all cases. Based on this analysis, the chosen design is 20–50% more efficient than a cylinder of the same volume and inside diameter would be.

Table 2.2 Estimated Efficiency of Reaction Chamber Designs, Based on Ray Tracing Analysis. Efficiency is defined as the fraction of the initial intensity of rays emanating from the specified points that reach the reaction chamber exit filter, assuming a 5% loss at each reflection and averaged over 360° of light emission direction.

Location of Photon Source		Efficiency	
Radial	Axial	Flared	Cylinder
On Axis	1/2 inch from filter	.717	.590
	2/3 height	.613	.424
1/8 inch from wall	1/2 inch from filter	.729	.597
	2/3 height	.619	.416

Both designs were 500 ml in volume and 1.25 inches in diameter at the point adjacent to the PMT.

The lower efficiency of the cylindrical chamber is a result of its large length-to-diameter ratio, necessitated by the PMT cooler size constraint. The required small diameter significantly reduced the estimated efficiency, even with the reaction chamber design that was chosen. The PMT photocathode has a diameter of 2.0 inches, so a larger-diameter reaction chamber would allow more efficient photon detection. For comparison, the reaction chamber designed of Ridley and Grahek (Figure 2.5c) has a diameter of 2.0 inches, matching the PMT diameter. Ray-tracing calculations indicate that a 2.0 inch diameter 500 ml cylindrical reaction chamber would be 3–10% more efficient in transmitting emitted photons to the PMT than the design used here, while a 250 ml cylindrical chamber (the Ridley and Grahek design) would be 13–30% more efficient. However, reaction chamber shape is just one of the variables controlling the ultimate instrument sensitivity. Since reported NO sensitivities using the Ridley and Grahek design range to 7 pptv [*Ridley and Grahek*, 1990], 5 times the value obtained with the chosen reaction chamber, it is clear that other variables affect the sensitivity as much or more than the reaction

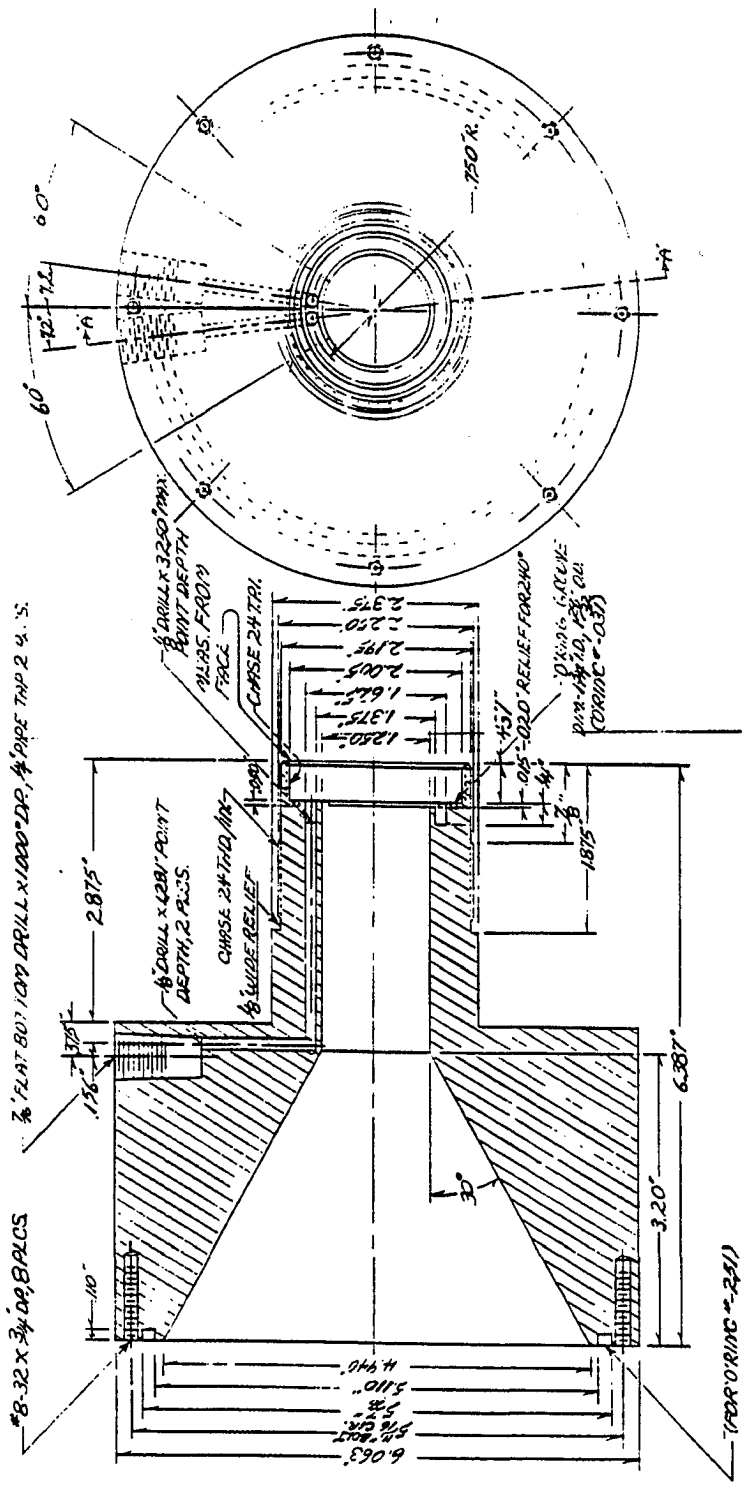

Figure 2.6 Reaction chamber design used in this study.

chamber shape.

In order to maximize the detection of photons exiting the reaction chamber, the chamber was designed to be inserted close to the PMT. This required removal of the stock TECO clear plastic window that thermally isolated the PMT from the TECO reaction chamber. The reaction chamber was fitted with an o-ring to prevent condensation of ambient water vapor on the PMT. However, the proximity of the large aluminum reaction chamber to the PMT resulted in heat transfer to the PMT. Tests after fabrication of the reaction chamber showed that positioning the chamber near the PMT did in fact result in an increased sensitivity (50% greater than that when the reaction chamber was located behind the clear window). However, the dark count was also significantly increased, due to the increased PMT temperature. The net result was little, if any, net improvement in detection limit.

2.2.4 Ozone Generation and Scrubbing

Generation of the quantity of ozone required by chemiluminescence NO detectors presents difficulties because the high-voltage discharge commonly used has a tendency to arc to nearby metal objects. Additionally, it is necessary to protect the pump oil from the large amounts of ozone, since O_3 will oxidize pump oil to form a material resembling varnish. Development and optimization of a safe ozone generator and scrubbing of ozone are described in this section.

2.2.4.1 Ozone Generation

In order to ensure that most of the ambient NO reacts within the reaction chamber, a high concentration of O_3 is needed. The necessary O_3 concentration in the reaction chamber is determined by the requirement that the NO mixing ratio be reduced by $>\sim$90% upon passage through the reaction chamber, i.e.,

$$0.1 \geq \exp(-k_{NO+O3}[O_3]_R t_R) \tag{2.13}$$

where $[O_3]_R$ and t_R are the ozone concentration and residence time in the reaction chamber, respectively, and k_{NO+O3} is equal to $k_{2.3} + k_{2.4}$ (page 12). The residence time in the reaction chamber can be calculated from the 1 slpm sample flow and the measured reaction chamber pressure of approximately 7 torr. This calculation gives a volume flow rate through the reaction chamber of 110 lpm and a residence time of 0.28 s in the 500 ml reaction chamber. (The volume flow rate calculated in this manner is less than the pump displacement of 190 lpm (section 2.2.8.3) due to a pressure drop across the tubing and ozone scrubber between the reaction chamber and pump.) Using the $NO+O_3$ reaction rate of 1.8×10^{-14} cm^3/molec./s at 298°K [*DeMore et al.*, 1987], the required O_3 concentration is 4.6×10^{14} molec./cm^3, or 0.2%. This requires an O_3 flow of at least 2 sccpm (cubic cm per min at standard conditions of 760 torr and 0°C). To generate this amount of O_3, a high-voltage discharge system was used, incorporating the electrode shown in figure 2.7 (Thermo Environmental Instruments, Incorporated, Franklin, MA).

Several of these electrodes were used in parallel to increase the O_3 production rate. The electrode consists of a glass tube, covered with silver paint, and a central electrode. During operation, oxygen flows through the annular space between these two conductors, and a high voltage (approximately 7000 VAC) is applied, generating a corona which produces ozone. The electrical connections are made via brass clips at each end of the electrode. The silver paint does not extend past a point about 1 inch from the opposite electrode clip, in order to prevent coronas from the silver paint to that clip. In addition, the entire surface of the tube between brass clips is covered with a corona-inhibiting paint.

In initial tests, ozone was generated using an ozonator designed for water purification. This component was operated at a pressure slightly above atmospheric, and had tygon tubing connected to its upstream end. After approximately one month of use, a fire destroyed the ozonator. The cause of the fire is uncertain, but it appeared to originate at the tygon tubing connection. Arcing from the ozonator

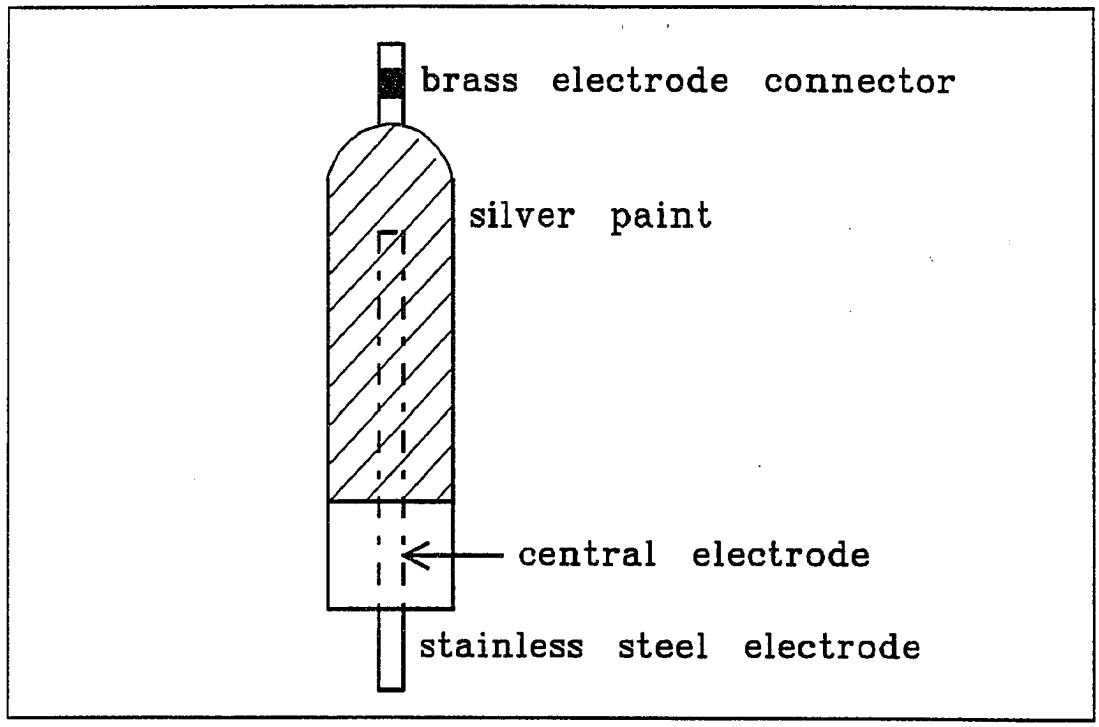

Figure 2.7 Ozone-generating electrode used in this work. The entire region between copper connectors was covered with corona-inhibiting paint.

electrode may also have been a cause, although excessive arcing was not observed prior to the fire. The water-purification ozonator was not operated long enough to determine whether it could have been operated safely. However, tubing connections to the ozonator were difficult to make and required tygon tubing, rather than teflon.

A more reliable O_3 generator was developed using TECO electrodes and the TECO power supply. For the summer 1988 measurements, 2 electrodes were used. A third electrode was added after that campaign. In both cases, the standard TECO power supply was sufficient to operate all of the electrodes.

The ozonator was operated at approximately atmospheric pressure until after the spring 1989 measurements. Under atmospheric pressure, approximately 3% O_3 was produced by 3 electrodes in a total O_2 flow of 230 sccpm, or about 7 sccpm O_3. The O_3 production rate was not regularly measured, however. Instead, the sufficiency of O_3 production was determined prior to the 1988 and 1989 measurement

campaigns by ensuring that the ozone amount was sufficient to react >99% of the NO present during zeroing in the 500 ml prereactor. This was tested by adding a known amount of NO to the sample flow and monitoring the resulting increase in the zero signal. Prior to the 1990 measurement campaign, the ozonator flow rate was decreased to 115 sccpm, resulting in a pressure of ~500 torr in the ozone generating electrodes. Tests of the effect on sensitivity of ozonator flow and pressure indicated that sufficient O_3 was produced under these conditions. Although the amount of O_3 produced was not monitored, changes in the O_3 amount would have resulted only in changes in sensitivity, and possibly zero level. These were monitored throughout all three measurement campaigns and there was no evidence of significant O_3 concentration changes.

Construction of a safe ozone generator that could run unattended for long periods proved problematic. This difficulty arose from the high voltage present on the ozonator electrodes. External arcing and coronas are possible and, in fact, likely from old, damaged, or modified electrodes. These processes result in production of O_3 external to the ozonator electrodes and can severely damage the ozonator over time. Therefore, great care must be taken in developing a safe ozonator. As a result of observations of corona discharge from ozonator electrodes to a grounded metal wall up to 5 cm away, an ozonator was constructed in a plastic box, with all walls at least 5 cm away from the electrodes. The three electrodes that were used were separated by approximately 10 cm and were connected in parallel using high-voltage automotive spark plug cable. A large amount of corona-inhibiting paint ("corona dope") was necessary to prevent arcing from the silver paint to the opposite electrode, and corona dope was also applied to the electrode clips, which otherwise glowed with a corona. The entire box was made of transparent plexiglass to ensure that coronas could be observed if present. Despite all precautions, a small amount of external corona was nearly always present. However, the amount remaining was observable only in an absolutely dark room, and resulted in negligible external ozone

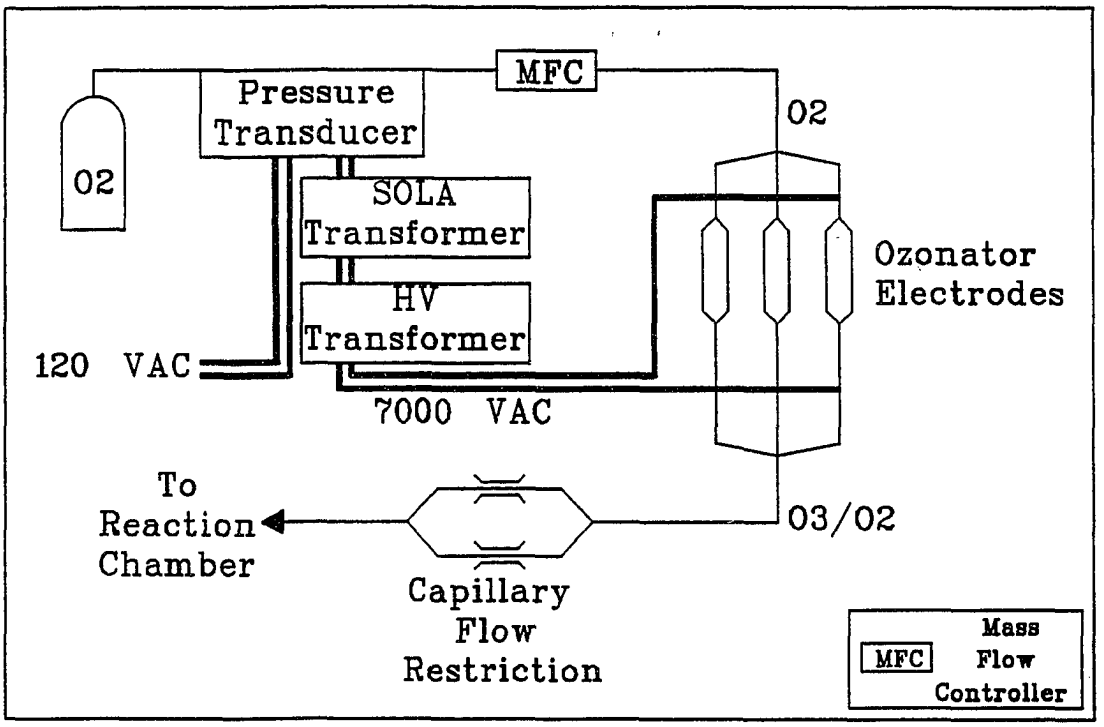

Figure 2.8 Schematic diagram of the ozonator designed for these measurements.

production. It should be noted that the ozonator used in commercial TECO NO detectors frequently displays a significant corona between the silver paint and the opposite electrode. The external ozone that results is immediately diluted by a cooling fan. However, it is likely that this corona significantly reduces the useful lifetime of the ozonator electrodes in the commercial ozonator.

Connections to the glass electrodes were made directly with teflon compression fittings to eliminate possible off-gassing from plastic or rubber tubing. The glass tube ends of the TECO ozonator electrodes are 1/4 inch o.d. and can be connected directly to 1/4 inch teflon compression fittings. As an additional safety precaution, a pressure transducer was installed on the oxygen tank. The transducer shut off power to the ozonator in the event that the oxygen tank ran empty. A schematic diagram of the entire ozonator system is shown in Figure 2.8.

2.2.4.2 Ozone Scrubbing

The high ozone concentration in the reaction chamber exhaust would quickly case damage if the ozone were allowed to enter the pump. During the first measurement campaign (summer 1988), activated carbon was used to scrub the reaction chamber exhaust. Granulated carbon sold for use in aquariums was used in a 160 ml acrylic scrubber. The carbon quantitatively captured O_3 when fresh. However, after operation for several weeks ozone breakthrough occurred, resulting in degradation of the pump oil. In addition, a large pressure drop (~50 torr) across the scrubber prevented operation of the reaction chamber at the desired low pressure. Furthermore, the activated carbon became hot and could catch fire when exposed to a high concentration of ozone in oxygen.

In order to avoid the problems encountered with activated carbon, a Hopcalite catalyst (a manganese dioxide-copper oxide mixture; Mine Safety Appliances Co., Pittsburgh, PA) was used after the first measurement campaign. Hopcalite quantitatively removed O_3, and did not lose its catalytic activity over a period of 1 year. However, the Hopcalite was initially used in the same acrylic scrubber, and still caused a large pressure drop. Therefore, an improved container for the Hopcalite was obtained after the spring 1989 campaign (Edwards High Vacuum Inc. inlet chemical trap ITC20, Grand Island, NY). The new container had a very low pressure drop and resulted in lower reaction chamber pressures during the 1989 and 1990 campaigns.

Hopcalite also catalyzed the oxidation of NO in air, with >99.9% removal of NO. However, very fine Hopcalite dust was always present and was difficult to filter. In several instances, Hopcalite dust from an inlet scrubber contaminated the system, requiring a complete cleaning. (Hopcalite can be removed with a solution of dilute sulfuric acid and oxalic acid. However, this solution will also slowly degrade stainless steel.) I recommend that Hopcalite not be used except downstream of the reaction chamber, and then only if a mechanism to prevent flow from the pump back to the

reaction chamber in the event of a power outage is included (such a reversal of flow could carry Hopcalite upstream into the reaction chamber). In the system used here, the pump was equipped with a device designed to prevent oil flow out of the pump, which effectively prevented back-flow of air during power outages. In addition, a solenoid valve was used to repressurize the reaction chamber with ambient air in the event of a power outage.

2.2.5 Zeroing System and Artifacts

Accurate measurement of the zero signal is a critical requirement of pptv-level NO measurements, and errors in this measurement can result in instrumental artifacts, as discussed in section 2.1.1.3. In the next section, the development of the zeroing systems used during the three measurement campaigns is discussed, followed by a presentation of the NO artifact values measured during each campaign.

As discussed in section 2.1.1.1, the instrument zero signal is due to PMT dark pulses and O_3 chemiluminescent reactions with compounds other than NO. In this instrument, the PMT dark count generally accounted for more than half of the total zero signal and varied with room temperature. This is the result of a combination of factors, including use of a non-thermostatted PMT cooler and the lack of thermal isolation between the PMT and the reaction chamber. The large variability in the dark count that can result from ambient temperature variations is shown in Figure 2.9, which was obtained by running the instrument in the laboratory with no ozone or sample flow while monitoring the dark count rate. During this period, the room temperature of the laboratory varied between approximately 15 and 21°C, peaking in the mid-afternoon, with corresponding PMT temperatures of $\sim$−6 to −2°C. A diurnal cycle in dark count resulting from the daily room temperature variation is apparent. In addition, an increase in room temperature to >25°C during day 1 of the figure was accompanied by a large increase in dark count, presumably a result of an increase in PMT temperature above −2°C.

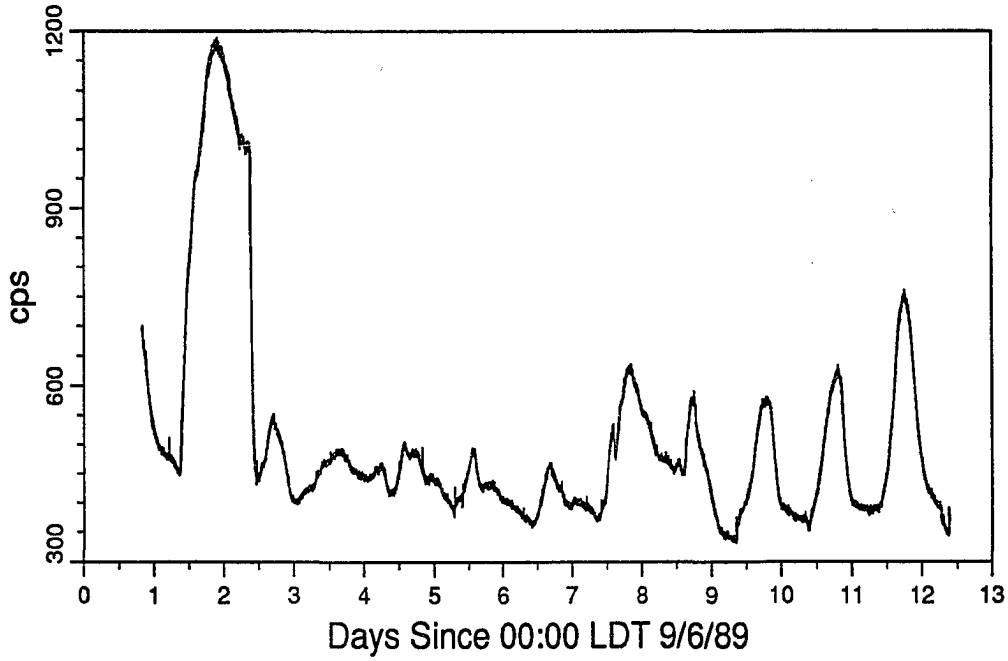

Figure 2.9 Variation of photomultiplier tube (PMT) dark count rate with time. Variation of the dark count rate is due to PMT temperature changes in response to room temperature variation. Room temperature was ~15–21°C during most of this period, except for an excursion to >25°C during day 1.

Dark counts of 300–600 cps were common during measurements at Barrow. In contrast, the contribution to the total zero signal from ozone chemiluminescent reactions was only about 100 cps after more than 1 day warmup. By comparison, other instruments with colder PMTs have reported dark count rates of ~100 cps [*Bollinger,* 1982; *Drummond et al.,* 1985; *Parrish et al.,* 1990]. Improvement in the PMT cooler/reaction chamber system of the instrument used in this work to reach a dark count rate of ~100 cps would result in a reduction in the detection limit of ~40% due to a reduction in zero count rate, provided the instrument sensitivity remained constant.

2.2.5.1 Zeroing System Development

As discussed above, a zeroing chamber is used to correct for the PMT dark count rate and non-NO_2^* photoemissions. The zeroing system used initially is shown in

Figure 2.10. In this system, the stainless steel prereactor was located in the ozone line, and sample flow was diverted to the ozone line during zeroing. The ozone concentration was kept high enough to ensure that >99.9% of the NO reacted within the 500 ml prereactor. The prereactor was located in the ozone line so that ozone would enter the reaction chamber from the same location during both measure and zero modes, to eliminate a potential cause of NO artifacts [*Bollinger et al.,* 1984]. Nevertheless, significant artifacts were observed, both positive and negative. This system was used at Barrow during the 1988 campaign, and measured artifacts during that period (presented in section 2.2.5.2 below) ranged from -11 to 68 pptv. The variable artifacts may have been partially due to transient effects resulting from changes in relative humidity over the stainless steel prereactor surface, as observed by *Bollinger* [1982].

To test whether this artifact was due to O_3 flow changes in the reaction chamber, the sample and O_3 flows were mixed upstream of the reaction chamber, so that the flow entering the chamber was unchanged between zero and measure modes. This setup, which is similar to that used by *Drummond et al.* [1985], is shown in Figure 2.11. Sensitivity was reduced by ~70% in this setup, due to partial reaction of O_3 and NO prior to the reaction chamber. However, negative NO concentrations were still observed during nighttime measurements, indicating that a negative artifact was still present. Therefore, the negative artifact problem was not primarily due to changes of ozone flow in the reaction chamber between the zero and measure modes.

Humidification of the O_2/O_3 flow has been reported to improve zeroing and artifact problems [*Drummond et al.,* 1985]. In an attempt to eliminate the artifact problem, a new zeroing system was developed using a humidified O_3 source. The total ozone flow was split into two parts as shown in Figure 2.12. One-third of the total flow was used for zeroing and was mixed with the sample flow immediately upstream of the reaction chamber. The remaining ozone was added directly to the

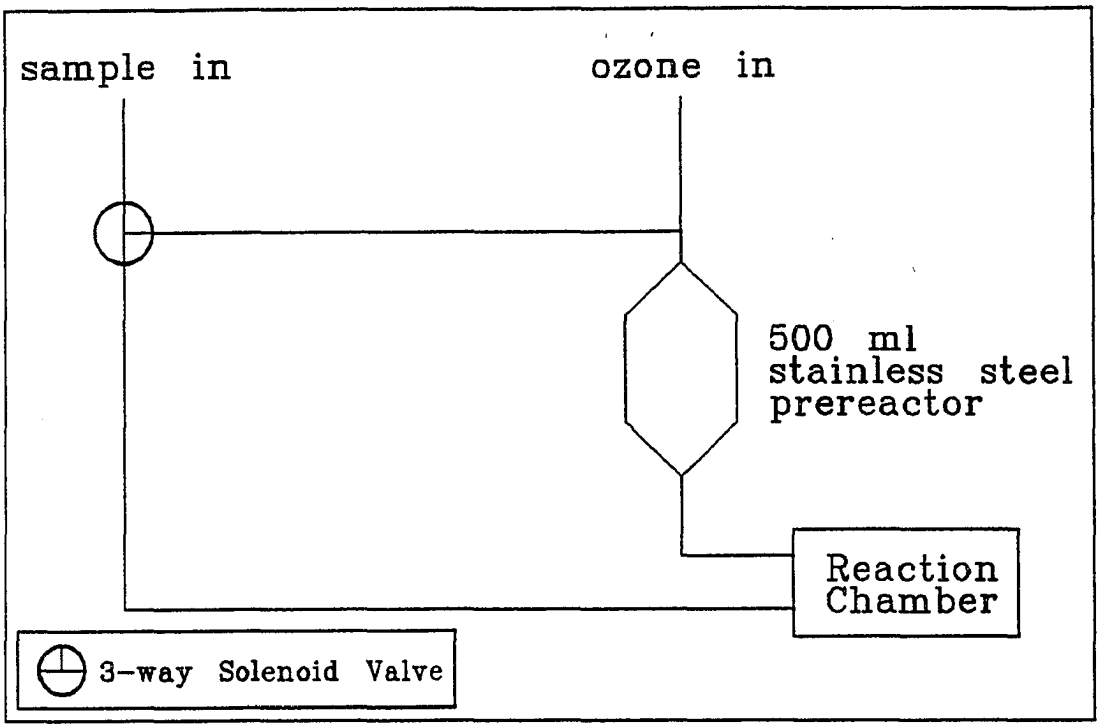

Figure 2.10 Initial zeroing system, used during the 1988 Barrow measurements.

reaction chamber. The effect on sensitivity (a reduction of ~20%) was less than in the previous system (Figure 2.11), since less ozone was added to the sample flow prior to the reaction chamber, and it was added at a point closer to the chamber. However, the use of less ozone for zeroing required a larger, one liter zeroing volume (stainless steel) to ensure complete reaction. Water addition was accomplished using a reservoir of double-deionized water, which was connected to the O_3 line with a short section of 1/4 inch o. d. stainless steel tubing. A water diffusion rate of about 15 ml/day was observed during operation at room temperature. However, heating tape was often used to increase the temperature of the reservoir to approximately 40°C, in order to increase the water addition rate.

This zeroing system did not remove the problem of significant and variable artifacts. Artifacts measured with this system at Barrow during the spring 1989 campaign ranged from -103 to 11 ppt. It appears that variability in the amount of

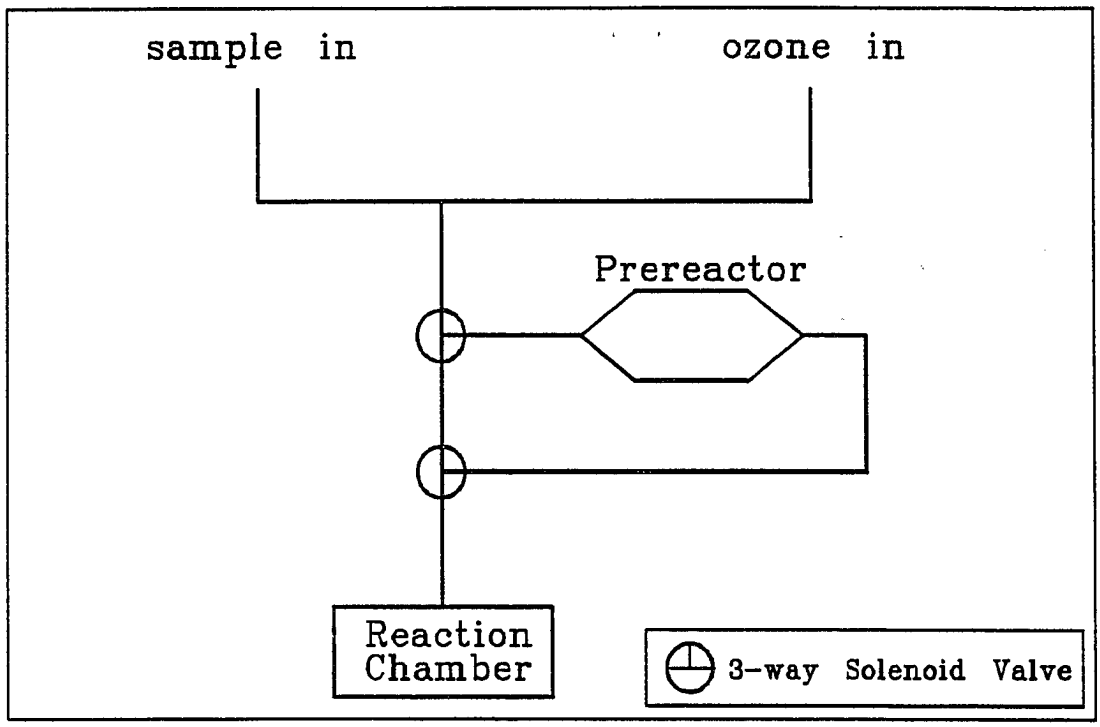

Figure 2.11 Zeroing system to test the effect on artifact of ozone flow changes in the reaction chamber.

water delivered by this system was at least partially responsible for these large and variable artifacts (see discussion of observed artifacts during the 1989 measurements in section 2.2.5.2 below).

To determine whether the source of these artifact problems was use of a stainless steel prereactor, a test was conducted in which the 1988 zeroing system (Figure 2.10) was used, but with a 500 ml pyrex zeroing volume. A large negative artifact was still observed (~ -500 pptv) in dried, scrubbed air. Since two different stainless steel prereactors and a pyrex prereactor all resulted in large negative artifacts at times, the prereactor material was not the cause of this problem. Additional tests to determine the cause of the problem were not conducted, however, because a new zeroing system was developed. At the same time, sections of tygon tubing that had been present in the oxygen line upstream of the ozonator were removed and replaced with teflon, in case hydrocarbon emissions from the tygon tubing had been affecting

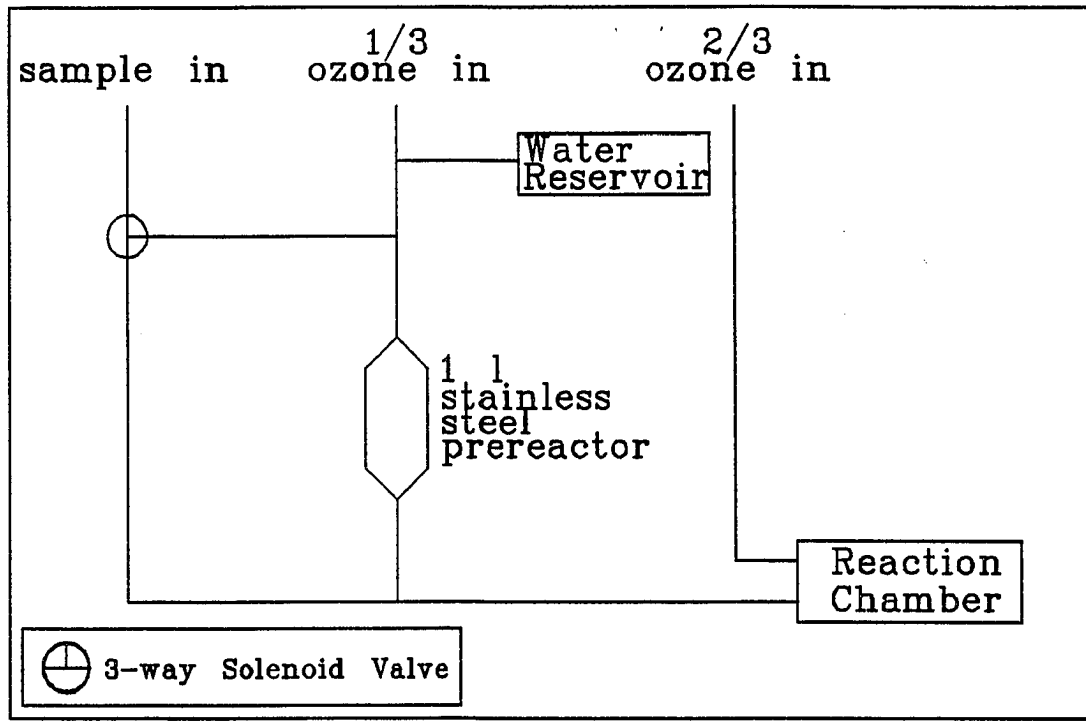

Figure 2.12 Zeroing system used during the 1989 Barrow measurements.

zeroing.

The new zeroing system was developed following the 1989 measurement campaign and operated at ambient pressure, with a separate small ozone source. In effect, this zeroing system allowed the NO-detector portion of the instrument to operate separately from the zeroing system, which was located in the sample line upstream of the mass flow controller. The ambient pressure zeroing system is similar in concept to that described by *Kaplan et al.* [1988], with several modifications (many suggested by P. Bakwin [private communication, 1989]). A schematic diagram of the system is shown in Figure 2.13. Zeroing was accomplished by passing the sample through a quartz cell that was illuminated by a mercury ultraviolet lamp (PenRay 11 SC-1, UVP Inc., San Gabriel, CA), producing O_3 from O_2 present in the sample air. The $NO+O_3$ reaction was then allowed to proceed to completion in a pyrex reaction volume.

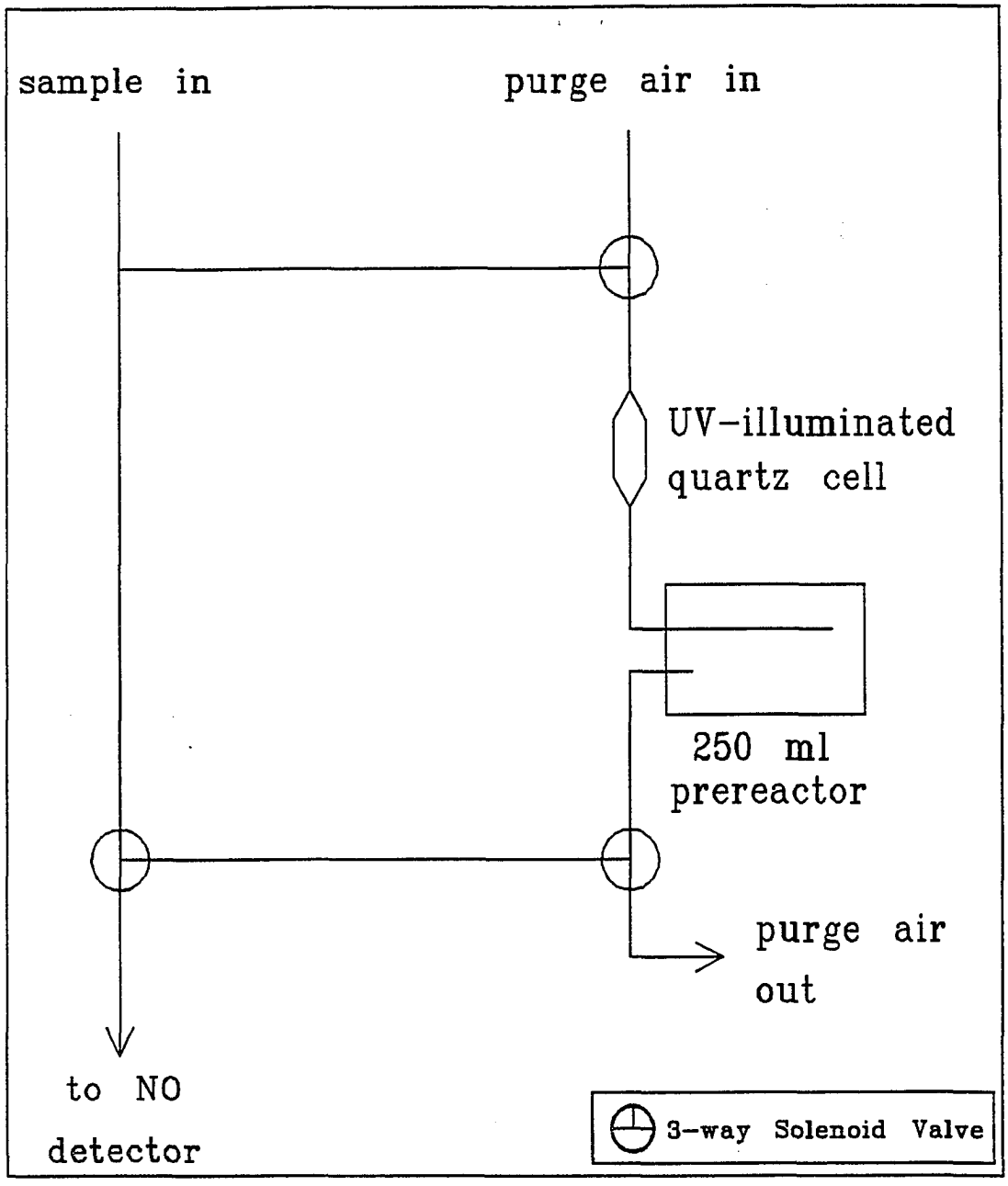

Figure 2.13 Ambient-pressure zeroing system, used during 1990 measurements.

The PenRay lamp emitted more ultraviolet light than was necessary to produce sufficient ozone for zeroing, so it was tightly wrapped with aluminum foil, leaving only 2–3 cm exposed. The lamp was then attached alongside the quartz tube, which was of an equal length, with wire, and both were wrapped tightly with aluminum foil. This wrapping was important to reduce formation of ozone in the surrounding air as well as to reduce the danger of stray ultraviolet light. Control of the amount of ozone produced in the quartz tube was possible by adjusting the fraction of the mercury lamp exposed. As the lamp aged, it was necessary to expose a larger amount of the lamp.

The residence time in the 250 ml zeroing reaction chamber was 15 s at the 1 slpm sample flow. The shape of the chamber (shown in Figure 2.13) was chosen based on tests which indicated that the chosen shape resulted in more efficient mixing than did a cylindrical chamber with inlet and outlet tubes on opposite ends. The fraction of initial NO remaining after passage through the zeroing chamber,

$$\frac{C}{C_0} = \exp(-k_{NO+O_3}[O_3]_z t_z), \tag{2.14}$$

was often slightly lower than the value expected, based on the measured O_3 concentration, the homogeneous NO+O_3 rate constant [*DeMore et al.*, 1987] and a 15 s residence time, and indicated an actual residence time or rate constant ~5–20% above the expected value. This result is attributed to a reaction rate higher than the homogeneous value, as has been observed previously (P. Bakwin, private communication, 1989).

When in operation, the quartz tube and mercury lamp become hot. In order to avoid temperature fluctuations that could lead to off-gassing of compounds from the quartz tube, the lamp was always left on. During measurement (non-zeroing) periods, a flow of purge air was maintained through the quartz tube and reaction volume.

The zeroing system, as used during the 1990 measurements, produced about

0.5 ppmv O_3 in the 1 slpm sample flow, and resulted in approximately 94–98% removal of ambient NO. The O_3 concentration was kept at a level below that sufficient for complete reaction to reduce the potential for significant reductions in the concentration of possible interfering compounds that could lead to artifacts [*Drummond et al.*, 1985]. In order to allow correction of the data for incomplete zeroing, the fraction zeroed was measured during each calibration cycle. It varied with time very slowly, and generally changed by less than 0.1% between measurements.

The revised zeroing system eliminated the large artifacts observed with the earlier systems, and resulted in artifacts between -2 and +2 pptv (presented in the next section).

In the development of the improved zeroing system, several experiments were performed, in addition to those described above. The results of some of these indicate that:

- Ozone is neither adsorbed nor desorbed from quartz, pyrex, or teflon surfaces.
- Viton o-rings experienced no discernable degradation, even at the high ozone concentrations they were exposed to in the NO-detector reaction chamber. Similarly, no degradation in performance of the sample mass flow controller, which has viton o-rings and stainless steel parts, was observed as a result of the ppmv-level ozone flow from the zeroing system ozone flow.
- Teflon parts, if in direct contact with the hot mercury lamp, will warp.

2.2.5.2 NO Artifacts

In this section, the artifacts observed during each measurement period at Barrow are presented and the artifact corrections to the data are discussed. As a result of the improvements in instrument design discussed in the previous section, artifact levels varied greatly between the three measurement campaigns.

Artifact levels were measured by averaging the apparent NO concentrations observed during night or when the sun was very low on the horizon (solar zenith angle $\geq 85°$). In the absence of recent NO_x emissions, NO will not be present at night due to reaction with ambient ozone, so the concentration measured (the apparent NO concentration) is equal to the artifact. Since the NO_x source nearest the CMDL site is approximately 1 km away, and most sources are much farther, the nighttime NO concentration at the site is expected to be essentially zero. Additional artifact measurements were made by sampling activated carbon-scrubbed ultra-pure synthetic air.

1988 measurements. Artifacts during the summer 1988 campaign at Barrow (based on nighttime NO measurements) are shown in Figure 2.14. The artifact values shown in Figure 2.14 range from -11 to +68 pptv, and exhibit large variability. The mean artifact was 18 pptv, and the standard deviation was 21 pptv. These values were obtained using nighttime NO measurements. To ensure that nearby local sources did not affect the artifact estimate, the NO measurements were also screened by variability; only values with an observed standard deviation less than twice that predicted by counting statistics were included in the nighttime averages. Such low standard deviations indicate that nearby NO_x sources did not affect the measurements used for artifact estimation.

All NO measurements during this period were corrected by subtracting the mean level of 18 pptv. Uncertainty in the resulting concentration estimates is dominated by the artifact uncertainty, and is estimated to be ± 50 pptv. This uncertainty level includes all of the nighttime NO average concentrations calculated using the standard deviation screening criterion.

The artifacts shown in Figure 2.14 tended to be larger during periods of clean-sector flow (marked with x in Figure 2.14) than during flow from the direction of local Barrow sources (+). The average during predominantly clean-sector periods

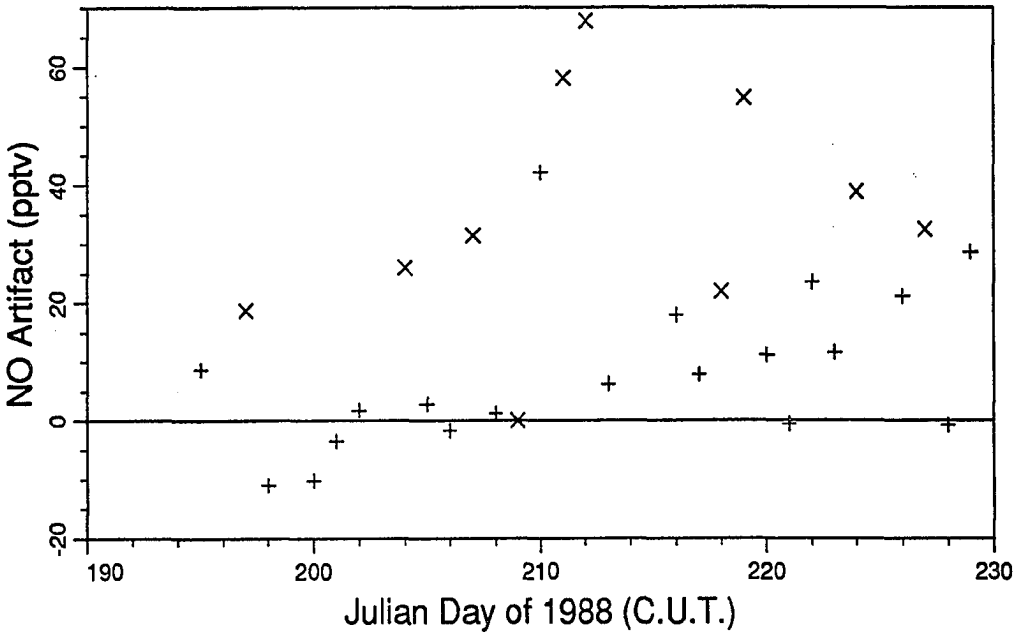

Figure 2.14 NO Artifact Measurements During the Summer 1988 Campaign. The artifact values are averages of the apparent nighttime NO concentration, after screening by variability as described in the text. Measurements during periods of clean sector flow are indicated by x's; + symbols indicate measurements obtained during flow from the direction of local Barrow sources.

was 35 pptv, while that during other nights was 8 pptv (significantly different at the 99% level).

1989 Measurements. Artifacts during the spring 1989 measurement period are shown in Figure 2.15 and and ranged from -103 to +11 pptv. The overall mean and standard deviation of the nighttime artifact measurements are -43 and 25 pptv, respectively. These artifacts were measured in two ways: using synthetic high-purity air (in this study, activated carbon-scrubbed Ultra-zero Ambient Monitory Zero Air [Scott, Fremont, California] was used), and using ambient air at night during periods when recent NO_x emissions were absent. The nighttime artifact measurements are averages of the NO concentrations observed during each night, after screening by standard deviation as described for the 1988 campaign. Prior to averaging for each

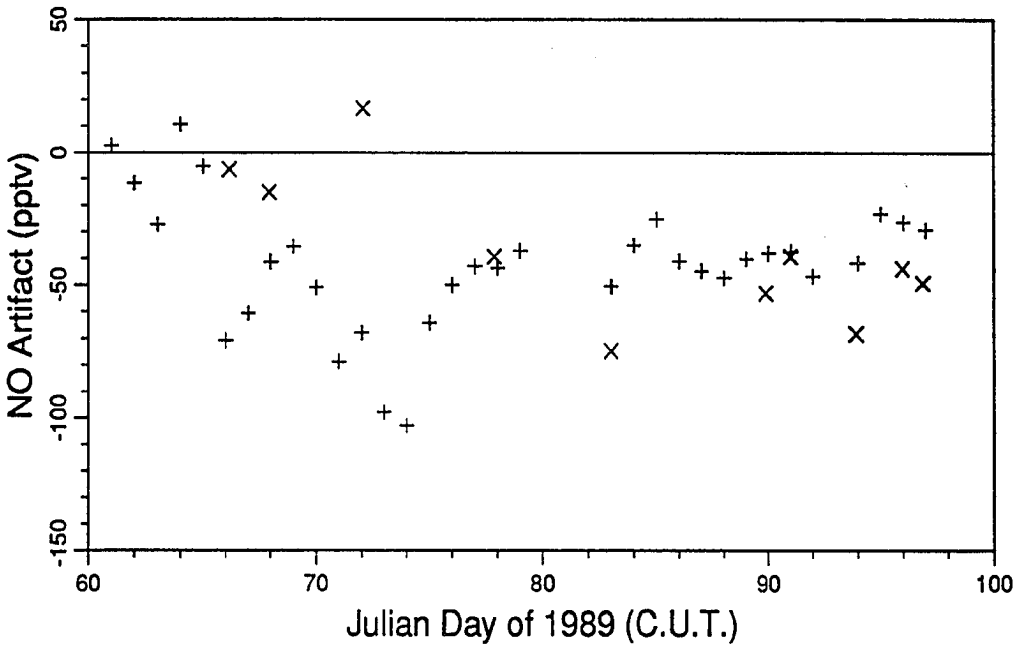

Figure 2.15 NO artifact measurements during the spring 1989 campaign. Nighttime NO measurements are indicated by + symbols; x's indicate synthetic air tests.

night, 22 outliers clearly affected by nearby sources, but which were not screened out by the standard deviation criterion, were removed. These outliers were each several times higher than the surrounding measurements.

The artifacts determined at night (marked with + in Figure 2.15) did not always coincide with those measured using high-purity synthetic air (x in the figure). However, since trace compounds in ambient air may affect the artifact, it was felt that the nighttime measurements provided a more realistic test of the artifact level. Therefore, only the nighttime NO measurements were used to estimate the artifact. There was no evidence during this period of higher or lower artifacts during clean-sector flow. However, this may be due to the large variations present in the artifacts.

Some of the variability in measured artifacts was apparently due to the water addition system. The water addition system apparently occasionally injected droplets

of water into the ozone flow when it was bumped. In addition, the temperature of the water reservoir was adjusted periodically during this period. Thus, it is likely that some of the variability in measured artifact was due to real artifact changes, related to the amount of water in the ozone line. The largest daily change in measured artifact occurred on Julian day 66, when the artifact changed by 66 ppt. This change coincided with a change in the water addition system (section 2.2.5.1). With the exception of that day, day-to-day artifact changes were ≤ 40 pptv.

The NO and NO_y measurements obtained during the 1989 campaign were corrected for artifacts by subtracting a value linearly interpolated between adjacent artifact measurements with the following exceptions. Data obtained after the water addition change on day 66 but before the next artifact measurement were corrected using the first artifact measurement after the change. In addition, during periods when missing data resulted in one or more nights without artifact measurements, the nearest artifact measurement was used without interpolation. The total uncertainty in the artifact correction during this period is conservatively estimated to be 75 pptv, a value larger than the total range of measured artifacts either before or after the water addition change on day 66.

1990 Measurements. Modifications to the zeroing system prior to the 1990 campaign (described in section 2.2.5.1) resulted in substantially improved NO artifact levels. The distributions of all 1990 artifact measurements, based on both nighttime NO observations and ultra-zero air tests, are shown in Figure 2.16. For the purpose of artifact correction, the entire 1990 data set was divided into 3 smaller data sets. Data sets 1 and 2 include all measurements through August (data set 1: March 3–30 and June 3–August 31; data set 2: April 18–May 29). The remaining data (after August) were analyzed later, and are included in data set 3 (September 1–December 31). Data sets 1 and 2 were separated because of a noise problem (described in Section 2.2.8.4) which resulted in the loss of some data between data sets 1 and 2. All

valid data during the period affected by the noise problem are included in data set 2, with the remainder of the valid data through August in data set 1. This separation was necessary because the noise problem occasionally caused large artifacts due to erroneously high photon count rates. Periods clearly affected by noise were omitted from the analysis, but there is an indication of a residual effect on artifacts on the remaining data set.

NO artifact values were estimated for periods of up to 8 hours during each night, using all valid NO observations obtained when the solar zenith angle was $\geq 85°$. Thus, up to three artifact values were obtained each night at Barrow. (Three artifact values were obtained during each 24 hr winter "night.") The valid NO measurements used in the averages include those in which the observed variability in 1s photon count totals during the 60 s averaging period (S_{obs}) was less than 1.5 times that expected from counting statistics (S_{cs}). In addition, the standard deviation of all observed NO measurements within each average was required to be $< 1.1S_{cs}/\sqrt{40}$ ($S_{cs}/\sqrt{40}$ is the standard deviation expected due to counting statistics for the 40 s average). Otherwise, the data from that average were not considered a valid measure of the artifact. Statistics of the nighttime artifact measurements for each data set are shown in Table 2.3.

Table 2.3 Statistics of Artifact Measurements During the 1990 Measurement Campaign.

Data Set	Type	Period Included (Julian Day of 1990)	Mean (pptv)	S.D. (pptv)	Range (pptv)	N
1	Nighttime NO	61–247[a]	0.5	1.3	-3.6–3.4	91
2	Nighttime NO	108–149	2.0	1.3	0.5–5.2	15
3	Nighttime NO	248–365	-0.3	1.4	-5.3–4.1	152
1–3	Nighttime NO	61–365	0.1	1.5	-5.3–5.2	258
1–3	Ultra-Zero Air	61–365	1.6	2.5	-2.3–6.0	9

[a]Excluding data set 2.

All nighttime artifact values in data sets 1–3 are displayed in Figures 2.17–2.19. Ultra-zero tests are also shown in the figures (indicated by x symbols). These results indicate that the ultra-zero tests were consistent with the nighttime artifact

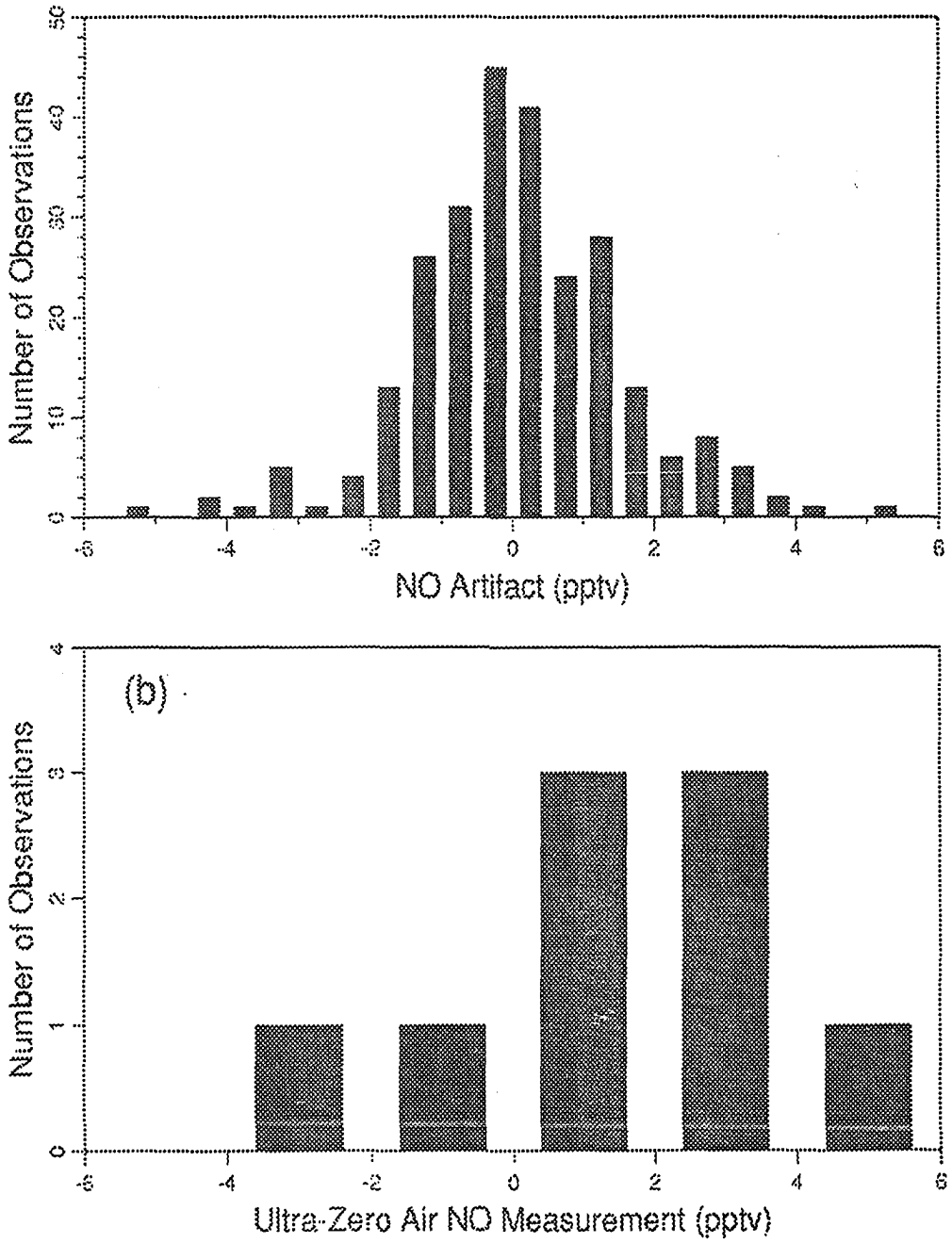

Figure 2.16 Frequency distribution of artifact measurements during the 1990 measurement period. (a) Nighttime NO measurements. (b) Ultra-zero cylinder air tests.

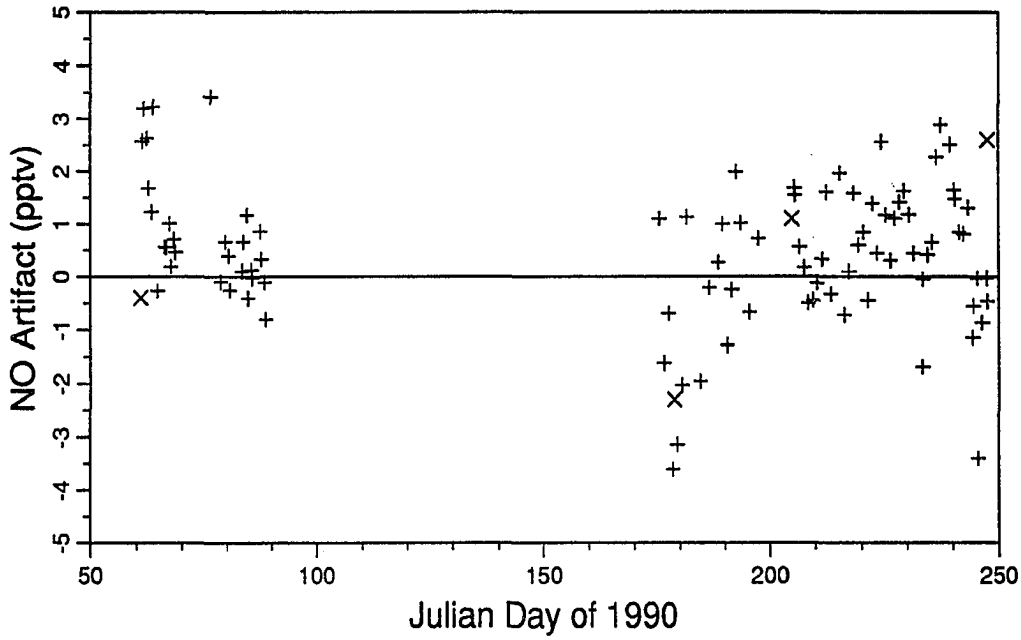

Figure 2.17 Time series plot of artifact measurements during data set 1, 1990. Measurements based on nighttime NO observations are plotted with + symbols; ultra-zero artifact tests are displayed with x's. Artifact measurements from day 108 to day 149 are shown in Figure 2.18.

measurements. In addition, it appears that, on some occasions, there was drift upward or downward in the artifact, in addition to random variations. As a result, all 1990 NO measurements were corrected for artifacts using linear interpolation between adjacent artifact values. If either adjacent artifact value was more than 48 hours away, then only the nearest artifact value was used for the artifact correction. The uncertainty of the 1990 artifact correction is estimated as twice the standard deviation of all nighttime artifact measurements in 1990, or 3.0 pptv.

2.2.6 Calibration

The sensitivity of the instrument (S_{NO}) was regularly measured using a reference standard of NO in N_2. Regular calibration was used to keep track of changes in sensitivity, which were $\leq$10% over 24 hr periods. Calibrations were conducted ap-

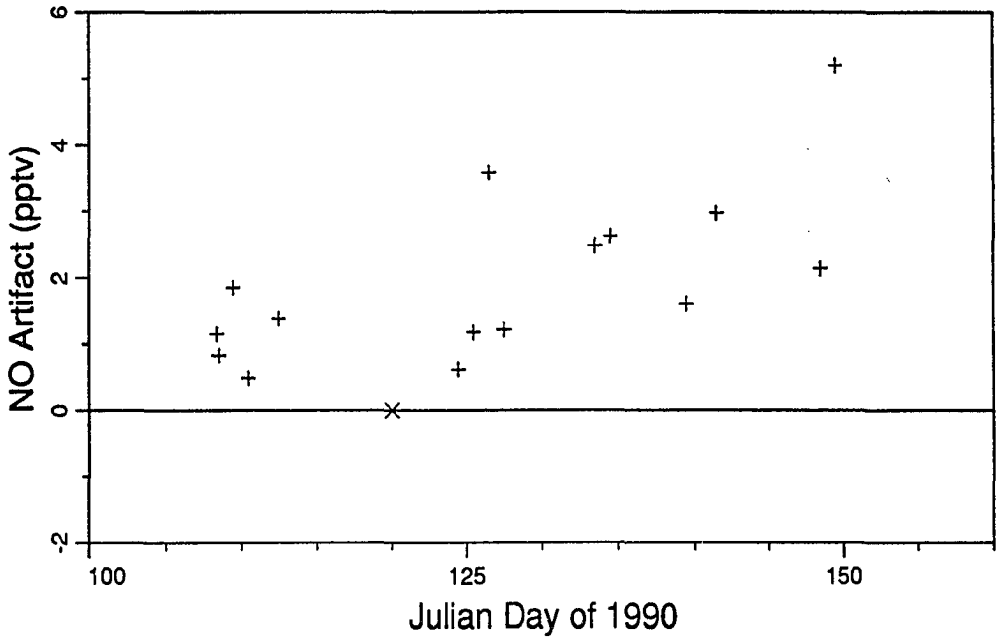

Figure 2.18 Time series plot of artifact measurements during data set 2, 1990. Measurements based on nighttime NO observations are plotted with + symbols; ultra-zero artifact tests are displayed with x's.

proximately once per hour, and S_{NO} changed by <2% between most adjacent calibrations. The efficiency of the NO_y converter was also regularly monitored, using NO_2 generated by gas phase titration of the reference NO standard. Since measurements of these calibration parameters depend critically on the accuracy of the sample and calibration mass flow controllers (MFCs), the MFCs were also calibrated regularly, using bubble flowmeters.

The following sections describe the procedures used for measurement of the NO sensitivity and the conversion efficiency and for calibration of the mass flow controllers.

2.2.6.1 NO Sensitivity Calibration

Instrument sensitivity was measured using cylinders of NO in N_2 (approximately 5 ppmv in concentration, with a specified uncertainty of 2%) (Scott Specialty Gases,

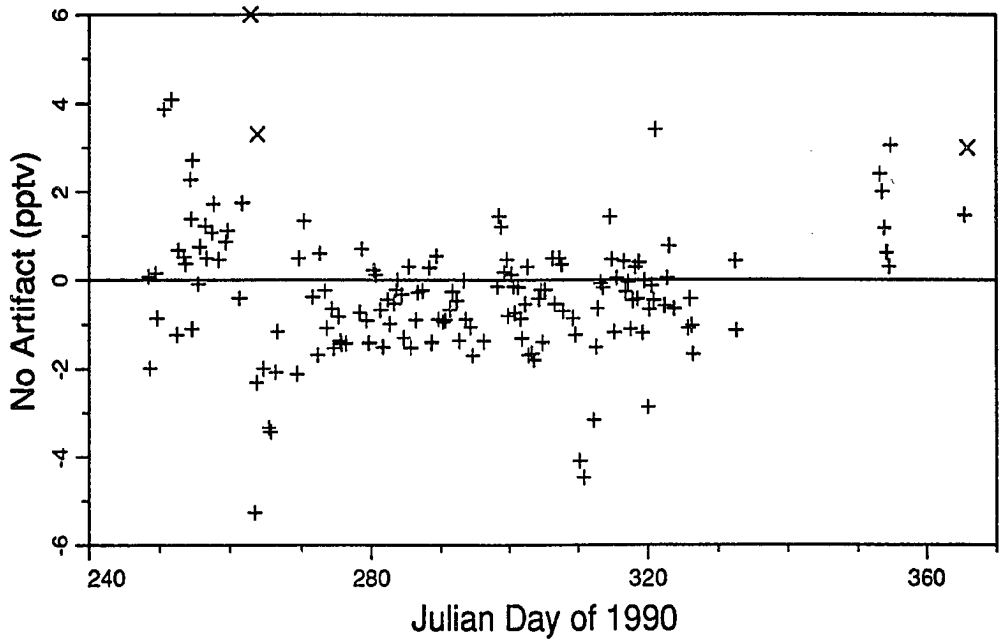

Figure 2.19 Time series plot of artifact measurements during data set 3, 1990. Measurements based on nighttime NO observations are plotted with + symbols; ultra-zero artifact tests are displayed with x's.

Fremont, California). The accuracy of the specified concentration was tested by comparing two different Scott cylinders and one National Institute of Standards and Technology (NIST) standard reference material (NIST, U.S. Dept. of Commerce, Gaithersburg, MD). In all cases, the stated concentrations of the different cylinders agreed to within the specified uncertainty of 2%. These comparisons were carried out by comparing the sensitivity of the instrument to calibration standards from the separate tanks. This was done by changing the tank connected to the calibration system and measuring the sensitivity with each cylinder for several hours. (The tests were repeated to take into account possible drift in the instrument sensitivity.)

The linearity of the NO response was tested over a range of 2.4–25 ppb, and no deviations were observed (within an uncertainty of 1%). The result of this test is shown in Figure 2.20. This instrument is expected to be linear over a much larger range, however, based on tests of similar instruments by other investigators (see

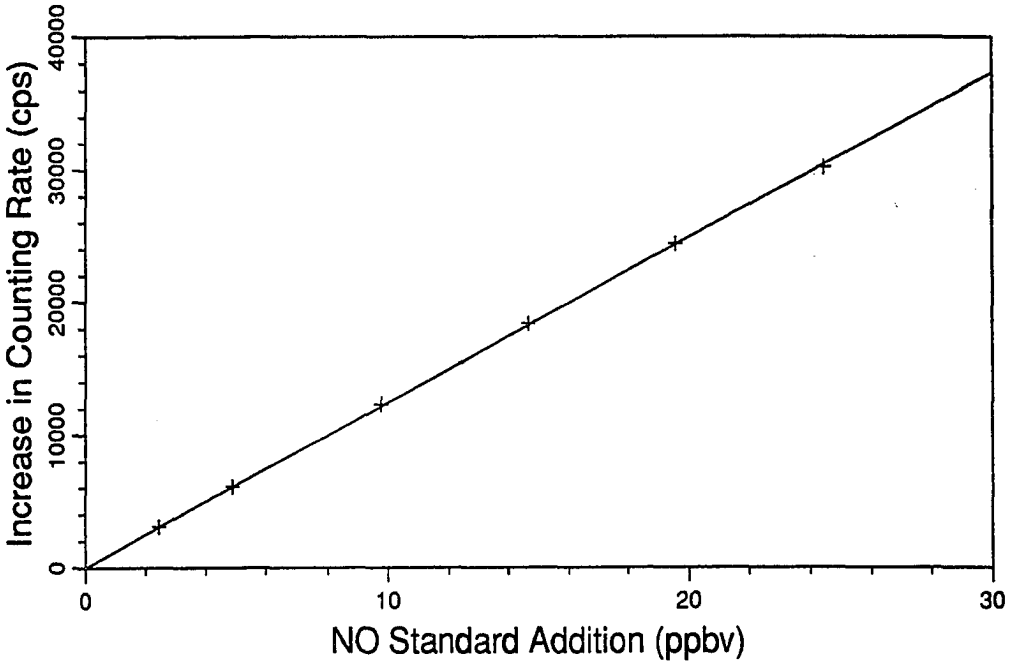

Figure 2.20 Linearity of the NO detector response.

section 2.1.1.3 above).

Calibration gas was added to the inlet line in two different ways, as shown in Figure 2.21. In the design used in 1988 (Figure 2.21a) calibration gas was simply added to the sample flow at a teflon tee. The tubing between the calibration solenoid and the tee was kept as short as possible. Nevertheless, after calibration, the pure calibration gas in that tubing section slowly diffused into the main sample flow, resulting in an long and slowly-decaying transient signal lasting for several minutes. In order to reduce this problem, the two-solenoid system shown in Figure 2.21b was developed and used during the 1989 and 1990 measurement campaigns. In this system, the sample flow is redirected during calibration by solenoid 1 (see Figure 2.21a) into the calibration gas flow, through solenoid 2, and back into the main sample line. After the calibration mode, calibration gas can still diffuse into the sample line from the short tube to solenoid 2, but the NO calibration gas concentration in this line

has been diluted by the sample flow, and thus presents less of a problem than did the undiluted calibration gas present in the system of Figure 2.21a. In both calibration systems, the calibration flow was continued uninterrupted during non-calibration periods, in order to eliminate potential transient effects from flow changes. During these periods, the calibration gas was vented.

An attempt to further reduce the mode-changing transients was made by inserting 1/8 inch o.d. teflon tube sections into the 1/8 inch i.d. tube sections between the two tees and solenoid 2 in Figure 2.21b to reduce the volume in these tubes. However, it was found that as long as these tube sections were kept as short as possible such inserts did not significantly affect the transients.

Location of Calibration Standard Addition. During the 1988 and 1989 campaigns, the calibration gas was added to the sample flow immediately prior to the sample mass flow controller. This provided an accurate measurement of the true instrument sensitivity but did not account for NO or NO_y losses in the inlet tubing.

During the 1990 measurement campaign the calibration gas was added near the instrument inlet in order to ensure than any potential losses of NO within the inlet lines were included in the calibration measurement. In accordance with theoretical expectations, NO loss due to reaction with ambient ozone often resulted in a reduction in sensitivity measured at the NO inlet. The 1990 calibration measurements indicate NO inlet losses of ~5–10%. The expected reduction of the ambient NO concentration due to oxidation by ambient O_3 in the 5 m inlet line can be estimated using the inlet residence time (5.8 s at 1 slpm in the 1/8 inch i.d. tubing), using the equation

$$\frac{[NO]_{detector}}{[NO]_{ambient}} = \exp(-k_{NO+O_3}[O_3]_{ambient} \times 5.8s). \qquad (2.15)$$

This calculation (at an assumed average temperature of 10°C) yields a factor of 96% at an ambient O_3 concentration of 20 ppbv, or 92% at an O_3 concentration of 40 ppbv, in agreement with the observations. Loss of NO is not observed when

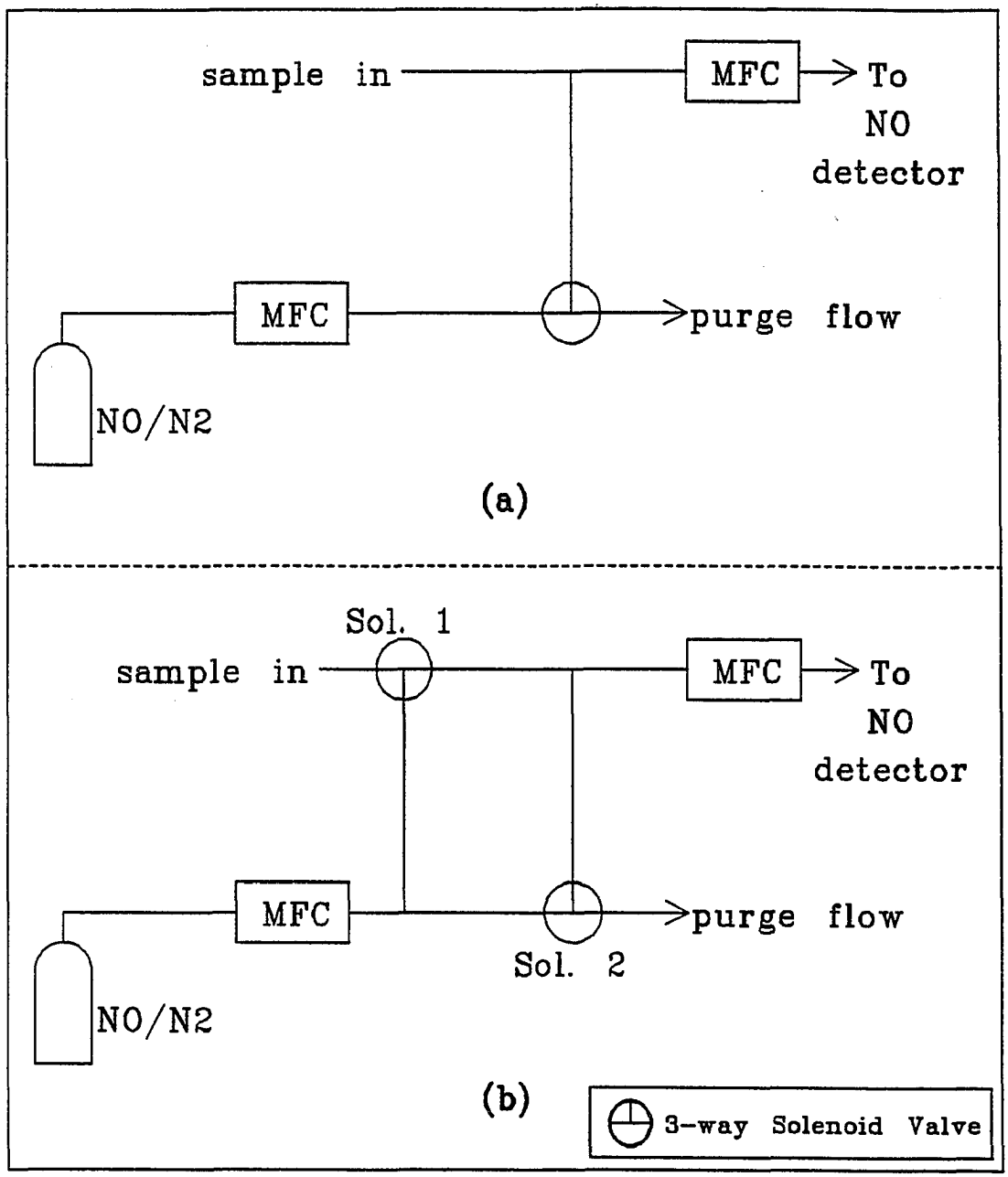

Figure 2.21 NO calibration systems: (a) Used during 1988 measurements. (b) Used during 1989 and 1990 measurements.

measuring NO_y, because the NO_y converter effectively removes ambient O_3 from the sample flow. Therefore, separate values of S_{NO} were used for analysis of NO and NO_y measurements made during 1990. Although the same S_{NO} value was used for both NO and NO_y measurements in the 1988 and 1989 campaigns, this introduced an error of <10%, for the NO measurements only. At the low NO levels observed during clean air flow at Barrow, this was a negligible contribution to the total uncertainty of NO measurements from those campaigns (see section 2.2.11).

2.2.6.2 Conversion Efficiency Calibration

Several methods for measuring the NO_y conversion efficiency were used. However, gas-phase titration of NO with O_3 to form NO_2 was found to give the most reliable and reproducible results.

Calibrations utilizing permeation sources of NO_2 and HNO_3 were used during 1988–1989. The permeation sources were temperature-controlled to ±1°C using a permeation oven (VICI Metronics, Santa Clara, California). Nitric acid permeation tests were conducted only a few times. They were difficult to perform reproducibly due to the high surface reactivity of HNO_3. NO_2 permeation tests were conducted more often, and were used to characterize the conversion efficiency during the 1989 measurements. In that case, the permeation tube was factory-calibrated gravimetrically to ±5%, and was used at a temperature of 30°C.

Gas-phase titration of NO with O_3 to produce NO_2 [*Stedman,* 1976] provided a more consistent source for NO_y conversion efficiency tests and produced an NO_2 standard directly referenced to the NO calibration standard. In this method, a small flow of ozone was added to the NO calibration gas, as shown in Figure 2.22, and the $NO+O_3$ reaction was allowed to proceed before the calibration flow was added to the sample.

When the lamp is turned on, O_3 is produced, and reacts with NO from the

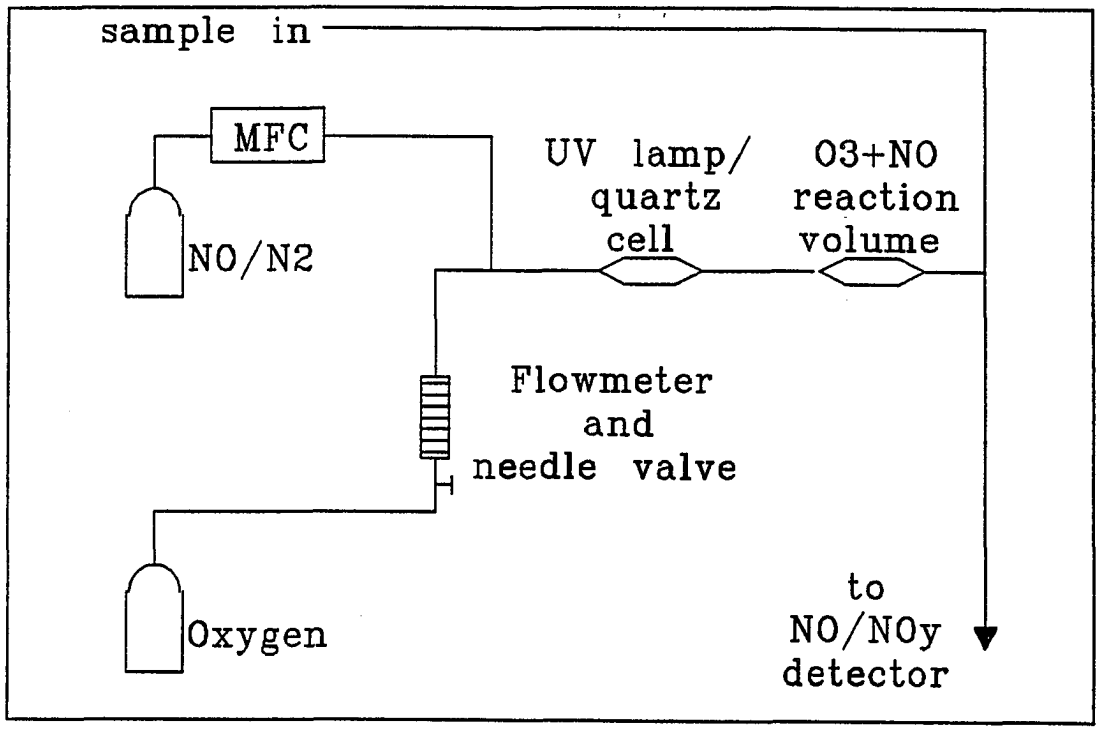

Figure 2.22 NO/O_3 titration system.

calibration gas. The amount of NO_2 produced is given by

$$[NO_2]_{produced} = [NO]_{ozone\ off} - [NO]_{ozone\ on}, \tag{2.16}$$

and the amount of NO_2 *not* converted back to NO by the NO_y converter is

$$[NO]_{not\ converted} = [NO_y]_{ozone\ off} - [NO_y]_{ozone\ on}. \tag{2.17}$$

Thus, the conversion efficiency η for NO_2 is given by

$$\eta = 1 - \frac{[NO_2]_{not\ converted}}{[NO_2]_{produced}} = 1 - \left(\frac{[NO_y]_{ozone\ off} - [NO_y]_{ozone\ on}}{[NO]_{ozone\ off} - [NO]_{ozone\ on}} \right). \tag{2.18}$$

Initial ozone titrations utilized an ozone calibrator (Columbia Scientific Industries Corp., Austin, TX) as the ozone source, and a reaction volume of ~30 ml. The large reaction volume, compared to the small NO and O_3 flows (10 sccpm each), resulted in long equilibration periods. Therefore, this method was used only in the laboratory to calibrate the NO_y converter used during 1988.

A new gas-phase titration system was developed prior to the 1990 measurements. In this system, the titration system forms an integral part of the automatic calibration system (see Figure 2.4). In consists of a quartz tube and ultraviolet lamp for ozone generation, similar to that used for the 1990 zeroing system (page 44), only with a much smaller reaction volume. Approximately equal flows af ~5 sccpm NO and O_2 were mixed upstream of the quartz tube. No reaction chamber was necessary, because sufficient reaction occurred within the quartz tube and short sections of teflon tubing prior to injection into the sample flow (volume ~4 ml). The UV lamp was entirely covered with aluminum foil, with only a pinhole to allow minimal light to escape and cause O_3 formation. The size of the hole in the UV lamp covering was controlled so that the O_3 formed titrated <100% of the initial NO. Preliminary tests under conditions of complete NO titration resulted in apparent NO_y loss within the titration system. This was probably a result of oxidation of NO_2 to NO_3 by excess O_3, followed by efficient removal of NO_3 by teflon surfaces (D. Fahey, private communication, 1989).

The primary advantage of this system is that once the calibration flow enters the sample line, the ozone is diluted to negligible levels (a few ppbv), so the $NO+O_3$ reaction is essentially quenched at that point. In addition, the absence of a separate reaction chamber reduces the time for equilibration when the lamp is turned off. There are two main limitations of this system. First, a needle valve (rather than a mass flow controller) was used to control the O_2 flow. As a result, it was important that the pressure in the calibration line not change between measure and calibration modes to prevent oscillation of the O_2 flow. Even with a mass flow controller, pressure changes associated with mode changes would likely result in transients of ~1 minute, due to variations in the O_3 concentration produced in the quartz tube. Second, the UV lamp used in this system did not reach full intensity for several minutes after it was turned on. This was not a significant problem, but it required that the lamp be allowed to warm up during the measurement periods prior to each

calibration.

2.2.6.3 Mass Flow Controller Calibration

Mass flow controllers (Tylan Corp., Carson, CA; Model FC-280) were used to control the sample and calibration gas flow rates, as well as the ozonator oxygen supply and the CO supply to the NO_y converter. These mass flow controllers (MFCs) have a specified accuracy of 1.0% of the maximum, or full scale flow. The accuracy of the sample and calibration gas MFCs was checked several times during this study. In several cases small adjustments in MFC response were made in response to small observed errors in flow rate. MFC calibration was conducted using bubble flowmeters connected to the MFC outlet. The MFC inlet was connected directly to a tank of nitrogen regulated to approximately 15 psi (pounds per square inch above ambient). Two bubble flowmeters were used for calibration, with ranges of 0–500 ml (100 ml increments) and 0–50 ml (10 ml increments). The 0–50 ml bubble flowmeter was itself calibrated using a more accurate 10 ml class A volumetric pipette (specified accuracy ±0.2%). The design of the 0–50 ml bubble flowmeter prevented calibration using a pipette, and it was used as received from the manufacturer (specified accuracy ±5%). Flow measurements made with the bubble flowmeters were corrected to standard temperature and pressure (0°C, 1 atm). The bubble flow measurements were not corrected for water vapor which arises from evaporation of the bubble solution. This resulted in errors of approximately 2% in the calibration of both the sample and calibration gas flow controllers. However, since the instrument calibration was based on the ratio of the calibration gas and sample flows, this did not affect calibration or measurement accuracy.

The first calibration of the MFCs occurred after the summer 1988 measurements. At that time, calibrations indicated that the sample (0–10 slpm) flow controller was within specifications. However, the calibration gas controller (0–10 sccpm) was out of specifications, with a relative error of 6.7% at the setting of 2 sccpm

used at Barrow. (The MFC was then readjusted to within specifications.) The flow measurements at this time were mistakenly not corrected to standard pressure. This may have led to a calibration error of up to ~1%, based on typical values of air pressure at the laboratory in Fairbanks. However, since the relative error was the same for both the sample and calibration flow controllers, this did not affect calibration or measurement accuracy.

The MFCs were next calibrated after the spring 1989 measurements. At that time, an error in the calibration flowmeter of 1.8% of full scale was found at the setting of 2 sccpm used during the measurement campaign (7.2% relative error). The flowmeter was again adjusted to within specifications. In both 1988 and 1989, it was not known whether the observed deviations in MFC response occurred before, during, or after the measurement period. However, the resulting uncertainty (±7%) was a minor contributor to the total NO and NO_y uncertainty in those campaigns (section 2.2.11), and the data were not adjusted for potential MFC errors.

After the 1989 measurement period, the sample flowmeter was found to be contaminated with dust, resulting in a reduction of the maximum flow achievable through the flow controller. Inadvertently contamination of the MFC may have occurred during tests after the measurement period, and inspection of the 1989 data revealed no evidence to indicate that the measurements were affected. The MFC was returned to the manufacturer for cleaning.

Prior to the 1990 measurements, the MFCs were again calibrated. The calibration MFC was found to be off by 1.2% of full scale (10 sccpm) and was adjusted. The sample MFC was adjusted by the manufacturer to a new full-scale range of 2 slpm, and laboratory tests indicated the manufacturer's calibration was accurate to 0.1% of full scale. The MFCs were recalibrated twice during and once after the 1990 measurements (June 21, 1990; September 19, 1990; and January 10, 1991), and in all cases both were found to be accurate within 0.5% of full scale.

2.2.7 NO_y Conversion

Three different NO_y converters were used during the three measurement campaigns at Barrow. The first two systems, based on molybdenum mesh and a molybdenum tube, respectively, proved to be inadequate for reasons discussed below. The final design incorporated a gold-tube/CO system, which was found to be reliable and easily maintained.

This section contains a description of the three NO_y converter systems, and discussions of tests of the conversion efficiency of each system and of the methods used to correct the data from each measurement campaign for non-unity conversion efficiency. (Additional information on conversion efficiency is contained in section 2.4—Instrument Intercomparison, and section 2.2.6.2—Conversion Efficiency Calibration—contains a discussion of the methods used to measure NO_y conversion.)

2.2.7.1 1988 Converter

During the summer 1988 measurements, a molybdenum mesh converter from a commercial instrument (Model 14 B/E, Thermo Environmental Instruments, Incorporated, Franklin, MA) was used. This converter had been previously used. Prior to the 1988 measurement campaign, the NO_2 conversion efficiency of the converter, operated at the standard temperature of 375°C, was measured and found to be >97%. Two measurements of the conversion of HNO_3 at this time indicated conversion efficiencies of 77 and 80%. These values are considered lower limits to the true HNO_3 conversion efficiency, as loss of HNO_3 within the calibration system was found to be a problem in later tests.

The conversion efficiency was not measured during the 1988 campaign. After the 1988 measurements, the converter was inadvertently operated for 5 weeks with the heater intermittently off. The conversion efficiency was not measured again until

after this period, when it was found to be 55%. Contamination of the converter likely resulted from operation without the heater, and this apparently caused the drop in conversion efficiency. An analysis of the NO_y measurements obtained at Barrow during 1988 revealed no evidence of a significant drop in NO_y conversion efficiency during the measurement campaign. Nevertheless, the lack of conversion efficiency measurements during or immediately after the Barrow measurement period results in significant uncertainty in the actual conversion. The Barrow measurements from 1988 were not corrected for potential non-unity NO_y conversion, and uncertainty in the NO_y measurements due to potential incomplete conversion is estimated to be 50%.

2.2.7.2 1989 Converter

Following the 1988 measurement campaign, a new converter based on a molybdenum tube was developed. A molybdenum tube system was selected to minimize the "memory effect" commercial molybdenum mesh converters exhibit following exposure to high NO_y levels, as well as avoid the use of CO required by gold-tube systems. In addition, use of a tube converter permits a comparison of experimentally-determined reaction parameters with those predicted from theoretical flow calculations [*Murphy and Fahey*, 1987; *Bollinger et al.*, 1983].

The molybdenum tube system was developed by J. Herring (University of Alaska Fairbanks), and had a length of 37 cm, an inner diameter of 0.42 cm, and a minimum purity of 99% (Rhenium Alloys, Elyria, Ohio). The tube was heated to 375°C, and the upstream fitting was heated separately to improve temperature uniformity throughout the tube. A short section of stainless steel tubing was used to cool the downstream flow, and a teflon filter prevented molybdenum migration from the converter.

Laboratory tests were conducted over a two-month period. During this time, the tube converter was exposed nearly continuously to NO_2 concentrations of 40–

70 ppbv in a 0.7 lpm flow. The measured NO_2 conversion efficiency during these tests ranged from 65 to 96%. Tube cleaning procedures included high-temperature N_2/H_2 (or vacuum) bake-outs at 500–600°C and/or HCl rinses. Generally, these cleaning procedures resulted in a significant increase in conversion efficiency, though not in all cases.

Using the methods of *Murphy and Fahey* [1987], the wall reaction probability for NO_2 on the wall of the molybdenum tube can be calculated. The minimum conversion efficiency of 65%, which was observed two weeks after a tube cleaning, corresponds to a reaction probability of approximately 2.5×10^{-5}. Based on this probability, a tube more than 2 m in length would be required to maintain a conversion efficiency of >99% in a 1 slpm flow over a two-week period of exposure to 40–70 ppbv NO_2.

During the measurement period at Barrow, the flow through the converter was 2 slpm. At this flow rate, the conversion efficiency would be 99% in the limit of infinite wall reaction probability (based on the Gormley-Kennedy solution; *Bollinger et al.*, [1983]). However, the measured conversion efficiency at Barrow ranged from 62 to 85%.

The NO_2 conversion efficiency was monitored frequently (3–4 times per week) during the Barrow campaign. These measurements were conducted with a permeation system which was switched between SPAN (standard addition of NO_2) and ZERO (no standard addition) modes. The first 60 seconds of each mode were discarded, and the following 30–40 seconds averaged. ZERO readings were interpolated to account for NO detector drift, and the measured permeation system flow rate was corrected to standard temperature. The permeation oven was maintained at 30.0 ± 0.4°C.

These NO_2 conversion efficiency measurements are shown in Figure 2.23. The overall mean and standard deviation of the conversion efficiency were 0.75 and 0.07, respectively. However, some of the observed variability was due to degradation of

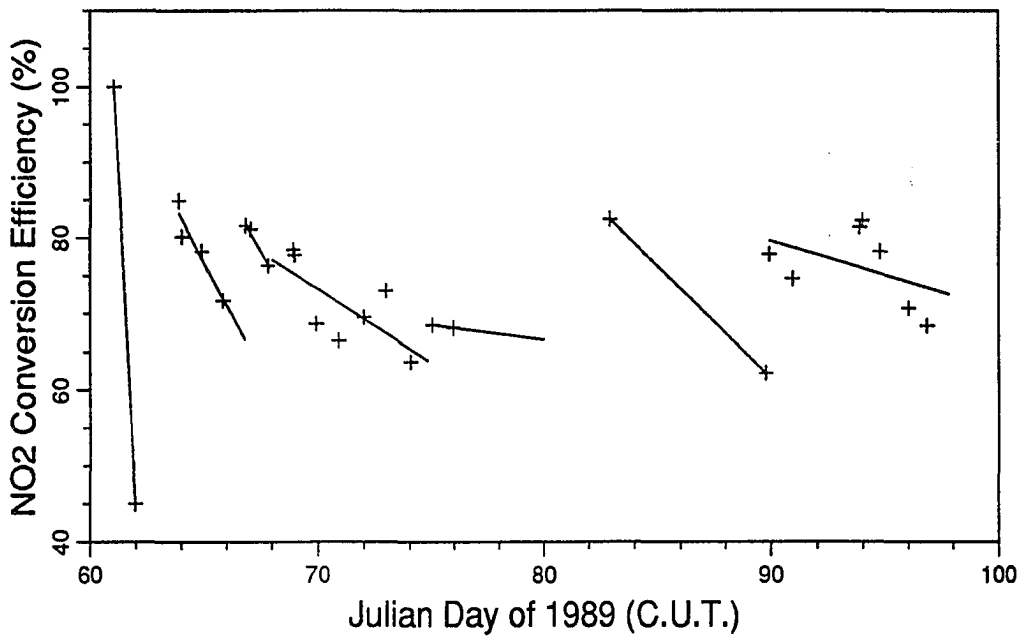

Figure 2.23 NO_2 conversion efficiency measurements during the 1989 campaign. Least-squares fits to the conversion efficiency measurements between successive cleanings are shown by the straight lines.

the conversion efficiency with time and increases in conversion efficiency resulting from tube cleanings. The converter was cleaned using bakeouts at 500–600°C under vacuum or nitrogen (combined with HCl rinses in the first two instances). Least-squares fits to the conversion efficiency measurements between successive cleanings are shown by the straight lines in Figure 2.23.

In order to take into account the reduction in conversion efficiency with time, the NO_y measurements were corrected for non-unity conversion based on the least-squares fits shown in Figure 2.23. There is a large uncertainty in these conversion efficiency estimates, due to the variability in the observed values. This uncertainty is conservatively estimated to be 3 times the overall standard deviation of conversion efficiency measurements, or 0.20. This translates into a maximum relative uncertainty in NO_y concentrations of 31%.

2.2.7.3 1990 Converter

As a result of the poor conversion efficiency of the molybdenum tube converter, a gold tube/CO converter was developed. As described in section 2.1.2.2, heated gold tubes have been found to catalyze the reduction of NO_y compounds to NO, using CO as a reducing agent. A gold tube, 37 cm in length, 1/4 inch o.d., 0.19 inch i.d. and of 99.95% purity was purchased for this use (Englehard Corp., Iselin, NJ). The tube was initially cleaned with an overnight soak in a 2% solution of Micro Laboratory Cleaning Solution (Cole-Palmer Instrument Co., Chicago, IL) in a sonic bath. The tube was cleaned further by soaking overnight in HCl. Stainless steel bulkhead fittings were attached to the tube ends, and the bulkhead fittings were attached directly to a tube furnace (Mini-Mite Model 55035, Lindberg Corp., Watertown, WI). The tube was thus supported at the ends, and was held in the center of the approximately 2.5 cm diameter tube furnace. Some distortion of the tube was observed after heating to temperatures above about 500°C, due to softening of the gold, but this was not a problem.

The temperature at the midpoint of the the tube was controlled to 300±0.5°C. When used with a 1 slpm air flow, the temperature at a point 5–10 cm from the inlet end was 265°C, while at a corresponding distance from the outlet end the temperature was 280°C. CO was added to the sample flow to a concentration of 0.3% v/v (3 sccpm) at a teflon tee located just upstream of the tube heater.

The conversion efficiency for NO_2 was checked with each calibration cycle (about once per hour) during the 1990 measurement period at Barrow. Initially, the tube was cleaned weekly by heating to 700°C. This temperature required the use of a section of stainless steel tubing downstream of the converter to cool the exhaust flow, instead of direct connection to the outlet teflon tubing. Later experiments showed that heating to 500°C was adequate to maintain a conversion efficiency for NO_2 above 95%. At 500°C, no change in the outlet tubing was required to cool the tube exhaust.

Conversion efficiency measurements require the subtraction of two large numbers with a small difference (the calculation method is discussed in section 2.2.10). In order to reduce the uncertainty of the conversion efficiency measurements, 5-point running averages of the conversion efficiency values measured during each calibration cycle were used to correct the NO_y data. The resulting running-average conversion efficiencies are shown in Figure 2.24.

Only data collected when conversion efficiency measurements were above 90% were considered valid; NO_y data obtained during periods of lower conversion efficiency were discarded. Several periods of low conversion efficiency are apparent from Figure 2.24. During days 87–88, a low conversion efficiency apparently resulted from a reduced CO flow, caused by an ice plug in the CO line. Apparently, there was a small amount of water in the CO tank which froze and accumulated at the point where the tube exited the building and reached ambient temperature, blocking the tube. Periods of conversion efficiency below 90% were also observed during days 111–113 and 126–130. The cause of these low values was not determined, and after the weekly cleaning cycles, acceptable conversion efficiencies were again observed. During days 288–302, the wire controlling the solenoids which directed flow through the NO_y converter malfunctioned, and neither conversion efficiency nor NO_y measurements were obtained. Finally, a significant drop in conversion efficiency was observed after about day 320 (November 16). The weekly converter bakeouts still resulted in an increase in conversion efficiency after that date, but the maximum conversion observed during each cleaning cycle dropped continually, reaching values as low as 5%. Due to the low conversion efficiencies, all data obtained after November 16 were excluded from further analysis.

Small but significant variations in NO_2 conversion efficiency are apparent in Figure 2.24. Some of these are due to the weekly bakeout cycle, but many reflect changes between bakeouts. The NO_y measurements during 1990 were corrected for non-unity NO_2 conversion efficiency using the 5-point running averages of conversion

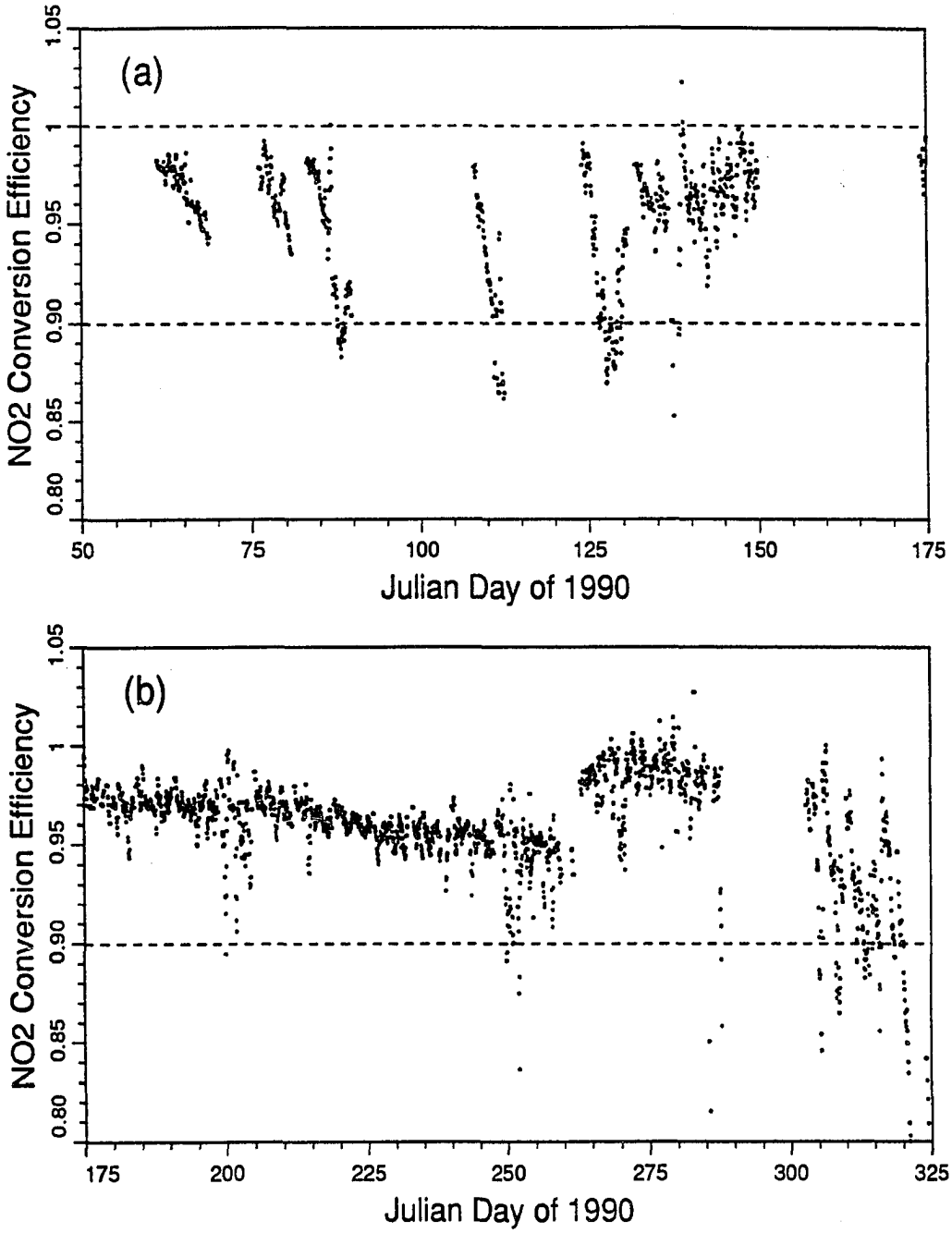

Figure 2.24 NO_2 conversion efficiency measurements during the 1990 campaign. Each point corresponds to a running average of 5 consecutive measurements. (a) Days 50–175 of 1990. (b) Days 175–320 of 1990.

efficiency measurements (Figure 2.24) centered nearest each NO_y measurement. The calculation procedure is presented in section 2.2.10.

2.2.8 Other Components

The remaining components of the NO/NO_y monitor include the instrument control and data acquisition system, the inlet system, and a variety of other components. These components are described briefly in this section. In addition, a short discussion of grounding and electrical noise problems encountered in this work is presented.

2.2.8.1 Instrument Control and Data Acquisition

The instrument was cycled automatically through a series of calibration and measurement modes (section 2.2.9.1) by a microcomputer (section 2.2.8.3), which also measured the photon counting rate. Input and output (I/O) from the computer were controlled through a DAS-16 I/O board (Metrabyte Corporation, Taunton, MA) using the the Labtech Notebook software (Laboratory Technologies Corporation, Wilmington, MA).

The Notebook program is run using "setups," which define a series of channels representing variables measured or calculated by the program. Through the DAS-16 I/O board, Notebook produced TTL signals that controlled the state of the solenoid valves and the calibration UV lamp. The TTL pulses were sent to a "solenoid control box" (built by B. McKibben, Geophysical Institute) which produced 12 volt output signals to drive the solenoid valves. To control the calibration UV lamp, one of the 12 V output signals was used to power a solid state relay, which switched the 110 VAC power to the UV lamp on and off.

The photon counting rate was monitored through a counter on the DAS-16 I/O board, which was queried each second by the Notebook program. The counter counted TTL pulses, which were produced by a discriminator/pulse amplifier (de-

scribed in Section 2.2.8.3). The counter could count to a maximum of 2^{16} (65,536). In practice, this limited use of the instrument to NO and NO_y levels below about 50 ppbv. (Higher maximum concentrations could be measured simply by querying the counter more frequently than once per second). Data were stored in the form of mean and standard deviation of the counting rate for each mode, based on 1 s observations (1990), or 4–5 s average count rates (1988–1989). In addition, 5 s-average counting rates were saved to allow for detailed inspection of the measurements when necessary.

Separate Notebook setups were used for each of the three measurement campaigns, as the instrument configuration and usage was improved. The setup used for the 1990 measurement campaign is included in Appendix A.

2.2.8.2 Inlet System

The inlet system is an integral part of the total measurement system, particularly in the case of NO_y. The inlet systems used in this work represent compromises between the goal of a minimum length of inlet tubing and the requirement of automatic calibration to ensure accuracy over periods of weeks to months. The inlet systems used during the three measurement campaigns are described here.

1988 and 1989 Inlets. During the 1988 measurements, the instrument was located in an outbuilding next to the CMDL station; in 1989, the instrument was located in the main CMDL building. In both cases, the sample inlet was located approximately 1 m above the roof, and was sheltered by a small plexiglass box (approximately 20 cm × 20 cm × 30 cm) to keep rain and snow out of the inlet. Separate downward-facing teflon tubes were used for NO and NO_y inlets.

Teflon tubes approximately 2m long extended from the inlet to the top of the instrument rack within the building, where the NO_y converter was located. Sections of the tubes outside the building were covered with aluminum foil to prevent

photolysis within the tubes and minimize temperature changes [*Carroll et al.*, 1985].

1990 Inlet System. The inlet configuration was modified for the 1990 measurements. These modifications were made with two goals. First, the length of tubing upstream of the NO_y converter was reduced to prevent losses of HNO_3 and other reactive species within the inlet line. Second, the location of calibration gas addition was moved to the inlet, rather than within the building, in order to account for NO loss within the inlet due to reaction with ambient ozone. To accomplish these goals, a weatherproof box was constructed to house the NO_y converter, all solenoids controlling flow through the converter and calibration, and the calibration UV lamp and quartz tube used in NO/O_3 titrations. The box was well-insulated, and heat from the tube heater was sufficient to keep the temperature inside the box above freezing even when ambient temperatures were below -30°C.

In order to minimize the length of inlet tubing, ambient air was sampled from a 120 cm galvanized steel sampling stack 30 cm in diameter, through which ambient air was pulled downward at high speed by a fan located at the bottom. The sampling stack reached to 1.8 m above the roof (a total height of 6.8 m above ground level), and was protected by a rain cover approximately 10 cm above the top. The instrument inlet consisted of teflon tubes (separate tubes for NO and NO_y), which protruded horizontally to the center of the sampling stack. The inlet box was located as close as possible to the stack. However, in order to automatically measure sensitivity and NO_2 conversion efficiency, it was necessary to include solenoid valves prior to the NO_y converter. These increased the total inlet length to a total of approximately 100 cm of 1/8 inch i.d. teflon tube.

2.2.8.3 Other Components

Pumps. A two-stage direct-drive pump with a displacement of 190 lpm was used to evacuate the reaction chamber (Model E2M8, Edwards High Vacuum, Grand

Island, NY). The pump was operated with an exhaust filter to recover oil mist. Oil was transferred from the exhaust filter to the pump when necessary, and the amount of oil thus recovered was large enough that it was rarely necessary to add pump oil. The pump was very reliable, and needed servicing only once, after it was contaminated with O_3 (section 2.2.4).

In addition to the main pump, a small pump (Air Cadet, Cole Palmer Instrument Co., Chicago, IL) was used to maintain necessary purge air flows. This pump was used to maintain a flow through the zeroing volume and NO_y converter when the main flow bypassed those systems and also collected the calibration gas flow during measurement periods.

Scrubbers containing Hopcalite (Mine Safety Appliances Co., Pittsburgh, PA) were used prior to each of the pumps to remove ozone and carbon monoxide. Exhaust from the pumps was directed outside the building as a safety measure in case a scrubber malfunction allowed CO to reach the pump exhaust and to keep the odorous exhaust out of the work area.

Computers. During the 1988 measurement campaign, a standard 80286 IBM type computer (EPIC-AT) was used for data acquisition and instrument control. Beginning in the 1989 campaign, a Compaq Portable II computer (Compaq Computer Corp., Houston, TX) was used. This computer was smaller and more easily transported.

Fittings and Tubing. All fittings and tubing exposed to the sample flow were constructed of teflon, with the exception of the NO_y converter. Thick-walled TFE tubing (1/4 inch o.d., 1/8 inch i.d.) was used in most cases as well as a smaller amount of thin-walled FEP tubing (1/4 inch o.d., 3/16 inch i.d.) (Fluorocarbon Co., Anaheim, CA). Compression fittings were constructed of PFA teflon (grab-seal fittings, Fluorocarbon Co., Anaheim, CA). Stainless steel compression unions

(Swagelock Co., Solon, OH) were used to connect the NO_y converters used during the three campaigns to upstream teflon tubing, and a short section of stainless steel tubing was used downstream of the converters to cool the hot air prior to downstream teflon tubing. In lines not exposed to the sample flow (e.g. the ozone and CO lines), both teflon and stainless steel compression fittings were used.

Solenoid Valves. The three-way solenoid valves used to control the calibration and sample flows were constructed of PFA teflon and were compatible with the teflon compression fittings (Delta Series valves, Fluorocarbon Co., Anaheim, CA).

CO Detector. A carbon monoxide detector was used with the NO/NO_y instrument as a safety device. The CO detector (Sierra Monitor Corp., Sunnyvale, CA) had an alarm which was activated at CO concentrations above 100 ppmv, in order to ensure that dangerous CO leaks would be detected if they occurred.

2.2.8.4 The Photon Counting System and Counting Noise

The photon counting system consisted of the photomultiplier tube, a pulse amplifier/discriminator (PAD), and a counter that was part of the DAS-16 I/O board (described above). The photomultiplier tube was a red-sensitive PMT that was originally part of the TECO 14T instrument (section 2.2.2). Pulses from the PMT were sent to the PAD (designed and constructed by B. McKibben, Geophysical Institute), which converted the photomultiplier pulses into TTL pulses that could be counted by the computer. The PAD was located in a drawer of the chassis containing the PMT, and received its input directly from a preamplifier in the base of the PMT. The discriminator portion of the PAD consisted of a circuit that compared the height of PMT pulses with preset reference voltages, and passed only those falling between two preset levels. The lower voltage level was set by monitoring the dark count rate as the voltage was increased from a value near 0 V. At a voltage cutoff

near 0 V, thermal (PMT) noise resulted in a large number of extraneous counts. The voltage cutoff was increased until the count rate began to drop sharply, and was then increased approximately 50 mV more. This procedure resulted in selection of a lower discriminator cutoff of 115 mV. The upper discriminator cutoff was set at 2.0 V, a value which allowed all PMT pulses to be counted. The instrument response was not sensitive to changes in the upper discriminator cutoff above 2 V.

Noise in the photon counting system was sometimes a problem during the 1988 and 1990 measurement campaigns. During 1988, single-second spikes in counting rate of several hundred cps above the background level were observed, at a rate of once every few minutes. The cause of the spikes was not determined, but they were easily edited out of the data record, as described in section 2.2.11.1. In addition, prior to the 1988 campaign, changes in the count rate of ~50 cps were observed, depending on how the wire connecting the PAD to the computer was connected. A shielded wire was used, and the count rate varied depending on whether the shield of the wire was connected to both the computer and PAD grounds or to only one of the two grounds.

Similar problems were observed during the 1990 campaign. For about three weeks, a much worse spiking problem was observed, with highly variable count rates of several ten-thousand cps. These data were not included in any analysis. At the same time, a curious negative NO artifact of ~-10 to -40 pptv was observed. The artifact was clearly a result of extraneous noise in the photon counting system, because it only occurred when the instrument was under computer control and was not present when the instrument was operated manually. During this period, the shield of the wire connecting the PAD and computer was connected to the grounds of both, and both the spikes and the negative artifact problem disappeared temporarily when the shielding wire was disconnected from both the computer and the PAD. The problems recurred after a few weeks, however. After the problems reappeared, a 10-gauge cable was used to connect the computer, PAD, and chassis grounds. This

was done under the theory that line noise was creating voltage between the grounds of the computer and PAD. After the grounding cable was connected, the problem disappeared and did not recur.

2.2.9 Summary of Instrument Configurations During the Measurement Campaigns

This section contains a description of the instrument operation routines used to calibrate and make NO and NO_y measurements during the three campaigns. These routines consist of a sequence of modes, which are described in the next section. After each mode change, the instrument was allowed to equilibrate to the new conditions, and then photon count measurements were averaged for a specified period. The procedures used to select the equilibration and averaging periods used during the 1990 campaign are also described below.

2.2.9.1 Modes of the Instrument

1988. The basic instrument sequence used during the 1988 measurements is shown in Figure 2.25. This sequence was modified somewhat for the 1989 and 1990 measurements, but the general sequence was the same in all three measurement campaigns. Each measurement cycle began with a calibration mode, in which NO calibration gas was added as a standard addition to the NO sample line. Thus, the instrument sensitivity was calculated from the difference between the C (calibration) and NO-1 (first NO measure) modes. NO and NO_y concentrations were calculated from the difference between the corresponding NO or NO_y mode and a zero level interpolated between the previous and succeeding Z modes.

Each mode was 140 s in length. The first 20–30 s were discarded, and the remainder were averaged for the mode result. (As a result of computer problems at Barrow, the raw data were stored in two different formats, and different equilibration

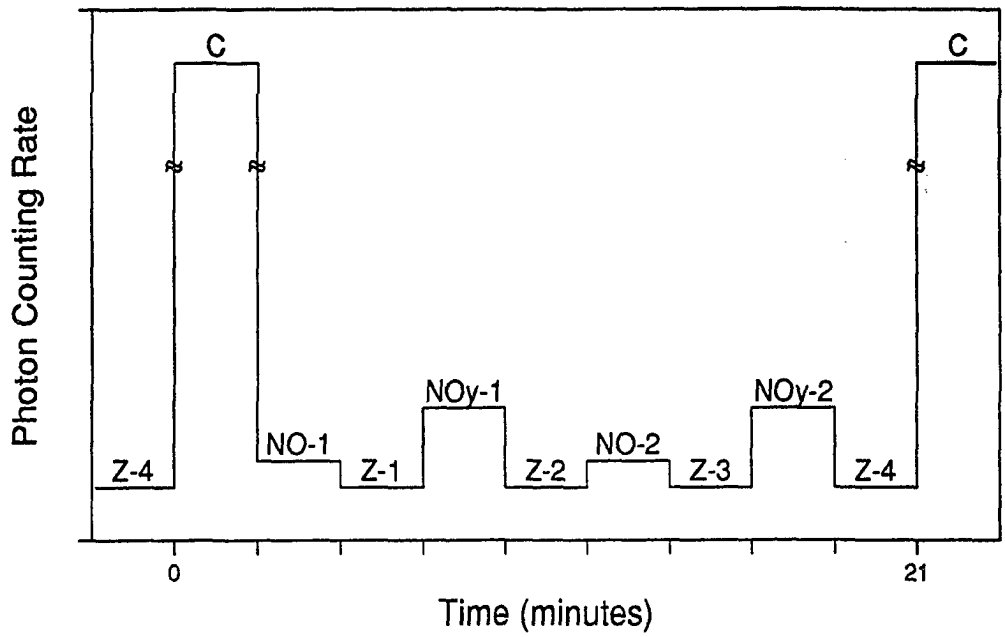

Figure 2.25 Instrument cycle used during the 1988 measurements. C—calibration mode; NO-1 and NO-2—NO measure modes; NO_y–1 and NO_y–2—NO_y measure modes; Z-1 through Z-4—zero modes. The ~ symbols indicate a discontinuity in the y-axis (photon counting rates during the calibration modes were much greater than those during the measure and zero modes).

periods were used for the two formats.) The standard deviation of the count rate during the averaging period was also stored, and this value was useful as an indicator of ambient variability.

1989. The mode sequence used in 1989 was identical to that used in 1988. However, different equilibration and averaging periods were used. For the first NO measure mode (NO-1) which followed calibration, 50 s were allowed for equilibration. For all other modes, 100 s of equilibration were allowed. A shorter equilibration period was used for mode NO-1 because preliminary tests indicated that the effect of the mode change from calibration to NO-measure was shorter than that due to switching from zero to measure or vice-versa. However, analysis of the resulting data indicated that a higher count rate was consistently observed during the NO-1 mode

than during NO-2, as a result of lingering effects from the previous calibration. As a result, only data from the NO-2 mode were used for further analysis. Averaging periods of 100 s were used for all modes except the calibration. For the calibration mode, a 20 s averaging period was sufficient, since the higher counting rates during that mode resulted in a reduced relative standard deviation.

1990. For the 1990 measurement period, a more complex sequence of modes was used. The setup was modified in two ways. First, additional calibration modes were added so that other calibration parameters (in addition to NO sensitivity) could be automatically measured (these include NO_2 conversion efficiency, zeroing efficiency, and NO sensitivity when passing through the NO_y converter). In addition, eight NO and NO_y measurements were made between successive calibrations, rather than two as in 1988 and 1989, resulting in 1 calibration every approximately 1.3 hr. Figure 2.26 shows the cycle used.

The first six modes consisted of calibration measurements. After the calibration period, 8 measurements of NO and NO_y were made. Each measurement consisted of three modes for NO: an NO zero mode (modes **Z|NO|1a, Z|NO|2a, ..., Z|NO|8a**), an NO measure mode (modes **NO|1, NO|2, ..., NO|8**), and a second NO zero mode (modes **Z|NO|1b, Z|NO|2b, ..., Z|NO|8b**). The three NO modes were followed by an NO_y measure mode (modes **NO_y|1, NO_y|2, ..., NO_y|8**) and an NO_y zero mode (modes **Z|NO_y|1, Z|NO_y|2, ..., Z|NO_y|8**). The five measurement modes were repeated a total of eight times. A separate NO_y zero mode was used because CO used in the NO_y converter during 1990 caused a significant increase in the instrument zero level, as observed previously [*Fahey et al.,* 1985]. In data analysis, the zero level during each measure mode was estimated by interpolating between the 2 adjacent **Z|NO** modes (for NO) and by interpolating between the 2 nearest **Z|NO_y** modes (for NO_y).

The calibration measurements were used to estimate the NO sensitivities ap-

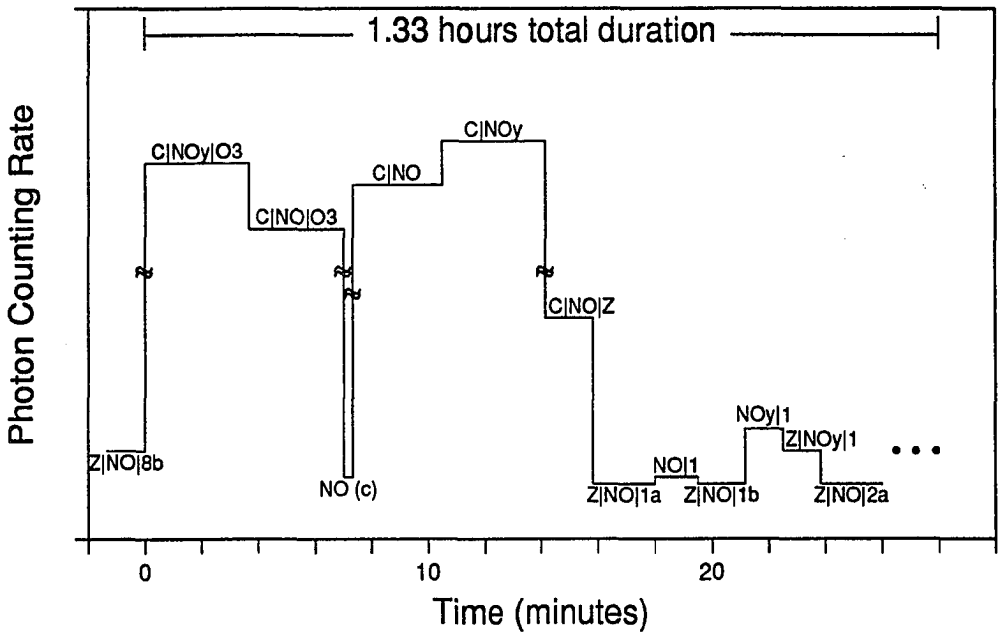

Figure 2.26 Instrument cycle used during the 1990 measurements. The individual modes are described in the text and summarized in Table 2.4. The ~ symbols indicate a discontinuity in the y-axis (photon counting rates during the calibration modes were much greater than those during the measure and zero modes). The six measurement modes (Z|NO|1a through Z|NO_y|1) were repeated eight times.

plicable to NO and NO_y measurements, the NO_2 conversion efficiency in the NO_y converter, and the fraction of NO removed during the zeroing mode (the "fraction zeroed"), using the equations presented in section 2.2.10. The 6 calibration modes (the first 6 modes in Figure 2.26) consisted of different settings of the calibration and NO/NO_y solenoids and the calibration UV lamp (used to create ozone for NO/O_3 titration) as shown in Table 2.4. The calibration UV lamp and calibration solenoids were ON during the first 2 modes; thus a flow of $NO+NO_2$ was added as a standard addition to the inlet. During mode **C|NO_y|O_3**, this flow was directed through the NO_y converter; the NO_y converter was bypassed during mode **C|NO|O_3**. The next mode, **NO(c)**, was a measurement of ambient NO without any calibration gas addition. During this mode, the calibration UV lamp was turned off and the NO_2 in the calibration system was flushed out. In the next two modes, the calibration gas (now

consisting of NO only) was redirected into the inlet. In mode **C|NO**, the standard addition was directed through the NO channel; in mode **C|NO_y**, the calibration flow was directed through the NO_y converter. The last calibration mode, **C|NO|Z**, was identical to mode C|NO (NO calibration gas through NO channel), except that the zeroing system was switched on, allowing calculation of fraction of NO removed during zeroing.

Table 2.4 Summary of the Instrument Modes Used During the 1990 Measurements.

Mode Number	Mode Abbreviation[a]	Calibration	Gas-Phase Titration UV Lamp	NO/NO_y	Zeroing
Mode 0	$C\|NO_y\|O_3$[b]	ON	ON	NO_y	OFF
Mode 1	$C\|NO\|O_3$[c]	ON	ON	NO	OFF
Mode 2	NO(c)[d]	OFF	OFF	NO	OFF
Mode 3	C|NO[e]	ON	OFF	NO	OFF
Mode 4	$C\|NO_y$[f]	ON	OFF	NO_y	OFF
Mode 5	C|NO|Z[g]	ON	OFF	NO	ON
Mode 6[h], 11, 16, ...	Z|NO|1a[i,h]	OFF	ON	NO	ON
Mode 7[h], 12, 17, ...	NO|1[j,h]	OFF	ON	NO	OFF
Mode 8[h], 13, 18, ...	Z|NO|1b[k,h]	OFF	ON	NO	ON
Mode 9[h], 14, 19, ...	$NO_y\|1$[l,h]	OFF	ON	NO_y	OFF
Mode 10[h], 15, 20, ...	$Z\|NO_y\|1$[m,h]	OFF	ON	NO_y	ON
...	...	...	...	...	...

[a] C indicates a calibration mode; Z indicates a zero mode; NO or NO_y indicates measurements through the NO inlet or NO_y converter, respectively; and O_3 indicates and NO/O_3 titration calibration.
[b] NO/NO_2 calibration through the NO_y converter using NO/O_3 titration.
[c] NO/NO_2 calibration through NO inlet using NO/O_3 titration.
[d] NO measure mode used for calibration.
[e] NO calibration through NO inlet.
[f] NO calibration through NO_y converter.
[g] NO zero mode during NO calibration.
[h] Repeated a total of 8 times
[i] NO zero mode.
[j] NO measure mode.
[k] NO zero mode.
[l] NO_y measure mode.
[m] NO_y zero mode.

The equilibration and averaging periods for each mode are shown in Table 2.5. The equilibration periods after each mode change were selected based on a series of laboratory tests in order to ensure that long enough equilibration periods were used and that the equilibration periods were not unnecessarily long. These tests

are described below. The averaging periods were selected based on a consideration of the expected magnitude of the counting rate during each mode, and the relative uncertainty acceptable in each mode average. For example, the **C|NO** and **NO(c)** modes were used to calculate NO sensitivity, based on the difference in count rate between those modes. Since a very large difference was present due to the added calibration gas, short averaging periods were acceptable for those modes. In contrast, the difference between the **C|NO$_y$|O$_3$** and **C|NO$_y$** modes were used to calculate NO_2 conversion efficiency. In this case, a small difference between two modes, each with a high count rate, was measured. Therefore, a longer averaging period was necessary. For the NO and NO_y measure and zero modes, the averaging times were selected based on desired detection limits following equation 2.12:

$$\text{Detection Limit} \sim \frac{\sqrt{2Z}}{S_{NO}\sqrt{N}}$$

Typical zero levels for NO and NO_y were $\leq$1000 cps and $\leq$2000 cps, respectively, while typical NO sensitivities were 1.0–1.5 cps/pptv and 1.2–1.8 cps/pptv for NO and NO_y measurements, respectively. Thus, the averaging times chosen for NO and NO_y (40 s and 20 s) correspond to NO and NO_y detection limits (2σ) of about 10 pptv and 20 pptv, respectively.

2.2.9.2 Derivation of Equilibration Periods Used During the 1990 Measurements.

A series of laboratory tests were conducted to determine the minimum equilibration period necessary to avoid any bias in the calculated mode averages. The equilibration periods used in the measurements were selected based on these results, but included a safety margin to accommodate potential degradation of instrument performance in the field. In these laboratory tests, the instrument was cycled back and forth through a mode change (for example, **NO↔Z|NO**) while the photon count rate was recorded. The mode changes occurred every 120 s. Twenty second-average

Table 2.5 Equilibration and Averaging Periods Used in the 1990 Measurement Cycle.

Mode Number	Mode Abbreviation	Equilibration Period (s)	Averaging Period (s)
Mode 0	C|NO_y|O_3	180	40
Mode 1	C|NO|O_3	185	15
Mode 2	NO(c)	5	15
Mode 3	C|NO	175	15
Mode 4	C|NO_y	180	40
Mode 5	C|NO|Z	80	20
Mode 6[a], 11, 16, ...	Z|NO|1a[a]	90	40
Mode 7[a], 12, 17, ...	NO|1[a]	50	40
Mode 8[a], 13, 18, ...	Z|NO|1b[a]	60	40
Mode 9[a], 14, 19, ...	NO_y|1[a]	60	20
Mode 10[a], 15, 20, ...	Z|NO_y|1[a]	60	20
...	...	...	...

[a]Repeated a total of 8 times

values for each mode were then calculated as a function of equilibration period for each of a large number of repetitions, and the effect of equilibration period was determined through a comparison of these averages.

The results of one such test, in which the instrument was cycled between NO_y measure and NO_y zero modes, are displayed graphically in Figure 2.27. Shown in the figure are 20 s-average measurements of the Z|NO_y mode, as a function of equilibration period. Each line in the figure corresponds to a single replicate. The shape of the lines is determined by the features of the mode change. In this case, the count was initially high because the instrument was previously in NO_y measurement mode, and NO_y concentrations in the laboratory were relatively high. After the mode change, the count rate dropped quickly to the instrument zero level in the absence of CO, due to the fact that the zeroing volume was initially filled with ambient air from the zero purge air flow during measure modes. As the zeroing volume filled with CO-rich air from the NO_y converter, the count rate rose, reaching the Z|NO_y level after approximately 45s, or 3 flushes of the zeroing volume.

The actual determination of a minimum equilibration period was based on a comparison of the average value after specific equilibration periods with the average

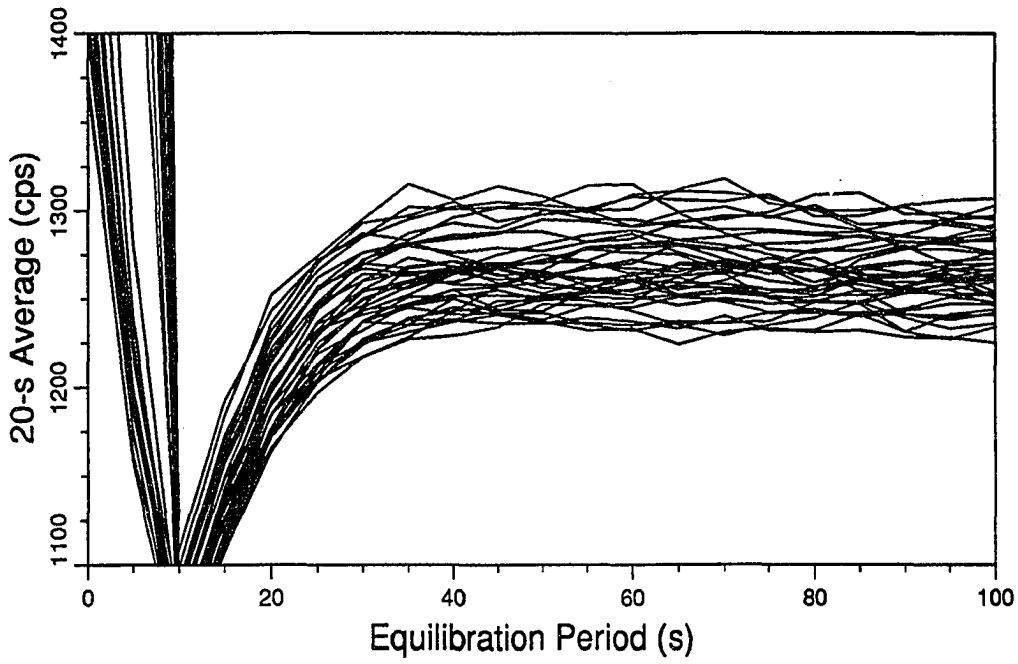

Figure 2.27 Results of a test to determine minimum equilibration period. This test corresponds to the mode change $NO_y \longrightarrow Z|NO_y$. Each line corresponds to a separate replicate. 20 s-average counting rates for the $Z|NO_y$ mode were calculated after equilibration periods ranging from 0–100 s. The resulting averages are plotted against the equilibration period.

after a 100 s equilibration. This comparison was made using a t-test on the mean difference between the two equilibration periods. For the mode change $NO_y \longrightarrow Z|NO_y$ shown in Figure 2.27, this analysis indicated that a bias of ≤ 2 cps was present at an equilibration period of 50 s. The minimum equilibration periods, and corresponding estimates of the remaining bias are shown in Table 2.6 for the measure and zero modes. The estimated bias shown in that table is the maximum estimated absolute difference between averages after the specified equilibration period and the average after a 100 s equilibration, based on a t-test at the 95% confidence level.

The equilibration periods that were selected for use during the measurement campaign are also shown in Table 2.6 and are somewhat longer than the estimated minimum equilibration periods. In the case of mode change $Z/NO_y \longrightarrow Z/NO$, a 4 cps potential bias was considered too large, since it could contribute to NO

Table 2.6 Minimum Equilibration Periods for Measure and Zero Modes, Based on Laboratory Tests.

Mode Change	Minimum[a] Equilibration Period (s)	Remaining Bias[b] (cps)	Actual[c] Equilibration Period (s)
$Z/NO_y \longrightarrow Z/NO$	50	≤ 4	90
$Z/NO \longrightarrow NO$	25	≤ 1	50
$NO \longrightarrow Z/NO$	30	≤ 1	60
$Z/NO_y \longrightarrow NO_y$	50	≤ 15	NA[d]
$NO_y \longrightarrow Z/NO_y$	50	≤ 2	60

[a]Result of the laboratory tests.
[b]Absolute value. See text for calculation method.
[c]Equilibration period actually used.
[d]Not applicable. This mode change was not present in the final instrument cycle.

artifact levels. A period of 90 s, long enough to allow for 6 flushes of the zeroing volume, was chosen as a conservative equilibration period instead. For the other modes, somewhat larger values were also chosen to allow for differences in instrument performance between the laboratory and the field.

The equilibration periods chosen for the calibration modes (shown in Table 2.5) were significantly longer than those required for the measure and zero modes. Laboratory tests similar to those used for the measure and zero modes indicated long minimum equilibration periods were needed (approximately 80 s). However, even after an 80 s equilibration period small, low-frequency fluctuations in the count rate were observed (amplitude $<10\%$ of the total count rate change resulting from the calibration gas addition). These oscillations may have resulted from pressure variations within the long tube carrying the calibration flow from the mass flow controller to the instrument inlet. Since calibrations were conducted less than once each hour, longer equilibration periods in these modes had less impact on the number of data points obtained than would longer equilibration periods in measure and zero modes, and therefore the calibration equilibration periods were chosen conservatively.

2.2.10 Data Reduction and Calibration Parameters

This section describes the procedure used to convert counting rates observed during each mode to calibration parameters and NO and NO_y concentrations and presents a summary of the measured calibration parameters during each measurement campaign. The data acquisition program stored the mean and standard deviation of the counting rate during each mode to a file on the instrument's computer. This file was later used by a data analysis program (included in Appendix B), which carried out the calculations described below. The following discussion focuses on analysis of data from the 1990 measurement period. However, with the exception of NO_2 conversion efficiency and fraction zeroed calculations (which were not part of the 1988 and 1989 automated measurements), the 1988 and 1989 calculations were the same.

2.2.10.1 Calibration Parameters.

The calibration parameters include NO sensitivity through the NO inlet line (referred to as Sens); with units of cps/ppt), NO sensitivity through the NO_y converter (NOySens; cps/ppt), NO_2 conversion efficiency (CnvEff; unitless), and fraction zeroed (FrcZrd; unitless). Each of these was measured once per 1.3 hours (once per measurement cycle). In the following equations, measurements from the calibration modes of the 1990 setup are abbreviated as shown in Table 2.4. (Descriptions of the instrument settings are given in Section 2.2.9.1 above.) The name of the mode in brackets, for example {C|NO}, is used to refer to the average counting rate during the mode. Similarly, $S_{\{C|NO\}}$ refers to the observed standard deviation of the counting rate (based on the 1 s observations), $N_{\{C|NO\}}$ is the number of seconds in the averaging period for the mode, and $T_{\{C|NO\}}$ is the time at the center of the averaging period.

Four values were calculated for each calibration parameter. The parameter esti-

mate (symbolized by an overbar, e.g. $\overline{\text{Sens}}$) was calculated using the average count rate from each relevant mode. The standard deviation of the parameter (e.g. S_{Sens}) was calculated using error propagation, based on the standard deviation of the counts observed during the relevant modes. The ratio of the observed standard deviation to that expected from counting statistics alone ($S_{obs}/S_{counting\ statistics}$) was also calculated, and is referred to as SRatio(e.g. SRatio_{Sens}). Finally, the time at the midpoint of the averaging period for the most critical mode used in the calculation was assigned to each parameter (e.g. T_{Sens} was assigned the time from the {C|NO} mode).

The equations for these parameters are as follows.

Sens — NO Sensitivity. The NO sensitivity was calculated as

$$\overline{\text{Sens}} = \frac{\{\text{C|NO}\}-\{\text{NO(c)}\}}{[\text{NO}]_{cal.\ gas}}, \tag{2.19}$$

where $[\text{NO}]_{cal.\ gas}$ is the NO concentration increase due to the calibration gas standard addition, calculated from the NO concentration in the calibration gas tank ($[\text{NO}]_{cal.\ tank}$) and the sample and calibration gas mass flow controller flow rates ($[\text{NO}]_{cal.\ gas} = [\text{NO}]_{cal.\ tank} \times \text{MFC}_{cal.\ gas}/\text{MFC}_{sample}$). The equations used for the other parameters for NO sensitivity were

$$S_{Sens} = \overline{\text{Sens}}\sqrt{\frac{\frac{s^2_{\{\text{C|NO}\}}}{N_{\{\text{C|NO}\}}}+\frac{s^2_{\{\text{NO(c)}\}}}{N_{\{\text{NO(c)}\}}}}{(\{\text{C|NO}\}-\{\text{NO(c)}\})^2}}, \tag{2.20}$$

$$T_{Sens} = T_{\{\text{C|NO}\}}, \text{ and} \tag{2.21}$$

$$\text{SRatio}_{Sens} = \sqrt{\frac{\frac{s^2_{\{\text{C|NO}\}}}{N_{\{\text{C|NO}\}}}+\frac{s^2_{\{\text{NO(c)}\}}}{N_{\{\text{NO(c)}\}}}}{\frac{\{\text{C|NO}\}}{N_{\{\text{C|NO}\}}}+\frac{\{\text{NO(c)}\}}{N_{\{\text{NO(c)}\}}}}}. \tag{2.22}$$

The value of SRatio_{Sens} is simply the ratio of S_{Sens} to the value of S_{Sens} that would result if the observed variance of count rate during each mode were equal to the

average count rate divided by the number of seconds in the average (i.e., if the counts observed during each mode followed a Poisson distribution).

The NO_y sensitivity (NO_ySens) was calculated identically, except that it was based on modes {C|NOy} and {NOy|1}.

CnvEff — NO_2 Conversion Efficiency. The equations used for NO_2 conversion efficiency were

$$\overline{\text{CnvEff}} = 1 - \left(\frac{\{\text{C|NOy}\} - \{\text{C|NOy|O3}\}}{\{\text{C|NO}\} - \{\text{C|NO|O3}\}} \right), \tag{2.23}$$

$$S_{CnvEff} = \overline{CnvEff} \times \sqrt{\frac{\frac{s^2\{\text{C|NOy}\}}{N\{\text{C|NOy}\}} + \frac{s^2\{\text{C|NOy|O3}\}}{N\{\text{C|NOy|O3}\}}}{(\{\text{C|NOy}\} - \{\text{C|NOy|O3}\})^2} + \frac{\frac{s^2\{\text{C|NO}\}}{N\{\text{C|NO}\}} + \frac{s^2\{\text{C|NO|O3}\}}{N\{\text{C|NO|O3}\}}}{(\{\text{C|NO}\} - \{\text{C|NO|O3}\})^2}}, \tag{2.24}$$

$$T_{CnvEff} = T_{\{\text{C|NOy|O3}\}}. \tag{2.25}$$

The value of SRatio_{CnvEff} was calculated in the same manner as SRatio_{Sens} (equation 2.22).

The conversion efficiency calculated using equation 2.23 is actually an approximation, for two reasons. First, it is based on the assumption that the sensitivities appropriate for NO_y and NO measurements are identical, although (as discussed in section 2.2.6.1), the sensitivity for NO can be as much as 10% lower than the NO_y sensitivity, due to titration by ambient O_3. This approximation results in an overestimation of the value in parentheses in equation 2.23 by up to 10%. However, since only conversion efficiencies above 90% were used (i.e., the value in parentheses was $\leq$0.10), the result was an underestimation of the conversion efficiency of <1%.

The second approximation results from the ozone titration procedure. During O_3 titration calibration modes, a small amount of O_3 was added to the sample flow, resulting in an O_3 concentration increase in the inlet line of $\leq$30 ppbv. This O_3 increase did not affect the NO_y calibration modes, since O_3 was destroyed by the NO_y converter. However, it resulted in a reduction of the signal during the

{C|NO|O3} mode by <10%. Under typical titration conditions, this resulted in an overestimate of the conversion efficiency of ≤1%. Thus, these two approximations resulted in negligible errors in conversion efficiency estimates and tended to cancel each other.

FrcZrd — Fraction Zeroed. The following equations were used for the fraction of NO removed by the zeroing procedure:

$$\overline{FrcZrd} = 1 - \frac{\{C|NO|Z\}-\{Z|NO|1a\}}{\{C|NO\}-\{NO(c)\}}. \quad (2.26)$$

$$S_{FrcZrd} = \overline{FrcZrd} \times \sqrt{\frac{s^2_{\{C|NO|Z\}}}{N_{\{C|NO|Z\}}}+\frac{s^2_{\{Z|NO|1a\}}}{N_{\{Z|NO|1a\}}}} \Big/ (\{C|NO|Z\} - \{Z|NO|1a\})^2 + \frac{s^2_{\{C|NO\}}}{N_{\{C|NO\}}}+\frac{s^2_{\{NO(c)\}}}{N_{\{NO(c)\}}} \Big/ (\{C|NO\} - \{NO(c)\})^2, \text{ and} \quad (2.27)$$

$$T_{FrcZrd} = T_{\{C|NO|Z\}}. \quad (2.28)$$

The value of $SRatio_{FrcZrd}$ was calculated in the same manner as $SRatio_{Sens}$ (equation 2.22).

2.2.10.2 Concentrations

Calculation of the NO and NO_y concentrations was straightforward once the calibration parameters were estimated. The estimated concentrations were based on sensitivities and zero values linearly interpolated between the preceeding and succeeding measurements (indicated by $Sens_{int}$, $\{Z|NO\}_{int}$, and $\{Z|NOy\}_{int}$). The fraction zeroed and the NO_2 conversion efficiency of the instrument did not vary significantly over short periods, and any variations between successive measurements were attributable to measurement uncertainties. Therefore, a running average of five consecutive measured values of those parameters was used in the calculations ($FrcZrd_{ra}$ and $CnvEff_{ra}$).

Concentrations during the eight NO and NO_y measurements in each instrument cycle were treated identically. The following equations show the calculations for the

first NO and NO_y concentration of each cycle.

NO Concentration. The NO concentration estimate, standard deviation, time, and SRatio ($S_{obs}/S_{counting\ statistics}$) value were calculated using

$$[NO] = \frac{\{NO|1\} - \{Z|NO\}_{int}}{Sens_{int} \cdot FrcZrd_{ra}}, \tag{2.29}$$

$$S_{[NO]} = [NO] \times \sqrt{\frac{s^2_{\{NO|1\}}}{N_{\{NO|1\}}} + s^2_{\{Z|NO\}_{int}}}{(\{NO|1\} - \{Z|NO\}_{int})^2} + \frac{s^2_{FrcZrd_{ra}}}{(FrcZrd_{ra})^2} + \frac{s^2_{Sens_{int}}}{(Sens_{int})^2}, \tag{2.30}$$

$$T_{[NO]} = T_{\{NO|1\}}, \text{ and} \tag{2.31}$$

$$SRatio_{[NO]} = \frac{s_{\{NO|1\}}}{\sqrt{\{NO|1\}}}, \tag{2.32}$$

where $\{Z|NO\}_{int}$ and $Sens_{int}$ are the zero counting rate and sensitivity, respectively, linearly interpolated to the time of NO measurement, and $FrcZrd_{ra}$ is a running average of 5 FrcZrd measurements, centered at the time of NO measurement.

NO_y Concentration. If NO_y were converted with 100% efficiency, the NO_y concentration would be

$$A = \frac{\{NOy|1\} - \{Z|NOy\}_{int}}{NOySens \cdot FrcZrd}. \tag{2.33}$$

In general, however, it is necessary to correct for non-unity conversion. This was done based on a 5-point running average of the measured NO_2 conversion efficiency. The conversion efficiency correction was applied after first subtracting the NO concentration $[NO]_{int}$ (interpolated to the time of NO_y measurement), since NO was fully detected regardless of the NO_2 conversion efficiency. Thus,

$$[NO_y] = \frac{A - [NO]_{int}}{CnvEff_{ra}} + [NO]_{int}, \tag{2.34}$$

$$
\begin{aligned}
S^2_{[NO_y]} &= \left(\frac{A-[NO]_{int}}{CnvEff_{ra}}\right)^2 \\
&\times \left[\frac{s^2_{CnvEff_{ra}}}{(CnvEff_{ra})^2}\right. \\
&\left. + \frac{A^2\left(\frac{s^2_{\{NOy|1\}}}{N_{\{NOy|1\}}} + s^2_{\{Z|NOy\}}\right)}{(\{NOy|1\} - \{Z|NOy\})^2} + \frac{s^2_{NOySens_{int}}}{(NOySens_{int})^2} + \frac{s^2_{FrcZrd_{ra}}}{(FrcZrd_{ra})^2}\right) + s^2_{[NO]_{int}} \\
&+ \frac{}{(A-[NO]_{int})^2} \\
&\left. + s^2_{[NO]_{int}}\right] \\
&+ s^2_{[NO]_{int}}, \qquad (2.35)
\end{aligned}
$$

$$
T_{[NO_y]} = T_{\{NOy|1\}}, \text{ and} \qquad (2.36)
$$

$$
SRatio_{[NO_y]} = \frac{s_{\{NOy|1\}}}{\sqrt{\{NOy|1\}}}. \qquad (2.37)
$$

2.2.10.3 Calibration Parameter Measurements

The measured values of the various calibration parameters are presented in this section (with the exception of NO_2 conversion efficiency, which is discussed in Section 2.2.7). During the 1988 and 1989 campaigns, only NO sensitivity and zero levels were monitored; laboratory experiments prior to those measurements indicated that the zeroing procedure completely removed ambient NO, so it was unnecessary to monitor the fraction zeroed. Frequency distributions of the NO sensitivities and zero levels observed during the 1988 campaign are shown in Figure 2.28. The NO sensitivity was approximately 0.4–0.7 cps/pptv, and the zero level was most frequently in the range 200–400 cps, but often reached $\geq$2000 cps due to high room temperature. During the 1989 campaign, a sensitivity of 0.9–1.2 cps/pptv was observed, with a zero of 500–2000 cps. Frequency distributions of these parameters are shown in Figure 2.29. (Values off the plot scales are included in the first or last bin.)

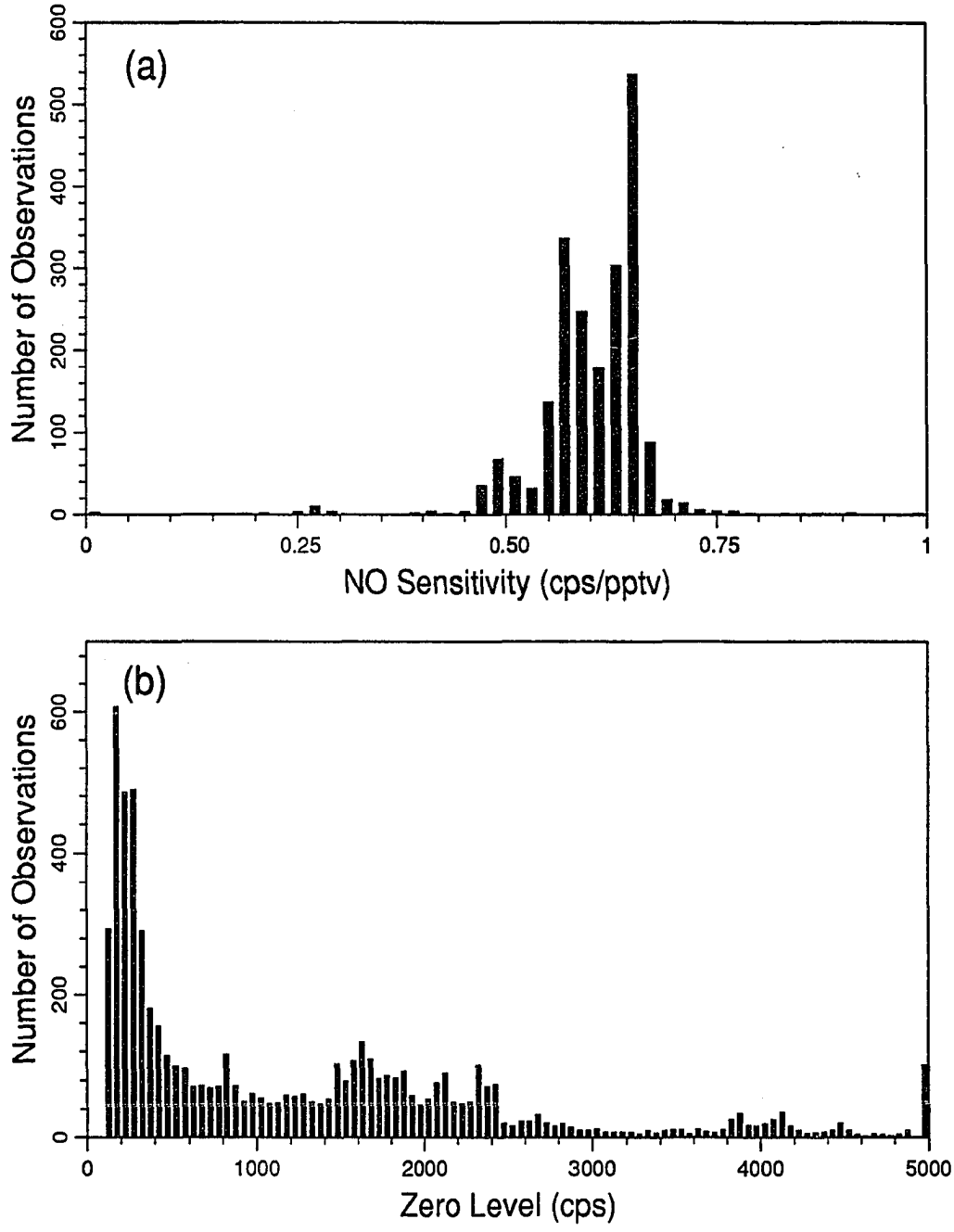

Figure 2.28 Frequency distributions of calibration parameters monitored during the 1988 campaign. (a) NO sensitivity. (b) Zero count rate.

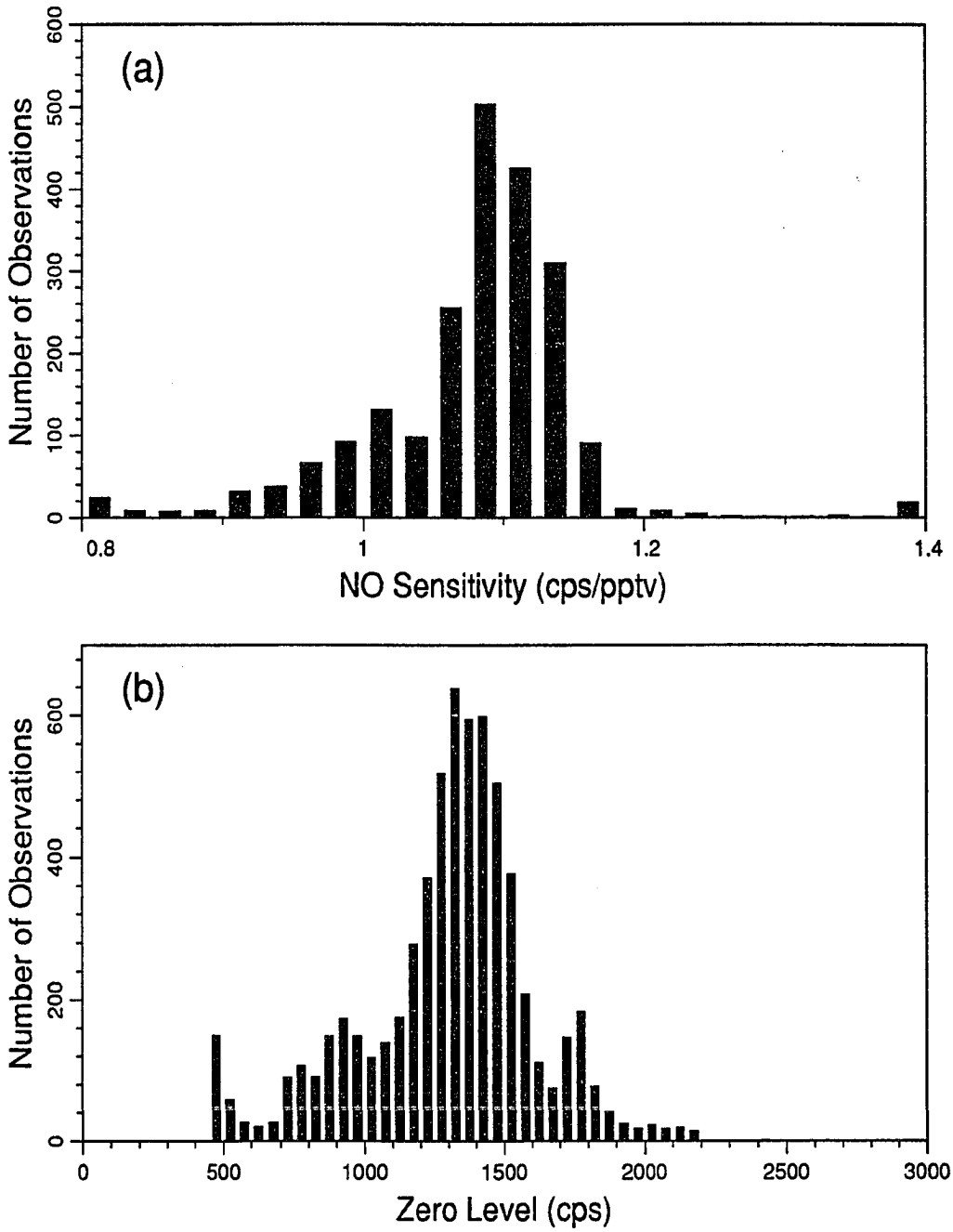

Figure 2.29 Frequency distributions of calibration parameters monitored during the 1989 campaign. (a) NO sensitivity. (b) Zero count rate.

During 1990, the full suite of calibration parameters was monitored, including NO sensitivity and NO sensitivity through the NO_y converter, the fraction of ambient NO removed by the zeroing procedure (fraction zeroed), and separate NO and NO_y zero levels, in addition to NO_2 conversion efficiency. The distributions of NO sensitivities are shown in Figure 2.30. Most of the measurements were in the range 1.0–1.4 cps/pptv for NO and 1.2–1.5 cps/pptv for measurements through the NO_y converter. Sensitivities measured through the NO_y converter were higher because the converter destroys ambient ozone [*Fahey et al.*, 1985], which otherwise reacts with ambient NO in the inlet tubing. The distribution of measured zeroing efficiencies is displayed in Figure 2.31. Most values prior to the fall were ~0.92–0.97. However, degradation of the ultraviolet lamp over time resulted in a lower zeroing efficiency, reaching values as low as 0.86 in December. The zero levels observed during 1990 are shown in Figure 2.32. NO_y zero count rates were generally 300–1500 cps, higher than those for NO (~300–800 cps) due to a contribution from the CO flow [*Fahey et al.*, 1985].

2.2.11 Uncertainty of the NO and NO_y Measurements

In the next sections, the quality control checks that were applied to ensure data validity are discussed, followed by uncertainty estimates for each of the three measurement campaigns.

2.2.11.1 Quality Control Checks

A number of methods were used to ensure that the instrument was operating correctly and producing reliable NO and NO_y measurements. These include

1. Checks on calibration parameters (sensitivity, fraction zeroed, and NO_2 conversion efficiency) to ensure that the calibration measurements were not erroneous due to transient impacts from nearby NO_x sources (e.g. vehicles at the

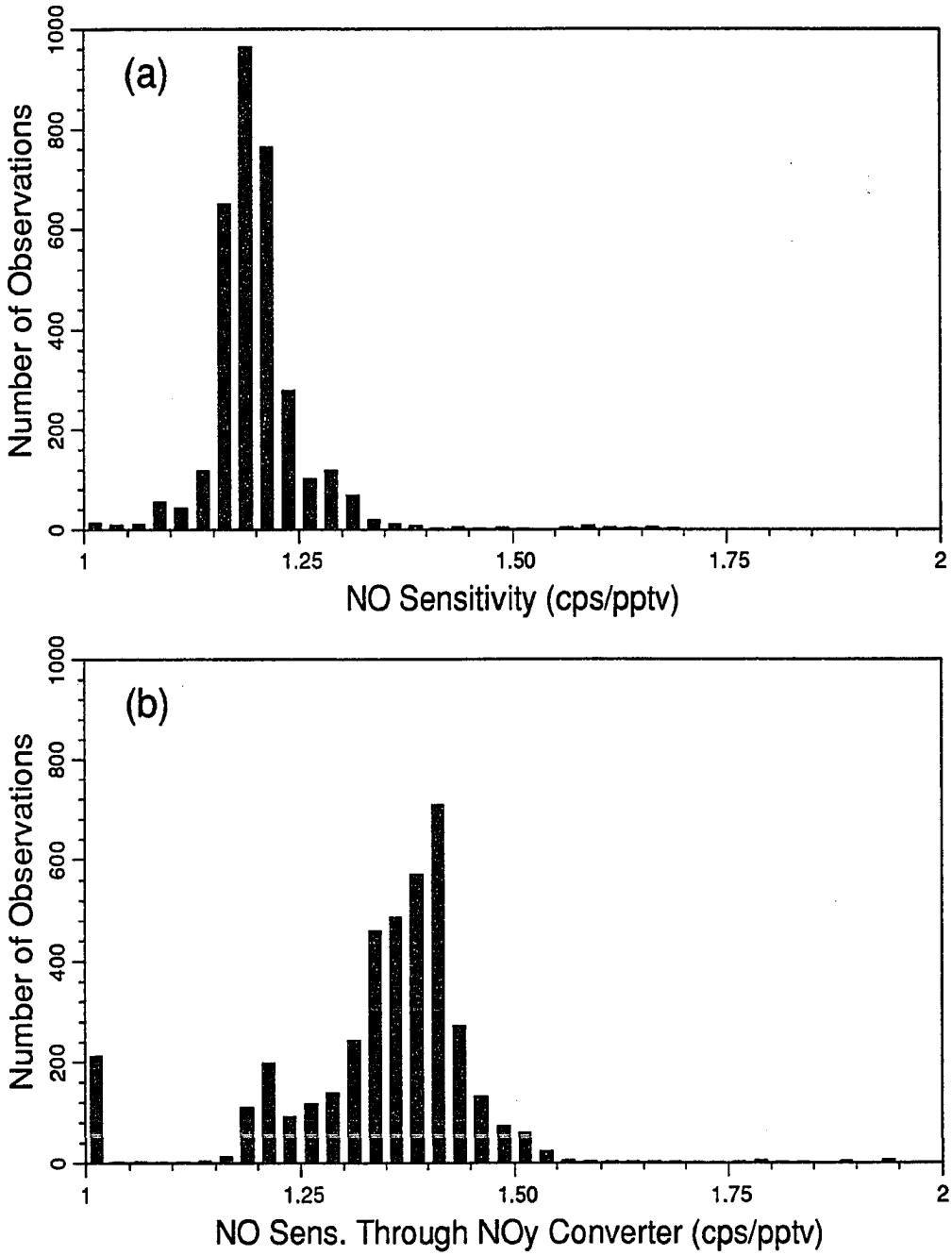

Figure 2.30 Frequency distribution of NO sensitivity measurements during the 1990 campaign. (a) NO sensitivity through the NO inlet. (b) NO sensitivity through the NO_y converter.

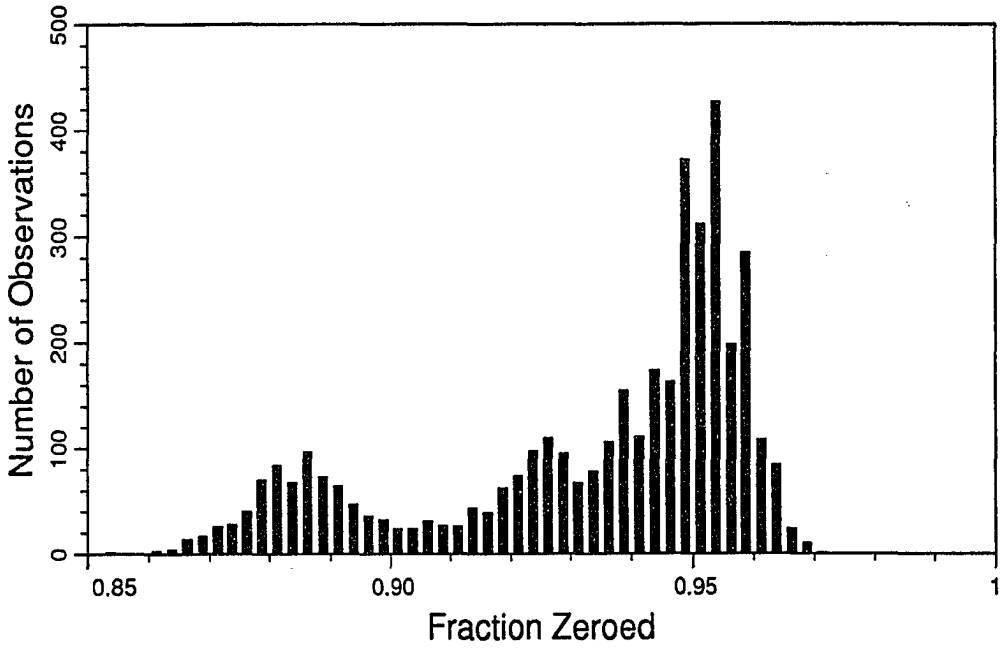

Figure 2.31 Frequency distribution of zeroing efficiency measurements during the 1990 campaign.

station) and to ensure that the instrument was operating normally.

2. Checks on the instrument zero levels to ensure that they were within the expected range and to ensure that variability in the counting rates observed during individual zero modes was close to that expected from counting statistics.

3. NO artifact tests, to ensure that the accuracy and precision of low-level NO measurements were adequate.

The checks on calibration parameters and zero levels used during the three measurement campaigns are discussed in this section. NO artifact tests were discussed in section 2.2.5.2.

1988 and 1989. The validity of the measurements made during the 1988 and 1989 campaigns was monitored using the ratio of the standard deviation of the NO

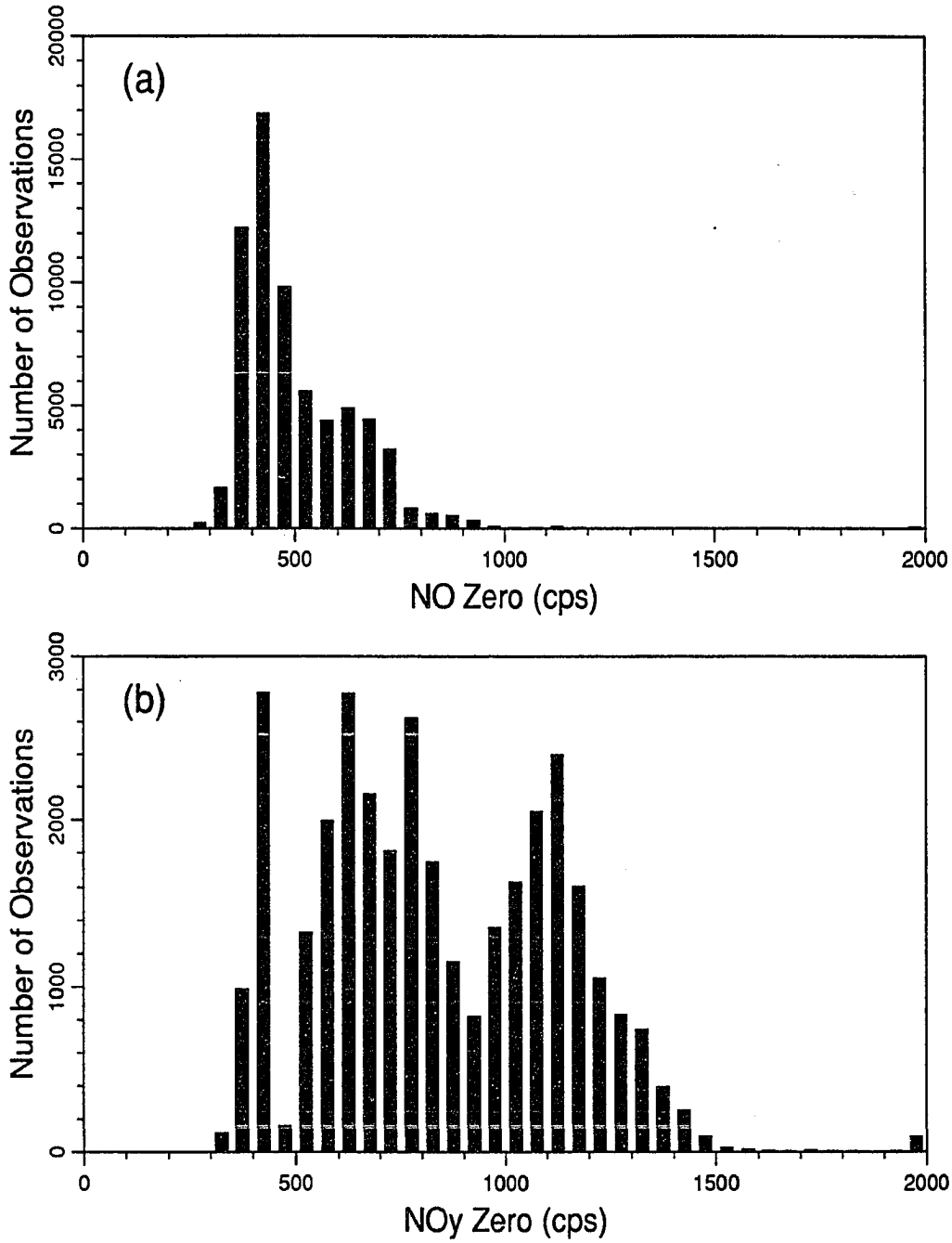

Figure 2.32 Frequency distribution of zero level measurements during the 1990 campaign. (a) NO zero. (b) NO_y zero.

and NO_y concentration estimates calculated by error propagation ($S_{[NO]}$ and $S_{[NO_y]}$) to the standard deviations expected from counting statistics alone. High values of this ratio accompanied errors in sensitivity measurement due to transient nearby NO_x sources (e.g. vehicles at the station). The measurements during 1988 and 1989 were screened by the standard deviation ratio, as described in chapters 3 and 4, and this screening effectively removed effects of erroneous calibrations. In addition, the spurious counts observed during 1988 (in which single-second spikes in the count rate were observed once every few minutes, as described in section 2.2.8.4) were screened from the raw data prior to calculation of any calibration parameters or concentrations. This was done by scanning the count rate measurements during the averaging period for each mode and calculating the mean and standard deviation for the period. Any count rate values more than two standard deviations from the mean were then discarded, and a new mean and standard deviation were calculated for each mode.

1990. Additional data validity checks were instituted prior to analysis of the 1990 data to further ensure the accuracy of the measurements. The data analysis program used to analyze the 1990 raw data (contained in Appendix B) contained checks on the validity of each calibration parameter. Calibration parameter and zero level measurements were considered valid only if the values fell within an acceptable range and if the variability in count rate observed during the calibration or zero mode was low. The variability criterion was met if the SRatio value for the mode was below a cutoff. The range and SRatio cutoffs that were used were selected based on an analysis of the 1990 data collected through August and are shown in Table 2.7, which also shows the fraction of calibration and zero measurements satisfying each test. These tests effectively screened out calibration measurements affected by temporary local pollution such as a vehicle driving to the station, as well as periods of instrument malfunctions. Relatively high SRatio values were necessary

for the calibration parameters. This was a result of small fluctuations in count rate observed during the calibration modes (section 2.2.9.2).

Table 2.7 Checks on Validity of Calibration Parameters During 1990.

Parameter	Acceptable[a] Range	Fraction[b] in Range	Maximum[c] SRatio	Fraction[b] With Lower SRatio
NO Sensitivity	1.0–2.0[d] cps/pptv	99.0%	10	97.0%
NO_y NO Sensitivity[e]	1.0–2.0[d] cps/pptv	98.5%	10	94.9%
Fraction Zeroed	0.85–1.0	95.8%	3	91.2%
NO_2 Conversion Efficiency	0.90–1.05[f]	86.1%	10	95.8%
NO Zero	300–2000 cps	95.6%	2	93.5%
NO_y Zero	300–2000 cps	95.1%	2	93.0%

[a]Ranges of the calibration parameters considered valid.
[b]Fraction of measurements during March–August satisfying the given constraint.
[c]Maximum acceptable value of SRatio(ratio of the observed standard deviation to that expected from counting statistics).
[d]1.0–1.5 for data set 3.
[e]NO sensitivity through NO_y converter.
[f]The acceptable range for conversion efficiency extends above 1.00 to allow for random variability in the conversion efficiency measurement.

Invalid calibration parameter or zero measurements were dealt with as follows. In the case of interpolated parameters (sensitivity, zero level, and fraction zeroed), if only one adjacent measurement was invalid, then the valid adjacent measurement was used. If both were invalid, then concentration estimates using that parameter were considered invalid and were flagged with an error code. For the conversion efficiency, which was based on a 5-point running average, all valid measurements among the nearest 5 observations were included. If none were valid, then NO_y concentration estimates at that time were flagged as erroneous.

For the valid calibration parameter and zero measurements, the standard deviation of the interpolated parameter was estimated using error propagation. This estimate of standard deviation was compared to the difference between the two measurements used in the interpolation and, if necessary, the estimated standard deviation was increased so that both adjacent measurements were within two standard deviations of the interpolated value. This was necessary only for zero measurements, and only when ambient concentration changes between successive zeros

changed dramatically, resulting in changes in zero level due to incomplete zeroing. As a result, this adjustment was rarely, if ever, necessary while measuring clean background air at Barrow.

2.2.11.2 Uncertainty Estimates

As discussed in section 2.1.1, uncertainty in the NO measurements results from three sources: calibration uncertainty, random variability due to photon counting noise, and uncertainty in the instrumental artifact correction. For NO_y measurements, uncertainty also results from uncertainty in the NO_y conversion efficiency. Estimates of the contributions of these components to the total uncertainty, discussed individually in the previous sections, are summarized here and used to estimate NO and NO_y uncertainties applicable to each measurement campaign.

NO Calibration. The NO concentration in the calibration gas was known to ±2% (section 2.2.6.1). Estimated accuracy of the calibration gas mass flow controller (MFC) was 7%, 7%, and 2% during the 1988, 1989, and 1990 measurement campaigns, respectively (section 2.2.6.3). The corresponding accuracies for the sample MFC were 5% for all three measurement campaigns. Thus, the total accuracy of the NO sensitivity measurements were 9%, 9%, and 6% for the 1988, 1989, and 1990 measurements, respectively.

Artifact Correction. Uncertainty in the NO artifact correction was the primary determinant of the NO detection limit during the 1988 and 1989 campaigns (section 2.2.5.2). The accuracy of the artifact correction was estimated to be 50 pptv in 1988 and 75 pptv in 1989. In 1990, reduced artifact variability resulted in an estimated accuracy of ±3 pptv in the artifact level.

Photon Counting Noise. In the absence of artifact correction uncertainty, random variability due to counting statistics would determine the NO detection limit.

The 2σ uncertainty due to counting noise (at low NO concentrations) is given by

$$\text{NO Uncertainty (pptv)} = \frac{2}{S_{NO}}\sqrt{\frac{2Z}{N}}, \tag{2.38}$$

where S_{NO} is the sensitivity (cps/pptv), Z is the zero count rate (cps), and N is the averaging period (s). Typical values of S_{NO} and Z (section 2.2.10.3) and averaging periods (see section 2.2.9.1) for the three campaigns result in estimated NO uncertainties (2σ) of 4–29 pptv, 4–10 pptv, and 4–9 pptv for the 1988, 1989, and 1990 campaigns, respectively. For the 1990 campaign, a higher zero level during NO_y measurements resulted in a somewhat higher NO_y detection limit of 5–14 pptv,

NO_y Conversion. During the 1988 and 1989 campaigns, uncertainties in the NO_2 conversion efficiency measurements resulted in estimated accuracies of the NO_y measurements of 50% and 31%, respectively. During the 1990 measurements, regular measurement of the NO_2 conversion efficiency resulted in much lower uncertainty in its value (<10%). The conversion efficiency for other NO_y compounds was not measured during 1990. Tests with the same converter during an instrument intercomparison shortly after the 1990 measurement period (section 2.4) indicated complete conversion of PAN but only partial (~50%) conversion of n-propyl nitrate. Based on these results, and the current understanding of NO_y speciation in the Arctic (discussed in the following chapters), the uncertainty resulting from the assumption that the NO_y conversion efficiency was equal to the NO_2 conversion efficiency is estimated to be 25%.

Total Uncertainty. The total estimated uncertainties of NO and NO_y measurements from the three campaigns are calculated by propagation of errors and are presented in Table 2.8, along with a summary of the contributions from the individual error sources discussed above.

Table 2.8 Uncertainty of the NO and NO_y Measurements.

	Source of Uncertainty				Total Estimated Uncertainty	
	Calibration	NO Artifact	Photon Counting Noise	NO_y Conversion Efficiency	NO[a]	NO_y[a]
1988	9%	50 pptv	4–29 pptv	50%	50 pptv or 9%	50 pptv or 51%
1989	9%	75 pptv	4–10 pptv	31%	75 pptv or 9%	121[b] pptv or 32%
1990	6%	<10[c] pptv	4–9 pptv	20%	3 pptv or 6%	15[d] pptv or 26%

[a]Total uncertainty is the larger of the two values listed.
[b]Calculated based on the NO uncertainty of 75 pptv and the minimum observed NO_2 conversion efficiency of 62%.
[c]Uncertainty of a single 40 s-average measurement. Uncertainty can be reduced by averaging many measurements, to a minimum uncertainty of 3 pptv.
[d]Based on photon counting statistics, using the higher NO_y zero count rate (see text).

2.3 The Measurement Site

The measurements presented in this thesis were made at the National Oceanic and Atmospheric Administration (NOAA) Climate Monitoring and Diagnostics Laboratory (CMDL) station at Barrow, Alaska (formerly designated a Geophysical Monitoring for Climatic Change (GMCC) station) [*NOAA*, 1989]. This station (at 71°19′ N, 156°37′ W, 9 m msl) is located approximately 7 km from the town of Barrow, as shown in Figure 2.33. The site was established in 1972 and was chosen as a location where the prevailing winds would minimize contamination from local anthropogenic emission sources [*Bodhaine et al.*, 1981]. The prevailing wind blows from the northeast, with calm periods (wind speed <1 mph) being rare (<1% of observations) [*Bodhaine et al.*, 1981].

The "clean" sector between the headings of 20° and 145°is free of local anthropogenic NO_x sources save an occasional snowmobile or all-terrain vehicle. Winds are from this sector >50% of the time [*Bodhaine et al.*, 1981]. There are a number of important local sources in other directions, most of which are located along the coast beginning at the town of Barrow and continuing to the northeast. The town of Barrow (population 3,100) is located at a heading of 235° from the measurement site. Along the coast NE from the town and continuing to a heading of due north from

the CMDL site are a number of other NO_x sources. These include the Barrow dump (where garbage is frequently burned); the Ukpeagvik Inupiat Corporation/Northern Arctic Research Laboratory (UIC/NARL) complex (a hotel/office/laboratory complex); and the distant early warning (DEW) site and runway used by the U.S. military. Winds blowing from any of these sources are enriched in NO_x from fuel combustion emissions. Somewhat further up the coast is the "Duck Camp," located at a heading of approximately 20°, which is used during the summer by some local residents for outings and as a temporary residence. Automobile traffic and fuel combustion in and around the camp occur intermittently during summer. In addition, a dirt road which continues past the Duck Camp to Point Barrow is occasionally travelled during summer. Two additional areas—the South and East Barrow Gas Fields—are sometimes sources of NO_x emissions. The fields are located at headings of approximately 145° and 185° from the measurement site. Buildings associated with natural gas wells in these fields are electrically heated, and no pumps are used to recover the pressurized natural gas. Prior to 1990, there were no combustion sources associated with the fields, aside from occasional vehicle usage within the fields. However, gas-fired heaters were installed at well heads in the two fields during 1990 (11 18,000-BTU and 3 5,000-BTU heaters), and these were operated on a continuous basis after installation (B. Allen, Allen and Crouch Engineers, Barrow, AK; private communication, 1990).

The Barrow site is characterized by cold temperatures and frequent low-level temperature inversions year-round. Monthly-average temperatures range from a low of -28°C in February to 3.7°C in July. The frequent low-level temperature inversions are surface-based approximately 39% of the time on a year-round basis [*Kahl*, 1990]. Wind reaching the measurement site is frequently of marine character—the upwind fetch from the site includes <2 km of land within the nearest 14 km when winds are between 0° and 120°. The land surface near the station is of low relief and characterized by short tundra plants and many lakes and ponds.

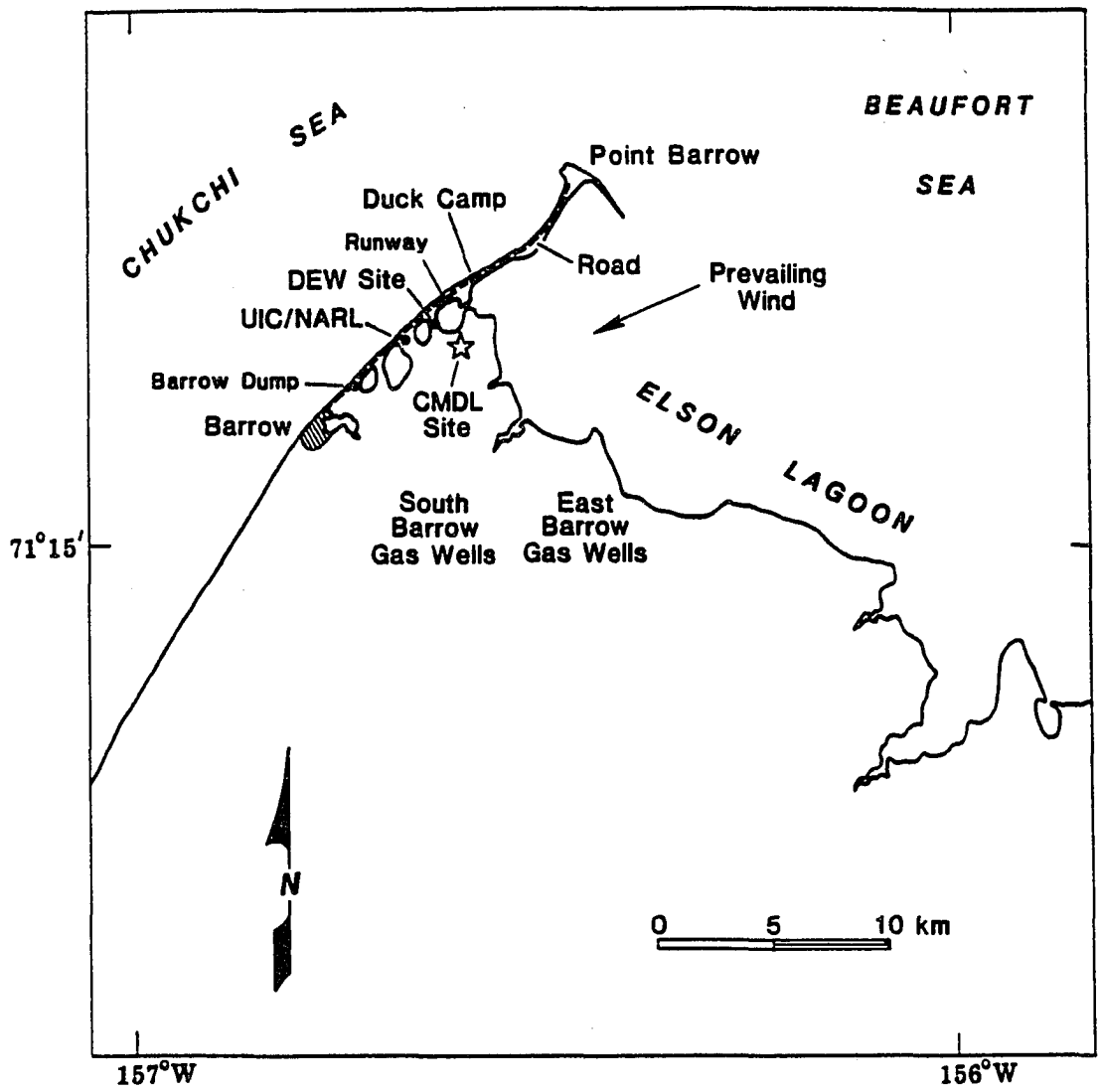

Figure 2.33 The location of the measurement site and nearby pollution sources. Nearby sources of NO_x emissions identified on this figure are discussed in the text (Based on *Bodhaine et al.*, [1981]).

The CMDL site was staffed by two full-time technicians who provided experimental support. In addition, during the 1988 and 1989 measurement campaigns other researchers at the site monitored the operation of the NO/NO_y instrument during periods when the author was absent. During the longer 1990 measurement period, CMDL staff conducted weekly instrument checks and maintenance, activities which required approximately 1–2 hr per week of CMDL staff time. These included checks of a number of instrument parameters, a 4–8 hr bakeout of the NO_y converter, and retrieval of the previous week's data to a floppy disk, which was mailed to the author. The data were generally reviewed weekly so that instrument malfunctions could be quickly identified. In addition, approximately five trips to the CMDL site were made by the author during 1990 for instrument setup/takedown and for maintenance.

Meteorological parameters (wind, temperature, and dewpoint) were measured at the site [*NOAA,* 1991], and these measurements were used in analysis of the NO and NO_y data. In addition, twice-daily temperature soundings were conducted from a National Weather Service station in Barrow.

2.4 Instrument Intercomparison

An intercomparison was conducted between the UAF NO/NO_y monitor used at Barrow during 1990 and a similar instrument developed and operated by a group from the NOAA Aeronomy Laboratory (AL). The goal of the intercomparison was to test the UAF instrument against a more fully characterized machine. The AL group had previously taken part in another instrument intercomparison in which their instrument performed well [*Fehsenfeld et al.,* 1987]. During this intercomparison, measurements of NO and NO_y in ambient air were used to determine the relative accuracy and precision of the two instruments. In addition, standard addition tests of NO and other NO_y compounds (NO_2, PAN, n-propyl nitrate, and HNO_3) were

used to assess the relative accuracy of NO_y measurements by the two groups. Participants in the intercomparison included the author, Daniel Jaffe (UAF), David Parrish (AL) and James Carpenter (AL). Paul Goldan (AL) acted as the intercomparison referee.

2.4.1 Site and Instrument Descriptions

The intercomparison took place from February 5–15 1991 on the Green Mesa, approximately 1 km west of and 110 m above the Department of Commerce laboratories in Boulder, Colorado [*Fehsenfeld et al.*, 1987]. Air reaching the intercomparison site can range in characteristics from polluted to relatively pristine, as winds vary from the direction of the Denver-Boulder corridor to the unpopulated region to the west. As a result of such wind shifts and inversion height changes, NO and NO_y concentrations at the site can vary over several orders of magnitude in a matter of minutes. During the intercomparison, NO_y concentrations ranged from ~800 pptv to more than 100 ppbv and NO concentrations ranged from below detection limit to 72 ppbv.

The two groups' instruments were set up in adjacent trailers, with both inlets on the roof of the AL trailer, approximately 1 m apart. Both groups used downward-facing 1/4 inch o.d. teflon tubing as inlets. The UAF instrument was configured as described in Section 2.2.1, except for the modifications required to reduce the inlet tubing upstream of the NO_y converter to approximately 20 cm, in order to reduce potential tubing equilibration and adsorption problems. To accomplish this, the inlet and calibration solenoid valves upstream of the NO_y converter were removed, separate inlets were used for the NO and NO_y channels, and calibrations were performed manually. As a result, the calibration procedure was modified somewhat. The sequence of modes was identical to that described in section 2.2.9.1 on page 80, but the line carrying the calibration gas was manually inserted into tees in the NO and NO_y inlets at the proper times and the equilibration periods for each mode were

increased to allow time for the operator to do this. Because human intervention was necessary during calibration, the instrument was calibrated less frequently (once each 4–12 hr). During the remaining time, NO and NO_y measurements were made (i.e., modes 6–10 of Table 2.5 were repeated indefinitely). In order to obtain simultaneous measurements from the UAF and AL instruments, the equilibration and averaging times shown in Table 2.5 were modified—60 s equilibration and averaging periods were used for each mode.

The AL group used two instruments: one cycling between two NO_y converters and one cycling between NO and NO_x measurements. These instruments have been described elsewhere [*Fehsenfeld et al.*, 1987]. Concentration estimates from the two groups were based on 60 s averages for both NO and NO_y for the purposes of this intercomparison. The timing of the two sets of NO and NO_y measurements was synchronized in order to eliminate differences due to short-term ambient variability. Nevertheless, differences of 1–10 s built up over the 4–12 hr data acquisition cycles. As a result, some scatter between the two measurements was expected during periods of rapidly changing ambient concentrations.

2.4.2 Specified Uncertainties and Preliminary Observations

Prior to beginning the intercomparison, each group supplied the referee with estimated uncertainties for their NO and NO_y measurements. The uncertainties of the AL measurements were expected to be similar to previously reported values for the AL instruments: an NO uncertainty of $\pm 10\%$, with a 2 pptv detection limit [*Parrish et al.*, 1990]; and an NO_y uncertainty of $\pm 15\%$, with a detection limit of <10 pptv [*Fehsenfeld et al.*, 1987].

The estimated uncertainty of the UAF NO_y measurement was based on the fact that the NO_y conversion efficiency was measured only for NO_2, so the conversion efficiency for other NO_y compounds could potentially be different from the measured value. The resulting uncertainty was estimated to be approximately 20%.

For NO, uncertainty at high concentrations was estimated to be approximately 6%, the value estimated for the 1990 Barrow measurements (section 2.2.11). At lower concentrations, however (below ~1 ppbv), the initial performance of the instrument indicated that an uncertainty significantly higher than that estimated for the 1990 Barrow measurements was appropriate. During the initial setup period, the standard deviations of observed photon counting rates were higher than expected from counting statistics (by a factor of ≥ 4), even in the absence of ambient concentration changes. The standard deviation of individual nighttime NO measurements (when ambient NO was apparently absent) was approximately 20 pptv, and the distribution of nighttime NO measurements did not appear to follow a Poisson distribution, as expected from counting statistics. Based on these observations, the precision of the NO measurements was estimated to be 60 pptv (3σ) prior to the beginning of the intercompared measurements.

The observed high variability in photon counting rates is attributed to electronic noise problems. Two potential sources of electronic noise which may have contributed to the observed increase in detection limit were identified. First, the ozonator was damaged in transit and two of the three electrodes were broken. They were replaced with used electrodes, but it was not possible to adequately cover the replacements with "corona dope." Significant coronas and/or arcing were observed around the electrodes throughout the intercomparison and may have led to radio-frequency and electrical (line) noise. Indeed, moving the ozonator from its initial location on a shelf above the PMT to the top of the rack resulted in a reduction of the observed photon count noise level. Second, the electrical wiring in the trailer containing the UAF instrument had been damaged, such that the ground wire in one circuit was not properly grounded. This resulted in a 60 VAC potential between the grounds in two circuits in the trailer and apparently damaged the I/O board in the computer, which had to be replaced. All portions of the instrument were subsequently connected to a single circuit, but grounding problems may still have

contributed to the observed noise problem.

2.4.3 Results

2.4.3.1 Ambient Measurements

NO_y Measurements. There were 905 simultaneous NO_y measurements ranging from 0.8–100 ppbv. (Periods when AL reported NO_y concentrations above 100 ppbv were not intercompared, since the UAF photon counter was configured such that concentrations above 100 ppbv were not measurable.) Figure 2.34a shows a scatter plot of the NO_y data, with a 1:1 line and the least-squares linear regression fit to the data. The regression results are summarized in Table 2.9. The slope of the regression line (0.939±0.002; one standard deviation of the slope) is significantly different from unity, indicating a small bias between the two groups' measurements. However, the bias is within the estimated accuracy of the two groups.

Table 2.9 Regression of UAF and AL Measurements During the Intercomparison.

	Slope	Intercept	r^2	Degrees of Freedom
NO_y (all data)	0.939 ± 0.002	31 ± 46	0.994	903
NO (all data)	1.043 ± 0.003	37 ± 19	0.997	598
NO[a]	1.043 ± 0.003	23 ± 21	0.997	523

[a]Before 5 p.m. February 14.

Analysis of the ratio of $[NO_y]_{UAF}/[NO_y]_{AL}$ yields a similar result. Figure 2.34b shows values of this ratio as a function of $[NO_y]_{AL}$. The data are divided into bins of 100 measurements of increasing $[NO_y]_{AL}$ (with 105 points in the rightmost bin), and the lines in the figure cross at the mean AL concentration and mean ratio (UAF/AL) for each bin. The vertical lines extend ±1 standard deviation of the ratio, while the horizontal lines show the range of $[NO_y]_{AL}$ for each bin. The mean and standard deviation of the ratio over the entire data set are 0.94 and 0.07, respectively. The mean value is statistically different from unity at the 99% confidence level, again indicating a small bias between the two sets of measurements. An estimate of the

precision of the agreement between the two groups can be gained from the standard deviation of the ratio. Over the range 10–100 ppbv, one standard deviation of the ratio is approximately 5%. The standard deviation increases to ~7% from 2–10 ppbv and increases further to ~10% below 2 ppbv.

NO Measurements. The NO data set contains 600 points and is shown in Figure 2.35a, together with a 1:1 line and the linear regression fit. The horizontal dotted line in the figure indicates the UAF detection limit of 60 pptv, and it is clear that there is substantial scatter in the UAF results at low NO levels, well above the estimated uncertainty of 60 pptv. However, an inspection of the data revealed that most of the scatter is due to measurements during the last night of the intercomparison (the night of February 14–15, 1991). During that night, there were several periods when the UAF measurements indicate significant NO was present ($\geq$100 pptv), while the AL measurements were <10 pptv.

The results of both the UAF and AL measurements during the last night have been inspected and do not indicate a malfunction of either group's instrument. The raw UAF data (five second-average cps values) do not indicate measurement error. Similarly, inspection of the level and variability of count rates observed during UAF zero modes did not indicate an instrument malfunction. The UAF instrument was operated in the laboratory after the intercomparison and at that time the instrument was still capable of determining NO at levels of <10–20 pptv. NO_y concentrations during this period were high (~10–50 ppbv) and the two groups' NO_y measurements agreed well.

Despite analysis of the raw data, the cause of the discrepancy in NO measurements during the last night was not identified. Possible explanations include (*i*) a leak from the UAF calibration line (which was manually attached to a purge vacuum); (*ii*) conversion of a small fraction of the ambient NO_y to NO within the UAF inlet lines by an unknown contaminant; and (*iii*) malfunction of the AL instrument

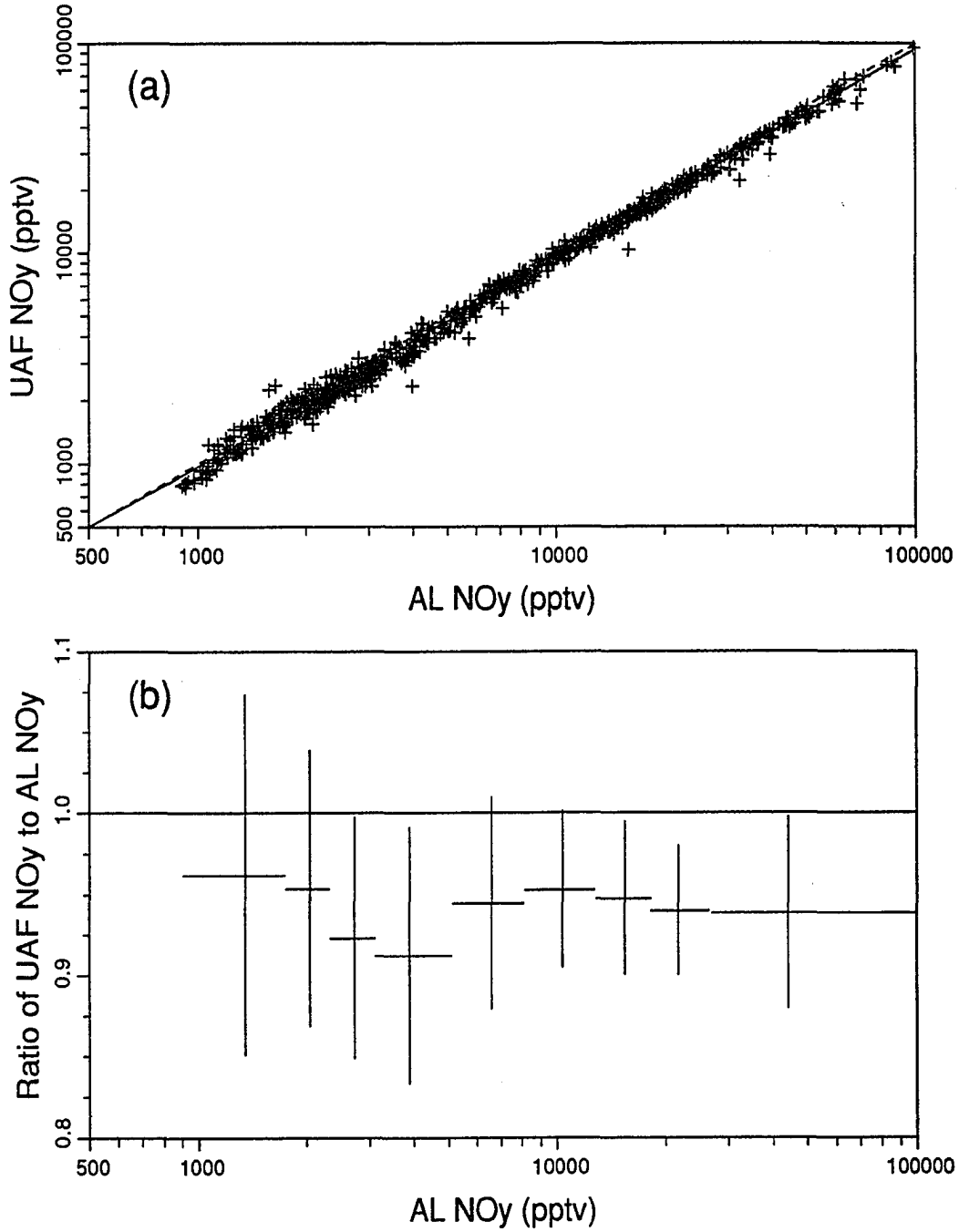

Figure 2.34 Ambient NO_y measurements during the intercomparison. (a) Scatter plot of all simultaneous NO_y measurements with $[NO_y]_{AL}$<100 ppbv. The solid line indicates a 1:1 relationship, and the result of a least-squares linear regression of the data is shown by the dashed line. (b) Plot of $[NO_y]_{UAF}/[NO_y]_{AL}$ versus $[NO_y]_{AL}$. The measurements are binned into groups of 100 points of increasing $[NO_y]_{AL}$ (with 105 points in the rightmost bin). The crosses indicate the average value of $[NO_y]_{UAF}/[NO_y]_{AL}$, while the horizontal lines span the range of $[NO_y]_{AL}$ in each bin. The vertical lines extend ±1 standard deviation of the concentration ratio.

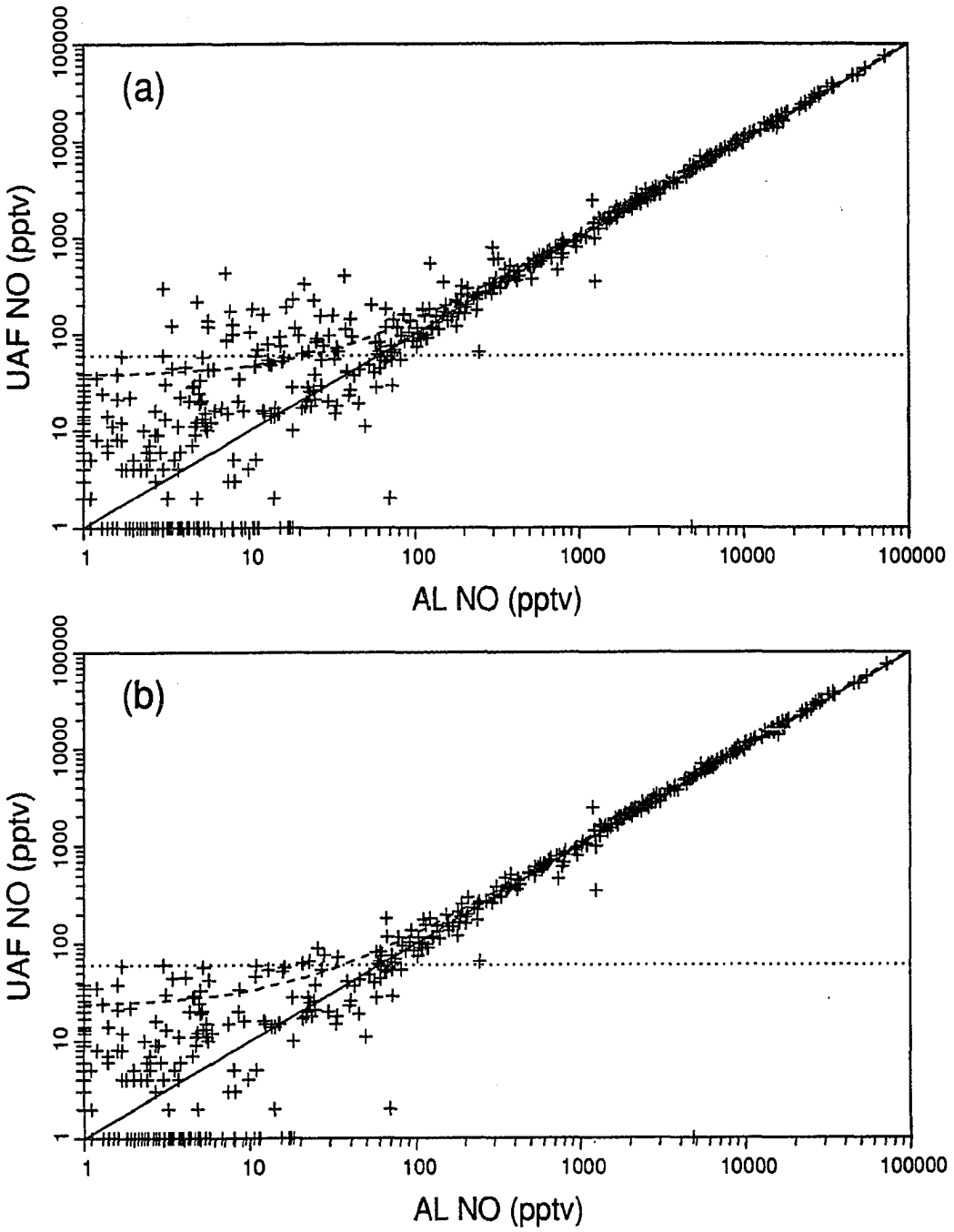

Figure 2.35 Scatter plots of UAF and AL NO measurements during the intercomparison. Measurements below 1 pptv are plotted as 1 pptv. The solid line corresponds to $[NO]_{UAF}=[NO]_{AL}$ and the dashed line shows the result of a least-squares linear regression of the measurements. The UAF detection limit of 60 pptv is indicated by the dotted line. (a) All data. (b) All data before 5 p.m. February 14, 1991.

resulting in erroneously low NO measurements.

Although it was not possible to identify a cause of the divergence in results from the last night, the results from that night are clearly different from those from the rest of the intercomparison. Therefore, the measurements from that night were removed from the data set described below. The remaining data set includes all measurements before 5 p.m. February 14, a total of 525 points, with NO concentrations from below detection limit to >70 ppbv. These data, displayed in Figure 2.35b, are highly correlated (r^2 =.998). It is apparent from that figure that 60 pptv was an adequate estimate of the UAF detection limit prior to the last night. There are some remaining outliers in Figure 2.35b. However, an individual inspection of each of the outliers (with concentration differences greater than 60 pptv and 20% of $[NO]_{AL}$) indicates that all occurred during periods of rapidly changing ambient concentrations, indicating that the differences were likely due to imperfect synchronization of the two instruments.

Results of a regression analysis of the NO data prior to the last night (shown by the dashed line in Figure 2.35b and summarized in Table 2.9) indicate excellent agreement between the two datasets, with no significant intercept and a slope less than 5% different from 1. The ratio of $[NO]_{UAF}$ to $[NO]_{AL}$, shown in Figure 2.36 for all measurements with $[NO]_{UAF}$ above 100 pptv, is also close to 1. The average ratio for all the points included in that figure is 1.06 (SD_{mean} = 0.01, N=272). For lower concentrations, the ratio is larger—for points with UAF NO from 60–100 pptv, the average ratio is 2.1 (SD_{mean}=0.8, N=24). However, the mean absolute difference in this range is only 30 pptv, and only 2 points have a difference greater than the UAF detection limit of 60 pptv again indicating that the measurements were in agreement to within the stated uncertainties.

A comparison between the UAF and AL data at low NO levels in lightly polluted air can give additional information concerning any possible bias in the data sets. Measurements obtained during nighttime periods (19:00–05:00 local time) when

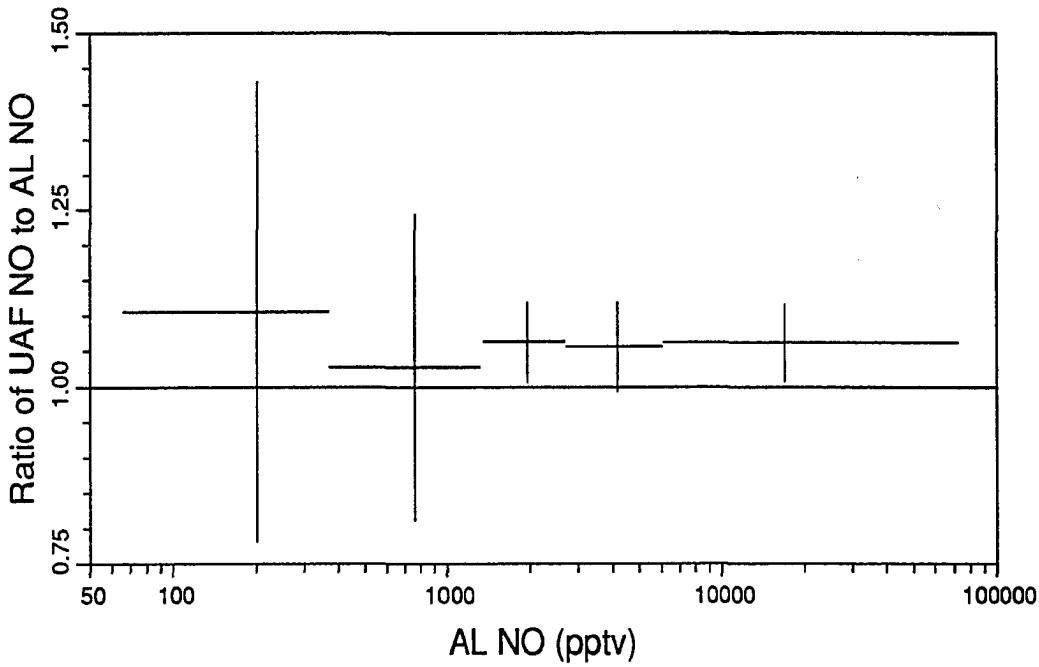

Figure 2.36 Ratio of $[NO]_{UAF}$ to $[NO]_{AL}$ during the intercomparison. The measurements are binned into groups of 50 points of increasing $[NO]_{AL}$ (with 72 points in the rightmost bin). The crosses indicate the average value of $[NO]_{UAF}/[NO]_{AL}$, while the horizontal lines span the range of $[NO]_{AL}$ in each bin and the vertical lines extend ± 1 standard deviation of the concentration ratio.

ozone was at least 25 ppbv were extracted from the data set (D. Parrish, private communication to D. Jaffe, 1991). A total of 312 points satisfied these criteria. Of these, six had NO concentrations of 100 pptv or greater in either data set. If these 6 points are excluded, the AL data average 2.6 pptv with a standard deviation of 7.6 pptv and the UAF data average 2.4 pptv with a standard deviation of 19.3 pptv. Thus, there is no evidence of a bias larger than $\sim$3 pptv in either data set. In addition, this analysis is consistent with the estimated UAF detection limit of 60 pptv (3σ).

2.4.3.2 Standard Addition Tests

A number of standards were intercompared, including NO, NO_x, PAN, HNO_3, and n-propyl nitrate (NPN). The results of the standard intercomparisons are shown in

Table 2.10. These tests were conducted by adding a small flow (<10 sccpm) of the specified standard at the sample inlet while sampling ambient air. The standard was added either through a tee or by inserting a 1/8 inch o.d. tube containing the standard into the 3/16 inch i.d. inlet tube.

Table 2.10 Calibration Gas Standard Addition Tests.

	Emission Estimate (nmole/min.)		
Standard Source	UAF	AL	$\frac{\text{UAF}}{\text{AL}}$
UAF NO standard	1.05	1.038	1.01
AL NO standard	0.521	0.517	1.01
UAF NO_x (g.p.t.)[a] standard	1.08[b]	1.13	0.956
AL NO_x(g.p.t.) standard	0.501[b]	0.51	0.98
AL NO_x(perm.)[c] standard	1.97[b]	2.02	0.975
PAN source	0.22[b]	0.20	1.1
NPN source	0.054[b]	0.104	0.52
NPN source (500°C)[d]	0.102[b]	0.098	1.04
HNO_3 source	0.528	0.25	2.11
HNO_3 source	—[e]	0.59	(0.89)[f]

[a]Gas phase titration.
[b]Uncertainty due to ambient variability during measurements is approximately 20%.
[c]Permeation source.
[d]Converter at 500°C to ensure complete conversion.
[e]Measurement was not made.
[f]Estimated using the UAF HNO_3 measurement from the first HNO_3 test and the second AL HNO_3 measurement.

Tests using the two groups' NO and NO_x standards indicated agreement within estimated accuracies. The agreement between the NO emission estimates was very good (1%). For the NO_x sources, the UAF measurements were 2-4% lower than those of the AL group, still within estimated accuracies. The PAN intercomparison also showed agreement between the two groups well within the reported 20% uncertainty of the UAF measurements during standard addition tests using ambient air. (A 20% uncertainty was estimated for the ambient-air standard addition tests, based on variation of ambient NO_y concentrations during the tests.)

The NPN comparison was conducted somewhat differently than than the others, because initial tests indicated that the NPN source was unstable. To ensure that both groups were measuring the same NPN concentration, the NPN flow was

diluted with approximately 2.5 slpm of humidified zero air in a manifold and was sampled simultaneously by the two groups. As shown in Table 2.10, the NPN test indicated a poor conversion by the UAF converter at the standard temperature of 300°C. To quantify the NPN conversion efficiency, both groups measured the NPN concentration at a converter temperature of 500°C, which is expected to result in complete conversion [*Bollinger et al.*, 1983]. At 500°C, the measurements agreed well. Comparisons of the UAF and AL measurements at 300° and 500° indicates that NPN conversion by the UAF instrument at 300°C was approximately 50–55%. It should be noted that the UAF conversion of NO_2 was measured to be >98% at this time, at 300°C.

Tests of nitric acid were conducted on two occasions, using a permeation source in the AL trailer. However, the results of these tests were not reproducible. For example, on one occasion the AL measurement varied by a factor of two, depending on whether the calibration source was added at a tee on the inlet or inserted into the inlet.

2.4.3.3 Zero Air Tests

A synthetic zero air cylinder was evaluated by both groups for its NO and NO_y content. The results of these measurements are shown in Table 2.11. Measurement difficulties prevented precise determinations of NO or NO_y in the synthetic air with the UAF instrument. During the dry synthetic air tests, large increases in the UAF instrument's zero level were observed (several thousand cps). In addition, the zero level was not stable, but rose and fell. By averaging for a long period, it was possible to obtain an NO determination with a precision of <10 pptv. The increase in zero level was even larger when measuring NO_y, however, and a reproducible NO_y measurement was not possible.

This behavior was in contrast to that observed during synthetic zero air tests at Barrow during 1990, when increases in the instrument zero level of <100 cps were

Table 2.11 Synthetic Zero Air Tests.

Zero Air Test	AL Result (pptv)	UAF Result (pptv)
Dry zero air		
NO	7.1	4±9
NO_y	29.0	330[a]
Moist zero air		
NO_y	107	130 [a]

[a]Measurement uncertainty was not determined, but was believed to be high due to a high and fluctuating instrument zero signal (see text).

generally observed. Since the absolute humidity at Boulder was quite high, relative to the dry zero air and relative to typical conditions at Barrow, equilibration to the dry zero air was considered a possible cause of the high count rates, and an attempt was made to use humidified zero air to reduce the equilibration period. The humidification did greatly reduce the problem, but zero levels and variability were still much higher than those observed at Barrow. In addition, the AL determinations of NO_y in the same zero air tank were different, depending on whether dry or humidified zero air was used. This problem was not solved, and as a result the NO_y zero air comparisons are considered highly uncertain.

2.4.3.4 Performance of the UAF Instrument

Performance of the UAF instrument during the intercomparison was degraded somewhat in comparison to the previous operation at Barrow. As discussed above, elevated standard deviations of NO measurements were noted during the setup period and persisted throughout the intercomparison. However, an additional indicator of degraded instrument performance was noted after the intercomparison. There was a systematic difference between the instrument zero measurements made before and after each NO measurement, with the second zero approximately 18 cps greater than the first. Although the cause of this discrepancy could not be identified, the primary difference between the two zero measurements is that the first came after an NO_y

zero measurement, while the second followed an ambient NO measurement. Thus, the problem may have been related to equilibration of the zeroing system to the sample flow, particularly if the zero purge flow were not equal to the sample flow. However, it was not possible to determine whether this was the case. Alternatively, the problem may have been related to the electronic noise problems described above, but a mechanism for such a relationship has not been identified. Data from the last night of the intercomparison were specifically evaluated to determine whether differences between the two zeros could have caused the discrepancy between UAF and ALl NO measurements during that night. There was no evidence that this was the case.

In order to determine whether this problem was limited to the Boulder intercomparison, the last data set from Barrow (December 1990) was checked for any difference between the two zeros. None was found. In addition, the instrument was set up in the laboratory after the intercomparison and a similar test was conducted. Although a small difference between the two zeros was still observed, the magnitude (about 8 cps) was significantly less than that during the intercomparison.

Because of the difference observed between the two zero measurements, it was necessary to modify the data analysis procedure somewhat. Instead of using a zero level calculated by interpolating between the zeros surrounding each measure mode, only the zero before each measure mode was used. The true zero level was still estimated by interpolation, but the interpolation used the next valid (i.e., immediately before a measure mode) zero reading. It was necessary to use the first zero for these calculations—use of the second zero would have resulted in an NO artifact of approximately -15 pptv. By using the first zero only, the artifact was much closer to zero. Based on the seven nights during which low NO levels were observed, the average artifact level was 0.3 pptv, with a standard deviation of the seven nightly-average values of 2.0 pptv. (Each nightly-average artifact value was based on approximately 200 60-s-average NO observations during the ~14 hour night.)

Finally, the large amount of variability in ambient NO and NO_y concentrations at the intercomparison site resulted in uncertainties in the standard addition calibrations of the UAF instrument above those present in the previous Barrow measurements. Concentrations often varied enough within a single calibration cycle to significantly affect the calculated calibration parameters. Calibrations were generally attempted every 4–8 hours, but exceedingly large ambient variability resulted in only about one valid calibration per day, on average. As a result, no attempt was made to follow changes in the calibration parameters within the comparison period. Instead, a single value of each calibration parameter was used throughout the study. (The NO_y conversion efficiency was an exception—separate conversion efficiencies were used before and after a converter bakeout that was conducted on February 8.)

Table 2.12 summarizes the calibration parameters used in data reduction. These values were calculated by averaging all calibration measurements that were not affected by large ambient variability. Also shown in Table 2.12 are the estimated uncertainties of each calibration parameter, calculated as twice the standard deviation of the approximately 15 values.

Table 2.12 UAF Calibration Parameter Values During the Intercomparison.

Calibration Parameter	Average Value	Estimated Uncertainty
NO Sensitivity	1.24 cps/pptv	9.6%
NO_y Sensitivity[a]	1.38 cps/pptv	12%
Fraction Zeroed	0.983	0.2%
NO_2 Conversion Efficiency	0.95–0.99[b]	8–13%[b]

[a]NO sensitivity through the NO_y converter.
[b]Separate values were used before and after a converter bakeout conducted February 8, 1991.

2.4.4 Conclusions

The results of this intercomparison indicate that NO and NO_y measurements made by the two groups agreed to within the specified measurement uncertainties in most

cases. The ambient NO measurements above 100 pptv agreed to within approximately 6%. The results indicate that the UAF measurements were slightly higher than the AL values, but the difference was within the specified measurement accuracy. The ambient NO_y measurements were also in reasonable agreement, with the AL measurements approximately 6% higher than the UAF values, again within the specified accuracies. Measurements of low ambient NO concentrations obtained prior to the last night of the intercomparison indicated that the precision of each group's measurements was approximately equal to the value estimated prior to the intercompared measurements, and further indicated that no bias greater than approximately 3 pptv was present in either group's results. However, NO measurements obtained during the last night diverged to a much larger extent than expected from the estimated measurement uncertainties. The cause of this divergence could not be determined, although malfunction of either of the instruments cannot be excluded.

The standard addition tests of NO, NO_x, and PAN support the conclusion of no significant differences in the two groups' measurements. However, tests of NPN indicated that the UAF NO_y instrument detected only approximately 50% of the total NPN concentration when operating under standard conditions. Standard addition tests of nitric acid were also conducted. The results of these tests were not reproducible, apparently as a result of inlet losses of HNO_3 or an unstable HNO_3 source. In one pair of sequential measurements by the two instruments, the AL result was ~50% of the UAF measurement.

Measurements of NO in synthetic zero air were in agreement and indicated a low concentration (4–7 pptv) of NO in the zero air. The results of NO_y zero air tests were inconclusive. This was due to of equilibration difficulties encountered with the UAF instrument when sampling zero air and variable AL results which depended on whether the zero air was dry or humidified.

In conclusion, the results of this intercomparison indicate that the estimates of

instrument uncertainties submitted by the two groups prior to the intercompared measurements were adequate estimates of the true uncertainties in ambient measurements. Low conversion of NPN by the UAF instrument and irreproducible nitric acid measurements by the AL instrument underline the value of regular conversion efficiency tests of NO_y species besides NO_2. The UAF NO_y converter apparently converted only about half of the NPN during these tests. However, even if the conversion efficiency for NPN and other alkyl nitrates were only 50% throughout the 1990 Barrow measurement campaign when this converter was used, it is unlikely that this would result in an error of more than 25% in the Barrow NO_y measurements, based on measurements of alkyl nitrates in the Arctic (*Bottenheim et al.*, [1991]; discussed in section 5.2.3.1).

Chapter 3

Summer 1988 Measurement Campaign

The first field use of the NO/NO_y detector took place at the Barrow CMDL site July 14—August 19, 1988. As discussed in the previous chapter, a variable NO artifact signal resulted in an uncertainty of the NO measurements of approximately ±50 pptv. Uncertainty in the NO_y measurements is primarily due to imprecise knowledge of the NO_y conversion efficiency of the molybdenum converter used during this campaign, as described in section 2.2.7.1, and is conservatively estimated to be ±50%. The values reported here are not corrected for non-unity NO_y conversion.

The use of computer data acquisition made it possible to store information on the variability of ambient concentrations during each 120-second data acquisition mode. The expected standard deviation of photon counts is known, based on counting statistics. The actual standard deviation of the counts observed during each second of the 120-second period was stored, and could be compared with the expected value to gain information on the ambient variability. During periods in which clean

This chapter is based on material previously published as Honrath, R. E. and D. A. Jaffe, Measurements of nitrogen oxides in the Arctic, *Geophys. Res. Lett.*, *17*, 611–614, 1990.

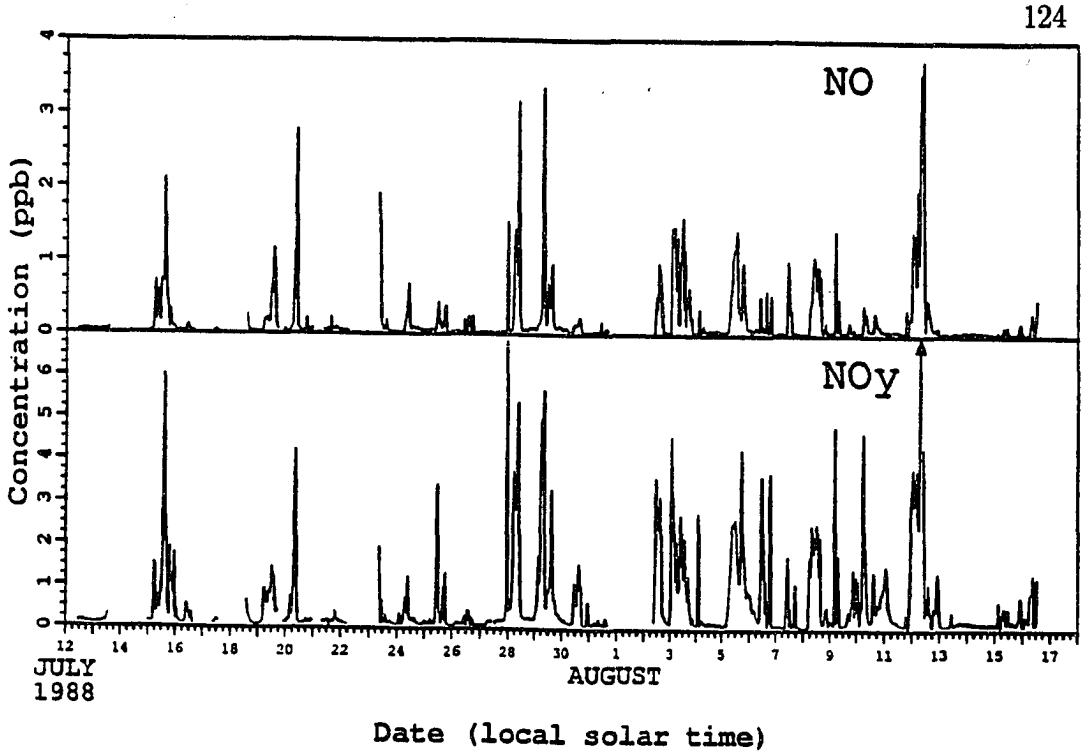

Figure 3.1 Hourly averages of the unscreened NO and NO_y measurements during July–August, 1988.

air was being sampled, the ambient variability was small, but when local (Barrow) sources impacted the site, variability increased. This observation was used to screen the data. In the screened data reported below, all values with observed variability greater than twice that expected from photon counting statistics have been omitted. This procedure was very effective in screening out effects of local sources, such as emissions from vehicles driving to and from the monitoring site and local (Barrow) stationary sources.

3.1 Results

Concentrations measured during the 37-day sampling period (July 14 - August 19, 1988) reached maxima of 6.5 ppb NO and 13.7 ppb NO_y, before any screening procedures. Hourly averages of these measurements are shown in Figure 3.1.

The high concentrations shown in Figure 3.1 were accompanied by large variability, indicating local pollutant sources. To eliminate these effects, the data were screened based on variability as described in the previous section. This screening greatly reduced the range of concentrations—maximum screened NO and NO_y concentrations are 1.7 and 2.8 ppbv, respectively. The median, mean, and standard deviation for NO_y are 130, 245, and 354 pptv, respectively. The median and mean for NO are both below detection limit (50 pptv). These data were screened only by variability, and not by wind direction, and they demonstrate the frequency of low concentrations at the Barrow site under all wind conditions, as well as the occasional occurrence of much higher concentrations.

During the sampling period, winds from the direction of local sources (section 2.3) were unusually frequent. In order to ensure that all concentrations reported here are of clean background air unaffected by local anthropogenic sources, the data were screened again to include only periods in which the local wind direction was from a sector containing no local sources (45–130°). In addition, data after a wind shift were omitted until measured values reached an apparent steady-state. This screening removed all of the high-NO_y periods apparent in Figure 3.1, with one exception. On August 11, NO_y concentrations were elevated (to 1.5 ppbv), despite winds from 65–90°, a sector in which local sources are absent. This period was also eliminated from the clean-sector data record. However, measurements made during 1989 and 1990 (chapters 4 and 5) demonstrated that events similar to the one that occurred on August 11, 1988, are not infrequent at the Barrow measurement site and are generally attributable to NO_x emissions from the Prudhoe Bay oil-producing region 300 km to the ESE.

The screened, clean-sector data include 65 hours in portions of 8 days. These screened, clean-sector data are discussed in the remainder of this chapter. A histogram of the clean-sector NO_y concentrations is shown in Figure 3.2. The 175 values range from below 50 to 300 pptv. The median, mean, and standard devi-

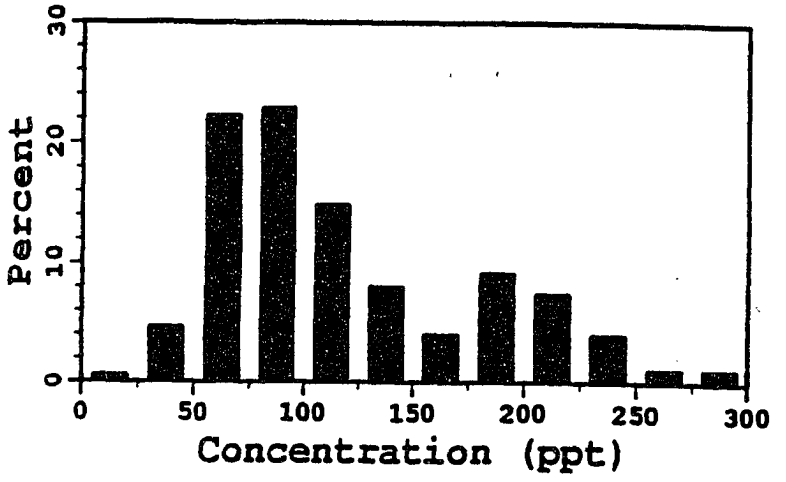

Figure 3.2 Histogram of clean-sector NO_y measurements during July–August, 1988 (N=175).

ation are 100, 120, and 60 pptv, respectively. NO concentrations were generally below our detection limit of 50 pptv, and the maximum observed was 100 pptv.

3.2 Analysis and Discussion

Hourly averages of the clean-air NO_y concentrations are shown in Figure 3.3 for each day, as a function of time of day. The concentrations exhibit a tendency to increase during midday, with lowest values near midnight. The mean daytime concentration of 140 pptv (6 am – 6 pm local solar time) is 40 pptv greater than that at night (6 pm – 6 am local solar time) (significant at the 99.9% confidence level). However, this difference is based on only 5 separate periods of clean-air measurements, most of which were significantly less than 24 hr in length. Therefore, the presence of a diurnal cycle cannot be identified conclusively.

There are several possible causes of the observed diurnal variation. First, variations in boundary-layer conditions could produce the observed NO_y cycle. On most days during our sampling period, a low cloud cover and/or fog formed in late evening, and remained until mid-morning the next day. NO_y removal at night (by cloud droplets or dry deposition) followed by daytime mixing with elevated concen-

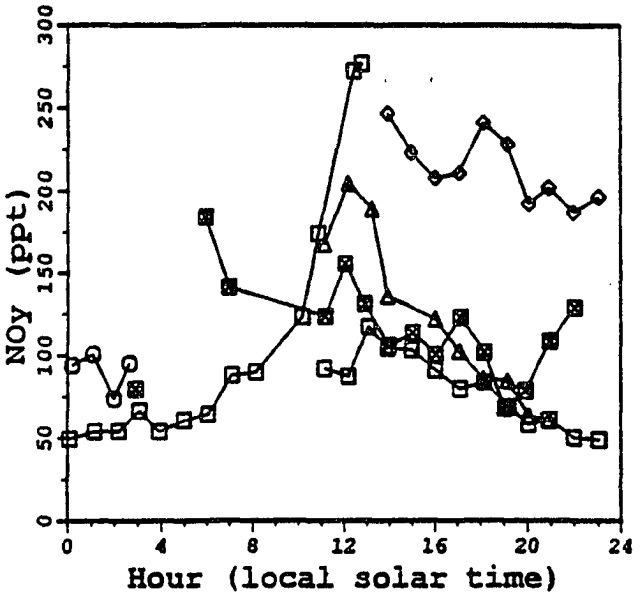

Figure 3.3 The diurnal cycle of clean-sector NO_y during July–August, 1988. Hourly-average data from separate periods are plotted with different symbols: squares, 11am July 12, 1988—1pm July 13; circles, midnight July 14–3am July 15; triangles, 11am–9pm July 24; diamonds, 2pm–11pm July 28; crossed squares, 6am August 4–3am August 5.

trations aloft could account for the observed cycle. Second, biological production of NO, which increases with soil temperature [*Williams et al.*, 1987], is also a potential cause of the diurnal cycle. During this period, the ambient temperature ranged from −2 to 15°C, and averaged 4°C. Apparent diurnal variation due to instrumental drift is considered unlikely, since instrument parameters were closely monitored. Since only clean-sector measurements were included in this analysis, it is unlikely that the diurnal trend is due to local anthropogenic activities. However, as noted above, the observed diurnal cycle may be an artifact resulting from the fact that the clean-air data set was composed of a small number of relatively short periods. Therefore, the observed difference between daytime and nighttime NO_y could be a result of concentration changes between the separate periods rather than a true diurnal cycle. Additional measurements are necessary to conclusively demonstrate the presence or absence of a diurnal NO_y cycle at Barrow. (See section 5.2.3.3 for analysis of diurnal variations in the 1990 NO_y measurements.)

The low NO_y concentrations reported here are similar in magnitude to those observed in other regions remote from anthropogenic NO_x sources, which range from 100 to 250 pptv (median values) [*Kelly et al.*, 1980; *Helas and Warneck*, 1981; *Stedman and McEwan*, 1983; *Hübler et al.*, 1989]. However, they are much lower than concentrations observed previously during springtime aircraft flights in the Arctic, which ranged 600–1000 pptv in the boundary layer [*Dickerson*, 1985]. The strong seasonal dependence indicated by this comparison indicated a need for additional measurements to adequately characterize nitrogen oxides in the Arctic. The measurements presented in the following chapters, made at Barrow during 1989 and 1990, address this need. Summertime NO_y measurements at Barrow are discussed further in section 5.2.3.1 of chapter 5—The 1990 Measurement Campaign.

Chapter 4

Spring 1989 Measurement Campaign

This chapter presents NO_y data from a 5-week measurement campaign conducted at the NOAA CMDL station near Barrow, Alaska, during the spring of 1989. These data support the general notion of "arctic haze:" the long-range transport of pollution to the Arctic from distant anthropogenic sources. However, the NO_y observations additionally indicate the existence of a significant regional pollution source which should be taken into account in future arctic air pollution studies.

Section 2.2.11.2 contains an analysis of the sources of measurement uncertainty during this campaign. The NO detection limit is estimated to be 75 pptv, a value which resulted from variability in the instrument artifact level. Above the detection limit, NO uncertainty is the greater of 15% and 75 pptv. The uncertainty of the NO_y measurements is estimated to be the greater of 31% and 120 pptv, primarily

This chapter is based on material material previously published as Jaffe, D. A., R. E. Honrath, J. A. Herring, S.-M. Li, J. D. Kahl, Measurements of Nitrogen Oxides at Barrow, Alaska During Spring: Evidence for Regional and Northern Hemispheric Sources of Pollution, *J. Geophys. Res.*, *96*, 7395–7405, 1991.

due to uncertainty in NO_2 conversion efficiency.

During this measurement period the background NO concentration was always below the detection limit, while the maximum NO level measured in air unaffected by Barrow was 1.4 ppbv (see discussion of "events" below). Background NO_y concentrations ranged from 230–1200 pptv. Thus, although measurement uncertainty limits the utility of the NO data set, its impact on the NO_y data is less severe.

4.1 Results

NO and NO_y were measured nearly continuously from March 2–April 7, 1989 (Julian days 61–97). The total data record includes many periods when emissions from local (Barrow) sources impact the site. These sources include the town of Barrow, the UIC/NARL complex, and the DEW Line site covering the upwind sector from 235°–320°, as described in section 2.3. Over about one-half of the remaining wind sector, intermittent small sources may be present. These consist of occasional vehicles several km from the site and airplanes (generally <1/day) using a runway ~1.5 km away. In addition, vehicles traveling to and from the station (about 2 trips per day) and occasional snowmobile use at the station can affect measurements.

To avoid impacts of local (Barrow) sources, the data were screened using an objective method based on ambient variability. First, all data were discarded when winds were from within 10° of the large continuous sources (225°–330°). In the remaining sector, data affected by intermittent local sources were screened using ambient variability, based on the standard deviation of the counting rate during each 100-s data accumulation period. During periods when local sources impact the site, the ambient variability is high, while the variability is much lower when clean air is sampled. In this screening method the expected standard deviation of counting rate (accumulated over each 10 s) was calculated, based on counting statistics ($s_{cs} = \sqrt{\overline{x}/10}$, where $\overline{x}$ = the average counting rate in counts per second).

The data were then screened by requiring all valid data to have an observed counting rate standard deviation s_{obs} such that $s_{obs} \leq \alpha s_{cs}$, where α is the maximum ratio allowed (discussed below).

The data presented here are thus divided into several periods, each of which is free of local (Barrow) impacts. These periods each satisfy the following criteria: (1) wind is not from the "dirty sector" (225°–330°); (2) Ambient variability is low ($s_{obs} \leq \alpha s_{cs}$); (3) average wind speed is >2 m/s (a level sufficient to avoid local impacts); and (4) NO and NO_y data are continuous, or the missing sections include only winds from the "clean sector." (The clean sector contains no continuous or intermittent local sources, and includes the sector 5°–130° during spring). To avoid residual effects after a wind change, the first 4 hours of any period satisfying these criteria were discarded (unless previous NO_y data were missing and only clean-sector winds were observed for at least 4 previous hours). One exception to the ambient variability criterion was allowed: if a single data point did not satisfy criterion (2), but the surrounding points did, it was assumed to be due to a vehicle at the CMDL site or an instrumental malfunction, and only that data point was discarded. It is believed that this screening process effectively removed all effects of local emissions on the data record. In some cases the objective screening method required the rejection of periods that did not appear to be affected by local sources. However, this is preferable to the use of a subjective screening method which is less clearly defined and reproducible.

In the data presented below 2 types of periods satisfying the above criteria are described: "background periods" and "events." "Background periods" correspond to times when NO and NO_y concentrations were relatively constant and were low (relative to the overall data record). They include all periods satisfying the above criteria with $\alpha = 2.0$. This value of α requires that ambient variability be very low. Inspection of the raw data also revealed several "events," during which ambient concentrations changed smoothly and reached high values while winds were generally

from the clean sector (5°–130°). During these events, which are described in detail below, s_{obs}/s_{cs} was greater than 2, but the relatively high s_{obs} was due to smooth changes in ambient concentrations, rather than random ambient variability. Therefore events are defined as periods satisfying the above criteria with $\alpha = 6.0$ and a maximum NO_y concentration of >3 ppbv. In several cases background periods and events were contiguous. In these cases the background period was ended and the event started before NO_y concentrations began to increase.

Eleven background periods were identified, and are summarized in Tables 4.1 and 4.2. Concentrations varied very little during individual periods, but larger differences were observed between periods. In at least some cases, these differences are related to meteorology, as discussed below. A histogram of all NO_y measurements during background periods (N = 885) is shown in Figure 4.1. The mean and median of the background NO_y data are 598 and 616 pptv, respectively. NO concentrations during the background periods were all below the detection limit of 75 pptv. There was no systematic variation in background levels with wind direction, indicating that the screening methodology was adequate.

Table 4.1 Summary of Spring 1989 Background Periods.

Background Period Number	Time (C.U.T.)[a] Start Day	Start Hour	End Day	End Hour	Wind Direction (Degrees)	Average Wind Speed (m/s)	Average Temperature (°C)
1	69	0647	69	1839	178–220	10.6	-4.8
2	71	1023	71	1400	124–167	6.5	-12.0
3	73	0238	73	1624	51–128	2.4	-8.9
4	75	1307	76	0939	338–10	6.6	-23.5
5	78	0300	78	1100	345–8	5.6	-24.2
6	83	0234	85	1700	46–109	10.6	-24.0
7	86	0351	87	1800	112–175	6.0	-22.2
8	90	0344	90	1000	119–137	5.5	-23.3
9	94	0417	94	1356	125–197	9.2	-17.3
10	96	0534	96	1841	153–191	9.4	-14.3
11	97	0443	97	1400	195–213	11.9	-3.7

[a]Coordinated Universal Time.

Four events were observed during the sampling period—they are shown in Fig-

Table 4.2 NO_y Concentrations During the Spring 1989 Background Periods.

Background Period Number	NO_y Concentration (pptv)				
	N	Median	Mean	S.D.	Range
1	64	473	467	56	354–720
2	18	352	353	19	314–385
3	76	278	284	32	230–378
4	101	689	694	64	512–937
5	44	732	736	30	687–864
6	214	617	622	64	537–793
7	153	559	562	48	482–743
8	36	845	850	48	768–921
9	55	547	611	99	514–875
10	72	734	764	79	665–1203
11	52	578	596	45	545–706

Note: NO was below the detection limit of 75 pptv.

Table 4.3 Summary of the Spring 1989 Events.

Number	Time (C.U.T.)[a] Start		End		NO_y Range, ppbv	NO Range, ppbv	Wind Direction, Degrees	Wind Speed,[b] m/s	Average Temperature, °C
1	67[c]	1100[d]	68	2143	.53–16.38	0–1.13	115–155	8.0	-20.1
2	85	1700	86	0351	.55–3.09	0–1.15	104–135	7.7	-20.6
3	87	0800	89	1830	.56–9.87	0–1.40	98–173	5.7	-24.1
4	90	1000	90	2148	.77–4.22	0–1.17	130–166	4.3	-26.3

[a]Coordinated Universal Time.
[b]Averaged over each background period.
[c]Julian day.
[d]Hour.

ure 4.2 and summarized in Table 4.3. NO concentrations were well above detection limits and highly correlated with NO_y levels during daylight periods. NO_y reached a peak of 16.4 ppbv (during event 1), and NO reached 1.4 ppbv (during event 3).

4.2 Analysis and Discussion

4.2.1 Background Periods

The 11 background periods include those times when NO_y concentrations were the lowest measured, were relatively constant, and were unaffected by local NO_x sources.

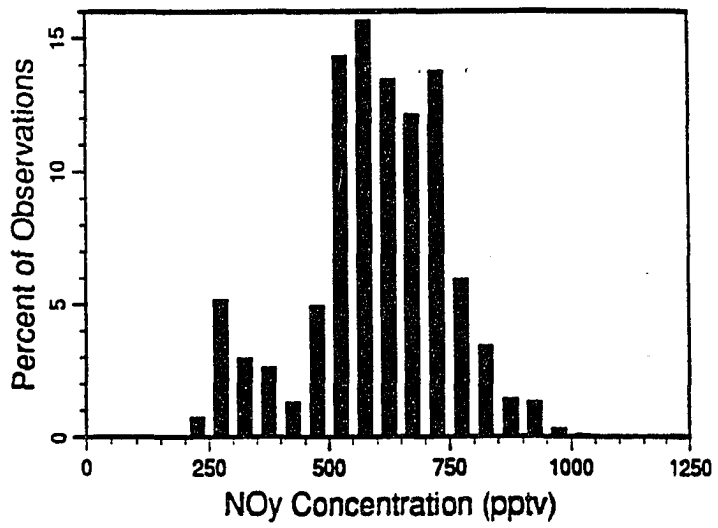

Figure 4.1 Histogram of NO_y concentrations during the spring 1989 background periods.

NO_y levels during these periods ranged from 230–1,200 pptv, with an overall median of 616 pptv. Median levels during individual periods ranged from 280–850 pptv. NO concentrations were always below the detection limit of 75 pptv. Based on the photostationary-state calculations described below (section 4.2.2.1), NO_x levels must have been below ~150 pptv during clear midday periods.

Springtime arctic NO_y concentrations have been measured previously by *Dickerson* [1985]. After correction for artifact measurement errors (R. Dickerson, personal communication to D. Jaffe, 1988), those aircraft measurements are in broad agreement with the present ground-level observations. Dickerson's measurements in the boundary layer ranged from 600 to 1000 pptv, with a few higher values. These are in the upper portion of the range observed at Barrow, or slightly higher. Free-tropospheric NO_y reached 1000–1600 pptv in polluted layers, and was about 300–400 pptv outside the layers. The NO_y concentrations measured at Barrow are similar to Dickerson's outside polluted layers, and are 1/3 to 1/2 of the levels in polluted layers.

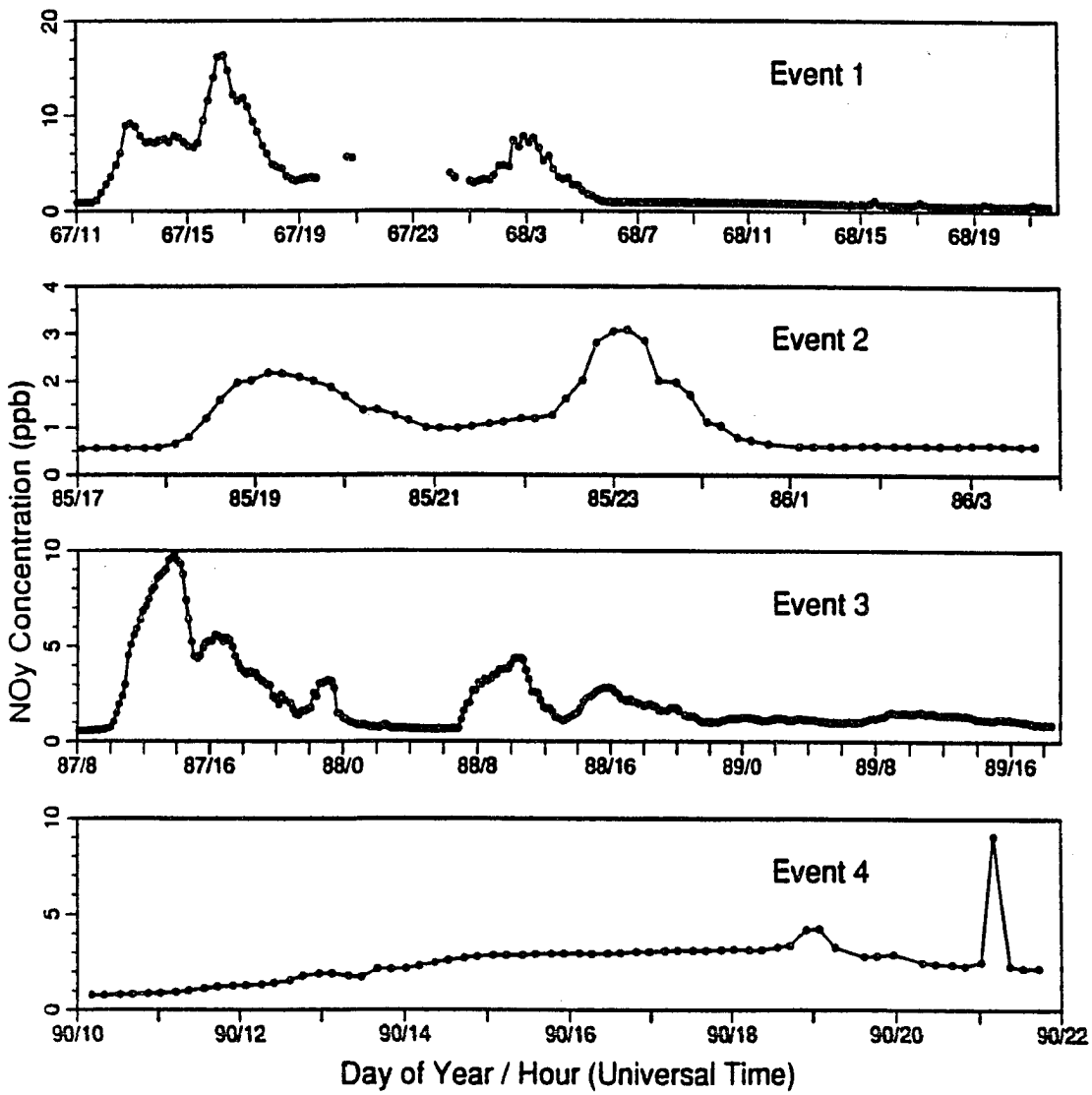

Figure 4.2 NO_y concentrations during the spring 1989 events. X-axis labels show day of year/hour (Coordinated Universal Time).

4.2.1.1 Trajectory analysis

Ten-day isobaric back-trajectories at 850-mbar [*Harris*, 1982] have been used to gain an understanding of the past history of the air sampled during each background period. However, large uncertainties often exist in the results of isobaric trajectory calculations applied to the Arctic [*Kahl et al.*, 1989]. Comparison of 850- and 1000-mbar trajectories during some background periods indicates that significant vertical wind shear was present and implies that the 850-mbar trajectories may not accurately represent transport in those cases [*Kahl et al.*, 1989]. Trajectories during the remaining periods, which have consistent 850- and 1000-mbar trajectories, may be divided into two types: (1) Arctic type, which pass over the Arctic Ocean (including the Beaufort and/or Chukchi Seas); and (2) Bering/south type, which pass over the Bering Sea and/or the Pacific Ocean. Examples of the two trajectory types are shown in Figure 4.3.

The highest background NO_y levels were observed during periods with Arctic trajectories—3 of the highest 5 are of this type (periods 4, 5, and 6). In addition, the second-highest (period 10) occurred during a transition between Arctic and Bering/south.

Lower NO_y levels occurred during periods with Bering/south trajectories. During period 3, with the lowest NO_y concentration, trajectories indicate that the air being sampled had spent the previous ≥ 7 days south of the Brooks Range in the Alaskan interior. Periods 1 and 2, with the third and second lowest NO_y concentrations, respectively, also occurred during transport from the south. During these two periods, 850-mbar trajectory indicates transport from south of the Brooks Range for ≥ 5 days. However, significant wind shear is apparent in a comparison of the 850- and 1000-mbar trajectory levels, so a more precise identification of the source region during those periods is not possible.

This trajectory analysis is consistent with the understanding of a generally con-

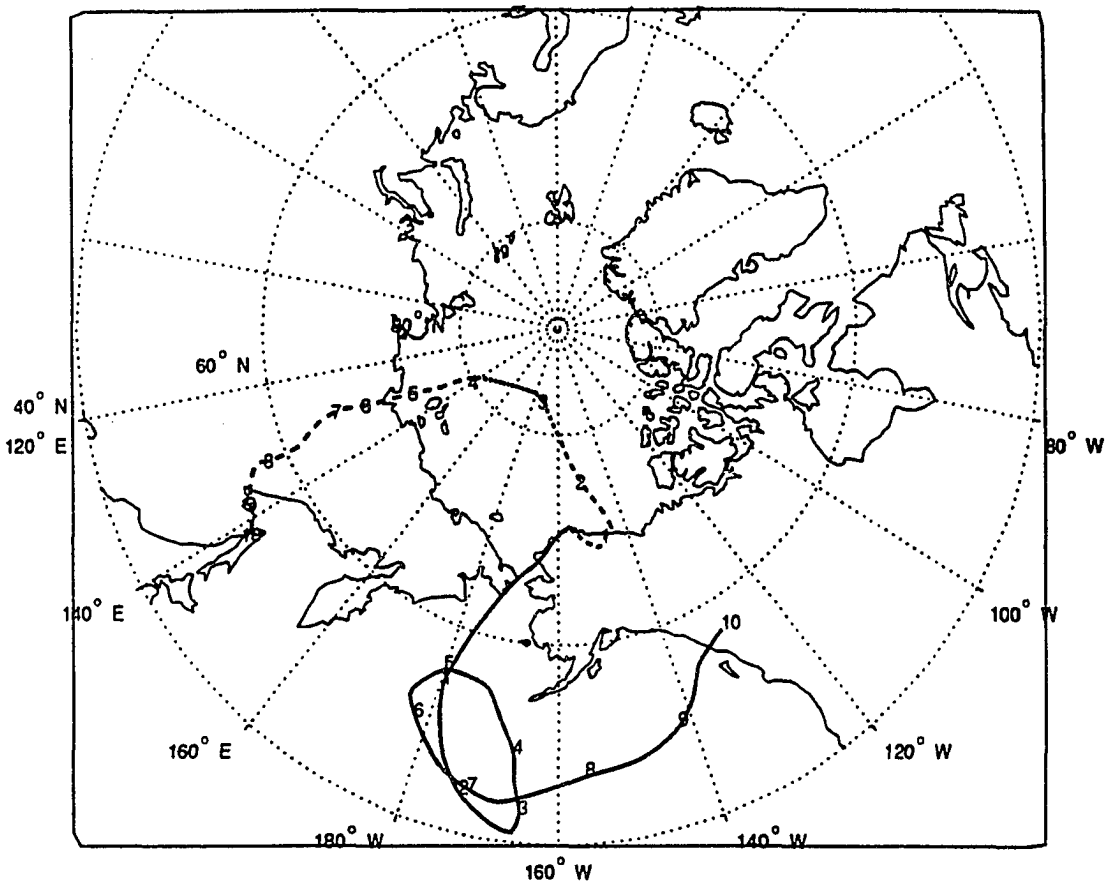

Figure 4.3 Typical 10-day back-trajectories at 850 mbar during the spring 1989 background periods. "Arctic" trajectory (solid, March 25, 1989, 1900 C.U.T.) and "Bering/south" trajectory (dashed, March 10, 1989, 1900 C.U.T.). Numbers on the trajectories indicate the number of days upwind.

taminated reservoir of air over the arctic basin during winter and spring, regenerated by episodic transport from source regions. Although no evidence of rapid transport from source regions was observed, the relatively constant and high NO_y levels observed during Arctic trajectories are indicative of the importance of this arctic NO_y reservoir.

It is interesting to note that NO_y levels during spring were higher than summer even during background periods 1–3, which were associated with southerly flow. This is consistent with the increased lifetime of reservoir NO_y compounds such as PAN during winter [*Singh and Hanst*, 1981]. Since upwind washout and/or deposition apparently removed most of the HNO_3 originally present in the air masses sampled (Table 4.4) and NO was non-detectable, NO_y at Barrow was apparently primarily composed of such reservoir compounds. Measurements of PAN and NO_y at Niwot Ridge, Colorado, show similar results [*Fahey et al.*, 1986; *Singh et al.*, 1985]. At Niwot Ridge, clean-air PAN levels were higher during fall than during summer [*Singh et al.*, 1985], and PAN accounted for a much greater fraction of NO_y in low-NO_y samples during fall [*Fahey et al.*, 1986]. The fall measurement period at Niwot Ridge was characterized by snow cover and low temperatures, which apparently led to a greater PAN lifetime [*Singh et al.*, 1985]. However, this is in contrast to free-tropospheric measurements during late spring at Mauna Loa in the central Pacific Ocean, where nitric acid accounted for 45% of the NO_y concentration [*Hübler et al.*, 1989].

4.2.1.2 Filter data

The results of simultaneous filter measurements during this sampling period can be used to further elucidate source regions and air mass history. Gaseous and particulate sulfur and nitrogen compounds (SO_2, HNO_3, and particulate NO_3^- and $SO_4^=$) were collected on sequential Nuclepore polycarbonate and base-treated polypropylene filters and analyzed by ion chromatography (Jaffe et al., 1991). The filter

samples were collected for approximately 12-hour periods, ending at 10 a.m. and 10 p.m. local time, yielding daytime and nighttime samples.

The combination of 12-hour filter samples and relatively short individual background periods resulted in only a few filters that were exposed entirely during single background periods. Results from those filters are shown in Table 4.4. NO_y concentrations averaged over the same periods as the respective filters are also shown in Table 4.4. Four background periods have filter data for comparison. Two of these (periods 4 and 6) have Arctic trajectories. A third (period 10) occurred during a transition between Arctic and Bering/south trajectories. Comparison of 850- and 1000-mbar trajectories for the fourth period (number 7) indicates large vertical wind shear. However, both trajectory levels indicate flow from the Arctic.

Table 4.4 Filter Measurements During the Spring 1989 Background Periods.

Period Number	Trajectory Classification	$SO_4^= + SO_2$	t-NO_3^- [a]	NO_y [b]	$\frac{NO_y}{SO_4^= + SO_2}$	$\frac{SO_2}{SO_4^= + SO_2}$
4	Arctic	601	28	668	1.1	0.15
6	Arctic	645	21	625	0.97	0.02
7	Arctic	435	131	568	1.3	0.04
10	Transition	235	8	765	3.3	0.08

Concentrations are in pptv.
[a]Nitric acid + particulate-nitrate.
[b]Averaged over the same period as the corresponding filter.

There are two main points to note from Table 4.4. First, the NO_y:SO_x ratio (where SO_x is defined as SO_2+particulate $SO_4^=$) is very close to 1 for the three periods of arctic flow. The ratio is higher (3.3) for period 10. This higher ratio is primarily due to a reduction in SO_x, which is <50% of the average for the other 3 periods, rather than an increase in NO_y. Period 10 occurred during a transition between Arctic and Bering/South trajectories, and may reflect transport of aged arctic air across the Bering Strait region en-route to Barrow. The increased ratio in this case may thus be related to enhanced scrubbing of $SO_2+SO_4^=$ relative to NO_y over the Bering Sea. A comparison of the observed concentration ratios to estimated

emission ratios in potential arctic haze source regions similarly indicates that NO_y is removal-resistant relative to SO_x. The emission ratio of NO_x:SO_2 estimated for Europe and the Soviet Union is approximately 1.7 (on a molar basis) (Hov et al., 1988). The higher concentration ratios observed at Barrow indicate a loss of sulfur relative to NO_y, and suggest that the arctic NO_y reservoir is composed of removal-resistant species.

Also shown in table 4.4 are total-nitrate (HNO_3+particulate NO_3^-) filter concentrations. Total-nitrate was <25% of NO_y during each of the 4 periods with filter data, and was <4% in 3 of the 4 periods. Since HNO_3 and particulate-NO_3^- are relatively efficiently removed from the atmosphere (relative to PAN), low total-nitrate concentrations are consistent with a removal-resistant NO_y reservoir.

4.2.2 Events

During this campaign, four identifiable pollution "events" were observed, lasting from 12–60 hours each as shown in Figure 4.2. The suddenness at which these events appeared in the data record and the extremely high NO_y concentrations observed for a background site, to 16 ppbv, are not characteristic of "arctic haze." However, the relatively smooth changes in NO_y concentration during these events contrast sharply with the well-characterized high-variability signatures of local (Barrow) pollution sources [*Bodhaine et al.*, 1981; chapter 3]. Table 4.3 provides a summary of the four events.

4.2.2.1 NO_x Estimation

Although only NO and NO_y were measured, NO_x ($NO+NO_2$) concentrations can be estimated during the day using the photostationary-state approximation [*Leighton*, 1961]. This approximation makes use of the rapid equilibrium achieved between the reactions

$$NO_2 + h\nu \longrightarrow NO + O(^3P) \quad (4.1)$$

$$O(^3P) + O_2 \xrightarrow{M} O_3 \quad (4.2)$$

$$NO + O_3 \longrightarrow NO_2 + O_2. \quad (4.3)$$

In the absence of oxidants other than ozone that convert NO to NO_2, the steady-state concentration of NO_2 is given as

$$[NO_2]_{ss} = \frac{k_{4.3}[NO][O_3]}{J_{4.1}}.$$

Although significant deviations from this relationship have been observed at higher NO levels [*Parrish et al.*, 1986], at the low NO levels measured at Barrow it is likely that the relationship is accurate within a factor of 2 or 3. Ozone concentrations at the Barrow site were provided by S. Oltmans (NOAA CMDL), and recommended values for $k_{4.3}$ [*DeMore et al.*, 1987] were calculated for temperatures measured at the site. The major uncertainty in these calculations results from estimation of the NO_2 photolysis rate constant, $J_{4.1}$, which was not measured. The radiative transfer model of *Stamnes and Tsay* [1990] was used to estimate $J_{4.1}$ during periods when the solar zenith angle was less than 85°. These calculations are based on clear sky, no aerosol, an 85% surface albedo, and a plane-parallel atmosphere. During the sampling period the land and ocean near the site were snow-covered, with the exception of occasional open leads over the ocean, so a high surface albedo for $J_{4.1}$ is expected [*Dickerson et al*, 1982]. The assumptions of clear sky, no aerosol, and a plane-parallel atmosphere without spherical correction imply that the calculated $J_{4.1}$ values are upper limits to the true rates, and thus the estimated NO_2 concentrations are lower limits. The assumption that ozone was the sole oxidant also implies a possible underestimation of NO_2 levels.

During this period the minimum solar zenith angle was 69°. The estimated NO_2 photolysis rate at that angle is $\sim 8.9 \times 10^{-3} s^{-1}$. This relatively large value

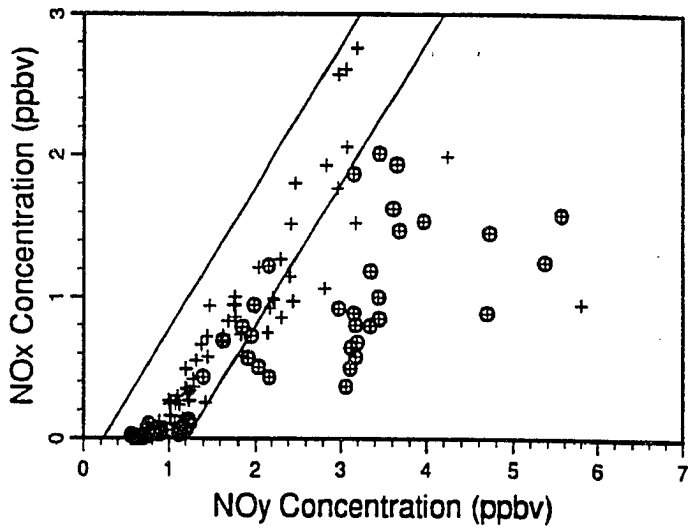

Figure 4.4 Estimated NO_x concentration versus NO_y during the spring 1989 events. NO_x is estimated based on the photostationary-state approximation (see text). Circled data points correspond to periods with solar zenith angle greater than 75°. The two lines delineate the region consistent with an enrichment of background air with pure NO_x (discussed in text).

of $J_{4.1}$ is a result of the high sensitivity of $J_{4.1}$ to surface albedo [*Madronich et al.*, 1983; *Luther and Gelinas*, 1976]. Under photostationary state conditions, with a typical Barrow springtime O_3 concentration of 40 ppbv and a temperature of -20°C, the corresponding ratio of $[NO_2]$:[NO] is 0.9. Thus the NO concentration would be above the detection limit of 75 pptv whenever NO_x levels were above about 150 pptv near local solar noon (under clear skies).

During the four events, NO concentrations were always above the detection limit during daylight hours and were frequently a large fraction of NO_y. The NO_x:NO_y ratios during the events were very high, reaching a maximum value of 0.9. This is in contrast to the low NO_x:NO_y ratio during background periods, where NO (and thus estimated NO_x) was always below the detection limit. (As discussed above, these NO_x estimates are lower limits due to the assumptions of clear sky, no aerosol, and no oxidants other than ozone.) The estimated NO_x concentrations are plotted against NO_y in Figure 4.4, which includes all data during periods in which the solar zenith angle (SZA) was less than 85°.

Since photochemical reactions transform NO_x to other NO_y compounds, the relative enrichments in NO_x and NO_y can be used as a measure of the photochemical age of an airmass. The lines plotted on Figure 4.4 correspond to the minimum and maximum NO_y concentrations observed during background periods, enriched with varying amounts of NO_x. If the NO_y enhancement during the four events were due to NO_x only, all points would be expected to fall between these two lines. However, a large amount of scatter in the data is apparent from Figure 4.4. Some of the scatter appears to be due to errors in estimating the NO_2 photolysis rate at high solar zenith angles. At high zenith angles, errors arising from omission of aerosols or clouds and use of plane geometry in the radiative transfer calculations are amplified, due to the increased atmospheric path length. Omission of data points corresponding to periods with SZA $> 75°$ (circled in Figure 4.4), reduces the scatter considerably. One remaining apparent outlier, at $NO_y \sim 6$ ppbv, was observed during a period of complete cloudiness. (No general relationship to cloudiness is apparent in the data, however.) Although it is clear that the high NO_y concentrations during events are largely due to NO_x enrichments, the difficulty in estimating NO_2 concentrations using the photostationary-state approximation at high solar zenith angle prevents an accurate determination of the NO_x:NO_y ratio during these events.

4.2.2.2 Filter Data

The simultaneous SO_2 and $SO_4^=$ filter data support the hypothesis of a plume enriched primarily in NO_x and NO_y. The 12-hour time resolution of the filter samples makes a direct comparison to the NO_y data difficult; however, some information can be gleaned from the combined sulfur and nitrogen data record during periods when individual filters were obtained during a single event. Events 1 and 3 encompass a total of five such filter samples, and the filter data during those events are summarized in Table 4.5.

The SO_x (SO_2+$SO_4^=$) concentration during events one and three averaged 479

Table 4.5 Filter Measurements During the Spring 1989 Events.

Event Number	$SO_4^= + SO_2$	t-NO_3^- [a]	NO_y [b]	$\frac{NO_y}{SO_4^= + SO_2}$	$\frac{SO_2}{SO_4^= + SO_2}$
1	643	130	3,576	5.6	0.04
	437	45	768	1.8	0.01
3	562	162	1,423	2.5	0.04
	348	122	2,441	7.0	0.04
	583	67	1,151	2.0	0.05
	219	62	1,253	5.7	0.03

Concentrations are in pptv.
[a]Nitric acid + particulate-nitrate.
[b]Averaged over the same period as the corresponding filter.

pptv, which is not significantly different than the average of 465 pptv during the four background filters (see Table 4.4). This indicates that the source responsible for the substantial NO_y enrichments did not significantly affect the background arctic haze sulfur concentrations. The molar ratio of NO_y:SO_x, calculated using NO_y concentrations averaged over the periods of filter collection, also indicates a sulfur-poor source. The NO_y:SO_x ratio ranges from 1.8–7.0, with the highest values during periods of highest NO_y concentrations. The values during periods of highest NO_y levels are much larger than those calculated during background periods (Table 4.4). Since SO_x was composed primarily of $SO_4^=$ (Table 4.5), while NO_y was typically about half NO_x, the NO_x:SO_2 ratio was even higher than the ratio of NO_y:SO_x. These observations are again consistent with a source rich in NO_x but SO_2 poor.

Finally, the extent of sulfur photochemistry can be gauged using the SO_2:($SO_4^= + SO_2$) ratio in a manner similar to the NO_x:NO_y ratio described above. Rapid transport across the Arctic of emissions from an "arctic haze" source that brought fresh NO_x emissions to Barrow would also bring fresh SO_2 emissions [*Barrie and Hoff*, 1984]. The SO_2:SO_x ratio, shown in Tables 4.4 and 4.5, is not increased during the events as compared to the background periods. This is consistent with enrichment of only NO_x by a regional source during the events.

These chemical data clearly indicate that emissions from a relatively nearby

source with a high NO_x:SO_2 ratio caused the events at Barrow. The only major NO_x source on the arctic coast of Alaska satisfying these conditions is the Prudhoe Bay oil production region. Prudhoe Bay has large NO_x emissions—estimated at 10,000–15,000 metric tons/year (J. Coutts, Alaska Department of Environmental Conservation, personal communication to D. A. Jaffe, 1990), which result primarily from operation of natural gas-fired turbines. Permitted SO_2 emissions are relatively low, at 618 metric tons/year, leading to a NO_x:SO_2 molar emission ratio of 22–33.

4.2.2.3 Meteorological Analysis

Figure 4.5 shows a plot of the observed NO_y concentrations (hourly average) during events and background periods versus the local wind direction. The events were observed to occur when wind directions were in the range of 98°–173°(although there were many occasions when winds were in this range but there was no evidence of Prudhoe Bay impacts, as shown by the background periods in Figure 4.5). The highest NO_y concentrations were observed when local winds were from 110°–120°, suggesting that the nitrogen oxide source responsible for these events is located in that sector. This is again consistent with the identification of the Prudhoe Bay industrial region as the source of the NO_y enrichments. The main Prudhoe Bay sources are located at 111° from Barrow and are approximately 300 km distant.

As a result of the stability of the arctic boundary layer during springtime and the flat terrain of the Alaskan arctic coastal plain, it is possible that emissions from Prudhoe Bay could travel 300 km in the boundary layer. However, the potential for transport at higher altitudes was also investigated, using rawinsonde data from the Barrow National Weather Service (NWS) station (8 km distant from the CMDL observatory). In assessing the possibility of transport from the Prudhoe Bay region, local wind data were used instead of the global gridded winds typically used in long-range transport studies of arctic air pollution [*Kahl et al.*, 1989]. The justification for this choice is based on the following: (1) long-range, multi-day trajectory analyses

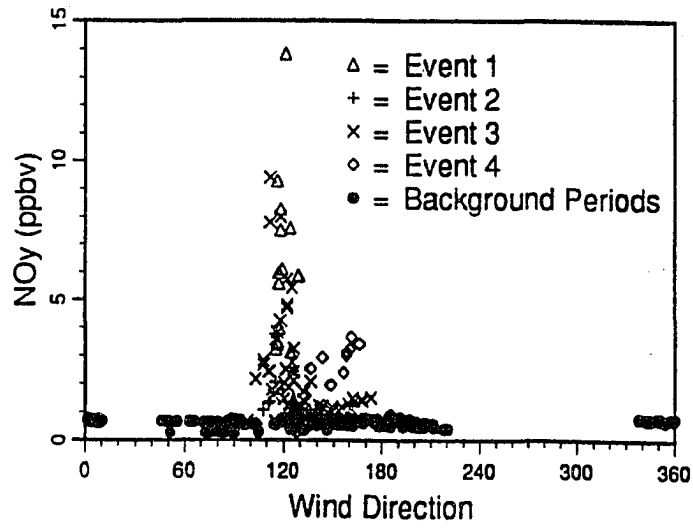

Figure 4.5 NO_y concentration during the spring 1989 events and background periods versus barrow surface wind direction (measured at the CMDL site).

are, in general, of limited usefulness in assessing transport problems on scales of a few hundred kilometers or less [*Kahl and Samson*, 1986]; and (2) the wind analyses upon which the multi-day trajectories are based are not always representative of local conditions [*Harris*, 1982].

Figure 4.6 shows 12-hour estimated trajectories at 1000- and 850-mbar, based on Barrow rawinsonde measurements during events 1–3 (data are not available during event 4). Estimated trajectories based on surface wind measurements at the CMDL site are also shown, depicting a constant wind speed and direction for 12 hours upwind of Barrow. The trajectories based on the CMDL surface winds support the hypothesis of rapid (<1 day) transport from the Prudhoe Bay area, although upper air data from NWS measurements are considerably different in several cases. The NWS measurements further indicate a significant amount of vertical wind shear, suggesting that the air sampled at Barrow may be a mixture of air parcels that were located in widely separated areas 12 hr earlier, which limits the usefulness of the trajectory analysis in identification of a source region. In addition, there is a large difference between the winds at 1000 mbar measured by the NWS rawinsonde and the CMDL surface winds during event 2. (The NWS surface measurement at

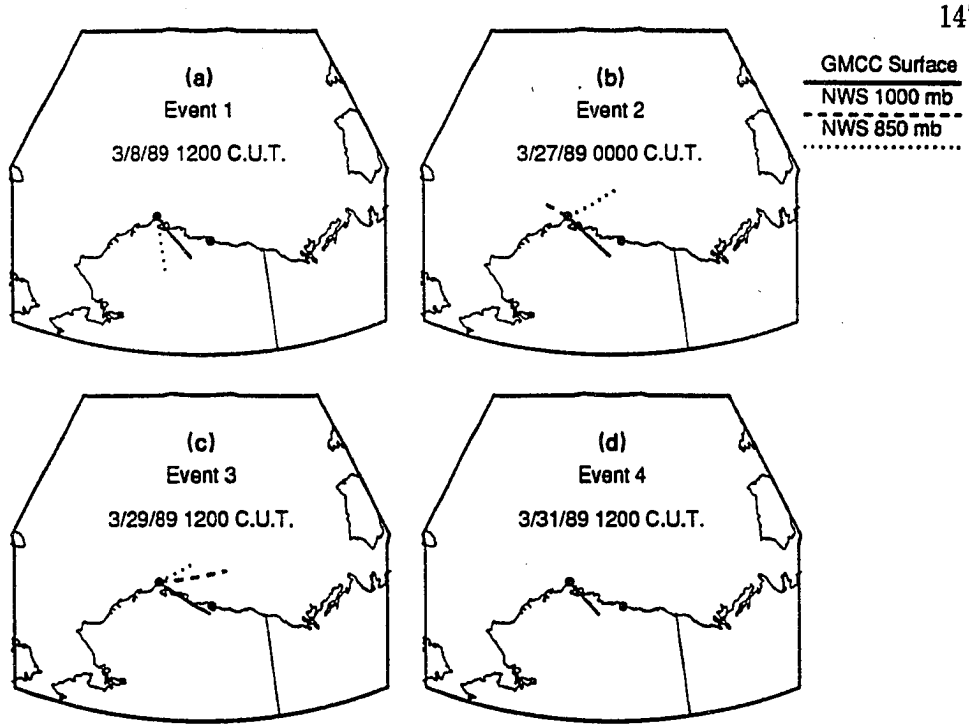

Figure 4.6 Twelve-hour back-trajectories based on barrow surface wind measurements during the spring 1989 events. Wind data are from the CMDL (formerly GMCC) surface (solid line), NWS 1000 mbar (dashed line), and NWS 850 mbar (dotted line) observations. Solid circles indicated the locations of Barrow and Prudhoe Bay. Data not shown are missing.

that time was consistent with the NWS 1000-mbar observation.) A brief review of the NWS and CMDL records during this periods shows that such large divergences were not uncommon. When interpreted in light of the chemical measurements, however, these analyses suggest that short-range trajectories based on the CMDL surface winds (Figure 4.5) may be the most reliable indicator of small-scale transport during the events.

An interesting observation arising from these analyses is that transport on scales of a few hundred kilometers is apparently occurring under the low-level arctic temperature inversion. Inversions along the Alaskan coast tend to be deep ($\sim$ 900 m) and strong ($\sim$ 10°C temperature difference across the inversion) during March [*Kahl*, 1990]. This suggests that spatial variability in the inversion structure may be of fun-

damental importance in diagnosing atmospheric transport in the Arctic.

4.2.2.4 Previous Measurements

Regional impacts due to pollutant emissions from Prudhoe Bay have been suggested previously, but the potential effects of these emissions are not generally considered in analyses of measurements at Barrow. Emissions from Prudhoe Bay were first suggested as a possible influence on Barrow measurements by *Radke et al.* [1976]. In measurements near the current CMDL site they found high condensation nuclei (CN) concentrations during periods when winds were from the direction of Prudhoe Bay, and attributed the increased levels to emissions from construction activities at Prudhoe Bay, which was not yet producing oil.

In several other cases Prudhoe Bay was not identified as a source, but published results indicate that events such as those described here may have contributed to elevated pollutant levels. In the Barrow CN measurements of *Bodhaine et al.* [1981], there is evidence of a pollutant source in the direction of Prudhoe Bay. Figure 3 of that paper shows elevated CN levels when local winds are from 120°–140°. Consistent with the NO_y data, the CN source exhibits a variability which is much lower than the local (Barrow) pollution sources. More recent measurements conducted by *Bodhaine et al.* [1989] in 1986 reveal two events in which smooth peaks in CN, accompanied by black carbon peaks, occurred during periods when the wind was from near the direction of Prudhoe Bay. Simultaneous diffusion battery measurements indicated that the CN peak was primarily a small-particle event.

Correlations of CO_2, CH_4, and black carbon during one of the 1986 events apparent in the Bodhaine et al. (1989) data have been discussed by *Hansen et al.* [1989]. For example, the event labeled 5 by Hansen et al. shows a pattern very similar to the events presented here and was observed during a period when the wind direction was $111 \pm 13°$ (1 standard deviation).

Although these previous observations have attributed increased pollutant levels

to long-range transport [*Bodhaine et al.*, 1989; *Hansen et al.*, 1989], the similarity of the events presented here with those reported previously suggests an identical source for at least some of the previously identified events. Although it is not necessarily true that all such events at Barrow are due to Prudhoe Bay pollution, the data strongly suggest that the Prudhoe Bay region is occasionally an important pollution source at Barrow.

A comparison of NO_y concentrations during the 1989 events with simultaneous CO_2, CH_4, black carbon, and condensation nuclei (CN) concentrations, measured at Barrow by NOAA CMDL, shows a significant correlation among all these species. This correlation indicates that the Prudhoe Bay region is a source of CO_2, CH_4, black carbon, and CN, in addition to NO_x. Emissions of these compounds may result from a variety of Prudhoe Bay activities, including natural gas combustion, oil and natural gas handling, and natural gas flaring. Further analysis of these data is not part of this thesis but will be presented in a separate publication.

4.3 Summary

NO and NO_y were measured during a 5-week period from March 2–April 7, 1989, at Barrow, Alaska. The data were separated into "background periods" and "events" using objective criteria to remove the effects of local (Barrow) contamination.

NO_y levels during the 11 background periods are representative of concentrations unaffected by local or regional NO_x sources. Median NO_y concentrations during individual background periods ranged from 280–850 pptv, with an overall median concentration of 616 pptv. These measurements indicate that

1. NO_y concentrations in the Arctic are significantly higher in spring than in summer. Surface NO_y levels at Barrow appear to be comparable to concentrations in the free troposphere outside of arctic haze layers [*Dickerson*, 1985], and about 50% of the levels in haze layers.

2. NO_y concentrations during southerly flow (as indicated by 850-mbar trajectories) were ~50–70% of the levels observed when trajectories indicate arctic air was being sampled at Barrow.

3. NO_y during background periods was apparently composed primarily of removal-resistant reservoir compounds. Springtime NO_y levels were higher than those in summer even in air masses that were apparently not affected by arctic haze. This observation provides evidence for a greatly increased NO_y lifetime during the colder months over a large region of the background troposphere.

Substantially elevated NO_y concentrations (to >16 ppbv) were observed during four events lasting from 12–60 hours. Events of elevated concentrations of condensation nuclei, methane, carbon dioxide, and black carbon similar in many respects to these NO_y events have previously been attributed to Eurasian sources. However, substantial evidence indicates that emissions from the Prudhoe Bay industrial region were responsible for the elevated NO_y observations:

1. Slow and smooth concentration variations during the events indicate that local (Barrow) sources were not the cause.

2. The ratio of NO_x:NO_y estimated during these events is very high (to 0.9) and indicates that the NO_y enrichment is almost entirely due to NO_x. This implies that fresh NO_x emissions were responsible for the events.

3. Filter measurements of $SO_4^=$ and SO_2 do not indicate enrichment of sulfur compounds during the events. This is consistent with a source, such as Prudhoe Bay, which is low in SO_x emissions.

4. The SO_2:(SO_2+$SO_4^=$) ratio was not enhanced during the events. This also indicates that the recent emissions responsible for a high NO_x:NO_y ratio were SO_2-poor.

5. The correlation with local wind direction indicates that the source is in the 110°–120° sector, consistent with Prudhoe Bay, which lies at a 111° bearing from

Barrow. Back-trajectories calculated from Barrow CMDL surface meteorological data are consistent with the identification of Prudhoe Bay as the source. The trajectory calculated for event 3 indicates that the air sampled during that event may have passed within 40 km of Prudhoe Bay approximately 12 hours earlier.

Although the CMDL site at Barrow is in a remote region, it is affected by local, regional, and hemispheric pollutant sources. In order to differentiate between these sources, data collected at such a site must be selected with great care so that measurements are representative of specific, identifiable air masses. These data indicate that atmospheric transport processes can bring different air masses to the Barrow site on a time scale of hours. Daily, weekly, or monthly means may therefore not be adequate to discriminate among different air masses. In general, measurement systems which provide high time resolution data will provide greater insight into complex atmospheric processes at a site such as Barrow.

Chapter 5

1990 Measurement Campaign

The 1990 measurement campaign covered the period from March 2 to December 31 and is discussed in this chapter. The data set obtained during this campaign constitutes the most comprehensive record of NO_y and NO concentrations in the arctic troposphere yet obtained. Operation of the instrument was continuously monitored, and any measurements that did not satisfy the quality control checks described in chapter 2 were omitted from further analysis. The resulting valid data set includes NO_y measurements during 178 days and NO measurements during 242 days (21,903 NO_y and 31,261 NO data points). The detection limits and uncertainty were 15 pptv and 21% for $NO_y$and <10 pptv and 6% for NO, respectively (Table 2.8).

5.1 The Complete Unscreened 1990 NO_y and NO Data Sets

The frequency distributions of all 40 s-average NO and 20 s-average NO_y measurements during 1990 (6 each hour) are shown in Figure 5.1. As described in chapter 4, local pollution from Barrow and regional (Prudhoe Bay area) emissions frequently impact the measurement site. These effects are apparent in the long tails on the

distributions shown in Figure 5.1. Concentrations above 10 ppbv were sometimes observed during periods of flow from nearby sources and are included in the rightmost bin of Figure 5.1; the maximum concentrations observed were 48 ppbv (NO_y) and 18 ppbv (NO).

Local effects can most clearly be seen from observations of nighttime NO. Since the lifetime of NO at night is <0.5 hr due to reaction with ozone under typical conditions at Barrow (temperature -40–0°C, ozone 10–60 ppbv), the presence of nighttime NO is indicative of sources in the Barrow area. Figure 5.2 shows the distribution of hourly-average NO measurements during night (defined as periods with solar zenith angle ≥85°) by wind direction for all measurements made during 1990. The data in this figure have been separated into 40° wind sectors using hourly-average surface wind measurements at the CMDL site [*National Oceanic and Atmospheric Administration (NOAA)*, 1991]. Within each sector, the 50th, 75th, 90th, and 95th percentile and maximum nighttime NO concentrations are shown. Each of the hourly-average concentrations is the average of ~5-6 individual measurements, with individual uncertainties of ≤10 pptv. Thus, the detection limit for hourly-average values is <~5 pptv.

Major nearby NO sources in the 200–320° sector are apparent from Figure 5.2. These include the town of Barrow, the Barrow dump, the NARL site, and the DEW station (see section 2.3 for a description of nearby sources). In addition, frequent emissions from traffic and airstrip operations in the 320–360° sector are apparent. Occasional observations of nighttime NO in the 0–40° sector may reflect traffic to Point Barrow or combustion sources at the Duck Camp, while nighttime NO in the 120–200° sector probably reflects occasional traffic to the East Barrow gas fields. Infrequent observations of significant nighttime NO in the rest of the 0–200° sector probably reflect snowmobile use near and upwind of the station, as well as vehicle traffic at the station. These observations indicate that local pollution is occasionally observed under all wind directions, but is very frequent in the southwest

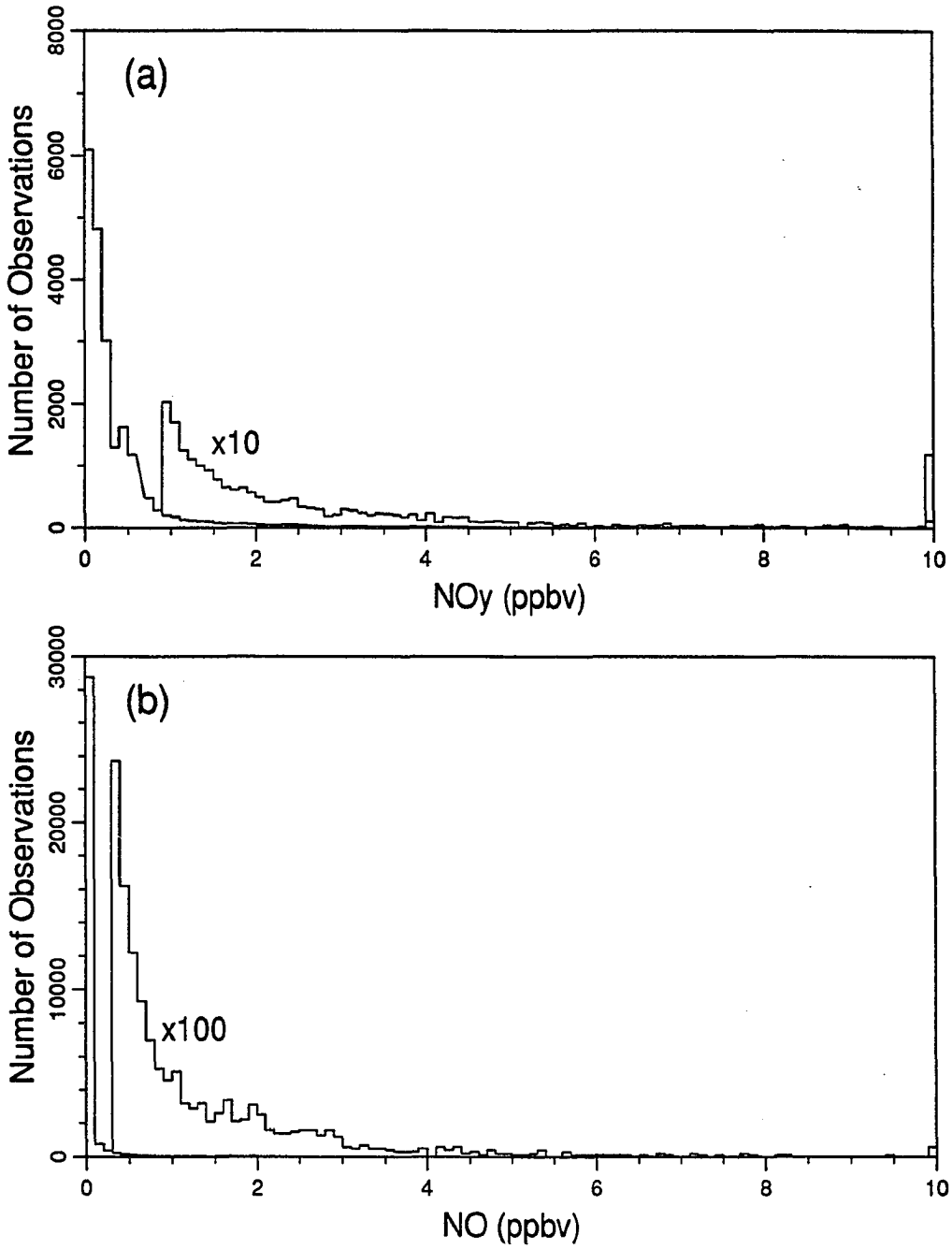

Figure 5.1 NO_y and NO distributions in the unscreened 1990 data set. Concentrations beyond the maximum shown are included in the rightmost bin. (a) NO_y. (b) NO.

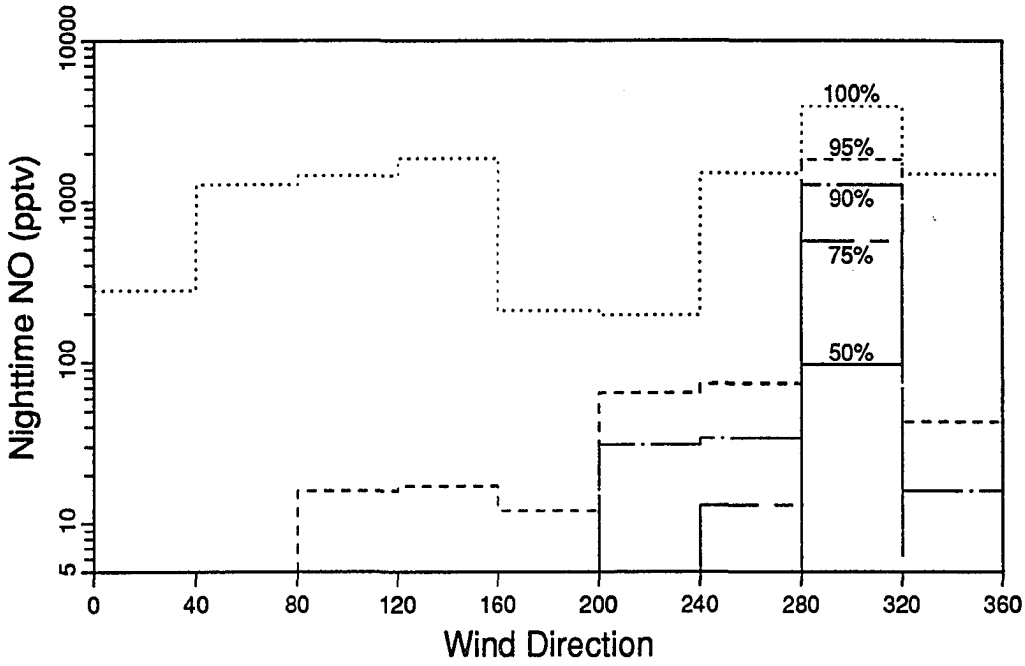

Figure 5.2 Distribution of nighttime NO by wind direction in the unscreened 1990 data set. All measurements with solar zenith angle at least 85° are included. Within each 40° wind sector (0–40°, 40-80°, ...), the 50^{th}, 75^{th}, 90^{th}, and 95^{th} percentile values and the maximum are shown.

and northwest sectors. This result underscores the need for careful screening of data from the Barrow site. An analysis of the relationship between the variability of ambient NO_y concentrations and wind direction was also conducted, and the results are consistent with those shown in Figure 5.2.

Daytime NO measurements are also a useful indicator of local, as well as regional, pollution at the Barrow site. Background arctic tropospheric NO levels are very low, both during the arctic haze season [*Dickerson*, 1985; results discussed in chapter 4 and below] and during summer [*Bakwin et al.*, 1991; results discussed below]. Thus, elevated daytime NO levels are indicative of local or regional NO_x sources. Nevertheless elevated daytime NO levels were often detected at the CMDL site, even within the sector that was free of local (Barrow) sources. Figure 5.3 shows the distribution of hourly-average NO during daylight hours (solar zenith angle below 80°) by wind direction, in the format of Figure 5.2. NO levels above 5 pptv

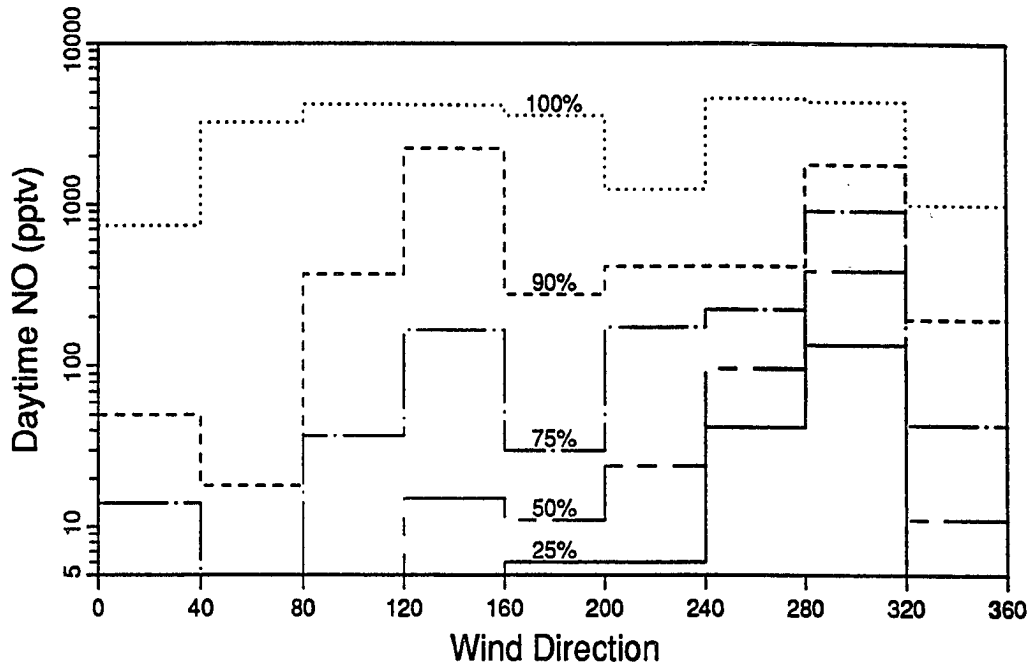

Figure 5.3 Distribution of daytime NO by wind direction in the unscreened 1990 data set. All measurements with solar zenith angle less than 80° are included. Within each 40° wind sector (0–40°, 40–80°, ...), the 25th, 50th, 75th, and 90th percentile values and the maximum are shown.

are seen much more often during daylight than during night, of course, and the frequent impact of local pollution in the 240–320° wind sector is particularly apparent. However, frequent elevated daytime NO is also observed in the 80–160° sector. This is consistent with the 1989 measurements (chapter 4), which showed impacts from Prudhoe Bay NO_x emissions when wind was from the east to southeast. The analysis of the 1990 results discussed below indicates that the high NO levels observed in the 80–160° sector during 1990 were also primarily due to emissions from Prudhoe Bay (located at a 111° heading from the Barrow site). Finally, elevated daytime NO was sometimes observed when wind blew from the south to southeast. This is probably a result of activity in the Barrow gas fields, which are located in that sector. Vehicles occasionally drive within the gas fields, and several small natural gas-fired heaters were installed at the gas wells during 1990 (section 2.3).

After removing all local/regional pollution episodes based on the NO_y data record, the NO data for each remaining period were scanned and outliers were removed in some cases, in the same manner as (g) above.

Three potential background periods chosen using screening criteria (a)–(e) are shown in Figure 5.4 with + symbols. NO_y measurements before and/or after the potential background periods are also displayed to show trends. Although these periods satisfied criteria (a)–(e), it is clear that they were not entirely representative of background conditions. Therefore, screening criteria (f) and (g) were applied to eliminate pollution events and outliers. First, hours within the potential background periods with NO_y standard deviations greater than 40 pptv were flagged (these hours are identified with an X on the x-axis of Figure 5.4). The measurements within these hours were then evaluated.

The potential background period shown in Figure 5.4a contained the beginning of an event which satisfied screening criterion (f). Wind direction during the hour flagged with an X was 129°, close to the 111° heading to Prudhoe Bay. Concentrations continued to rise after this hour, with wind directions closer to 111°, reaching a maximum above 5 ppbv. The last 2 hours of this period (i.e., the last 9 points plotted with + symbols) were deleted to remove the effects of the pollution event.

An example of a preliminary background period containing an outlier (satisfying criterion (g)) is shown in Figure 5.4b. Wind directions were in the 10–30° range during this time and there was no evidence of potential pollution except in the single outlier, so only that data point was removed.

The period shown in Figure 5.4c satisfied criterion (f) above, with winds outside the Prudhoe Bay sector during the potential background period (shown with the + symbols). Concentrations were dropping throughout the selected period, from a maximum of ~1.5 ppbv somewhat earlier. Wind directions were 7–48° during the flagged hours. However, the wind direction had been >111° a few hours earlier, and the NO_y pulse to 1.5 ppbv coincided with the wind shift past the 111° heading,

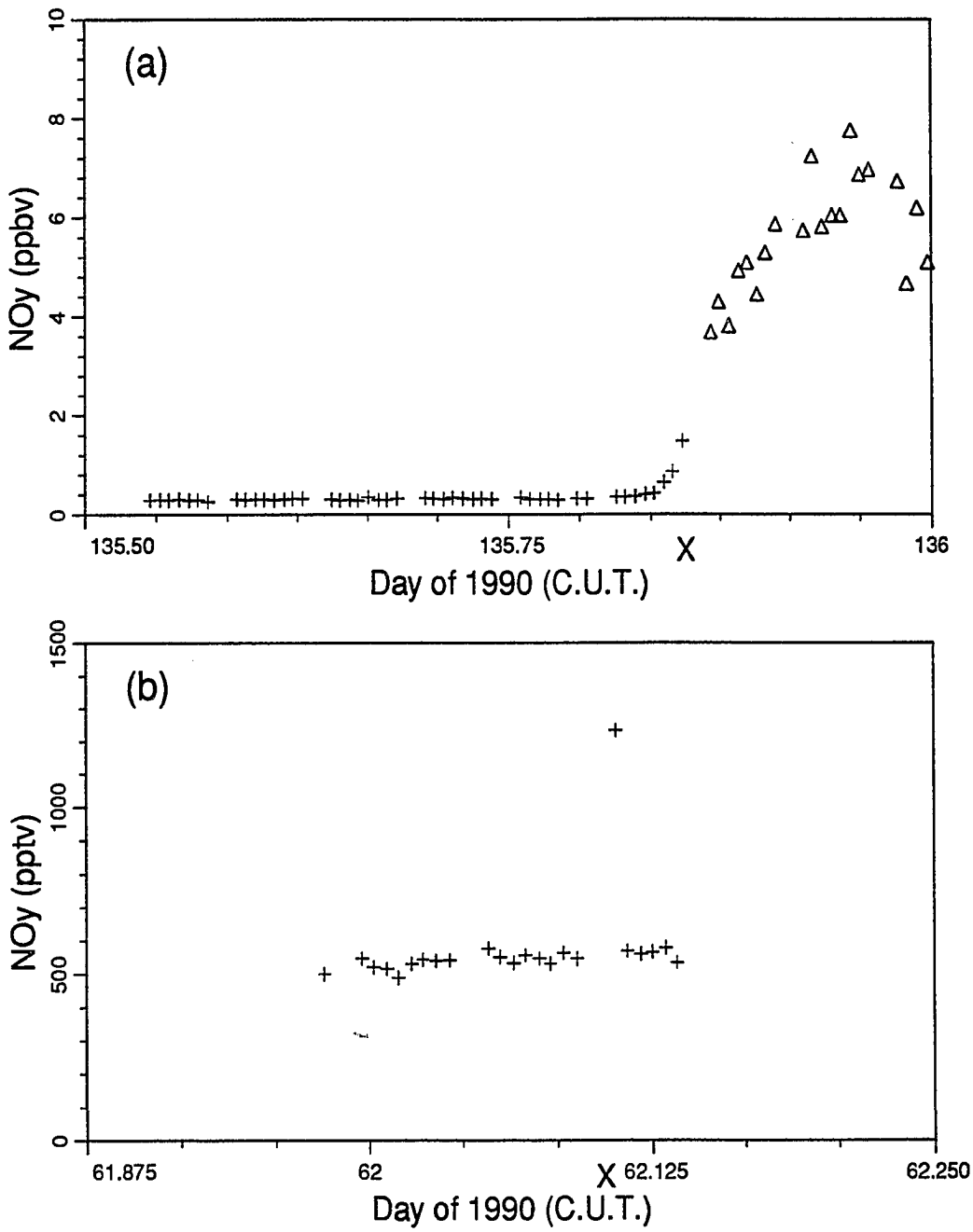

Figure 5.4 Examples of potential background periods that required additional screening. Potential background periods chosen with screening criteria (a)–(e) are shown with + symbols. Surrounding data not included in the potential background periods are shown with triangles. Hours within the potential background periods that have a standard deviation of NO_y measurements within the hour greater than 40 pptv are flagged with X's on the x-axis. See text for a discussion of the examples. (a) Example of a period affected by a regional pollution event with winds near the direction from Prudhoe Bay. (b) Example of a period with an outlier. Continued on next page.

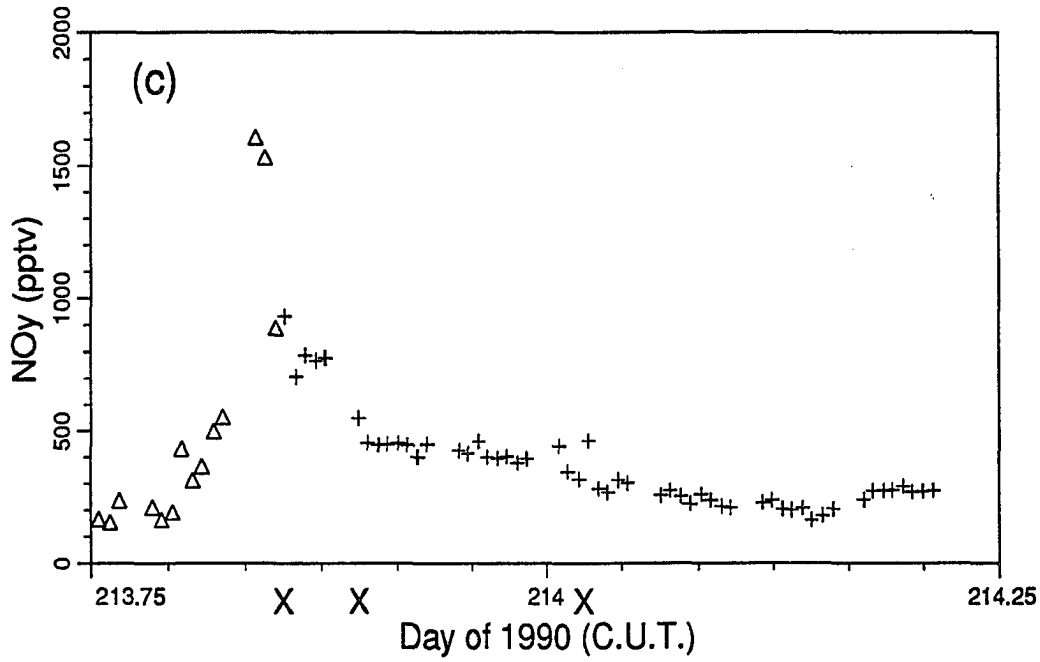

Figure 5.4 (continued) Examples of potential background periods that required additional screening. (c) Example of a period affected by an apparent clean-sector pollution event.

indicating that the high levels in Figure 5.4c were due to a snaking plume from Prudhoe Bay. The data in Figure 5.4c were eliminated from the background data set. (In the discussion of regional pollution events below, the measurements in Figure 5.4c are identified as event number 11.)

After the full screening procedure, 65 background periods remained. The background periods include measurements from March 2 through November 15, with some gaps during the months of April and June. The screening procedure was stringent, and while it allows a high degree of certainty that local and regional pollution did not affect the background data, it resulted in the exclusion of a large fraction of the total NO and NO_y sets from the background data set. Exclusion of data obtained during wind flow from 200–360° resulted in the loss of 25% of the total measurements, and the other screening criteria resulted in the exclusion of 39% of the measurement hours from the background data set. Thus, the selected background data set includes 36% of the total measurement hours.

5.2.2 Results

The timing and duration of each of the 65 background periods are shown in Table 5.1, which also summarizes meteorological parameters during the periods. NO and NO_y concentrations during the periods are shown in Table 5.2, and Figure 5.5 shows median NO_y concentrations and the total concentration range observed during each period. A well-defined seasonal cycle is clearly apparent, with high concentrations during March, followed by a sharp drop through April and May to very low summertime values in late June through August. Concentrations began to rise again in September, and continued to rise until the end of the measurements in November. Based on the results shown in Figure 5.5, four temporal regions may be defined: March, when relatively constant and high levels were observed; "spring transition" (April and May), when levels dropped rapidly; summer (June–August), with very low NO_y levels; and "fall transition" (September–November), when concentrations were rising once again. Thus March includes background periods 1–10, the spring transition includes periods 11–18, summer includes periods 19–43, and the fall transition includes periods 44–65. Median NO_y concentrations during background periods in March were 467–674 pptv, with an overall median of 557 pptv. The high March levels are in sharp contrast to those in summer, which ranged from 63–151 pptv with an overall median of 70 pptv, giving a seasonal amplitude (spring–summer) of ~500 pptv.

Table 5.1 Summary of 1990 Background Periods.

Background Period Number	Time (C.U.T.) Start Day	Start Hour	End Day	End Hour	Wind Direction (Degrees)	Average Wind Speed (m/s)	Average Temperature (°C)
1	61	7	61	16	22–86	5.8	-28.4
2	61	22	62	3	4–29	4.1	-27.5
3	62	17	63	12	37–146	4.5	-26.6
4	66	11	68	16	39–173	5.3	-31.1
5	78	12	78	22	126–167	6.7	-21.5
6	80	4	80	15	126–164	6.1	-21.3
7	83	3	85	12	3–78	6.0	-19.2
8	87	5	88	0	15–57	4.3	-24.9
9	88	6	88	10	33–37	7.6	-20.2
10	88	16	88	21	44–54	5.2	-17.1
11	109	2	110	15	10–107	3.5	-21.3
12	128	2	128	7	111–112	9.1	-6.9
13	135	12	135	18	98–112	5.7	-1.8
14	138	23	141	17	66–103	8.1	-2.5
15	142	1	142	7	78–83	9.7	-2.4
16	147	0	147	21	19–103	4.7	-1.2
17	148	3	149	2	14–34	5.2	-0.5
18	149	5	149	20	31–63	6.9	-1.6
19	175	7	175	13	106–111	7.0	0.8
20	178	3	178	15	76–107	7.7	1.6
21	179	2	179	14	75–96	3.7	0.4
22	179	21	180	12	75–104	6.1	1.2
23	184	2	184	13	47–72	5.3	3.7
24	185	17	187	0	58–97	5.6	3.0
25	189	5	190	14	16–75	4.6	-1.3
26	191	2	192	11	60–104	7.4	0.7
27	195	8	196	3	151–188	9.4	14.3
28	197	3	197	10	88–189	6.4	7.8
29	201	0	201	6	147–198	5.0	15.6
30	205	16	206	19	41–77	8.4	1.1
31	207	0	207	17	24–63	6.0	-0.2
32	209	7	211	16	48–84	5.5	0.8
33	212	3	213	13	76–105	5.4	4.4
34	215	9	215	14	5–46	4.0	1.5
35	216	3	218	8	54–93	8.1	0.1
36	219	1	221	15	8–92	6.4	-0.5
37	223	0	224	2	72–101	5.9	3.1
38	226	11	226	21	87–101	11.4	2.5
39	227	13	228	9	77–101	13.5	2.0
40	228	14	228	20	74–78	14.7	0.5
41	229	8	231	15	58–90	11.4	2.0
42	233	13	234	8	87–135	6.1	0.1
43	235	7	235	20	85–95	9.2	0.2

Continued on next page.

Table 5.1 (continued) Summary of 1990 Background Periods

Background Period Number	Time (C.U.T.) Start Day	Start Hour	End Day	End Hour	Wind Direction (Degrees)	Average Wind Speed (m/s)	Average Temperature (°C)
44	244	19	247	15	19–94	6.3	-1.0
45	248	2	249	2	69–87	9.9	0.6
46	256	11	257	7	142–186	5.8	4.4
47	263	6	263	15	34–71	7.7	-2.2
48	263	20	264	5	13–51	4.3	-3.9
49	264	9	264	18	24–60	3.4	-4.2
50	265	16	266	13	29–167	5.2	-1.7
51	266	14	266	21	31–43	8.3	-1.9
52	267	2	267	6	44–58	4.1	-1.3
53	267	11	267	15	36–47	4.1	-1.8
54	271	11	273	14	37–87	6.2	-3.8
55	273	18	274	10	62–75	5.9	-3.4
56	278	2	279	3	34–63	8.4	-6.8
57	280	11	281	17	77–113	13.6	-2.9
58	283	16	284	15	128–184	6.6	-5.7
59	302	22	303	15	44–92	2.2	-12.5
60	310	7	310	17	25–101	6.2	-16.9
61	312	11	312	20	37–118	3.6	-24.6
62	314	21	315	7	168–191	10.6	-17.5
63	315	9	315	13	193–197	15.4	-11.1
64	317	6	318	16	7–74	8.2	-16.6
65	319	3	319	10	12–44	3.1	-23.8

Table 5.2 NO and NO_y During 1990 Background Periods.

Background Period Number	NO_y					NO				
		Concentration (pptv)					Concentration (pptv)			
	N	Median	Mean	S.D.	Range	N	Median	Mean	S.D.	Range
1	56	535	535	19	489–575	55	-0.3	0.0	4.5	-10–9
2	33	541	542	21	488–578	31	-1.5	0.5	7.7	-18–16
3	115	467	470	20	432–524	112	0.5	0.5	5.9	-15–19
4	317	659	661	44	580–785	313	-0.1	0.1	4.9	-15–14
5	64	638	635	19	581–674	63	1.5	1.5	4.3	-8–10
6	70	585	590	24	548–667	70	-1.1	0.1	4.9	-11–12
7	334	528	523	34	446–606	333	0.7	0.7	5.0	-12–15
8	111	498	506	31	462–651	115	-0.4	0.1	5.2	-12–12
9	26	625	625	21	585–661	24	-1.4	-1.0	4.8	-10–8
10	26	674	679	20	653–723	25	4.4	5.5	5.1	-2–17
11	214	433	433	31	368–509	211	2.1	4.7	10.2	-12–45
12	32	437	435	23	380–482	30	4.5	4.5	4.9	-4–18
13	38	303	303	18	255–345	34	2.0	3.5	6.9	-6–20
14	266	229	233	26	160–300	261	1.8	1.7	5.4	-13–20
15	30	252	259	21	223–298	25	7.4	10.2	9.9	-3–28
16	116	195	194	16	156–254	112	8.4	8.6	8.0	-11–24
17	124	176	176	18	128–229	114	4.4	5.1	8.1	-15–24
18	85	180	182	21	148–244	82	-0.3	-0.7	4.8	-13–9
19	37	104	106	8	88–122	38	-0.3	-0.5	3.6	-9–5
20	73	88	89	8	74–111	73	0.7	1.1	4.3	-8–10
21	73	84	85	10	60–111	71	0.2	0.2	5.7	-11–27
22	90	75	76	8	54–97	91	1.8	1.8	3.9	-6–11
23	65	94	94	12	74–130	64	1.8	2.0	4.0	-7–11
24	186	70	70	8	51–92	187	2.4	2.5	3.8	-7–14
25	201	58	58	8	36–87	200	0.2	0.8	3.8	-8–12
26	198	63	63	8	38–90	200	0.0	0.2	4.1	-12–11
27	112	151	151	15	112–186	107	9.8	9.0	7.3	-8–29
28	43	94	95	12	75–131	42	1.6	1.4	4.0	-7–11
29	40	139	141	21	107–193	37	9.1	10.1	6.0	-4–23
30	166	60	60	8	43–96	167	0.0	0.0	3.5	-10–8
31	104	59	60	7	42–82	101	0.0	0.4	3.9	-9–10
32	340	67	68	11	41–134	340	0.5	0.5	3.9	-8–10
33	205	70	71	9	50–104	204	0.8	1.0	4.2	-7–13
34	35	63	66	11	49–92	34	-1.0	-0.8	4.2	-8–7
35	317	65	65	9	43–94	318	1.1	1.2	3.8	-6–14
36	355	60	61	9	37–95	357	0.0	0.2	3.6	-10–11
37	153	65	65	9	46–109	140	1.7	1.5	3.7	-7–10
38	59	78	78	9	57–100	62	0.9	0.7	3.8	-8–8
39	116	74	74	11	46–104	119	0.1	0.5	4.2	-13–11
40	31	83	84	10	58–102	32	0.8	0.3	4.1	-9–6
41	323	80	81	10	42–110	331	0.7	0.8	3.9	-11–11
42	118	82	83	8	62–100	119	2.9	2.8	3.9	-7–13
43	81	71	73	8	54–93	82	0.1	0.0	4.0	-12–10

Continued on next page.

Table 5.2 (continued) NO and NO_y During 1990 Background Periods

Background Period Number	NO_y					NO				
		Concentration (pptv)					Concentration (pptv)			
	N	Median	Mean	S.D.	Range	N	Median	Mean	S.D.	Range
44	382	87	87	10	58–128	383	1.0	1.1	4.6	-9–16
45	125	94	98	20	62–154	127	1.0	1.4	4.3	-8–14
46	121	134	135	20	94–235	120	1.0	1.8	4.2	-7–15
47	48	155	157	14	130–211	50	0.0	0.2	5.2	-10–11
48	46	162	160	17	126–204	40	0.0	1.0	6.8	-9–22
49	53	154	156	12	126–183	51	-1.0	0.4	5.9	-10–12
50	74	126	132	31	88–215	73	0.0	0.1	3.8	-8–10
51	41	113	112	10	92–139	41	2.0	2.3	4.5	-9–18
52	23	110	113	10	100–137	25	0.0	0.2	4.8	-9–13
53	23	113	112	11	76–128	21	0.0	2.9	8.5	-10–21
54	289	118	120	17	90–207	287	0.0	0.5	4.6	-9–15
55	97	129	135	18	102–191	94	0.0	0.8	5.0	-8–21
56	138	164	164	21	112–212	143	0.0	0.1	3.7	-10–10
57	176	170	171	14	145–207	178	0.0	0.4	3.8	-9–9
58	132	206	211	22	174–306	133	2.0	1.8	4.7	-10–14
59	105	231	229	15	188–260	102	-0.5	-0.1	4.4	-10–11
60	61	244	242	13	216–270	54	0.0	0.2	4.8	-9–11
61	54	240	240	15	201–282	53	-1.0	-0.4	4.1	-9–10
62	52	241	246	23	211–337	51	0.0	0.0	3.4	-10–6
63	24	228	229	15	202–264	24	0.5	0.7	3.0	-5–6
64	208	262	268	42	197–392	206	0.0	-0.1	4.0	-10–11
65	41	240	240	15	207–296	40	0.0	-0.1	4.0	-10–6

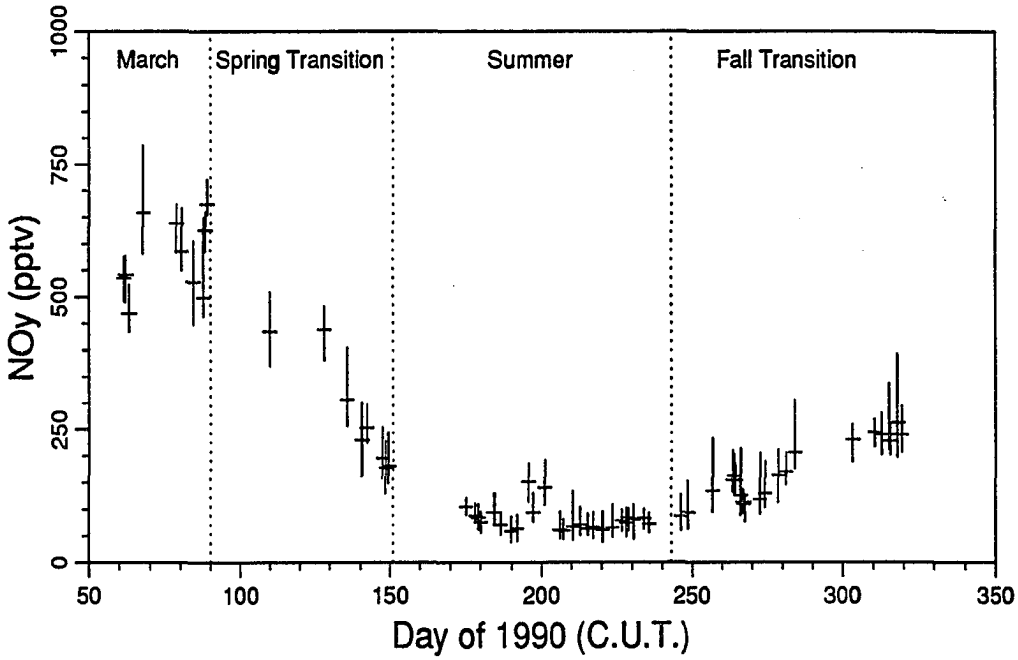

Figure 5.5 NO_y concentrations during the 1990 background periods. Median concentrations during each event are indicated by crosses, while the total range of 20-s average NO_y concentrations during each event is shown by the vertical bars.

Average daytime (solar zenith angle $\leq 80°$) NO concentrations during each background period are shown in Figure 5.6. Error bars on the figure are based on the variability of NO measurements within each period and are 2 standard deviations of the mean in length. At the low NO levels generally observed at Barrow, variability in the NO measurements results mainly from counting noise. The size of the error bars is a result of measurement variability (primarily due to counting noise—1 standard deviation of the 40 s observations is 3–6 pptv) and the number of daytime NO measurements during each period. However, artifact correction errors may contribute a larger uncertainty than results from measurement variability. A conservative estimate of the uncertainty in the artifact correction is based on the standard deviation of all artifact measurements made during 1990 as described in section 2.2.5.2. This calculation indicates a total uncertainty of ± 3 pptv (2σ), shown in Figure 5.6 by

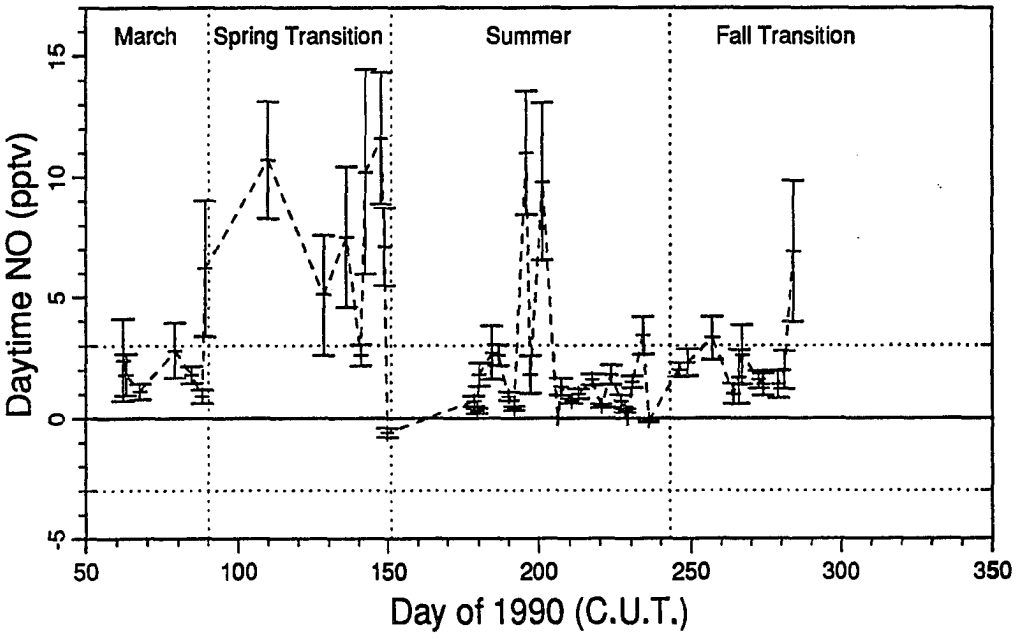

Figure 5.6 Daytime NO (solar zenith angle below 80°) concentrations during the 1990 background periods. The symbols indicate the average daytime NO concentrations during the background periods. Error bars extend 2 standard deviations of the mean above and below. The horizontal dotted lines about zero indicate the detection limit (see text).

horizontal dotted lines above and below zero. An indication of the adequacy of this uncertainty estimate can be derived by calculating the average nighttime NO during each period. These values are shown in Figure 5.7 and include all measurements when the solar zenith angle was at least 85°. In most cases, the nighttime NO estimates are much closer to zero than the conservative error estimate based on artifact variability, and no values significantly different from zero were observed. Thus, 3 pptv is an adequate estimate of the contribution of artifact correction errors to the NO measurements shown in Figure 5.6, and the observed daytime-average NO values between 3 and 15 pptv are above the detection limit.

As Figure 5.6 shows, daytime NO levels were below 3 pptv during most of the March and summer periods. An increase in NO was observed during the spring transition period, coincident with the NO_y drop. This NO pulse is likely a result of PAN decomposition, as discussed below.

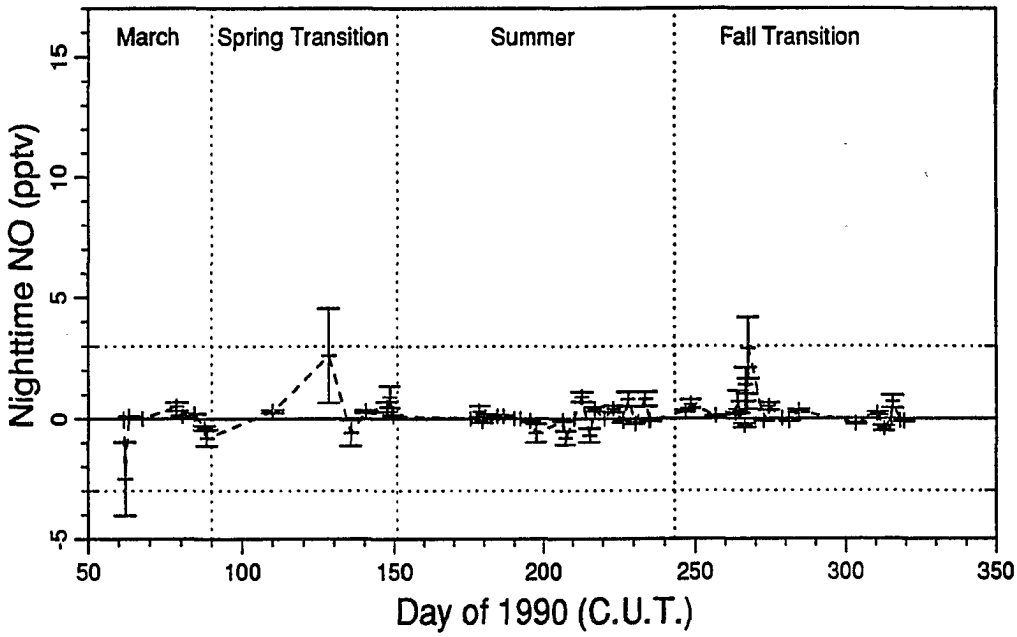

Figure 5.7 Nighttime NO (solar zenith angle greater than 85°) concentrations during the 1990 background periods. The symbols indicate the average nighttime NO concentration during each background period. Error bars extend 2 standard deviations of the mean above and below. The horizontal dotted lines about zero indicate the detection limit (see text).

Table 5.3 shows the maximum hourly-average NO concentrations observed during each background period. During periods 1–9 in March, hourly-average NO concentrations were below 6 pptv. In contrast, the NO pulse during the late spring periods 10–17 resulted in significantly higher hourly-average NO levels, reaching 34 pptv. Hourly-average NO concentrations during some of the late spring periods are shown in Figure 5.8. Figure 5.8 also shows solar elevations, and the diurnal cycle of NO concentrations that resulted from daytime NO_2 photolysis is apparent.

During summer (periods 19–43), peak hourly-average NO concentrations were generally low—reaching 4–7 pptv when the sun was at least 20° above the horizon—with the exception of periods 27 and 29. During periods 27 and 29, which are discussed in section 5.2.3.3, peak hourly-average NO levels reached 18 pptv. Figure 5.9a shows the diurnal variation of hourly-average NO during period 27.

Table 5.3 Maximum Hourly-Average NO Concentrations During 1990 Background Periods.

Background Period Number	Maximum Hourly-Average NO$\pm\sigma$[b] (pptv)	Solar Elevation[a] (degrees)	Background Period Number	Maximum Hourly-Average NO$\pm\sigma$ (pptv)	Solar Elevation[a] (degrees)
1	2.0±2.4	0	34	2.2±1.4	0
2	5.9±3.3	5	35	5.7±2.8	12
3	4.1±2.0	0	36	3.9±1.2	34
4	4.7±2.4	12	37	5.3±1.3	24
5	5.8±1.2	12	38	2.7±0.8	19
6	3.7±3.0	0	39	3.9±1.2	0
7	5.6±2.9	17	40	1.8±2.0	9
8	3.4±1.7	20	41	5.4±1.2	21
9	0.6±2.1	0	42	6.0±1.3	12
10	10.6±1.7	19	43	2.3±0.6	6
11	34.2±1.7	14	44	7.2±1.6	17
12	5.2±3.0	15	45	6.4±1.3	25
13	9.5±3.5	22	46	5.5±1.8	16
14	7.8±2.0	27	47	4.4±2.0	0
15	23.1±2.8	27	48	2.8±3.2	20
16	17.7±1.6	34	49	5.3±3.3	0
17	16.0±2.3	30	50	3.0±1.7	0
18	1.3±1.4	3	51	4.7±2.8	16
19	0.9±1.4	9	52	4.0±2.6	0
20	4.1±1.4	9	53	7.4±5.4	0
21	7.4±2.6	21	54	6.7±3.0	8
22	3.6±1.1	25	55	6.0±4.1	14
23	5.1±1.3	20	56	2.5±1.6	4
24	7.2±2.0	31	57	3.8±1.7	0
25	4.3±1.3	40	58	8.4±1.8	11
26	3.9±2.3	12	59	1.8±2.2	0
27	18.4±4.3	40	60	4.4±1.1	0
28	3.6±1.9	8	61	2.4±2.2	0
29	13.2±2.4	33	62	1.4±0.9	0
30	4.2±1.5	24	63	1.3±1.4	0
31	3.5±0.9	34	64	2.6±1.9	0
32	3.4±1.5	9	65	1.3±0.7	0
33	4.9±2.1	8			

[a]Solar elevation at the time of the maximum hourly-average NO concentration.
[b]Maximum hourly-average NO concentration ± one standard deviation of the average.

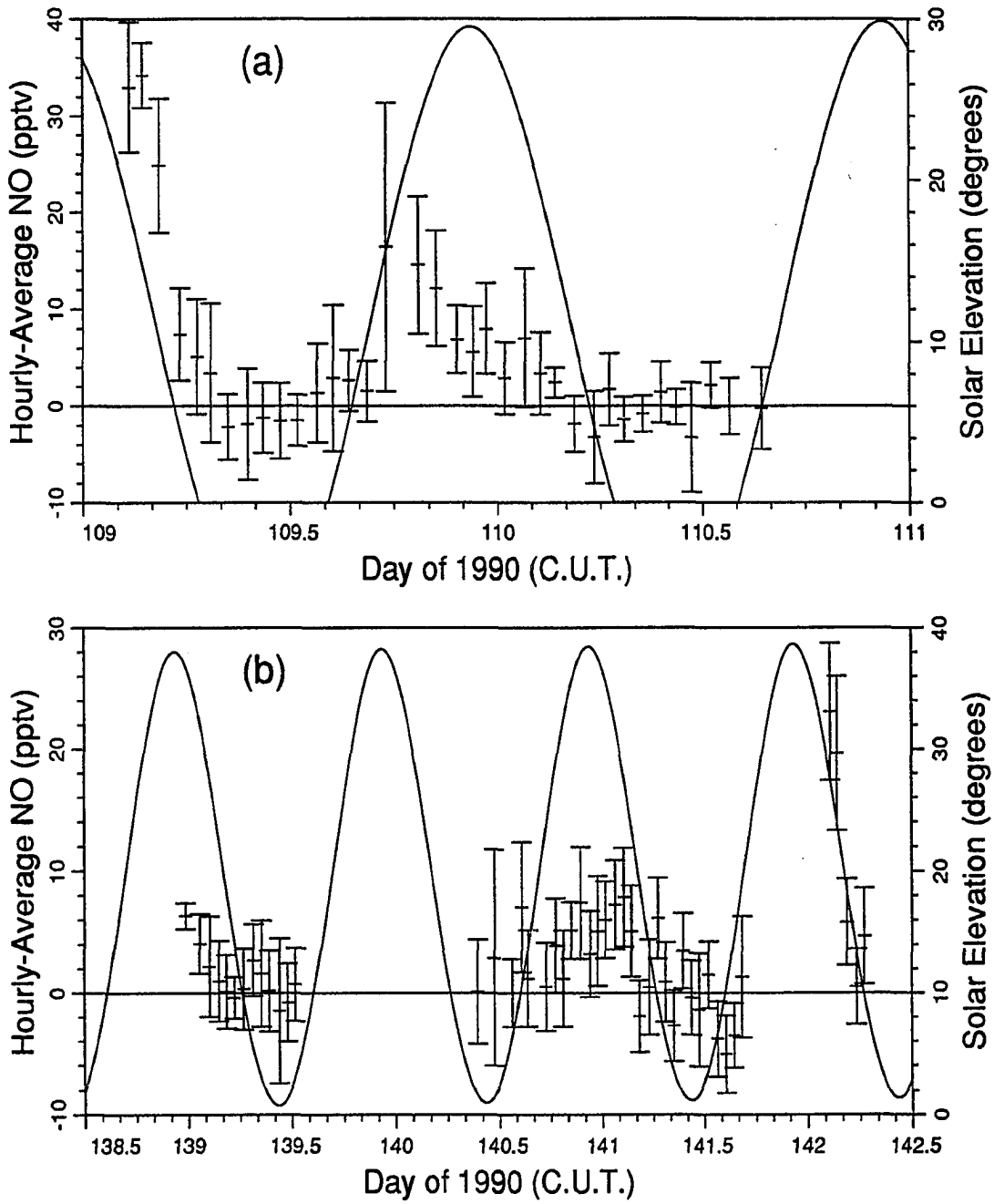

Figure 5.8 Hourly-Average NO concentrations during spring transition periods. Hourly-average NO concentrations are shown with error bars two standard deviations of the mean in length. The solid line shows solar elevation. The x-axis is in Coordinated Universal Time; local solar time is 13.6 hr (0.6 day) later. (a) Background period 11. (b) Background periods 14 and 15. Continued on next page.

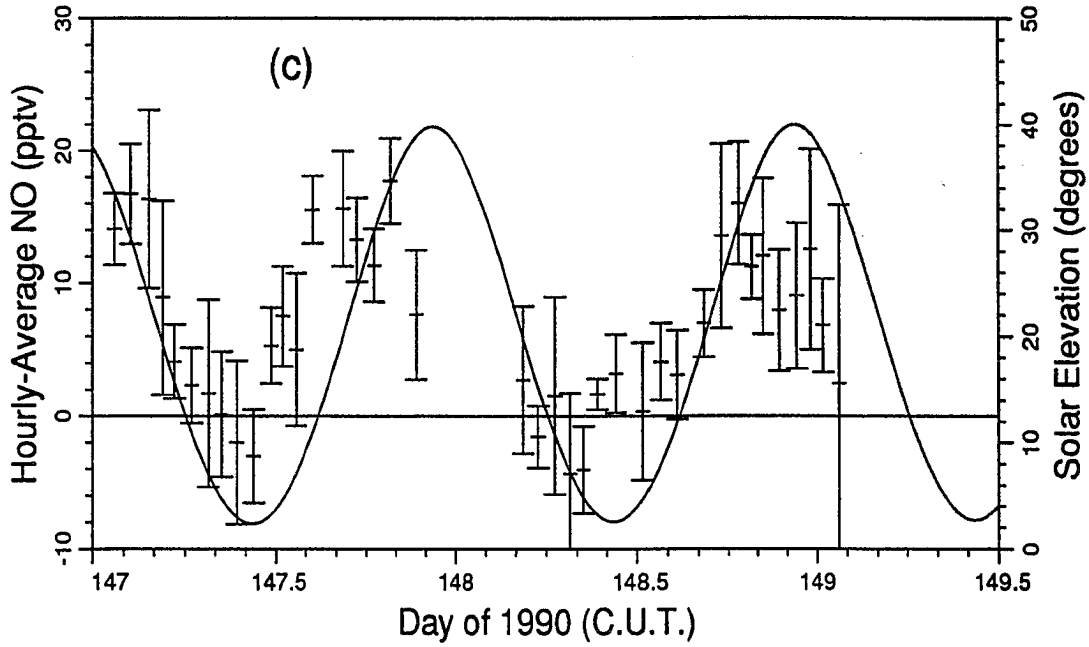

Figure 5.8 (continued) Hourly-Average NO concentrations during spring transition periods. Hourly-average NO concentrations are shown with error bars two standard deviations of the mean in length. The solid line shows solar elevation. The x-axis is in Coordinated Universal Time; local solar time is 13.6 hr (0.6 day) later. (c) Background periods 16 and 17.

Peak hourly-average NO concentrations during the fall transition periods (periods 44–65) were generally low (maximum 8 pptv). The diurnal cycle of NO during the fall period with the highest NO concentration—period 58—is shown in Figure 5.9b.

5.2.3 Analysis and Discussion

The 1990 measurements are compared to those obtained during the 1988 and 1989 campaigns and to measurements made by other investigators in the next section. In addition, the available information on NO_y speciation in the arctic troposphere is summarized. This information is used to guide discussion and further analysis of the 1990 measurements. Finally, modeling analyses that have produced NO_y

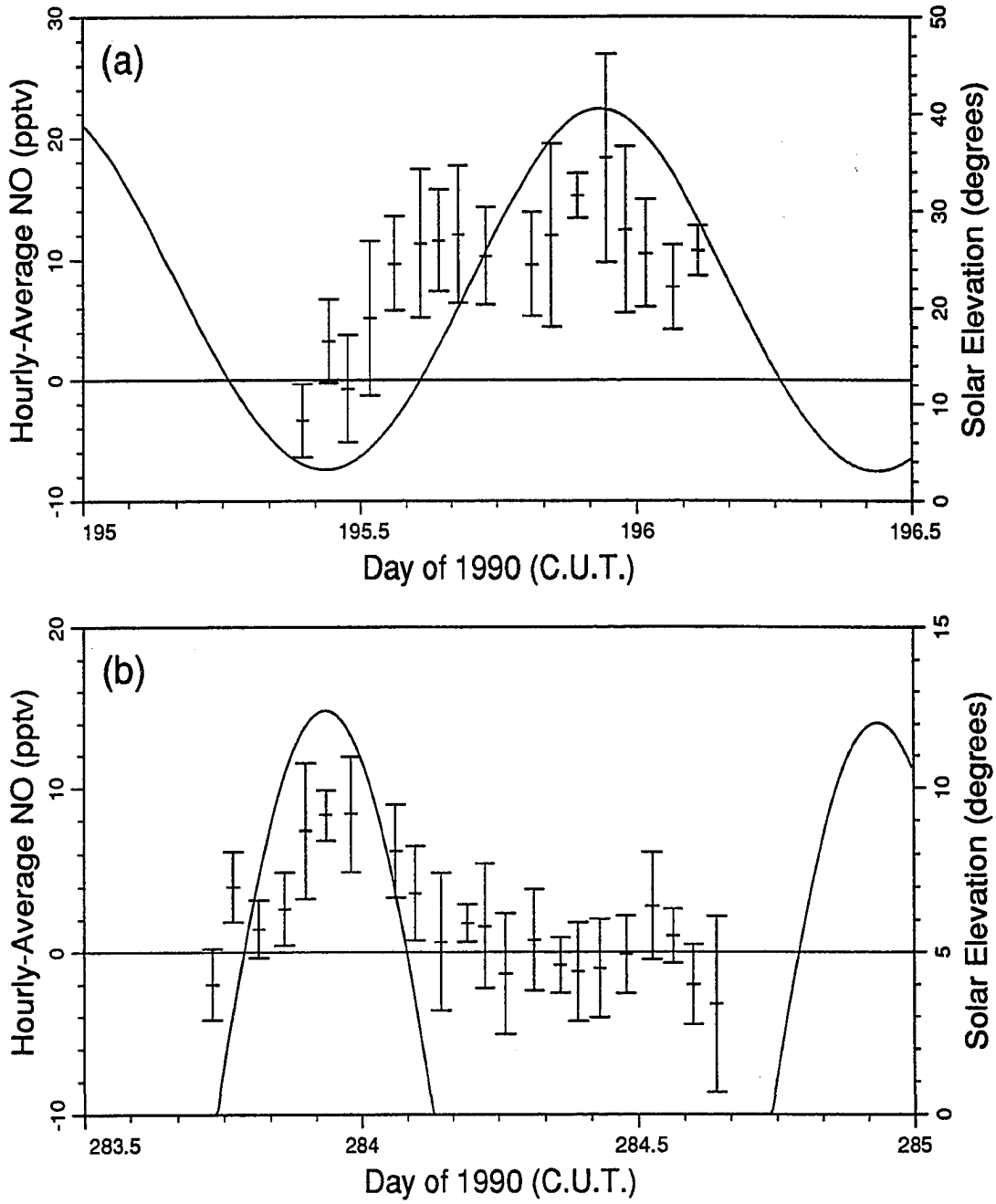

Figure 5.9 Hourly-Average NO concentrations during a summer and a fall transition period. Hourly-average NO concentrations are shown with error bars two standard deviations of the mean in length. The solid line shows solar elevation. The x-axis is in Coordinated Universal Time; local solar time is 13.6 hr (0.6 day) later. (a) Summertime background period 27. (b) Fall transition background period 58.

concentration predictions for the arctic troposphere are discussed and compared to the present measurements.

5.2.3.1 Previous Measurements

The NO_y concentrations measured at Barrow during 1990 are compared with those observed during 1988 and 1989 (presented in the previous 2 chapters) in Figures 5.10 and 5.11. Figure 5.10 shows the frequency distributions of background NO_y measurements obtained during the spring 1989 campaign (dashed line) and during March 1990 (solid line). The distributions are similar, with median concentrations of 616 pptv and 557 pptv during 1989 and 1990, respectively, although more variability was observed during the 1989 measurements. The estimated uncertainty of the 1989 measurements is higher than that of the 1990 values (32% versus 26%), as a result of NO_2 conversion efficiency variability during 1989. However, it is likely that the increased variability observed during 1989 reflects actual differences between the two periods to some extent. In particular, the lower 1989 concentrations have been attributed to relatively clean air associated with air mass trajectories from the south (chapter 4). As discussed below, such lower concentrations during southerly synoptic flow were not observed during the 1990 measurements.

Summertime NO_y measurements during 1988 and 1990 are compared in Figure 5.11. The 1988 measurements (N=175) are plotted with a dashed line. 1990 measurements during the summer background periods are shown with a solid line. (The 1990 distribution includes periods 19–43. The distribution of measurements during the marine-flow background periods 20–26 and 30–43 (discussed below) is shown with a dotted line.) Given the uncertainty of the 1988 data (estimated as $\pm$50%) the agreement is reasonable, and the two distributions are similar below 100 pptv. However, a significant fraction of NO_y concentrations observed during 1988 were above 120 pptv, in contrast to 1990. The only 1990 measurements above

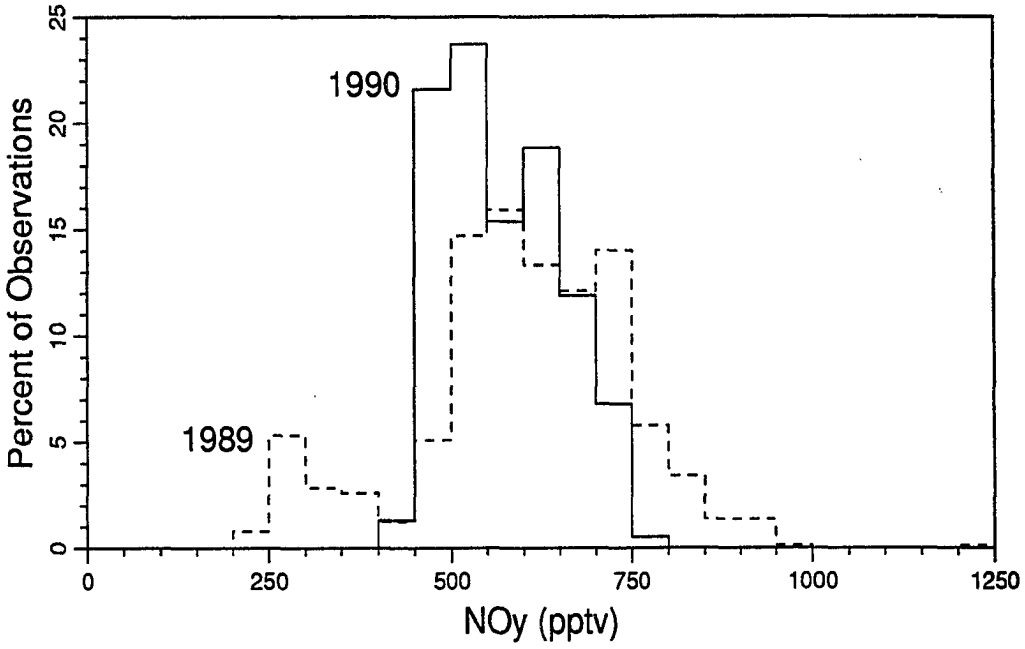

Figure 5.10 Comparison of NO_y measurements during spring 1989 and March 1990. The spring 1989 distribution (dashed line) includes 885 100-s average NO_y measurements. The March 1990 distribution (solid line) includes 1152 200-s average NO_y measurements.

120 pptv were associated with local surface flow over tundra (rather than marine flow), as discussed below. Since the 1988 measurements include only periods with surface wind directions 45–130° (i.e., primarily marine flow), it is unlikely that different flow patterns in the two summers are the cause of this discrepancy. In addition, since the summer 1990 measurements include much more data obtained over a longer period than in 1988, it is expected that if the higher background measurements obtained during 1988 were real, similarly high concentrations would have been observed during 1990. The higher NO_y levels during 1988 may instead be a result of a "memory effect" of the molybdenum mesh converter used in that campaign, in which high NO_y levels prior to the background periods (due to local contamination) resulted in erroneously high NO_y measurements during the background periods. Alternatively, residual effects from Prudhoe Bay NO_x emissions not removed by the 1988 screening procedure may be the cause.

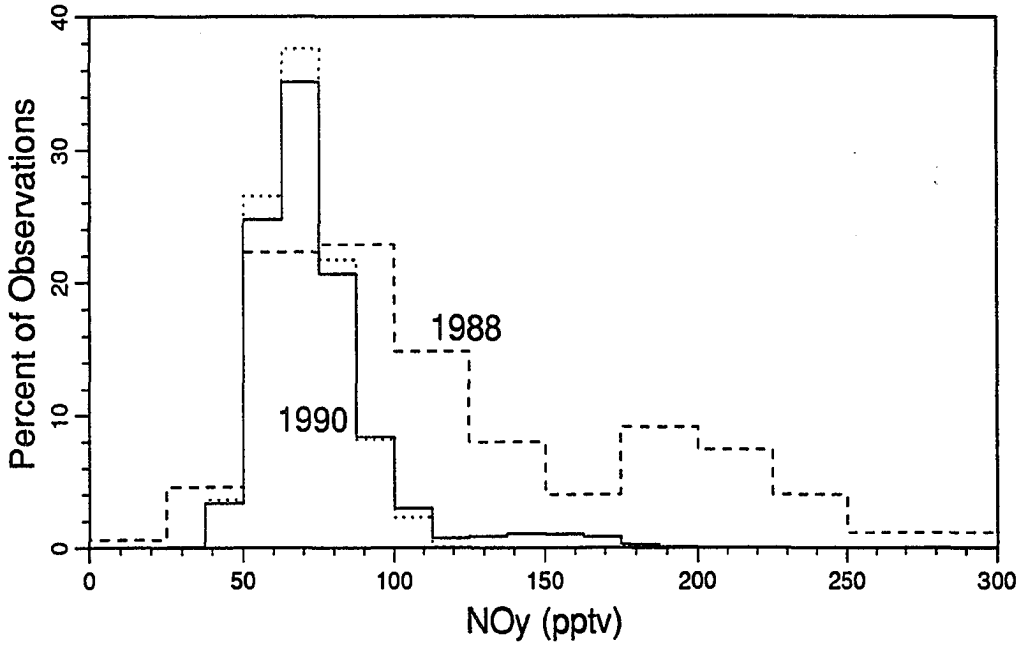

Figure 5.11 Comparison of NO_y measurements during summer 1988 and summer 1990. The summer 1988 distribution (dashed line) includes 175 120 s-average NO_y measurements. The summer 1990 distribution (solid line) includes 3521 measurements (periods 19–43). The summer 1990 distribution including only the marine-flow periods (periods 20–26 and 30–43; see section 5.2.3.3) is based on 3291 measurements and shown with the dotted line.

The low NO concentrations observed throughout the 1990 measurement campaign were below the 1988 and 1989 detection limits. Thus, the lack of detectable NO concentrations during 1988 and 1989 is consistent with the 1990 measurements.

Aside from the Barrow data presented here, few measurements of NO or NO_y in the Arctic have been reported. The reported measurements are from three aircraft flights during spring [*Dickerson,* 1985] and a surface and airborne campaign during summer [*Bakwin et al.,* 1991; *Singh et al.,* 1991a, 1991b]. Springtime NO_y concentrations were measured during aircraft flights at a latitude of ~80°N [*Dickerson,* 1985]. After correction for artifact measurement errors (R. Dickerson, private communication to D. Jaffe, 1988), those measurements are in broad agreement with the ground-level Barrow results. Dickerson's measurements in the boundary layer ranged from 600 to 1000 pptv, with a few higher values. These are in the upper por-

tion of the range observed at Barrow, or somewhat higher. Free-tropospheric NO_y reached 1000–1600 pptv in polluted layers, and was about 300–400 pptv outside the layers. Thus, the free-tropospheric measurements within and out of polluted layers span the Barrow surface measurements reported here.

NO measurements were also made during the springtime aircraft flights. NO concentrations were always below the detection limit of ~10 pptv, while solar zenith angles were $\geq$~80° [*Dickerson,* 1985]. This is consistent with our observations of daytime-average NO < 15 pptv during March at Barrow, when mid-day solar zenith angles reached <80°.

Summertime NO and NO_y concentrations were measured during aircraft flights based at Barrow and Bethel, Alaska, and at the surface at Bethel during the ABLE-3A campaign in 1988. Aircraft measurements in the Arctic and subarctic found NO_y concentrations generally 150–250 pptv near the surface [*Singh et al.,* 1991b]. However, a reservoir of elevated NO_y concentrations—500–2000 pptv—was present in the mid-troposphere. Surface measurements at the subarctic Bethel site also indicated relatively low boundary-layer NO_y values, as well as a significant diurnal cycle in NO_y concentrations, which ranged from ~130 pptv in early morning to ~210 pptv in late afternoon [*Bakwin et al.,* 1991]. NO_x concentrations during the same period were generally ~10–15 pptv [*Bakwin et al.,* 1991].

The Bethel surface NO_y measurements are 50–100 pptv higher than most of the concentrations observed at Barrow during the summer of 1990. However, they are similar in magnitude to the NO_y concentrations during Barrow tundra-flow periods which were ~100–200 pptv (see discussion of marine-flow versus tundra-flow in section 5.2.3.3 below). Thus, the lower concentrations generally observed at Barrow may reflect higher boundary layer stability over the arctic ocean [*Kahl,* 1990], relative to the subarctic region surrounding Bethel. It appears that boundary-layer NO_y concentrations in arctic and subarctic Alaska during summer are controlled primarily by vertical transport from the free-tropospheric NO_y reservoir [*Jacob et al.,*

1991]. More efficient vertical mixing at Bethel than at Barrow, due to warmer near-surface temperatures at Bethel, may cause higher surface NO_y concentrations at that site. In addition, NO_y concentrations at the Bethel site were occasionally enhanced by forest fire plumes during the ABLE-3A measurements [*Bakwin et al.*, 1991], which were not observed at Barrow. The airborne ABLE-3A NO_y measurements are also somewhat higher than the Barrow surface measurements, and this may reflect a steep vertical NO_y gradient in the arctic boundary layer during summer.

Measurements of boundary-layer NO_y in remote regions outside the Arctic are also sparse. Summertime NO_y at Mauna Loa, Hawaii [*Hübler et al.*, 1989] have been reported to be ~80–350 pptv in clean air, with a median NO_y level of approximately 250 pptv, based on a 1-month measurement period during May–June. Median NO and NO_x concentrations at the same site were 11 and 36 pptv, respectively [*Montzka et al.*, 1989]. *Stedman and McEwan* [1983] measured NO_y in clean air in New Zealand during February–May. They reported a range of 10 to >600 pptv, with a median of 130 pptv. At Cape Grim, Australia, concentrations from <50 to 300 pptv have been observed in marine air during May–August, with more than 90% of the observations between 100 and 200 pptv [*Galbally and Roy*, 1981]. Marine air off the North Atlantic, sampled by *Helas and Warneck* [1981] in Western Ireland during June, had a median NO_y concentration of 140 pptv, with a range from 0 to 1400 pptv. Somewhat higher concentrations were observed in the Amazon forest during July–August (median 455 pptv) near the city of Manaus, Brazil, even after discarding data apparently affected by regional or local pollution [*Bakwin et al.*, 1990].

In contrast to these measurements, the arctic summertime NO_y concentrations measured at Barrow during 1990 (median 70 pptv) were very low, while the arctic concentrations during March (median 557 pptv) were higher than those at other remote areas. This indicates isolation of the Arctic from major NO_x sources during summer as well as the stability of the summertime arctic boundary layer, which

apparently prevents effective mixing to the surface of elevated NO_y concentrations aloft. The high March arctic levels are a combination of "arctic haze" and increased stability of the NO_y reservoir during cold periods, as discussed below.

NO_y Speciation. Measurements of specific NO_y compounds in the Arctic indicate a distinct change in the speciation of ground-level NO_y from winter-spring to summer. In particular, the fraction of near-surface NO_y accounted for by PAN appears to be much higher during winter-spring than during summer, although this may not be the case in the free troposphere. Ground-level measurements made at Alert, Canada, during the springs of 1986–1988 indicate springtime PAN concentrations of 200–600 pptv [*Bottenheim et al.,* 1986; *Barrie et al.,* 1989; *Bottenheim et al.,* 1991] and alkyl nitrate levels as high as 50% of the simultaneous PAN concentration [*Bottenheim et al.,* 1991]. Simultaneous measurements of PAN and NO_y at the same location have not been made in the Arctic during the winter–spring arctic haze season. However, a comparison of the Alert PAN levels of 200–600 pptv with either the spring 1990 Barrow measurements of ~500–700 pptv or the March 1989 measurements of ~300–900 pptv (chapter 4) indicates that PAN is an important NO_y component. Since significant alkyl nitrate concentrations were also observed at Alert, it is likely that most of the springtime arctic NO_y reservoir is composed of organic nitrogen oxides such as PAN and alkyl nitrates. The simultaneous measurements of NO_y and total-NO_3^- in spring 1989 (described in chapter 4), which indicated low total-nitrate:NO_y ratios ($\leq$25%), support this conclusion.

During summer, PAN accounts for a smaller fraction of surface NO_y in the Arctic. Summertime PAN concentrations at Alert during 1988 were below 20 pptv [*Barrie and Bottenheim,* 1991]. Measurements of NO_y, PAN, and other NO_y components within the boundary layer over arctic Alaska during the ABLE-3A study also demonstrated low summertime PAN concentrations in the boundary layer (<10–50 pptv), with PAN accounting for only about 10% of the total boundary-layer NO_y. [*Singh et*

al., 1991a]. However, a significant PAN and NO_y reservoir was found in the free troposphere, with NO_y concentrations to >1000 pptv composed of ~40% PAN [*Singh et al.*, 1991b]. In addition, organic nitrates besides PAN appear to have been important NO_y components, both within the boundary layer and aloft, as the measured NO_y species (NO_x, HNO_3, PAN, and CH_3ONO_2) accounted for only 40–50% of the total NO_y observed throughout the troposphere [*Singh et al.*, 1991b]. Furthermore, modeling analysis of the ABLE3-A measurements indicates that the low NO_x levels observed near the surface can be explained by decomposition of PAN mixed down from above [*Jacob et al.*, 1991].

This discussion indicates that PAN and other organic nitrates are the dominant NO_y compounds in the Arctic, both during spring and summer. This is important because the lifetime of PAN is highly temperature-sensitive. Based on the thermal decomposition reaction alone, it varies from 2.6 yr at -30°C to 8.6 hr at 10°C. At night, surface deposition is expected to be the most important PAN removal process in mid-latitudes [*Singh,* 1987], but this process is inefficient in the arctic winter, since PAN deposition over seawater and fresh water is very slow [*Garland and Penkett,* 1976] and deposition to snow is also expected to be slow. Thus, the lifetime of PAN in the Arctic during winter is expected to be very long. In summer, warmer temperatures in the Arctic lead to an increased PAN decomposition rate and a shorter lifetime. The implications of changing PAN lifetimes on the seasonal cycles of NO_y and NO in the Arctic are discussed in the next section.

5.2.3.2 The Seasonal NO_y Cycle

The seasonal variation of NO_y at Barrow (Figure 5.5) closely mirrors that of a number of man-made pollutants which are components of "arctic haze." For example, measurements of aerosol light scattering coefficient (B_{sp}) at Barrow [*Bodhaine et al.*, 1981] indicated a similar plateau of high levels from about December–April, followed by a sharp drop during April and May to low summertime levels and a

fall increase beginning in September. Sulfur dioxide and sulfate concentrations in the Arctic exhibit a similar cycle [*Heidam,* 1983; *Joranger and Ottar,* 1984; *Barrie and Hoff,* 1985], as do many other pollutant tracers [*Barrie and Hoff,* 1985; *Barrie,* 1986]. Elevated winter–spring concentrations of these species are due to long pollutant lifetimes in the Arctic during winter, combined with enhanced transport from source regions. For example, based on measurements of the decay in hydrocarbon and halocarbon concentrations at Barrow, *Rasmussen et al.* [1983] reported that reductions in lifetime due to increasing OH concentrations could explain a large fraction of the observed March–June concentration decline. However, for the longer-lived species, there was a clear indication that transport times from the pollutant source region(s) were also increasing over this period [*Rasmussen et al.,* 1983].

In the case of NO_y, it is likely that the seasonal cycle is significantly mediated by chemical processes, primarily a reduction in the lifetime of the stable reservoir NO_y species, such as PAN, as temperatures and insolation rise in the spring. As discussed above, PAN and other organic nitrates are significant components of NO_y in the Arctic. The products of their decomposition (NO_x and, indirectly, HNO_3) have much shorter lifetimes than does PAN at low temperatures. Thus, the overall NO_y lifetime is expected to be highly temperature-dependent. This indicates a potentially important role of organic nitrate decomposition in determining the observed seasonal cycle.

Potential Role of Organic Nitrate Decomposition. Figure 5.12 shows the monthly-average background NO_y concentrations observed at Barrow and surface temperatures averaged over the same periods. A strong negative correlation is apparent, as expected if enhanced decomposition of PAN and/or other organic nitrates due to warmer late-spring and summer temperatures and/or greater insolation led to lower NO_y levels through formation of NO_x, and thence HNO_3, which is efficiently removed at the surface and by rainout. Additional evidence that decomposition of

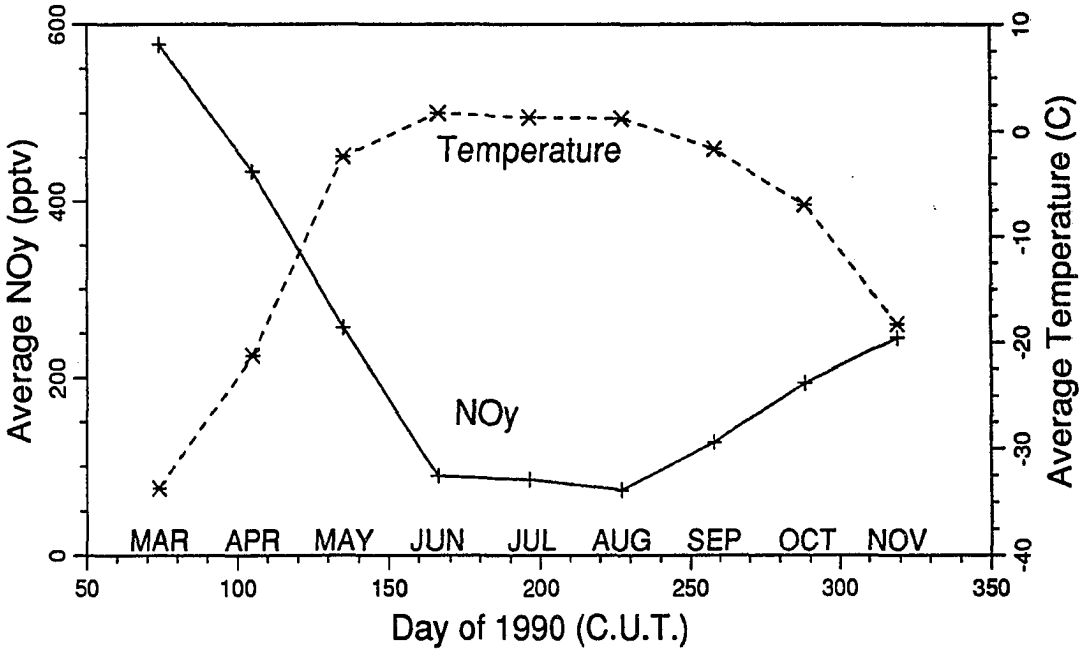

Figure 5.12 Monthly-average NO_y concentrations (solid line) and temperatures (dashed line) during the background periods. Values are averages of the concentration and temperature values for each background period within the respective month. The value for April is based on a single background period.

PAN and similar compounds contributed to the decay of the springtime NO_y reservoir is seen in the time series of daytime NO (Figure 5.6), which shows a pulse of NO coincident with the NO_y drop, presumably a result of NO_x released from organic nitrate decomposition.

The extent to which decomposition of PAN contributed to the drop in NO_y levels during the spring transition period can be assessed through a simple calculation. It is assumed that (1) NO_y is composed of PAN exclusively; (2) PAN decomposition represents a loss of NO_y (via deposition of NO_x or HNO_3); and (3) the transit time and dilution of air parcels transported from NO_y source regions to the Arctic is constant from March–June. As discussed above, the first assumption is likely only partially correct; PAN appears to be a major NO_y component, but other compounds, including other organic nitrates, are probably important as well.

The second assumption is equivalent to assuming that the lifetime of NO_x in the Arctic during spring is much less than that of PAN (~4–50 days during March–late May). However, since the PAN decomposition reaction is reversible, this assumption results in an underestimation of the true PAN lifetime [*Singh,* 1987]. The average transit time of air mass trajectories reaching Barrow from potential pollution source regions is estimated to be approximately constant through April and May, but is expected to increase somewhat in June [*Patterson and Husar,* 1981].

If these assumptions are accepted, then the NO_y concentration in the Arctic, C, is given by

$$C = fC_0 \exp(-T/\tau) \tag{5.1}$$

where C_0 is the concentration of the removal-resistant NO_y reservoir species in a pollution source region, T is the transport time from the source region to the Arctic, f is the dilution en-route, and τ is the NO_y (PAN) temperature-dependent lifetime. Equation 5.1 indicates that a plot of C versus $1/\tau$ should be linear on a semi-logarithmic scale:

$$\ln C = \ln(fC_0) - T(1/\tau). \tag{5.2}$$

Such a relationship was indeed observed, as displayed in Figure 5.13, which shows NO_y concentrations and estimated PAN lifetimes averaged for all background periods during March–June. The PAN lifetimes shown in Figure 5.13 must be interpreted with caution because they are based on thermal decomposition only, at the average Barrow surface temperature during each background period. Thus, the lifetimes calculated for the March periods are probably too long, since reaction with OH is expected to be more important than decomposition at the low March temperatures [*Singh,* 1987]. More importantly, it is likely that the Barrow surface temperature does not accurately reflect the actual temperature during transport from source regions. If transport occurred in the free troposphere (as indicated by the summertime ABLE-3A measurements of a free-tropospheric NO_y reservoir), then the actual temperatures would be lower, resulting in longer estimated lifetimes. Conversely, if

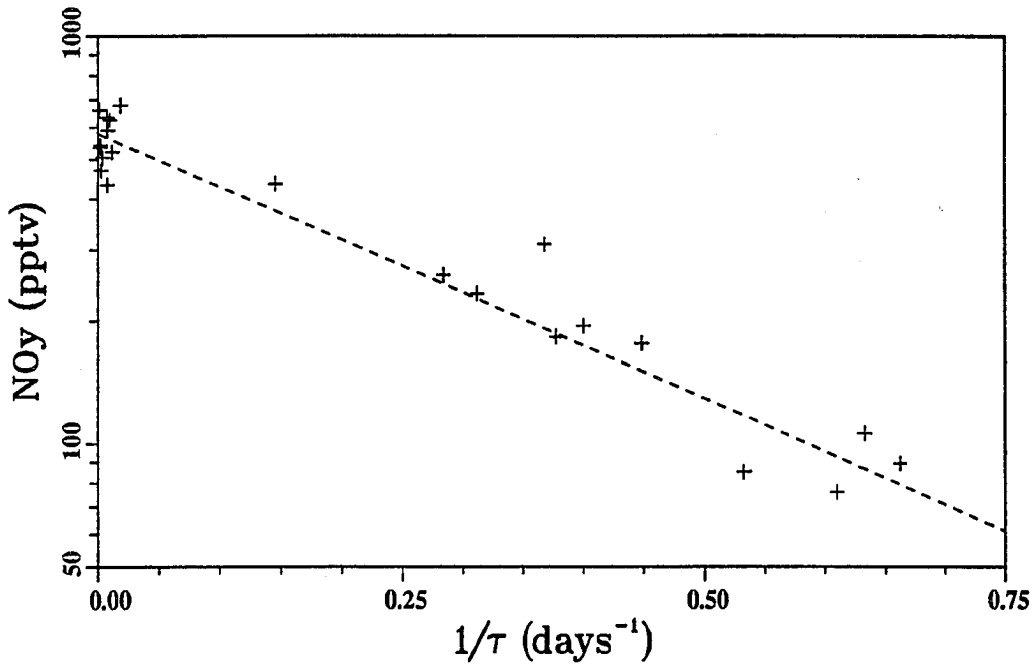

Figure 5.13 Correlation of NO_y concentrations during March–June with PAN lifetime. NO_y concentrations are averaged over each of background periods 1–22. The x-axis shows the reciprocal of PAN lifetime, based on the PAN decomposition rate only, at the average temperature of each background period. The dashed line is the result of a least-squares linear regression of $\log([NO_y])$ versus $1/\tau$. The regression parameters are given in the text.

transport occurred in the boundary layer, the average transport temperature would probably be higher.

A least-squares regression line based on equation 5.2 is also shown in Figure 5.13. The estimated regression parameters from that line are $fC_0 = 580 \pm 30$ pptv and $T = 3.0 \pm 0.2$ days ($\pm 1\sigma$). A transport time T of 3 days is significantly shorter than the expected period for transport from source regions, which has been estimated as 16–19 days [*Patterson and Husar,* 1981]. This could indicate that transport occurred in the free troposphere where temperatures were colder, consistent with the finding of elevated NO_y and PAN concentrations in the free troposphere during the ABLE3-A summertime flights [*Singh et al.,* 1991b]. Alternatively, the use of PAN decomposition lifetimes may have been inappropriate, since a reduction in NO_y lifetime could also result from increased rates of decomposition of other organic

nitrogen compounds due to either increasing temperatures or increasing sunlight. Nevertheless, this analysis supports the hypothesis that decomposition of PAN or other organic nitrates was largely responsible for the drop in NO_y concentration and the NO pulse observed during the transition period.

5.2.3.3 Modifications to the Seasonal Cycle

This section contains a discussion of factors that may have contributed to observed deviations from the general seasonal cycle of NO_y at Barrow. The roles of atmospheric flow patterns, temperature, and time of day in determining NO_y concentrations are presented below.

This discussion makes use of hourly-average meteorological parameters (surface wind and temperature) measured at the CMDL site [*NOAA*, 1991], temperature inversion data calculated from U. S. National Weather Service soundings at Barrow using the procedure of *Kahl* [1990] (J. Kahl, private communication, 1991), and 10-day back-trajectory calculations [*Harris*, 1982].

Effects of Local Wind Direction and Temperature. Figure 5.14a and b show the relationship between average NO_y concentrations in the summer periods and surface wind and temperature, respectively. Most of the summer periods coincided with wind directions of 0–120° (Figure 5.14a), and thus were representative of marine air. In contrast, wind directions during periods 27–29 occurred during surface flow from the southeast sector, and air sampled during those periods had an upwind fetch of tundra. With the exception of period 19 (discussed below), NO_y concentrations during the tundra-flow periods were higher than those during any of the marine-flow periods.

Temperatures were also elevated during the tundra-flow periods. The average temperatures during periods 27 and 29 were more than 10° higher than those of most of the other periods, which had average temperatures $\leq$4°C. The temperature

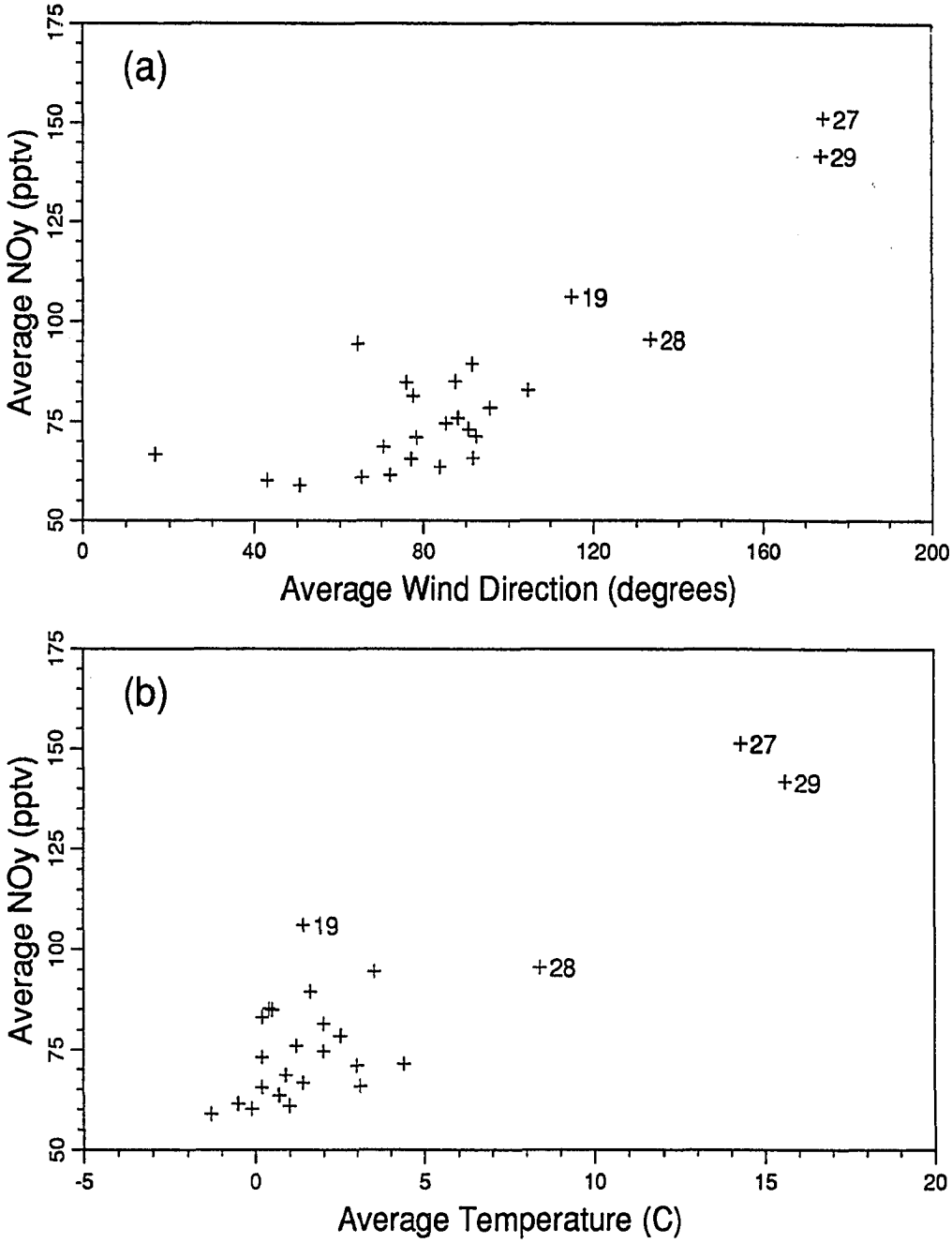

Figure 5.14 Average NO_y concentrations during the summer background periods versus surface wind and temperature. (a) X-axis gives surface wind direction, averaged over each background period. (b) X-axis gives average temperature for each period. Numerals identify periods 19 and 27–29.

during period 28 was also high. As shown in Figure 5.14b, the temperature variations during summer are correlated with NO_y levels. Higher temperatures may have affected the NO_y levels by causing weaker surface inversions. In fact, period 27 coincided with one of the few 1990 soundings which indicated no surface or elevated inversion. However, the sounding just after period 28 indicated a shallow surface-based inversion 24 m deep, and the soundings surrounding period 29 found surface-based inversions >200 m in depth. Higher temperature could also result in additional NO_x emissions from biogenic sources [*Williams,* 1987]. However, the ABLE-3A measurements at Bethel, which is considerably warmer than Barrow, indicated that the biogenic NO_x flux was a minor contributor to the NO_y budget at that location [*Bakwin et al.,* 1991], so increased biogenic emissions may not explain the ~50 pptv higher NO_y during the tundra-flow periods.

Other potential explanations include (1) a warmer and less stable boundary layer over land than over the ocean, which resulted in more efficient transport from the free troposphere to the surface over land; and (2) impacts from Alaskan wildfires during the southerly flow periods, which occurred during synoptic flow from the south (as indicated by 850 mb back-trajectories). However, without a full understanding of the stability of the boundary layer over the ocean and inland during those periods, it is not possible to draw a definite conclusion.

NO levels were also elevated during periods 27 and 29 (hourly-average NO concentrations reached 18 pptv), and this was probably a result of enhanced PAN decomposition due to the increased temperature. It should be noted that NO_x emissions from natural gas-fired heaters, installed at the Barrow gas wells to the south of the station during 1990 are also a possible cause of the increased NO and NO_y levels during the tundra-flow periods. However, there is no indication of increased concentration variability during these periods, as would be expected with nearby sources.

NO_y concentrations during period 19 were higher than those during any other

marine-flow, low temperature period. An inspection of the meteorological data record for the day prior to period 19 indicates that residual effects from local Barrow pollution may have been responsible. At the start of period 19, the wind heading was 111°. However, a wind reversal had occurred just prior to period 19. As recently as 7 hr before the beginning of period 19, the wind direction was 293°—opposite that observed during period 19—and winds from this direction, accompanied by NO_y concentrations to >10 ppbv, had persisted for approximately 1 day previous. Thus, it is considered likely that the relatively high NO_y levels during period 19 were a result of local pollution, rather than a true increase in background concentrations. The distribution of summertime background measurements during the marine flow background periods (i.e., periods 20–26 and 30–43) is shown in Figure 5.11.

There is no clear relationship between NO_y and temperature during March, when the maximum temperatures were much lower (the highest average temperature during a March background period was -17°C). Similarly, the much larger variability of NO_y levels in March (compared to summer) masks any effect of surface wind direction. There is much less difference between wind directions in terms of upwind fetch during spring than in summer, however, since the land and most of the ocean are covered with snow and ice. Therefore, the absence of a detectable effect of wind direction is not surprising.

During the spring and fall transition periods, NO_y concentrations changed more rapidly. As a result, it is not possible to separate differences in NO_y concentrations between background periods that result from local wind direction from those resulting from a changing NO_y lifetime and synoptic-scale processes. The role of increasing temperature on the NO_y decay observed during the spring transition period was discussed above (section 5.2.3.2).

Diurnal NO_y Variations. Diurnal variations in NO_y concentrations in remote areas have been observed in previous studies [*Kelly et al.*, 1980; *Helas and Warneck,*

1981; *Stedman and McEwan,* 1983]. Diurnal concentration cycles could arise from a variety of causes, including diurnal changes in mixing height, temperature-induced variations in biological NO_x production, and diurnal wind direction changes.

Figure 5.15a shows the diurnal variations of NO_y concentrations during the March background periods. The points plotted in Figure 5.15a represent average concentrations within each 2-hr interval. In order to remove effects of changes in NO_y concentration between background periods, the average concentration during each background period was subtracted from that observed during each hour of the respective period prior to averaging over 2-hr intervals for the figures. The error bars in Figure 5.15 extend ± 2 standard deviations of the mean and represent 95% confidence intervals on the means, which are averages of 7–58 values.

No significant diurnal trend was observed during the March periods. This may be a result of the removal-resistant nature of the springtime NO_y reservoir, which is apparently composed primarily of organic nitrate compounds such as PAN, with little HNO_3. Thus, diurnal mixing height changes would have less effect on NO_y concentrations than on concentrations of compounds such as $SO_4^=$ or HNO_3. Measurements of $SO_4^=$ and HNO_3 at Barrow during the spring seasons of 1986 and 1989 produced conflicting results regarding diurnal cycles of those species. In 1986, 12 hr-average $SO_4^=$ filter samples showed no detectable day-to-night differences [*Li and Winchester,* 1989]. However, measurements of $SO_4^=$ and HNO_3 in the spring of 1989 indicated significant day-to-night differences for both compounds (Shao-Meng Li, private communication, 1989). Analysis of the NO_y data from the spring 1989 measurement campaign indicates no significant diurnal cycle, consistent with the 1990 results.

In contrast, the diurnal cycles of NO_y during the spring transition, summer, and fall transition periods (shown in Figures 5.15b and 5.16a and b) were statistically significant at the 2 σ level. The daily amplitudes (based on 2-hr average data) are small: 25 ± 17 pptv (spring transition), 8 ± 2 pptv (summer) and 11 ± 7 pptv (fall

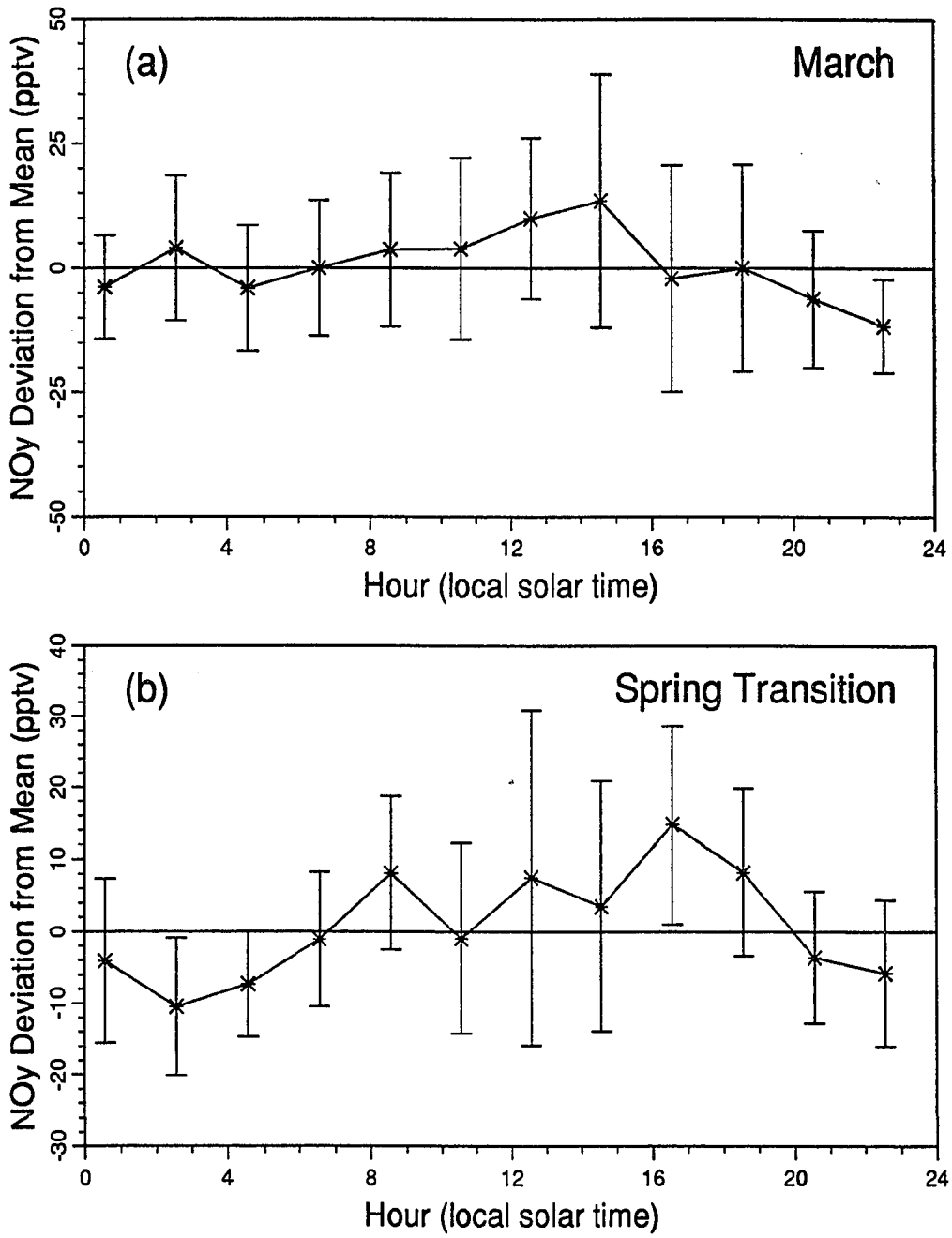

Figure 5.15 The diurnal cycle of NO_y during the 1990 march and spring transition background periods. The figures show the diurnal cycle of NO_y, averaged in 2-hr bins for all background periods in March (a) and the spring transition (b). Prior to averaging over 2-hr periods, the mean concentration for each period was subtracted from NO_y observations during the respective period, in order to minimize effects from concentration changes between periods. The error bars indicate the confidence interval on the average (2σ). At the 2σ level, there is no statistically significant diurnal cycle in the March data, but a significant diurnal cycle was present during the spring transition periods.

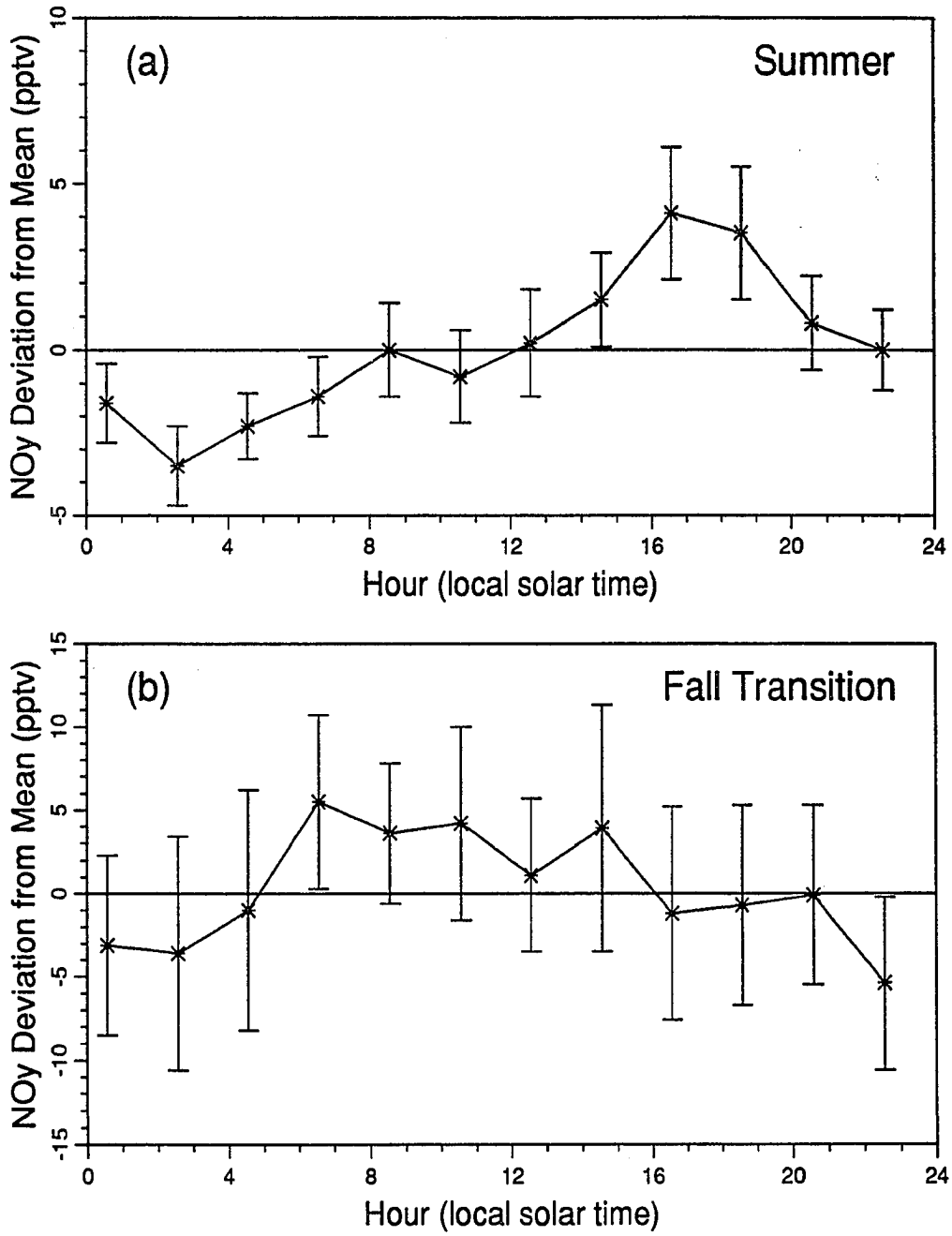

Figure 5.16 The diurnal cycle of NO_y during the 1990 summer and fall transition background periods. The diurnal cycles during the summer marine-flow periods (a) and fall transition periods (b) are shown in the format of Figure 5.15. At the 2σ level, the diurnal cycles in both the summer and fall transition background periods are significant.

transition), where the uncertainties are specified as $\pm 2\sigma$. The presence of significant diurnal variations during these periods may indicate that increased surface temperature resulted in PAN decomposition and, ultimately, NO_x and HNO_3 production and deposition. In this scenario, the diurnal cycle is a result of vertical mixing during mid-day and depletion of boundary-layer NO_y through removal at night. Alternatively, the diurnal NO_y cycles may be due to diurnal changes in biogenic NO_x production, at least during summer. The very low NO_x concentrations at Barrow and the expected low HNO_3 levels are reflected in the small observed daily amplitudes. (Although Figure 5.16a is based on the marine-flow summer periods only (periods 20-26 and 29-44); inclusion of all summer periods (periods 20–44) does not significantly alter the shape or amplitude of the diurnal cycle.)

These results support the finding of a diurnal cycle in the summer 1988 measurements (chapter 3), but indicate a much lower amplitude than that observed during 1988. The larger estimated amplitude during 1988 may have been an artifact of the small number and short duration of the background periods identified in 1988.

Summertime NO_y measurements at Bethel during the ABLE-3A study also indicated a diurnal cycle [*Bakwin et al.*, 1991]. Comparisons with simultaneous HNO_3 measurements indicated that nighttime HNO_3 deposition combined with daytime production and/or mixing from aloft was responsible for the observed cycle [*Bakwin et al.*, 1991]. The amplitude of the diurnal cycle observed at Bethel was larger than that observed at Barrow (~80 pptv versus ~10 pptv) and this may be due to greater vertical mixing at Bethel, as discussed above. In addition, the teflon inlet tube used in this study was longer (100 cm) than that used at Bethel (~15 cm; *Bakwin et al.*, [1991], and increased HNO_3 adsorption/desorption on the longer tube may have resulted in some flattening of the true diurnal cycle at Barrow.

Synoptic Flow Patterns. Trajectory calculations were used to investigate the effects of large-scale atmospheric flow patterns on background NO_y levels at Bar-

row during March. Trajectory analysis of results from the spring 1989 measurements (chapter 4) indicated lower concentrations during southerly flow (one-half to two-thirds of those during arctic flow periods), and this analysis was repeated to determine whether that was the case in 1990 as well.

Ten-day back trajectories at 850 mb, ending at Barrow at 0000 and 1200 Co-ordinated Universal Time (C.U.T.), were used to classify the flow patterns during each background period into Arctic and Bering/south, as was done for the 1989 measurements. In many cases, adjacent trajectories during, before and/or after a given background period were significantly different, and a clear identification of the flow during the period could not be made. Of the clearly identifiable periods, 3 occurred during arctic flow (periods 4, 8, and 9) and 2 during southerly flow (periods 3 and 6). Two of the arctic-flow periods (4 and 9) were among the highest in NO_y concentration (660 and 630 pptv), while NO_y levels were slightly lower during the southerly-flow periods (470 and 590 pptv). However, concentrations during period 8 (510 pptv average) were among the lowest measured in March. Trajectory calculations indicate that air sampled during period 8 originated in the Tamyr Peninsula region of the northern U.S.S.R. These results indicate only a weak effect of synoptic flow patterns on springtime NO_y at Barrow during 1990, with somewhat lower levels usually observed during southerly flow relative to arctic flow. However, concentrations observed during period 8 indicate that equally low levels can occur during periods of arctic flow. These results are in contrast to the 1989 measurements, which indicated NO_y levels during southerly flow only 50–70% of those during arctic flow.

850 mb trajectories were also used to classify background periods during the spring and fall transition and summer periods into arctic flow and southerly flow categories. However, any differences that may be present between arctic and southerly flow during the transition periods are not detectable because of the changing concentrations between periods. During the summer, the overall concentration range

between the separate periods is small, and the average concentration difference between arctic and southerly flow periods is also not significantly different from zero (-11±20 pptv (±1σ); 6 arctic flow periods – 5 southerly flow periods). Periods 19, 27, and 29, all of which occurred during large-scale southerly flow, were excluded from this analysis because of potential local contamination (period 19) and high NO_y levels associated with tundra-flow conditions (periods 27 and 29). Inclusion of periods 27 and 29 leads to a larger difference between arctic and southerly flow periods, but the difference is still not significant at the 2σ level.

5.2.3.4 The Relationship of NO_y and O_3 During the Background Periods

The relationship between nitrogen oxides and ozone in the arctic troposphere is of interest for several reasons. NO_x formation resulting from decomposition of PAN and/or other organic nitrates in the springtime arctic NO_y reservoir has the potential to affect springtime O_3 production both in the Arctic and at mid-latitudes. Since the springtime "arctic haze" NO_y reservoir is apparently a result of anthropogenic NO_x emissions, this represents a mechanism by which human activities may affect springtime O_3 concentrations in the Arctic. As discussed in chapter 1, increases in NO concentrations lead to increased net photochemical O_3 production. This process requires the presence of hydrocarbons, and elevated hydrocarbon concentrations have also been observed in the Arctic during spring [*Hov et al.*, 1984]. Thus, the springtime arctic NO_x pulse (observed at Barrow during April–May, 1990) may affect springtime O_3 concentrations in the Arctic.

The arctic NO_y reservoir may also affect the mid-latitude O_3 budget. Measurements of hydrocarbons near the UK made by *Lightman et al.* [1990] in arctic air masses not affected by recent anthropogenic emissions have demonstrated the presence of elevated hydrocarbon concentrations in spring, and indicate that transport of arctic air can affect pollution levels in remote mid-latitude areas. The hydrocarbon levels in these arctic flows were high enough that significant O_3 production

could occur, provided sufficient NO_x were present, and it was proposed that such O_3 formation may contribute to the springtime O_3 peak in the clean northern mid-latitudes, which is generally attributed purely to stratospheric injection [*Lightman et al.*, 1990]. Since NO_y levels in the Arctic are also elevated during spring, arctic air masses transported to lower latitudes during this period are expected to contain significant PAN concentrations. PAN decomposition in the warmer southerly regions is expected to release NO_x, possibly in quantities sufficient to contribute significantly to the springtime O_3 peak.

Furthermore, a proposed mechanism for the springtime O_3 depletion events observed at Barrow and other coastal arctic sites depends critically on N_2O_5 (and thus on NO_x) concentrations [*Finlayson-Pitts et al.*, 1990]. To determine whether there is evidence for any of these effects, the relationship of O_3 and NO_y during the background periods was investigated. Ozone concentrations at the CMDL site during 1990 were provided by S. Oltmans (NOAA CMDL, Boulder, Colorado; private communication, 1991).

Summer. Figure 5.17 shows hourly-average NO_y and O_3 concentrations during the June–August 1990 background periods (period 19 is excluded because of potential local pollution impacts, as discussed above). No trend is apparent from the entire data set. However, closer inspection revealed a significant difference in O_3 concentration between the periods with flow over tundra (periods 27–29) and the remaining, marine-flow periods. As discussed above, NO_y levels over tundra were higher than those over the ocean, presumably due to reduced boundary layer stability over land or surface NO_x emissions. The opposite was true for O_3, and this is a result of the large difference in O_3 deposition velocity to plants and soil relative to that over water or ice. The deposition velocity of O_3 to land is about an order of magnitude larger than is that to either water or snow [*Wesely et al.*, 1989]. Figure 5.18 shows a comparison of the frequency distributions of all O_3 measurements

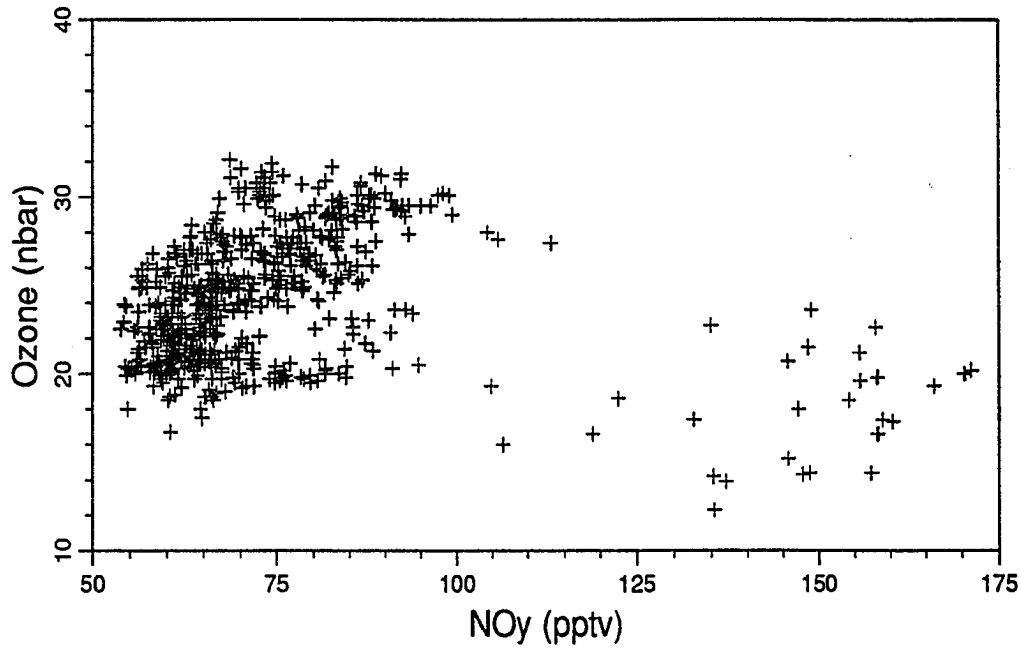

Figure 5.17 Hourly-average ozone and NO_y concentrations during the summer background periods. Period 19 is excluded (see text).

during June–August 1990 made during flow over tundra (surface wind direction 130–200°) and over the ocean (surface wind direction 0–120°), and a reduction in O_3 over the tundra is apparent. Since marine-flow and tundra-flow conditions were so different, they were analyzed separately. The following discussion is based on results of an analysis of the marine-flow periods. Only 3 periods (a total of 35 hr) occurred during flow over tundra, and no consistent NO_y/O_3 relationship is apparent during those periods (shown in Figure 5.19).

Figure 5.20a shows all 1 hr-average measurements of NO_y and O_3 during marine-flow summer background periods (periods 20–26 and 30–43), and NO_y and O_3 concentrations averaged over each background period are shown in Figure 5.20b. There is a clear trend, with higher NO_y levels associated with higher O_3, in both figures. Least-squares linear regression analysis of the data indicates a slope of 0.17–0.18 nbar O_3/pptv NO_y for both data sets, with intercepts of 13 nbar O_3 (all

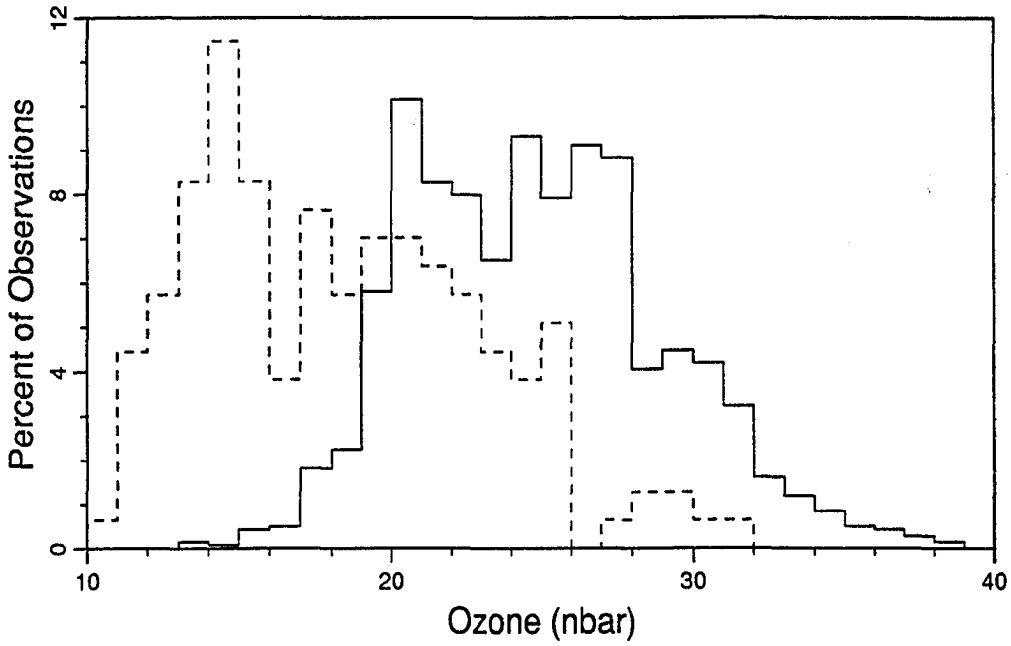

Figure 5.18 Comparison of the ozone frequency distributions during flow over land and ocean. The solid line includes measurements made during marine flow (surface wind direction 0–120°; N=1428); the distribution of measurements made during flow over tundra (surface wind direction 130–200°; N=157) is dashed. (Ozone measurements from S. Oltmans, NOAA CMDL, unpublished data).

coefficients are significant at the 95% level). Analysis of 850 mb trajectories and synoptic weather maps did not indicate any clear differences between the low NO_y-low O_3 periods and the high NO_y-high O_3 periods.

To determine whether the NO_y-O_3 relationship held within specific background periods, a similar analysis was conducted for the 5 periods with substantial changes in NO_y concentration ($\geq$20 pptv) and duration ($\geq$24 hr). Table 5.4 shows the results of this regression analysis for these 5 periods, as well as for the March, spring transition, and fall transition periods with substantial NO_y concentration changes and duration. Four of the five periods exhibited a significant slope, with values ranging from 0.12$\pm$0.04 to 0.28$\pm$0.16 nbar O_3/pptv NO_y. There is no apparent dependence of the slopes shown in Table 5.4 on Barrow surface temperature. Two examples of background periods which exhibited a significant slope are shown in

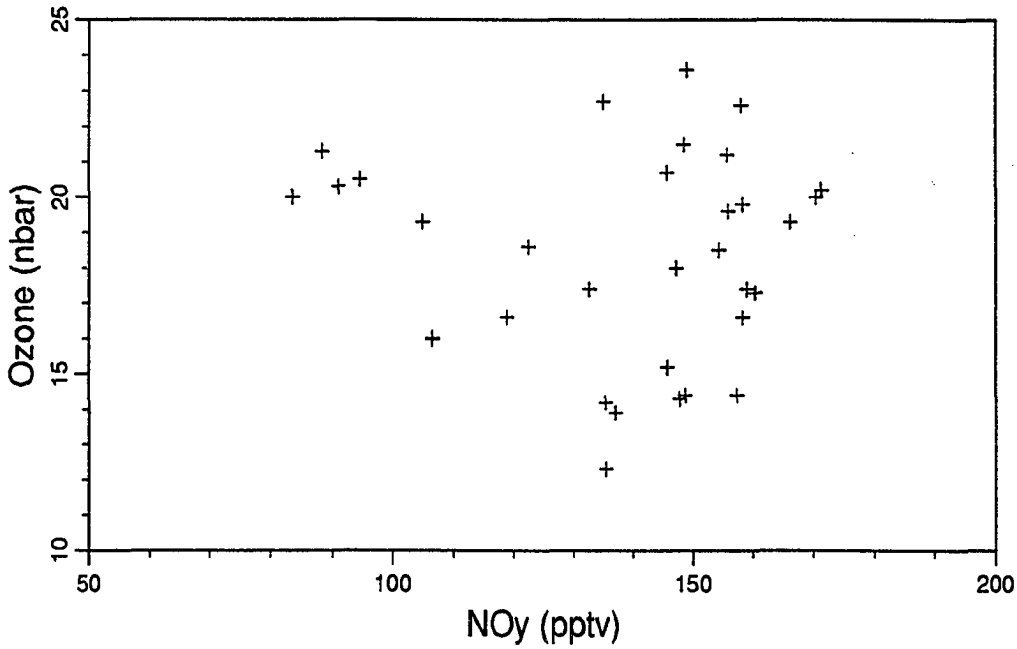

Figure 5.19 Hourly-average ozone and NO_y concentrations during the tundra-flow periods (periods 27–29).

Figure 5.21.

The slope of the regression lines indicates an approximately 170-fold enrichment of O_3 relative to NO_y, on a molar basis. The positive slope may indicate O_3 formation (or reduced destruction) resulting from the NO_y enrichment. In that case, the size of the slope implies substantial NO_y loss (relative to O_3). This may indicate O_3 formation due to NO_x emissions in an upwind (lower latitude) source region, associated with the formation of nitric acid and stable NO_y compounds (such as PAN and organic nitrates), and followed by preferential loss of HNO_3 before the remaining NO_y and O_3 reach the Arctic. However, to some extent the NO_y/O_3 correlation is probably a result of down-mixing of air from the mid-troposphere, which was enriched in O_3 due to stratospheric intrusion and carried to the surface along with NO_y from a mid-tropospheric NO_y reservoir. Unfortunately, the available data are insufficient to separate these two scenarios.

Increases in NO_y and O_3 during the summer were not generally correlated with

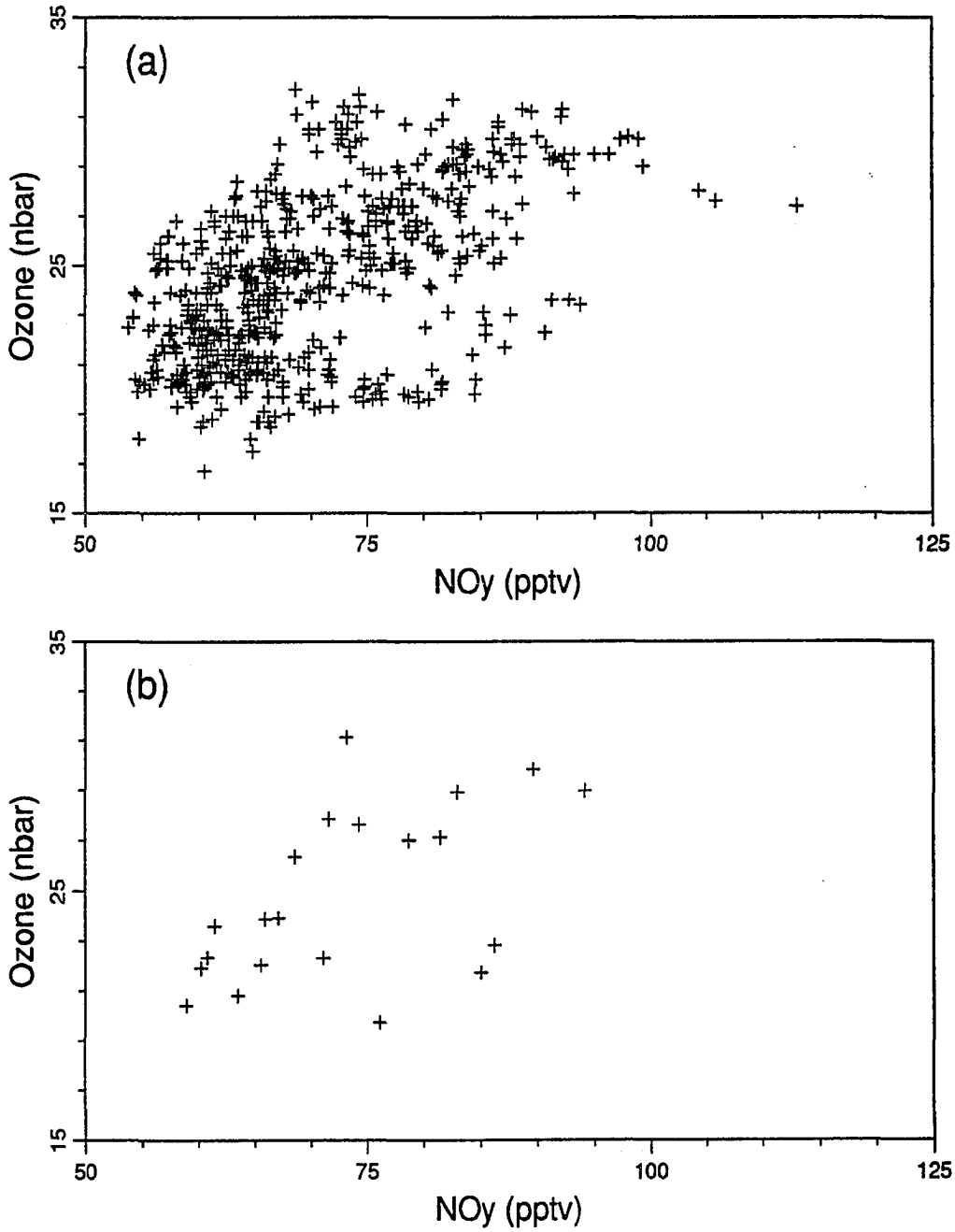

Figure 5.20 NO_y and O_3 concentrations during the marine-flow summer background periods. (a) Hourly-average values for background periods 20–26 and 29–43. (b) Values for the same background periods, averaged over each period.

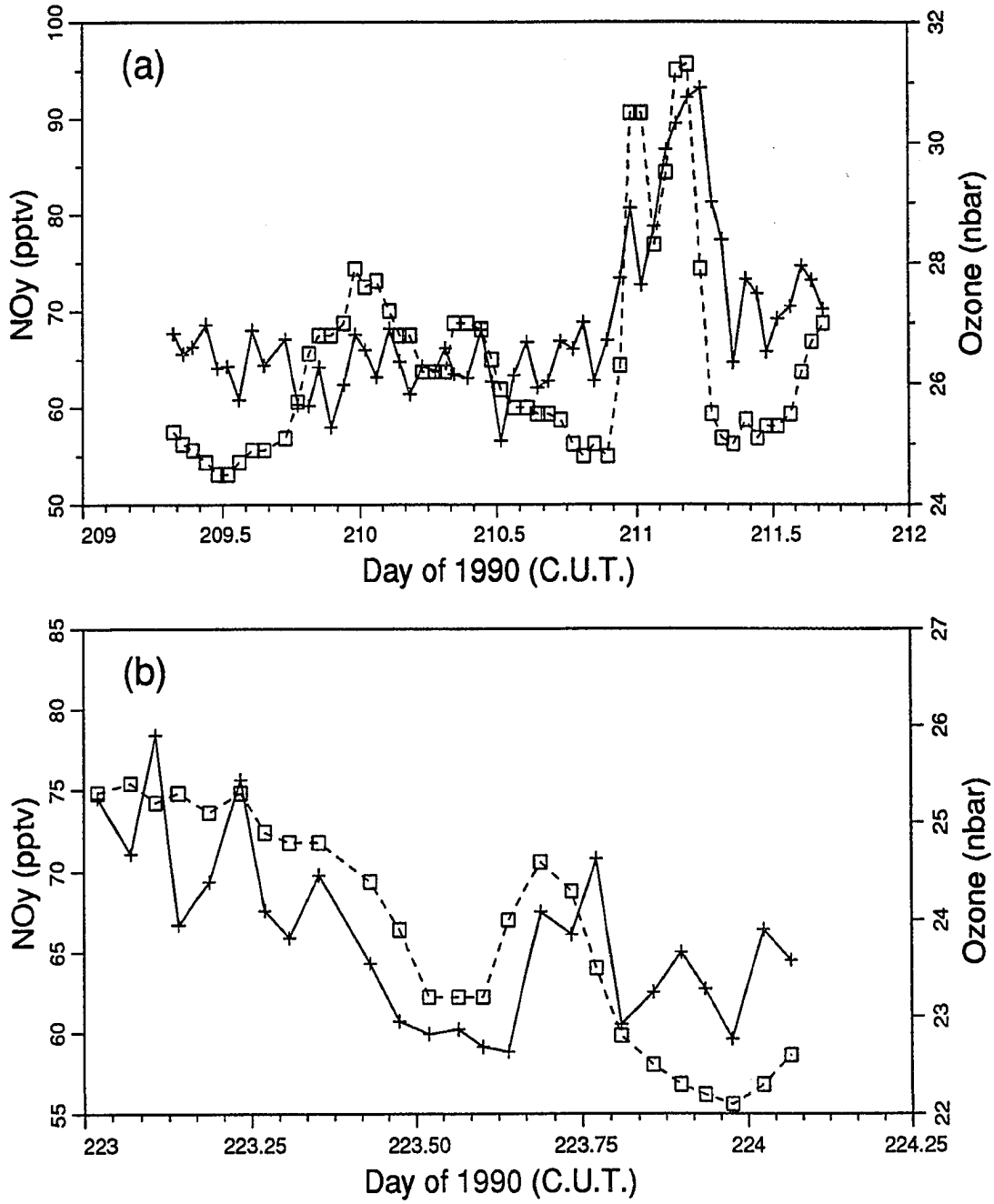

Figure 5.21 Examples of positive correlations of NO_y and O_3 during summertime background periods. Hourly-average NO_y concentration is shown by the solid line and + symbols; hourly-average O_3 concentration is shown with boxes and the dashed line. X-axis labels are in Coordinated Universal Time—local solar time is 13.6 hr (0.6 day) later. (a) Background period 37 (b) Background period 32.

Table 5.4 Regressions of NO_y and O_3 During Individual Background Periods.

"Season"	Period	Number of Hours	Slope[a] $\pm 1\sigma$	Intercept[a] $\pm 1\sigma$	r^2 of Regression
March	4	54	0.006±0.007 (NS[b])	25.5±4.6	0.0%
March	7	57	-0.18±0.02	120±13	51%
Spring Transition	11	38	0.001±0.002 (NS)	-0.2±0.7	0.0%
Spring Transition	14	45	-0.13±0.04	48±9	20.3%
Summer	32	57	0.12±0.02	18.1±1.6	32.7%
Summer	33	35	0.06±0.05 (NS)	23±3	2.9%
Summer	35	54	0.28±0.08	4±5	19.4%
Summer	37	25	0.15±0.03	14±2	21.0%
Summer	41	56	0.12±0.03	17±3	21.0%
Fall Transition	44	66	0.21±0.03	14±22	52.0%
Fall Transition	45	22	0.18±0.01	16±1	91.1%
Fall Transition	54	50	0.11±0.02	21.2±0.1	53.8%
Fall Transition	56	24	0.006±0.004 (NS)	35.1±0.6	8.2%
Fall Transition	57	30	-0.025±0.009	40±2	20.1%
Fall Transition	64	35	0.007±0.004 (NS)	33±1	4.5%

Includes all periods of ≥24 hr duration with NO_y range (hourly average) ≥20 pptv.
[a] $[O_3]$ = Intercept + Slope × $[NO_y]$.
[b] Not significant at the 95% level.

reductions in boundary-layer stability, as measured by vertical temperature soundings. However, the 12-hourly temperature soundings may have been too infrequent to identify transient changes in boundary layer stability.

March. Figure 5.22 shows concentrations of O_3 and NO_y, averaged over the March background periods. There is a significant correlation (r^2=0.80; linear regression indicates a slope of 0.07 nbar O_3/pptv NO_y, significant at the 95% level). However, inspection of the individual periods indicates that, although NO_y and O_3 are sometimes directly related, that is often not the case. Figure 5.23 shows NO_y and O_3 measurements during periods 1–3 (Figure 5.23a), when there was a significant positive correlation between NO_y and O_3, and during period 7 (Figure 5.23b), when O_3 and NO_y varied inversely or were unrelated. The sharp drop in both NO_y and O_3 in day 62 of Figure 5.23a coincided with a small wind shift, from a ~30° to ~50° heading, and a breakup of the surface-based temperature inversion to a height of 200m. 850-mb trajectories calculated for days 61–63 of 1990 indicate a shift from

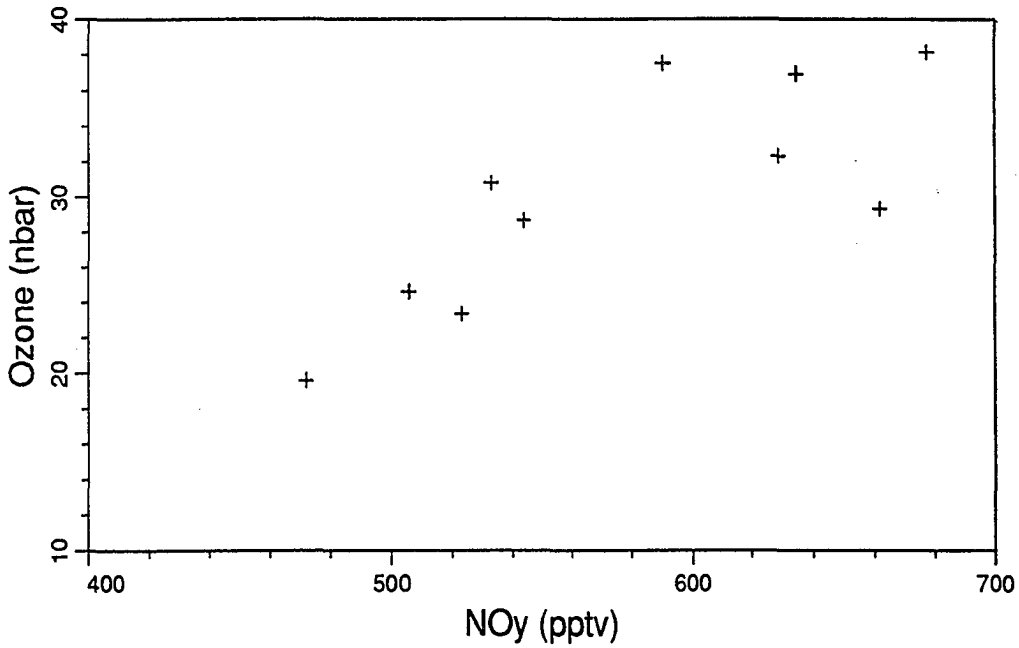

Figure 5.22 Average NO_y and ozone concentrations during the March background periods.

flow from the Arctic to flow from the south occurred between 1200 C.U.T. day 61 and 0000 C.U.T. day 62. Thus, the concentration changes may reflect the sampling of different air masses.

During period 7 (Figure 5.23b), O_3 concentrations were recovering from a partial O_3 depletion event, with wind direction constant at a heading of near 50°. There is an inverse correlation between NO_y and O_3 during parts of period 7, but not during others. Aircraft and ozonesonde observations have demonstrated that springtime arctic O_3 depletion events are limited to the boundary layer, and that fluctuations in the strength of the surface inversion can dramatically affect ozone concentrations [*Mickle et al.*, 1989]. The sharp increase in O_3 late in day 84 is thus likely related to a decay in the low-level temperature inversion. Temperature soundings at Barrow during this time do indicate a decay of the surface-based inversion during the first half of day 85. Although this inversion decay was not observed coincidently with the ozone increase, the 12-hourly temperature soundings may have been too infrequent

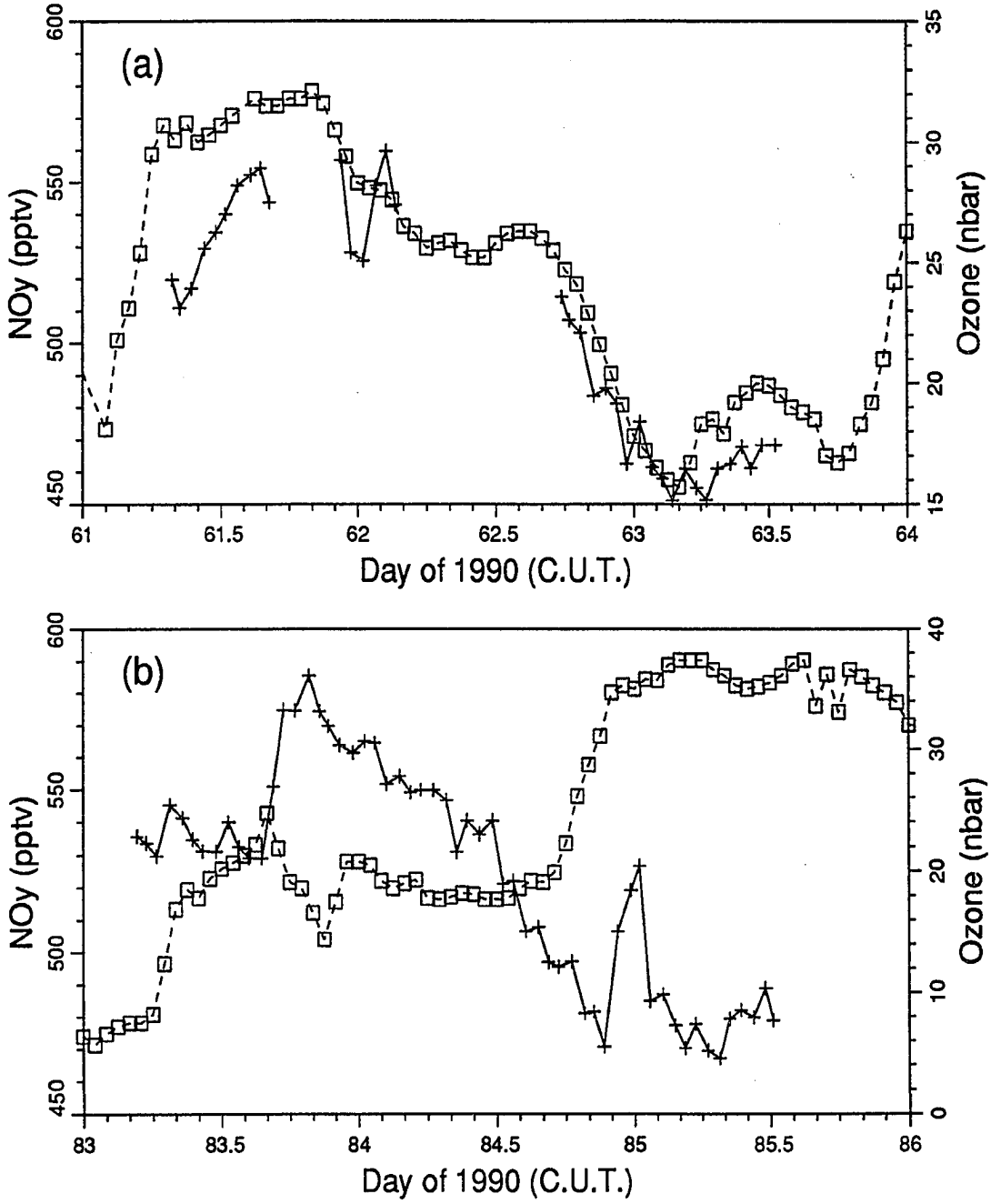

Figure 5.23 Hourly-average NO_y and O_3 concentrations during two periods in March. Hourly-average NO_y concentrations are plotted with + symbols and the solid line; hourly-average O_3 concentrations are shown with boxes and the dashed line. X-axis labels are in Coordinated Universal Time—local solar time is 13.6 hr (0.6 day) later. (a) Background periods 1–3. (b) Background period 7.

to identify an earlier transient inversion breakdown. If the ozone increase on day 84 was a result of enhanced vertical mixing, these data indicate that NO_y concentrations aloft were lower than those at the surface during this period.

In light of these results, the relationship of NO_y and O_3 during the spring 1989 measurement campaign (chapter 4) was also analyzed. Those data also indicate a complex relationship during spring, with some periods of negative correlation, some periods of positive correlation, and most periods exhibiting no apparent correlation.

Springtime Boundary-layer O_3 Depletion Events. NO concentrations observed during spring 1990 O_3 depletion events can be used to assess the adequacy of the mechanism for springtime O_3 depletion events proposed by *Finlayson-Pitts et al.* [1990], which is based on nitrile bromide ($BrNO_2$) photolysis. $BrNO_2$ formation requires the presence of N_2O_5, formed in the dark from NO_x. N_2O_5 exists in equilibrium with NO_2 and NO_3 [*DeMore et al.*, 1987] and is photodissociated during the daytime, and thus the presence of significant levels of NO_2 is a necessary condition for the proposed mechanism. *Finlayson-Pitts et al.* [1990] estimated a steady-state nighttime N_2O_5 concentration of 50 pptv, based on an assumed NO_2 concentration of 25 pptv. At this N_2O_5 concentration, they estimated that ~5–12 pptv of $BrNO_2$ could be formed over a ~2-week period, resulting in a modeled ozone loss of <30% over a 3-day period.

There were two partial and one complete O_3 depletion events during the springtime background periods. Ozone was almost totally absent during period 11 ($[O_3] <$ 1.5 nbar), and O_3 levels during periods 7 and 12 reached below 10 nbar. Daytime NO levels during these periods can be used to assess whether significant concentrations of NO_x would be available for nighttime formation of N_2O_5.

Hourly averages of NO measurements during background period 11, the near-total O_3 depletion event, are shown in Figure 5.8a, which also displays the solar elevation during period 11. NO concentrations were initially ~35 ± 4 pptv (±2

standard deviations of the hourly average), with a solar elevation of 18°. Concentrations dropped as the sun went down, but rose again at sunrise, reaching ~15 pptv the second day of period 11. The NO_x concentration during this period is difficult to estimate, but is likely 2–5 times the mid-day NO concentration (section 4.2.2.1), or 30–150 pptv. This range of NO_x concentrations is consistent with the O_3 depletion mechanism proposed by *Finlayson-Pitts et al.* [1990].

NO concentrations during the partial O_3 depletion events (background periods 7 and 12) were lower. The maximum hourly-average NO concentration during period 7 was 6 pptv with a corresponding solar elevation of 17°. During period 12, the maximum hourly-average NO concentrations was 5 pptv at a solar elevation of 15°. The NO measurements during periods 7 and 12 suggest much lower NO_x concentrations than were present during period 11, and do not support the *Finlayson-Pitts et al.* [1990] O_3 depletion mechanism, although NO_x loss could have occurred following O_3 depletion.

Transition Periods. Figures 5.24a and b are scatter plots of average NO_y and O_3 concentrations during the spring transition and fall transition periods, respectively. There is no significant correlation between NO_y and O_3 in these data sets, the large changes in NO_y concentrations during the transition periods (resulting from the seasonal NO_y cycle) overwhelming any NO_y–O_3 correlation that would otherwise be present. Regression analyses during each period with substantial NO_y variation ($\geq$20 pptv) and duration ($\geq$24 hr) are summarized in Table 5.4. The two spring transition periods shown there are similar to the March periods, with no correlation or a negative correlation. In contrast, the first three fall transition periods shown in Table 5.4 (periods 44, 45, and 54) exhibit significant positive slopes that are similar in magnitude to those observed during the summer periods, indicating that the processes resulting in the summer NO_y–O_3 correlations continued to operate through late September. There is no apparent correlation during the fall transition

periods after September.

5.2.3.5 Comparison to Modeling Results

A number of computer modeling studies conducted to assess global and regional NO_y and O_3 budgets have yielded NO_y concentration predictions for the Arctic. Due to computational limitations, the models generally include simplified chemistry, ranging from no explicit chemistry (tracer models) to chemistry including PAN and inorganic nitrogen compounds. A comparison of the model results to the data discussed here provides a useful indicator of the adequacy of current models used to simulate NO_y in the Arctic and other remote regions.

A three-dimensional tracer model has been used to assess the NO_x source which results from stratospheric N_2O oxidation and transport across the tropopause. These simulations included the stratospheric NO_x source [*Levy et al.*, 1980] or both stratospheric and subsonic aircraft sources [*Kley et al.*, 1981], and gave predicted arctic NO_y concentrations of <30 to ~100 pptv during summer, and between 120 and 300 pptv during spring. Although these models predicted summertime arctic NO_y levels comparable to those measured at Barrow during 1990, they assume that HNO_3 is the dominant lower-tropospheric NO_y compound [*Levy et al.*, 1980], which is not the case in the Arctic as shown by the discussion above. The presence of significant levels of PAN and other organic nitrates in the arctic troposphere argues against the dominance of the stratospheric NO_x source, which is expected to produce primarily NO_x and HNO_3 [*Singh et al.*, 1991a]. An additional use of a tracer model assessed the impacts of fossil-fuel NO_x emissions [*Levy and Moxim*, 1989]. However, without a chemical mechanism for production of stable organic nitrates, the model was unable to accurately predict the high arctic winter NO_y levels. Winter (January–March) concentrations of only ~100 pptv were predicted for arctic Alaska, with summertime levels of <50 pptv. In addition, no vertical concentration gradient was predicted for summer, in contrast to the ABLE-3A measurements [*Singh et al.*,

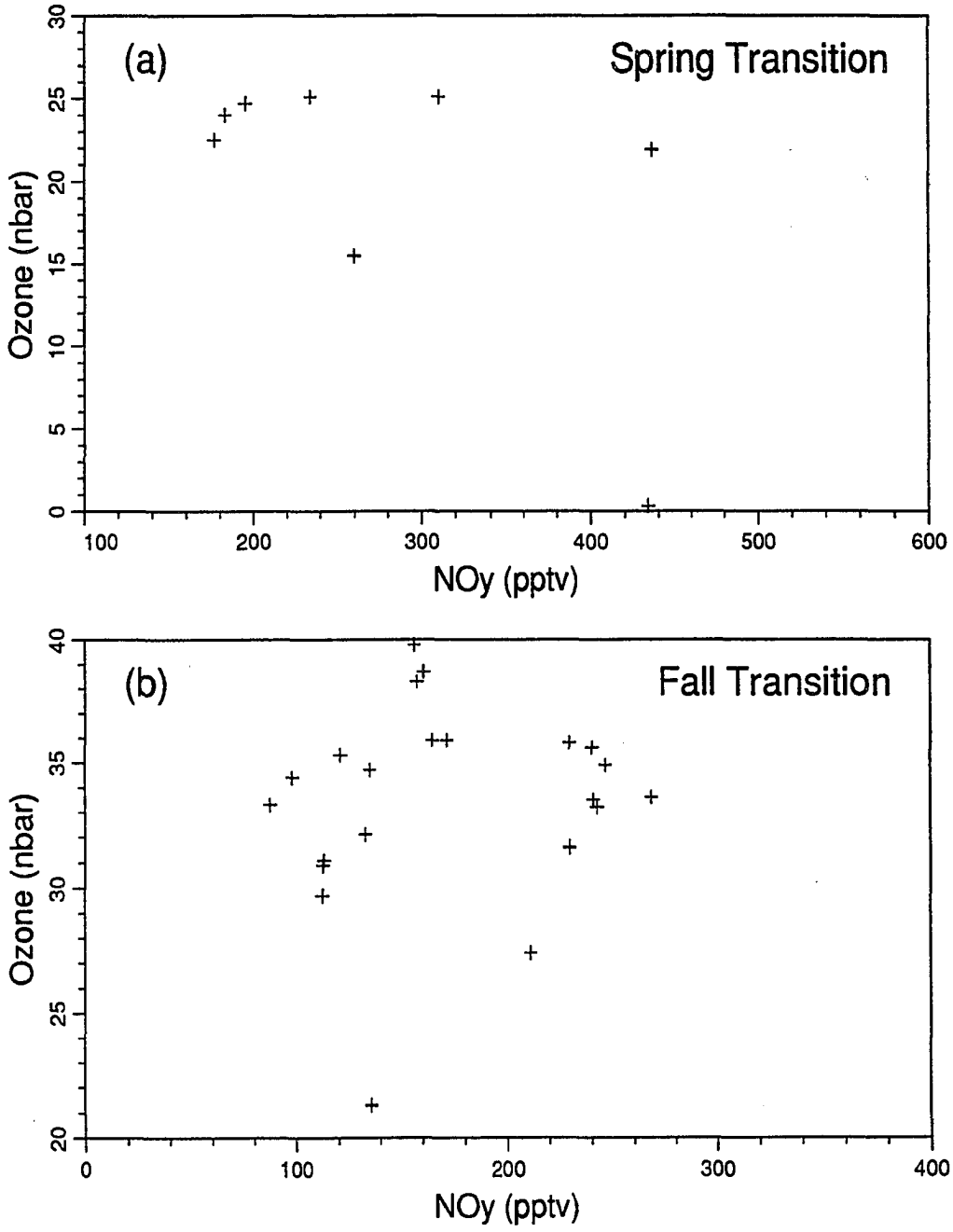

Figure 5.24 Average NO_y and O_3 concentrations during the spring and fall transition periods. NO_y and O_3 concentrations averaged over each background period are shown for background periods during the spring transition (a) and fall transition (b).

1991b].

Two-dimensional models with explicit chemistry have also been used. *Crutzen and Gidel* [1983] used a model with inorganic nitrogen chemistry to assess impacts of anthropogenic and natural tropospheric NO_x sources on ozone. Their model predicted arctic wintertime NO_y mixing ratios of >800 pptv, even higher than observed during March at Barrow. However, the high NO_y predictions were a result of N_2O_5 accumulation during the modeled arctic night, due to omission of heterogeneous N_2O_5 and NO_3 reactions with ice surfaces [*Crutzen and Gidel,* 1983]. NO_3 would photolyze during sunlit periods in late spring (producing NO_x and removing NO_3 and N_2O_5), so this simulation is not consistent with the March Barrow measurements of 500–700 pptv and near-zero daytime NO.

More complete chemical mechanisms were used by *Isaksen et al.* [1985] and *Singh et al.* [1985], who included PAN as well as inorganic nitrogen chemistry. *Isaksen et al.* [1985] predicted high December NO_y levels—to >1000 pptv—based on anthropogenic and natural tropospheric sources. However, the predicted surface composition was largely (~75%) inorganic nitrogen oxides including 500 pptv HNO_3, inconsistent with the filter measurements during 1989 (chapter 3). The predicted PAN concentration of 290 pptv was somewhat lower than the measurements of *Barrie and Bottenheim* [1991]. Summertime concentrations were predicted to be higher than the Barrow measurements at ~215 pptv. The model used by *Singh et al.* [1991b] also included the stratospheric NO_x source and predicted summertime surface concentrations of ~75 pptv, more in line with the 1990 Barrow measurements. However, a very weak concentration gradient with height was predicted, in contrast to the ABLE-3A observation of a mid-tropospheric NO_y reservoir [*Singh et al.,* 1991b].

The inability of current photochemical models to accurately simulate NO_y in the arctic troposphere indicates a need for additional model development if the potential impacts of anthropogenic NO_x emissions on remote tropospheric chemistry and O_3

levels are to be adequately assessed. However, the observation during the ABLE-3A campaign that unknown or unmeasured NO_y compounds made up a significant fraction of the arctic free tropospheric NO_y reservoir, at least during summer [*Singh et al.*, 1991b], and similar observations in other studies [*Fahey et al.*, 1986; *Jacob and Wofsey*, 1990], suggests that the current understanding of nitrogen oxides chemistry may be too limited to allow for the development of adequate models at this time.

5.3 Regional Pollution Impacts on the Barrow Measurement Site

Several episodes of high and smoothly varying NO_y concentrations were observed during the 1990 measurement period. These episodes were similar to the events observed during the 1989 measurement campaign which were attributed to emissions from the Prudhoe Bay region (chapter 4). In order to further characterize the Barrow measurement site and the regional impacts of Prudhoe Bay emissions, the events of apparent Prudhoe Bay impacts observed during 1990 were identified and are presented here.

5.3.1 Event Selection

Events were identified by scanning the 1990 NO_y data set for periods when wind direction indicated local Barrow sources did not affect the measurements, but NO_y levels were nevertheless well above background values. In this screening procedure, periods with wind directions of 0–200° were considered acceptable. These periods were scanned for NO_y levels above 1000 pptv during March, 750 pptv during the spring transition period (April-May), 250 pptv during summer (June-August), or 500 pptv during the fall transition period (September–November). These cutoff values are higher than the maximum concentrations observed during background

periods within each season. All periods satisfying these two constraints were reviewed, and those with smoothly-varying concentrations were selected as events. This selection was subjective, but resulted in the elimination of only one potential period, which coincided with a reversal of wind direction and resultant local (Barrow) pollution. Of the selected events, two more were discarded because they were very short (less than 3 hours with [NO_y] greater than 1.5 times the surrounding background level), leaving a total of 17 acceptable events. These 17 events alone account for 10% of the total measurement hours with wind in the 0–200° sector.

5.3.2 Results

The 17 events are summarized in Table 5.5. NO_y concentrations during the events reached 9 ppbv (excluding one outlier at 27 ppbv), and NO levels reached 6 ppbv. NO and NO_y concentrations during the events are shown in Figures 5.25 and 5.26. NO concentrations were highly correlated with NO_y during daylight periods, and frequently contributed more than half of the NO_y.

5.3.3 Analysis and Discussion

Wind directions during most of the events were close to the heading to Prudhoe Bay (111°). Event 10 is the only exception to this pattern. High NO_y levels during that event were accompanied by northeast flow but occurred a few hours after a wind direction reversal from the southwest. Thus, event 10 may reflect the return of local Barrow pollution that was transported over the Arctic Ocean. The correlation of hourly-average NO_y concentrations during the events with wind direction is shown in Figure 5.27. Most of the high NO_y observations coincided with wind in the sector of 45–130°, which is free from local sources (section 2.3) but contains Prudhoe Bay. These results support the conclusion reached in Chapter 4 that Prudhoe Bay NO_x emissions are sometimes responsible for significant increases in NO_y at Barrow

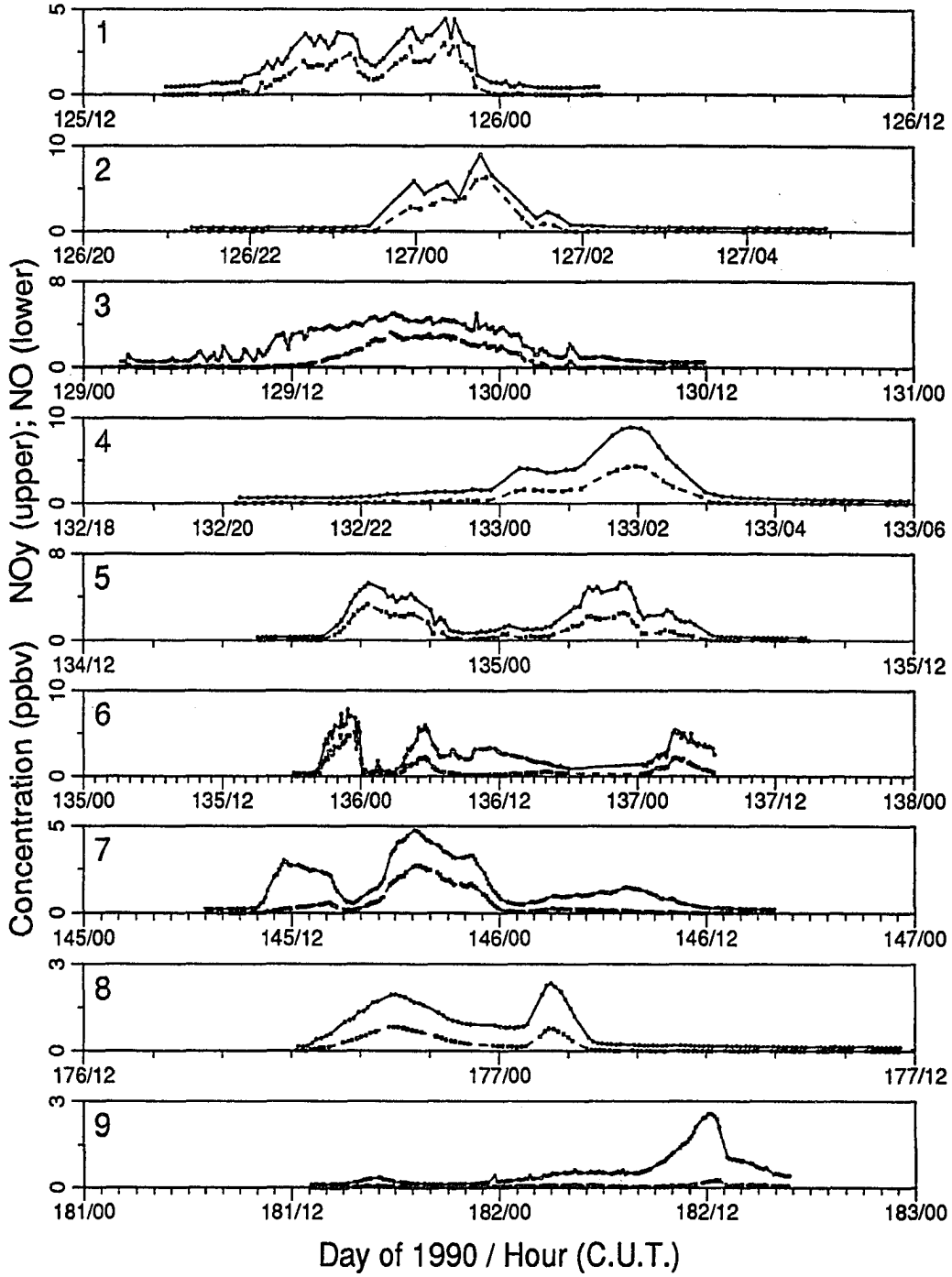

Figure 5.25 NO and NO_y concentrations during 1990 events 1–9. The event number is shown in the upper left corner of each plot. Measurements are shown by the solid markers. NO_y measurements are connected by solid lines and are above the NO measurements, which are connected by dashed lines. X-axis labels are in Coordinated Universal Time—local solar time is 13.6 hr (0.6 day) later.

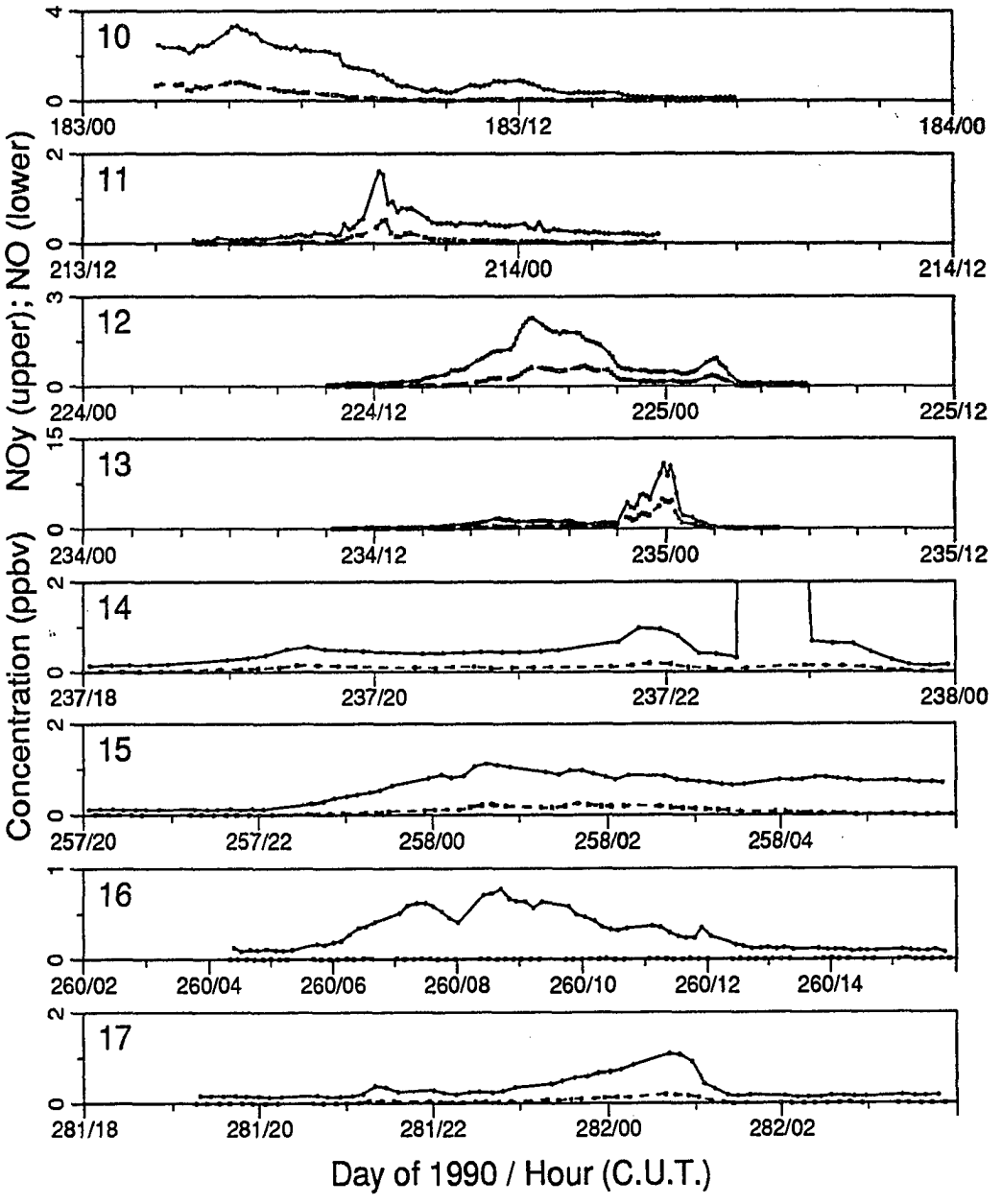

Figure 5.26 NO and NO_y concentrations during 1990 events 10–17. The event number is shown in the upper left corner of each plot. Measurements are shown by the solid markers. NO_y measurements are connected by solid lines and are above the NO measurements, which are connected by dashed lines. A single outlier in event 14 (in hour 237/22) is off scale at 26.9 ppbv. X-axis labels are in Coordinated Universal Time—local solar time is 13.6 hr (0.6 day) later.

Table 5.5 Summary of 1990 Events.

Event Number	Time (C.U.T.) Start Day	Start Hour	End Day	End Hour	Wind Direction (Degrees)	Average Wind Speed (m/s)	NO_y Range (ppbv)	NO Range (ppbv)
1	125	14	126	2	96–113	4.3	0.41–4.45	0.00–2.97
2	126	21	127	4	96–105	6.9	0.42–8.98	0.00–6.33
3	129	2	130	11	93–133	5.6	0.43–5.02	0.00–3.25
4	132	20	133	5	68–82	4.5	0.40–8.93	0.00–4.35
5	134	17	135	8	92–117	5.6	0.25–5.33	0.00–3.29
6	135	18	137	6	101–197	6.1	0.29–7.76	0.00–5.08
7	145	7	146	15	82–122	6.9	0.19–4.79	0.00–2.71
8	176	18	177	11	84–108	6.5	0.11–2.33	0.00–0.82
9	181	13	182	16	94–151	6.5	0.10–2.56	0.00–0.27
10[a]	183	2	183	17	18–70	4.7	0.11–3.33	0.00–0.82
11	213	15	214	3	7–114	2.7	0.06–1.61	0.00–0.52
12	224	10	225	5	72–106	7.9	0.06–2.27	0.00–0.67
13	234	10	235	4	84–107	7.0	0.07–10.76	0.00–4.78
14	237	18	237	23	96–109	7.9	0.13–26.92[b]	0.00–0.19
15	257	20	258	5	63–116	5.6	0.10–1.11	0.00–0.24
16	260	4	260	15	75–93	11.2	0.07–0.78	0.00–0.01
17	281	19	282	3	111–146	6.7	0.14–1.08	0.00–0.20

[a]This event occurred after a wind shift and may reflect the return of local Barrow pollution.
[b]The maximum value is a single outlier. Without this point, the maximum is 0.98 ppbv.

during periods when surface flow conditions preclude local Barrow impacts.

Figure 5.28 shows the seasonal variation of peak hourly-average NO_y concentrations during the 1990 events. Peak hourly-average NO_y concentrations from the four 1989 events (chapter 4) are also shown. Most of the high-concentration 1990 events were observed during May (Julian day 121–151), with lower concentrations later in the year. Consistent with this trend, two of the March and April, 1989, events had even higher concentrations.

The strength of the low-level temperature inversions normally present at Barrow is greatest during winter, and inversion strength decreases from March to September [*Kahl*, 1990]. Thus, less dilution of the Prudhoe Bay plume is expected during winter–spring than during summer, in agreement with the trend in maximum event NO_y concentrations. In addition, the strong surface-based inversions at Barrow during May frequently erode, often resulting in a mixed layer ~100–500 m deep

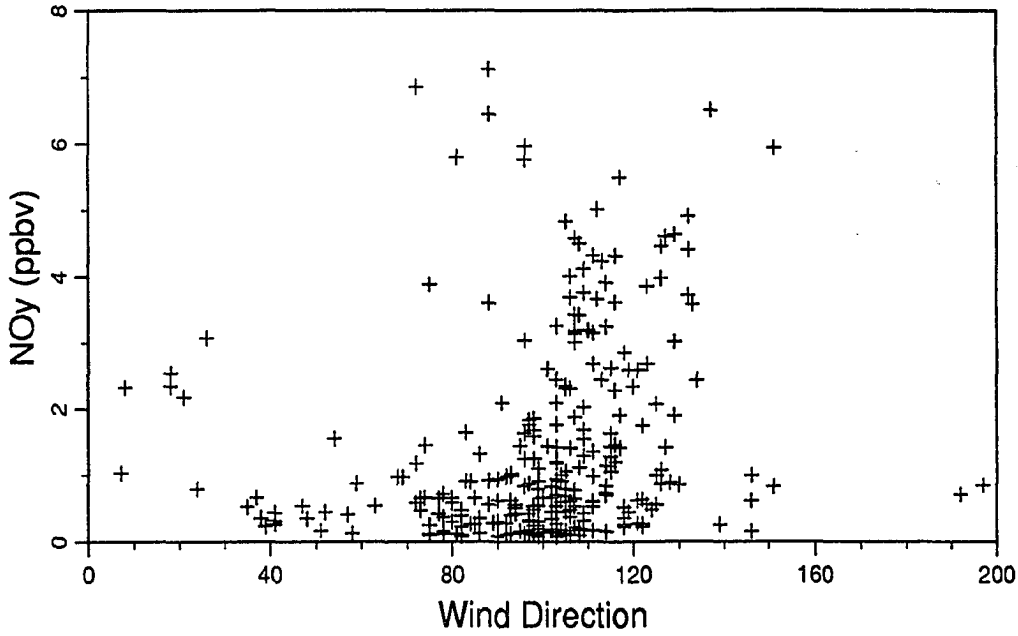

Figure 5.27 Hourly-average NO_y measurements versus wind direction during the 1990 events.

[*Kahl*, 1990]. During this period, most of the high NO_y concentrations in the events were observed during mid-day periods, when solar insolation is greatest and vertical mixing is expected to be most effective (see events 1–7 in Figure 5.25; local solar noon occurs at approximately 2330 C.U.T.), bringing elevated concentrations from the Prudhoe Bay plume (presumably located somewhat above ground level) to the surface. Surface-based inversions at Barrow are more persistent during summer and fall [*Kahl*, 1990], and this may partially explain the reduced frequency of events during summer and fall in 1990.

5.3.3.1 Impacts of Regional and Local NO_x Emissions on Ozone at Barrow

The presence of a major NO_x source (Prudhoe Bay) in arctic Alaska raises the additional possibility that regional O_3 levels may be affected by those NO_x emissions.

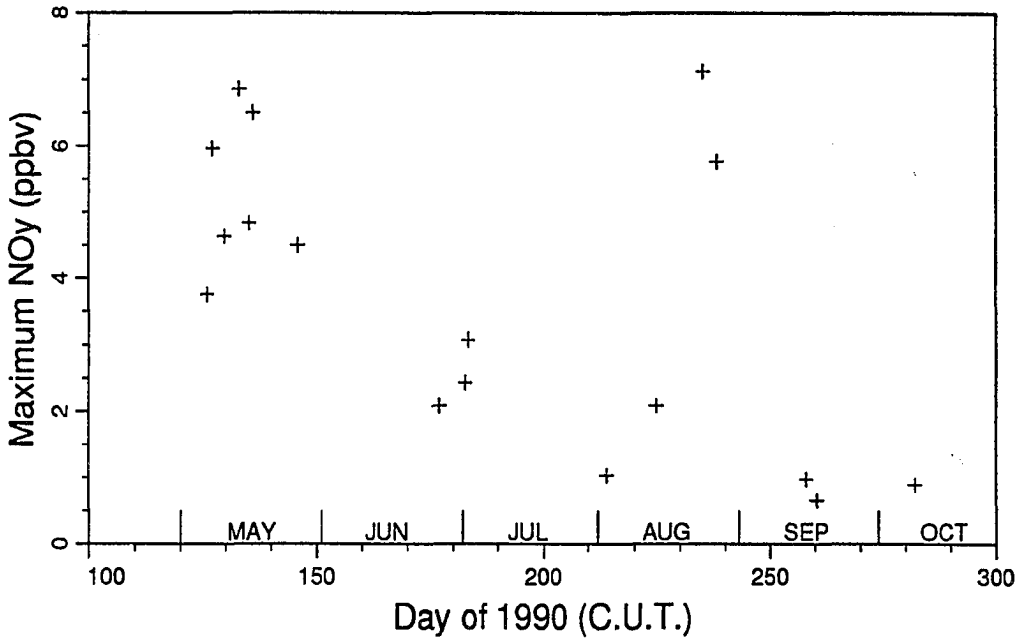

Figure 5.28 Seasonal variation of maximum NO_y concentrations observed during the events. The maximum 20 s-average NO_y concentration observed during each event is plotted against the time of observation.

This possibility is particularly intriguing since the record of surface O_3 at Barrow, which shows a summertime O_3 increase, began at approximately the time of Prudhoe Bay construction. To determine whether Prudhoe Bay NO_x emissions affected O_3 measured at Barrow, either through photochemical O_3 production or through O_3 titration, O_3 levels during the events were investigated. In addition, O_3 and NO_y levels during periods of flow from the town of Barrow were analyzed to determine whether local NO_x emissions affected the Barrow O_3 record.

The relationship of NO_y and O_3 during each of the 16 events attributed to Prudhoe Bay NO_x emissions was investigated. In most cases, changes in the ambient ozone concentrations during the events were much larger than the NO_y pulses and appeared to be unrelated to NO_y levels. There was no evidence of ozone formation in the Prudhoe Bay plumes. In three cases (events 3, 12, and 13), an inverse correlation

was observed; two of these cases are shown in Figure 5.29 (events 3 and 12). If it is assumed that the NO_y and O_3 variations during these events were due to variable dilution of a plume with ambient air of constant NO_y and O_3 concentration and that deposition during transport of the plume from Prudhoe Bay to Barrow was negligible, least-squares linear regression analysis can be used to estimate the ratio of NO_y enrichment to O_3 loss near the source [*Hansen et al.*, 1989]. This relationship can be used to test the hypothesis that titration of ambient O_3 by the NO source was responsible for the observed inverse correlation. In that case, the slope of the regression line should be ~-1 ppbv O_3 per ppbv NO_y.

This analysis was conducted for the periods of the three events during which O_3 and NO_y were inversely correlated (e.g., day 129 hour 8 through day 130 hour 3 in event 3 and all of event 8). The resulting slopes (nbar O_3/ppbv $NO_y \pm 2\sigma$) are -4.0 ± 1.2, -1.3 ± 0.8, and -0.4 ± 0.2 for events 3, 12, and 13, respectively. Only the measurements during event 12 are consistent with the hypothesis of O_3 loss through titration by NO emissions. O_3 and NO_y during the four 1989 events (chapter 4) were also analyzed in this manner. A clear correlation was present only during 1989 event 1. The slope of the regression line for that event is -1.7 ± 0.1 nbar O_3/ppbv NO_y.

The impact of local (Barrow) NO_x emissions on the Barrow O_3 record was investigated in a similar manner. In this case, all hourly O_3 and NO_y measurements made while the wind was blowing from major nearby sources (wind direction 235–320°) were used in a least-squares linear regression. Using the entire 1990 data set, the slope of the regression line was not significantly different from zero at the 90% level. Ozone concentrations at Barrow commonly varied by >10 nbar in the absence of significant NO_y concentration changes. Since <2% of all NO_y measurements were above 5 ppbv, even in this "dirty" sector, the absence of a statistically significant relationship is not surprising. The analysis was repeated for measurements conducted during the periods of March, March–May, June–August, and September–November.

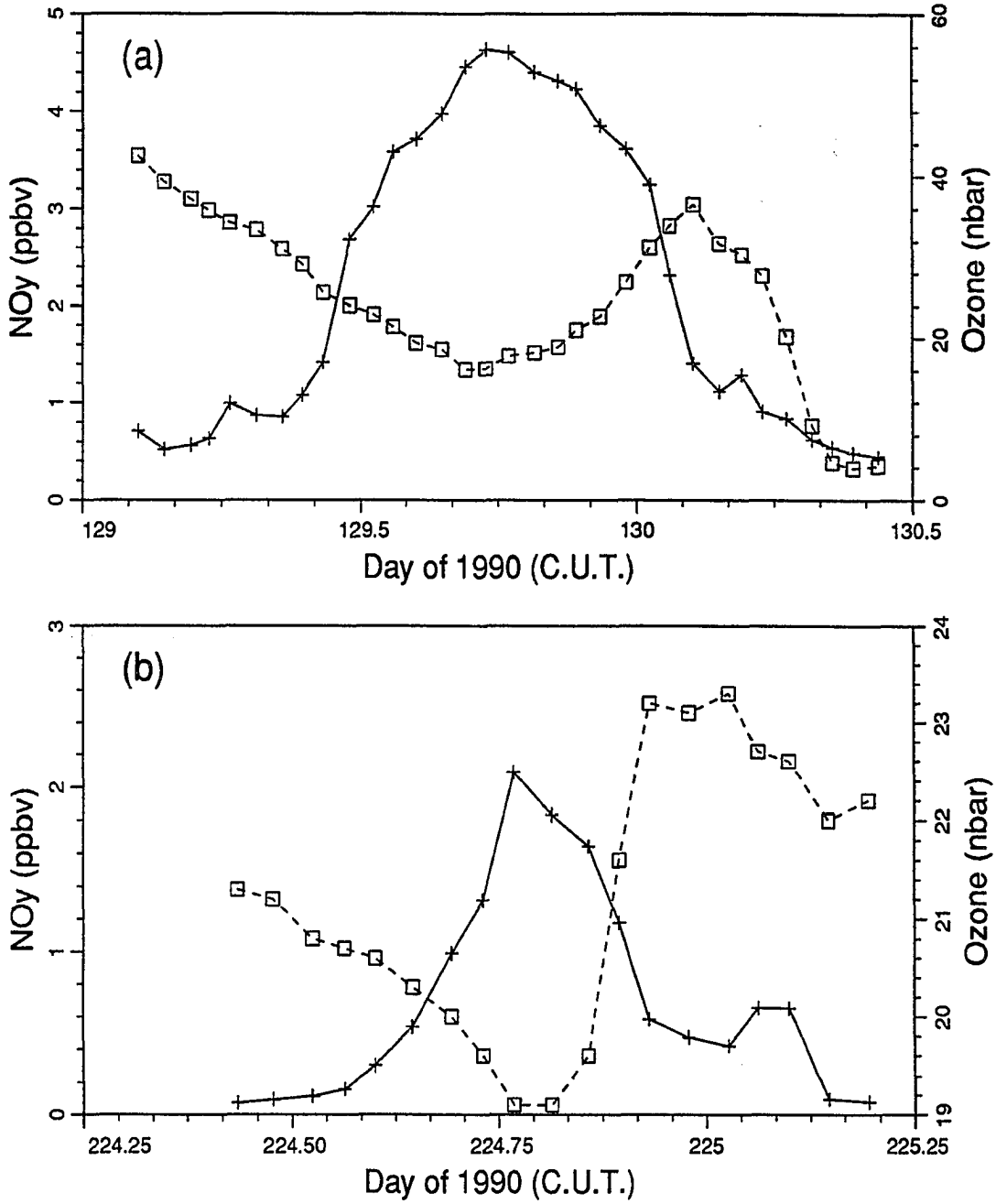

Figure 5.29 Two events which demonstrated an inverse correlation of NO_y and O_3. Hourly-average NO_y concentrations are shown with + symbols and the solid line; hourly-average O_3 concentrations are plotted with boxes and the dashed line. X-axis labels are in Coordinated Universal Time—local solar time is 13.6 hr (0.6 day) later. (a) Event 3. (b) Event 12.

Only the regression for September–November indicated a statistically significant relationship, with a slope of -0.8 ± 0.2 nbar O_3/ppbv NO_y. Thus, the impact of local NO_x emissions on the Barrow O_3 record appears to be negligible.

5.4 Summary

NO_y and NO measurements at the Barrow CMDL station were made from March–November, 1990. Within this time frame, 65 separate background periods, unaffected by local or regional pollution, were identified. Measurements during these background periods demonstrate a clear seasonal cycle in NO_y concentrations in the background arctic troposphere at Barrow. Elevated NO_y levels (~500–700 pptv) were observed during March. Concentrations dropped sharply during April–May, reaching very low values (generally <100 pptv) during summer (late June–August). Beginning in September, NO_y concentration began to increase once again.

The shape of the seasonal cycle is similar to that of other anthropogenic pollutants observed in arctic haze. However, the decay of NO_y levels in April–May coincided with an increase in temperature and was accompanied by an NO pulse, indicating that decomposition of PAN or other similar compounds (combined with NO_x and/or HNO_3 deposition) was at least partially responsible for the drop in NO_y concentrations. In addition, a comparison of these measurements with PAN and organic nitrate observations in the Canadian Arctic showed that both are consistent with the presence of a springtime arctic NO_y reservoir dominated by PAN and other organic nitrates. Through PAN decomposition as temperatures rise in the spring and through transport out of the Arctic, this NO_y reservoir may impact northern high- and mid-latitude O_3 levels during spring.

NO concentrations were generally below 6–8 pptv (hourly average) during the background periods. However, a pulse of NO was observed during April–May (to ~35 pptv hourly average), coincident with the decay of NO_y concentrations. This

NO pulse is attributed to the decomposition of PAN and/or other organic nitrogen compounds as temperatures and solar insolation increased. In addition, two relatively warm summertime periods were observed in which surface flow over the tundra was accompanied by an increase in temperature of ~10°C and elevated NO levels, consistent with the identification of PAN decomposition as the primary source of summertime NO_x in the arctic boundary layer [*Jacob et al.*, 1991]. Increased NO_y levels observed during the same two warm periods may have resulted from (1) enhanced vertical mixing over land, relative to the ocean, (2) wildfire plumes, or (3) biogenic emissions.

Synoptic flow patterns and diurnal changes had a minimal effect on background NO_y levels during the 1990 measurements. Springtime NO_y concentrations were generally somewhat higher during arctic flow than during southerly flow, but some of the lowest springtime NO_y levels were observed during arctic flow. A weak diurnal cycle was observed in the spring transition, summer, and fall transition periods, with mid-day concentrations ~10–25 pptv higher than those at night. This diurnal cycle may be a result of diurnal variations in vertical mixing, combined with depletion of nighttime NO_y by HNO_3 deposition.

NO_y and O_3 levels were positively correlated during summertime marine-flow clean-air periods. This correlation may indicate that the observed enrichments of both are the result of long-range transport of lower-latitude pollution, with preferential loss of part of the NO_y pollution component (e.g. HNO_3) through deposition en-route. However, the correlation is likely at least partially a result of variations in the amount of down-mixing of mid-tropospheric air, which was enriched in NO_y through long-range transport but enriched in O_3 through stratospheric downwelling.

During the spring, the relationship of NO_y and O_3 was complex, with some periods exhibiting a positive correlation and some a negative or no correlation, reflecting complex variations of O_3 in the arctic boundary layer during spring. NO concentrations (hourly-average) during one near-total boundary-layer O_3 depletion event

reached 15–34 pptv during daytime, indicating that sufficient NO_x may have been present for operation of the $BrNO_2$ O_3 depletion mechanism proposed by *Finlayson-Pitts et al.* [1990]. However, maximum daytime NO concentrations during two partial O_3 depletion events were $\leq$6 pptv (hourly average).

Regional and local pollution effects were frequently observed during the 1990 measurements. Seventeen events in which elevated NO_y and NO levels were observed while surface flow indicated no local (Barrow) pollution were identified. Sixteen of these events are attributed to NO_x emissions from the Prudhoe Bay industrial region 300 km to the southeast. These events accounted for 7.4% of the total measurements and were excluded from the background data set. In addition, frequent local pollution in the 200–360° wind sector necessitated the exclusion of an additional 25% of the total measurements from the background data set. A further 33% of the data were excluded due to transient local sources and/or impacts from Prudhoe Bay emissions not specifically identified as events, leaving 36% of the total measurements in the background data set. This result underscores the need for careful screening of measurements made at the Barrow site. An analysis of the impact of local and regional NO_x emissions on O_3 levels at Barrow revealed some cases of O_3 titration within apparent Prudhoe Bay NO_x plumes. However, O_3 variations unrelated to local or regional pollution episodes were much larger and therefore the impact of local and regional pollution sources on surface O_3 measurements at Barrow appears to be minimal.

Chapter 6

Summary and Conclusions

A high-sensitivity detector, designed and constructed as part of this research, was used to determine NO_y and NO concentrations at ground-level at a site near Barrow, Alaska. Measurements were made during three campaigns, in 1988, 1989, and 1990, with the detection limits and measurement uncertainties shown in Table 2.8. To eliminate impacts from local NO_x sources, the measurements were screened by wind direction and ambient variability. However, the remaining data set contained periods clearly affected by a major regional NO_x source—the Prudhoe Bay oil-producing region, which were termed "events." NO_y measurements remaining after exclusion of the events were not significantly affected by local or regional NO_x sources, and constitute a "background" data set, representative of the arctic boundary layer in the region of Barrow.

The NO_y and NO measurements were analyzed to assess the factors contributing to observed variations in background concentrations and to gain an improved understanding of the behavior of nitrogen oxides in the remote troposphere. In addition, the source of the elevated NO_y and NO levels observed during the events was identified, based on consideration of a variety of information sources. Finally, the relationship of NO_y to ozone was analyzed, both for the background measurements

and for the events. The results of these analyses, based on measurements during all three campaigns, are summarized below, followed by a brief statement of the broad conclusions of this research and its implications.

6.1 Background Measurements

The most striking feature of the background NO_y measurements is a distinct seasonal cycle in NO_y concentrations (Figure 5.5). NO_y concentrations measured in spring during the arctic haze season were extremely high for a remote site. Concentrations dropped sharply with the onset of warmer temperatures, reaching summertime levels as low as any reported boundary layer measurements of NO_y. Beginning in September, NO_y concentrations (measured during 1990) began to increase, and continued to increase until measurements were concluded in November. Because of the sharp seasonal cycle that was observed, it is useful to divide the measurements by time of year. In the following, the main conclusions regarding NO_y concentrations and speciation, based on background measurements during the early spring arctic haze season, during summer, and during the periods of transition from spring to summer and from summer to fall are presented separately.

6.1.1 Early Spring

NO_y concentrations during early spring were determined during the 1989 and 1990 measurement campaigns. Measurements obtained during the two campaigns agree well, despite use of different NO_y converters (molybdenum tube in 1989 and gold tube/CO in 1990). High concentrations were observed in both years, with median NO_y concentrations of the background data sets of 616 pptv (1989 measurements) and 557 pptv (March 1990 measurements). These concentrations, which are well above previous measurements of NO_y in other remote areas, indicate that the Arctic contains a significant reservoir of NO_y during spring. Simultaneous filter measure-

ments of SO_2 and $SO_4^=$—considered indicators of arctic haze—indicate that the ratio of NO_y to (SO_2+$SO_4^=$) in arctic air at Barrow is approximately one (on a molar basis). This ratio is significantly higher than estimated values at potential pollutant source regions, suggesting that the compounds making up NO_y at Barrow are less efficiently removed from the atmosphere than are SO_2 and $SO_4^=$.

A removal-resistant, stable springtime arctic NO_y reservoir is also indicated by consideration of NO_y speciation. Daytime-average NO concentrations during early March 1990 were always below 6 pptv (hourly average), indicating very low NO_x concentrations. Comparisons of the NO_y measurements reported here with simultaneous filter measurements of total-NO_3^- (HNO_3+particulate-NO_3^-) made during 1989 and with arctic organic nitrate concentrations measured previously provide evidence that PAN and other organic nitrogen compounds are the dominant components of the arctic NO_y reservoir during spring.

This springtime NO_y reservoir may provide a significant source of springtime NO_x to the high- and mid-latitudes, as temperatures and insolation increase during late spring or as arctic air masses are advected south to warmer regions where PAN decomposition would release NO_x. Through this process, the springtime arctic NO_y reservoir may affect springtime O_3 formation in the northern hign- and mid-latitudes. Furthermore, back-trajectory calculations indicate that elevated NO_y concentrations were present in a large region of the high-latitude troposphere. Although NO_y levels at Barrow were generally reduced somewhat during periods when back-trajectories indicated synoptic flow from the south (i.e., from the North Pacific or the interior of Alaska), even these lower concentrations were greater than most previous measurements at other remote sites.

6.1.2 Summer

Summertime NO_y concentrations—measured in the 1988 and 1990 campaigns—were very low. The summertime median concentration observed during late June–August

1990 was 70 pptv. The 1988 summertime measurements were somewhat higher (median 100 pptv), but uncertainties related to the use of a molybdenum mesh converter are probably responsible for this difference. Most of the 1990 background measurements were made during periods of marine flow. During three periods of flow over tundra, significantly higher NO_y concentrations were observed—to nearly 200 pptv—and this may have been a result of (1) enhanced vertical mixing due to heating at the ground, allowing down-mixing of free-tropospheric NO_y; (2) wildfire plumes; or (3) biogenic NO_x emissions. Daytime NO concentrations were also much higher during these periods, reaching 18 pptv (hourly average), in contrast to hourly-average NO levels below 8 pptv during the marine-flow periods. The elevated NO concentrations during flow over tundra were accompanied by temperatures ~10°C warmer than those during marine flow, consistent with the identification of the temperature-dependent decomposition of PAN as the primary source of NO_x in the arctic boundary layer (Jacob et al., 1991).

These measurements are generally consistent with the results of the ABLE-3A measurement campaign (Singh et al., 1991b; Bakwin et al., 1991), which also indicated low surface NO_y concentrations but which demonstrated high NO_y concentrations in the free troposphere.

A small but statistically significant diurnal cycle in NO_y concentrations was observed during the summer of 1990, with an amplitude of ~10 pptv, and is attributed to diurnal variations in boundary layer stability or biogenic NO_x emissions, combined with nighttime depletion of near-surface NO_y by deposition. The 1988 measurements also indicated a diurnal cycle. The larger amplitude derived from the 1988 measurements (40 pptv) may be a result of limited date coverage.

6.1.3 Transition Periods

During April and May of the 1990 campaign, NO_y concentrations dropped dramatically, from the March concentrations of ~600 pptv to the summertime levels of

~70 pptv. Concentrations were observed to increase more slowly in September–November. The springtime decay of NO_y concentrations was accompanied by elevated daytime NO concentrations—to ~35 pptv—suggesting that decomposition of PAN and similar compounds was at least partially responsible for the decreasing NO_y levels. Anticorrelation of temperature and NO_y concentrations during this period supports this conclusion. Through this NO_x pulse, the early-spring arctic NO_y reservoir may contribute to increased springtime O_3 concentrations in the Arctic.

Weak diurnal NO_y cycles were also observed during the spring and fall transition periods, with amplitudes of ~25 and ~11 pptv, respectively, and are attributed to diurnal variations in boundary-layer stability.

6.2 Regional Pollution Events

During a number of events in 1989 and 1990, substantially elevated NO_y levels were observed in air not impacted by emissions from the town of Barrow. The events were of approximately 8–60 hr duration, and peak NO_y levels reached more than 16 ppbv. Substantial evidence indicates that the source of the elevated NO_y levels was the Prudhoe Bay oil-producing region, located approximately 300 km to the ESE. This evidence includes: *i*) slow and smooth concentration variations during the events indicate that local (Barrow) sources were not the cause; *ii*) the ratio of NO_x:NO_y estimated during the events is very high (to 0.9), indicating that the NO_y enrichment was almost entirely due to NO_x and that relatively fresh NO_x emissions were responsible; *iii*) filter measurements of $SO_4^=$ and SO_2, made during 1989, do not indicate enrichment of sulfur compounds during the events, consistent with a source such as Prudhoe Bay which is rich in NO_x; and *iv*) NO_y concentrations during the events were highly correlated with surface wind direction, and highest concentrations coincided with winds in the 110–120° sector, the direction of Prudhoe Bay.

During 9 months of measurements in 1990, elevated NO_y levels apparently due

to the Prudhoe Bay plume significantly affected NO_y measurements at the Barrow site approximately 7% of the time that winds were from the 0–200° wind sector, which is free of major local NO_x sources. Other measurements made at the Barrow site may also be affected by Prudhoe Bay emissions, including methane, carbon monoxide, carbon dioxide, and ozone, and potential Prudhoe Bay impacts should be considered in future analyses of such measurements.

6.3 The Relationship of NO_y and O_3

Analyses of NO_y and O_3 during the 1990 measurements indicated significant correlations during some of the background periods and events. A positive correlation was observed in the summertime marine-flow background measurements, with a least-squares regression slope of ~170 (O_3/NO_y on a molar basis). Mechanisms that may explain the observed slope include: (*i*) long-range transport of both NO_y and O_3 from a lower-latitude pollution source region(s), with preferential loss of NO_y through deposition en-route; (*ii*) mixing of air from the mid-troposphere, with NO_y enrichments resulting from a anthropogenically-derived mid-tropospheric NO_y reservoir and O_3 enrichments from a stratospheric source; and (*iii*) mixing from the mid-troposphere, with both NO_y and O_3 enrichments a result of a stratospheric source. In-situ O_3 production is not believed to be possible due to the low observed NO concentrations and the high ratio of O_3 to NO_y molar enrichment. However, the cause of the observed correlation cannot be unambiguously identified based solely on the present measurements.

The relationship of NO_y and O_3 during spring was more complex. There was evidence of a direct NO_y/O_3 correlation in some springtime periods, but not in others. Peak hourly-average NO concentrations during three partial or near-total springtime O_3 depletion events were 6–34 pptv, indicating that sufficient NO_x may have been present at times for the $BrNO_2$ photolysis O_3 destruction mechanism of

Finlayson-Pitts et al. [1990] to operate. However, additional measurements of NO_2, NO_3 and/or N_2O_5 are necessary to determine whether the N_2O_5 required by this mechanism is present in significant quantities.

During some of the high-NO_y regional and local pollution events at Barrow, these measurements suggest that Prudhoe Bay or Barrow NO_x emissions resulted in reduced O_3 concentrations at Barrow, through NO/O_3 titration. However, the impact of these events on O_3 at Barrow was minimal, and local and regional NO_x emissions may not significantly affect O_3 measurements at the Barrow site.

6.4 Conclusions and Remaining Questions

These results indicate the presence of a reservoir of removal-resistant, stable NO_y compounds—predominantly PAN and other organic nitrates—in the Arctic during winter–spring, and this reservoir may encompass subarctic regions of the remote troposphere as well. Warmer temperatures—due to either the onset of spring or advection to more southerly regions—result in organic nitrate decomposition and the release of NO_x, as observed at Barrow during April–May, 1990. As a result, the arctic NO_y reservoir may impact O_3 concentrations during spring over a large region of the remote troposphere.

During summer, warmer surface temperatures and increased sunlight result in a reduced NO_y lifetime and low ground-level NO_y concentrations. However, measurements by other investigators during the ABLE-3A campaign indicate that a stable NO_y reservoir is present in the arctic mid-troposphere, even during summer (e.g. Singh et al., 1991b). The increased vertical concentration gradient resulting from the reduced surface NO_y concentration during summer is expected to result in a greater NO_y flux to the surface, and, ultimately, greater summertime HNO_3 deposition, despite lower surface NO_y concentrations. This type of process may be the cause of the observed summer maximum of NO_3^- concentrations in Greenland

snow (Davidson et al., 1989).

The present results also demonstrate a direct correlation between NO_y and O_3 in the summertime arctic boundary layer during late June–early September. This correlation may be a result of long-range transport of both NO_y and O_3 to the Arctic during summer, the transport occurring in the free troposphere. In this scenario, NO_x and hydrocarbon emissions in more polluted regions are mixed into the free troposphere where they result in O_3 formation prior to or during transport to the Arctic. Since anthropogenic NO_x emissions have increased significantly in the past decades (Hameed and Dignon, 1988), this process, if it occurs, may be the cause of the summertime surface O_3 increase observed at Barrow.

These measurements leave some unanswered questions that could be addressed by future research. First, the importance of the arctic NO_y reservoir in the springtime NO_x and O_3 budgets of mid-latitude regions should be assessed by further measurements. It would be useful to measure a suite of photochemically-active species in an arctic air mass that has been advected south over a region where NO_x concentrations are normally very low, such as the North Atlantic.

In addition, further work is needed to determine the cause of the observed summertime O_3-NO_y correlation, which, in addition to the process suggested above, could represent stratospheric O_3 brought to the surface along with NO_y from the free troposphere. Identification of an O_3 source associated with long-range NO_y transport, if it is present, will be difficult, since it probably represents a relatively small increase upon the stratospheric O_3 source. However, analyses of ground-level measurements of pollution tracers such as CO or vertical profile measurements of O_3 plus tracers of pollution and stratospheric influence may be useful in this regard.

Finally, the importance of unmeasured organic nitrogen compounds, indicated by the ABLE-3A measurements, as well as the inability of current models to accurately predict arctic NO_y concentrations and speciation, suggests that identification, mea-

surement, and characterization of the missing nitrogen compounds will be essential to an improved understanding of NO_y in the Arctic and other remote regions.

References

Bakwin, P. S., S. C. Wofsy, and Song-Miao Fan, Measurements of reactive nitrogen oxides (NO_y) within and above a tropical forest canopy in the wet season, *J. Geophys. Res.*, *95*, 16,765–16,772, 1990.

Bakwin, P. W., S. C. Wofsy, S. Fan, and D. R. Fitzjarrald, Measurements of NO_y and NO_y concentrations and fluxes over arctic tundra, *J. Geophys. Res.*, (in press) 1991.

Barrie, L. A., and R. M. Hoff, The oxidation rate and residence time of sulfur dioxide in the arctic atmosphere, *Atm. Env.*, *12*, 2711–2722, 1984.

Barrie, L. A. and R. M. Hoff, Five years of air chemistry observations in the Canadian arctic, *Atm. Env.*, *19*, 1995–2010, 1985.

Barrie, L. A., Arctic air pollution: an overview of current knowledge, *Atm. Env.*, *20*, 643–663, 1986.

Barrie, L. A., J. W. Bottenheim, R. C. Schnell, P. J. Crutzen, and R. A. Rasmussen, Ozone destruction and photochemical reactions at polar sunrise in the lower Arctic atmosphere, *Nature*, *334*, 138–141, 1988.

Barrie, L. A., G. den Hartog, J. W. Bottenheim, and S. Landsberger, Anthropogenic aerosols and gases in the lower troposphere at Alert Canada in April 1986, *J. Atmos. Chem.*, *9*, 101–127, 1989.

Barrie, L. A. and J. W. Bottenheim, Sulfur and nitrogen in the arctic atmosphere, in *Pollution of the arctic atmosphere*, W. Sturges, ed., Elsevier Press, (in press) 1991.

Bodhaine, B. A., J. M. Harris, and G. A. Herbert, Aerosol Light Scattering and Condensation Nuclei Measurements at Barrow Alaska, *Atm. Env.*, *15*, 1375-1389, 1981.

Bodhaine, B. A., E. G. Dutton, J. J. DeLuisi, G. A. Herbert, G. E. Shaw, and A. D. A. Hansen, Surface aerosol measurements at Barrow during AGASP-III, *J. Atmos. Chem.*, *9*, 213–224, 1989.

Bollinger, M. J., Chemiluminescent measurements of the oxides of nitrogen in the clean troposphere and atmospheric chemistry implications, Ph.D. thesis, Chem. Dept., Univ. Colo., Boulder, 1982.

Bollinger, M. J., R. E. Sievers, D. W. Fahey, and F. C. Fehsenfeld, Conversion of nitrogen dioxide, nitric acid, and n-propyl nitrate to nitric oxide by gold-catalyzed reduction

with carbon monoxide, *Anal. Chem.*, *55*, 1980–1986; 1983.

Bollinger, M. J., C. J. Hahn, D. D. Parrish, P. C. Murphy, D. L. Albritton, and F. C. Fehsenfeld, NO_x measurements in clean continental air and analysis of the contributing meteorology, *J. Geophys. Res.*, *89*, 9623–9631, 1984.

Bottenheim, J. W., A. G. Gallant, and K. A. Brice, Measurements of NO_y species and O_3 at 82° N latitude, *Geophys. Res. Lett.*, *13*, 113–116, 1986.

Bottenheim, J. W., and A. G. Gallant, PAN over the Arctic: Observations during AGASP-2 in April 1986, *J. Atmos. Chem.*, *9*, 301–316, 1989.

Bottenheim, J. W., L. A. Barrie, E. Atlas, L. E. Heidt, H. Niki, R. A. Rasmussen, and P. B. Shepson, Depletion of lower tropospheric ozone during arctic spring: the polar sunrise experiment 1988, *J. Geophys. Res.*, *95*, 18,555–18,568, 1990.

Bottenheim, J. W., L. A. Barrie, and E. Atlas, The partitioning of NO_y in the lower arctic troposphere during spring 1988, *J. Atmos. Chem.*, (submitted) 1991.

Carroll, M. A., M. McFarland, B. A. Ridley, and D. L. Albritton, Ground-based nitric oxide measurements at Wallops Island, Virginia, *J. Geophys. Res.*, *90*, 12,853–12,860, 1985.

Carroll, M. A., D. D. Montzka, G. Hübler, and K. K. Kelly, In-situ measurements of NO_x in the airborne Arctic Stratospheric Expedition, *Geophys. Res. Lett.*, *17*, 493–496, 1990.

Clough, P. N. and B. A. Thrush, Mechanism of chemiluminescent reaction between nitric oxide and ozone, *Trans. Faraday Soc.*, *60*, 359–370, 1967.

Cox, R. A., Some measurements of ground level NO, NO_2 and O_3 concentrations at an unpolluted maritime site, *Tellus*, *29*, 356–362, 1977.

Crutzen, P. J., The role of NO and NO_2 in the chemistry of the troposphere and stratosphere, *Ann. Rev. Earth Planet. Sci.*, *7*, 443–472, 1979.

Crutzen, P. J., and L. T. Gidel, A two-dimensional photochemical model of the atmosphere, 2, The tropospheric budgets of the anthropogenic chlorocarbons, CO, CH_4, CH_3Cl, and the effect of various NO_x sources on tropospheric ozone, *J. Geophys. Res.*, *88*, 6641–6661, 1983.

Davidson, C. I., J. R. Harrington, M. J. Stephenson, M. J. Small, F. P. Boscoe, and R. E. Gandley, Seasonal variations in sulfate, nitrate and chloride in the Greenland Ice Sheet: relation to atmospheric concentrations, *Atm. Env.*, *23*, 2483–2494, 1989.

Delany, A. C., R. R. Dickerson, F. L. Melchior, Jr., and A. F. Wartburg, Modification of a commercial NO_x detector for high sensitivity, *Rev. Sci. Instrum.*, *53*, 1899–1902, 1982.

DeMore, W. B., M. J. Molina, S. P. Sander, D. M. Golden, R. F. Hampson, M. J. Kurylo, C. J. Howard, and A. R. Ravishankara, Chemical kinetics and photochemical data for use in stratospheric modeling, evaluation number 8, JPL Publication 87-41, Jet Propulsion Laboratory, National Aeronautics and Space Administration, Pasadena, California, 1987.

Dickerson, R. R., D. H. Stedman, and A. C. Delany, Direct measurements of ozone and

nitrogen dioxide photolysis rates in the troposphere, *J. Geophys. Res.*, *87*, 4933–4946, 1982.

Dickerson, R. R., Measurements of reactive nitrogen compounds in the free troposphere, *Atm. Env.*, *12*, 2585–2593, 1984.

Dickerson, R. R., A. C. Delany, and A. F. Wartburg, Further modification of a commercial NO_x detector for high sensitivity, *Rev. Sci. Instrum.*, *55*, 1995–1998, 1984.

Dickerson, R. R., Reactive nitrogen compounds in the Arctic, *J. Geophys. Res.*, *90*, 10,739-10,743, 1985.

Drummond, J. W., A. Volz, and D. H. Ehhalt, An optimized chemiluminescence detector for tropospheric NO measurements, *J. Atmos. Chem.*, *2*, 287–306, 1985.

Drummond, J. W., D. H. Ehhalt, and A. Volz, Measurements of nitric oxide between 0–12 km altitude and 67°N to 60°S latitude obtained during STRATOZ III, *J. Geophys. Res.*, *93*, 15,831–15,849, 1988.

Fahey, D. W., C. S. Eubank, G. Hübler, and F. C. Fehsenfeld, Evaluation of a catalytic reduction technique for the measurement of total reactive odd-nitrogen NO_y in the atmosphere, *J. Atmos. Chem.*, *3*, 435–468, 1985.

Fahey, D. W., G. Hübler, D. D. Parrish, E. J. Williams, R. B. Norton, B. A. Ridley, H. B. Singh, S. C. Liu, and F. C. Fehsenfeld, Reactive nitrogen species in the troposphere: Measurements of NO, NO_2, HNO_3, particulate nitrate, peroxyacetyl nitrate (PAN), O_3, and total reactive odd nitrogen (NO_y) at Niwot Ridge, Colorado, *J. Geophys. Res.*, *91*, 9781–9793, 1986.

Fehsenfeld, F. C., R. R. Dickerson, G. Hübler, W. T. Luke, L. J. Nunnermacker, E. J. Williams, J. M. Roberts, J. G. Calvert, C. M. Curran, A. C. Delany, C. S. Eubank, D. W. Fahey, A. Fried, B. W. Gandrud, A. O. Langford, P. C. Murphy, R. B. Norton, K. E. Pickering, and B. A. Ridley, A ground-based intercomparison of NO, NO_x, and NO_y measurement techniques, *J. Geophys. Res.*, *92*, 14,710–14,722, 1987.

Fehsenfeld, F. C., J. W. Drummond, U. K. Roychowdhury, P. J. Galvin, E. J. Williams, M. P. Buhr, D. D. Parrish, G. Hübler, A. O. Langford, J. G. Calvert, B. A. Ridley, F. Grahek, B. G. Heikes, G. L. Kok, J. D. Shetter, J. G. Walega, C. M. Elsworth, R. B. Norton, D. W. Fahey, P. C. Murphy, C. Hovermale, V. A. Mohnen, K. L. Demerjian, G. I. Mackay, and H. I. Schiff, Intercomparison of NO_2 measurement techniques, *J. Geophys. Res.*, *95*, 3579–3597, 1990.

Finlayson-Pitts, B. J., F. E. Livingston, and H. N. Berko, Ozone destruction and bromine photochemistry at ground level in the arctic spring, *Nature*, *343*, 622–625, 1990.

Fishman, J., S. Solomon, and P. J. Crutzen, Observational and theoretical evidence in support of a significant in-situ photochemical source of tropospheric ozone, *Tellus*, *31*, 432–446, 1979.

Fontijn, A., A. J. Sabadell, and R. J. Ronco, Homogeneous chemiluminescent measurement of nitric oxide with ozone, *Anal. Chem.*, *42*, 575–579, 1970.

Galbally, I. E., Measurement of nitrogen oxides in the background atmosphere, in *Air Pollution Measurement Techniques*, Special Environmental Report No. 10, p. 179, World Meteorological Organization, Geneva, 1977.

Galbally, I. E., and C. R. Roy, Ozone and nitrogen oxides in the southern hemisphere troposphere, in Proc. Quad. Intern. Ozone Symp., J. London (ed.), Nat. Center for Atm. Res., Boulder, Colorado, 1981.

Galloway, J. N., and G. E. Likens, Acid precipitation: The importance of nitric acid, *Atm. Env.*, *15*, 1081–1085, 1981.

Garland, J. A. and S. A. Penkett, Absorption of peroxyacetyl nitrate and ozone by natural surfaces, *Atm. Env.*, *10*, 1127–1131, 1976.

Grosjean, D., and J. Harrison, Response of chemiluminescence NO_x analyzers and ultraviolet ozone analyzers to organic air pollutants, *Env. Sci. Tech.*, *19*, 862–865, 1985.

Hameed, S. and J. Dignon, Changes in the geographical distributions of global emissions of NO_x and SO_x from fossil-fuel combustion between 1966 and 1980, *Atm. Env.*, *22*, 441–450, 1988.

Hansen, A. D. A., T. J. Conway, L. P. Steele, B. A. Bodhaine, K. W. Thoning, P. Tans, and T. Novakov, Correlations among combustion effluent species at Barrow, Alaska: Aerosol black carbon, carbon dioxide, and methane, *J. Atmos. Chem.*, *9*, 283–299, 1989.

Harris, J. M., The GMCC atmospheric trajectory program, *NOAA Tech. Mem. ERL ARL-116*, Air Resour. Lab., Rockville, Md., 1982.

Heidam, N. Z., The components of the arctic aerosol, *Atm. Env.*, *18*, 329–343, 1984.

Helas, G., M. Flanz, and P. Warneck, Improved NO_x monitor for measurements in tropospheric clean air regions, *Intern. J. Environ. Anal. Chem.*, *10*, 155–166, 1981.

Helas, Günter and Peter Warneck, Background NO_x Mixing Ratios in Air Masses over the North Atlantic Ocean, *J. Geophys. Res.*, *86*, 7283-7290, 1981.

Honrath, R. E. and D. A. Jaffe, Measurements of nitrogen oxides in the Arctic, *Geophys. Res. Lett.*, *17*, 611–614, 1990.

Hov, Ø, S. A. Penkett, I. S. A. Isaksen, and A. Semb, Organic gases in the Norwegian Arctic, *Geophys. Res. Lett.*, *11*, 425–428, 1984.

Hov, Ø., A. Eliassen, and D. Simpson, Calculation of the distribution of NO_x compounds in Europe, in *Tropospheric Ozone*, I. S. A. Isaksen (ed.), D. Reidel Publishing Co., pp. 239–261, 1988.

Hübler, G., D. D. Montzka, C. Hahn, R. B. Norton, M. A. Carroll, F. C. Fehsenfeld, B. A. Ridley, J. G. Walega, F. Grahek, J. D. Shetter, E. Atlas, S. Schauffler, B. J. Huebert, and W. Warren, Total reactive odd nitrogen (NO_y) measurements and the NO_y budget in the remote troposphere, Eos *Trans. AGU*, *70*, 1014, 1989.

Isaksen, I. S. A., Ø. Hov, S. A. Penkett, and A. Semb, Model analysis of the measured concentration of organic gases in the Norwegian Arctic, *J. Atmos. Chem.*, *3*, 3–27, 1985.

Jacob, D. J. and S. C. Wofsy, Budgets of reactive nitrogen, hydrocarbons, and ozone over the Amazon forest during the wet season, *J. Geophys. Res.*, *95*, 16,737–16754, 1990.

Jacob, D. J., S. C. Wofsy, P. S. Bakwin, S.-M. Fan, R. C. Harriss, R. W. Talbot, J. D. Bradshaw, S. T. Sandholm, H. B. Singh, G. L. Gregory, G. W. Sachse, M. Shipman, D. R. Blake, and D. R. Fitzjarrald, Summertime photochemistry of the arctic troposphere, *J. Geophys. Res.*, (submitted) 1991.

Jaffe, D. A., R. E. Honrath, J. A. Herring, S.-M. Li, and J. D. Kahl, Measurements of nitrogen oxides at Barrow, Alaska during spring: evidence for regional and northern hemispheric sources of pollution, *J. Geophys. Res.*, *96*, 7395–7405, 1991.

Joranger, E. and B. Ottar, Air pollution studies in the Norwegian Arctic, *Geophys. Res. Lett.*, *11*, 365–368, 1984.

Kahl, J. D., and P. J. Samson, Uncertainty in trajectory calculations due to low resolution meteorological data, *J. Clim. Appl. Meteorol.*, *25*, 1816–1831, 1986.

Kahl, J. D., J. M. Harris, G. A. Herbert, and M. P. Olson, Intercomparison of three long-range trajectory models applied to arctic haze, *Tellus*, *41B*, 524–536, 1989.

Kahl, J. D., Characteristics of the low-level temperature inversion along the Alaskan arctic coast, *Int. J. Climatol.*, *10*, 537–548, 1990.

Kaplan, W. A., Wofsy, S. C., Keller, M., and J. M. Da Costa. Emission of NO and deposition of O_3 in a tropical forest system, *J. Geophys. Res.*, *93*, 1389–1395, 1988.

Kelly, T. J., D. H. Stedman, J. A. Ritter, and R. B. Harvey, Measurements of oxides of nitrogen and nitric acid in clean air, *J. Geophys. Res.*, *85*, 7417–7425, 1980.

Kley, D. and M. McFarland, Chemiluminescence detector for NO and NO_2, *Atmos. Tech.*, *12*, 63–69, 1980.

Kley, D., J. W. Drummond, M. McFarland, and S. C. Liu, Tropospheric Profiles of NO_x, *J. Geophys. Res.*, *86*, 3153-3161, 1981.

Kondo, Y., H. Muramatsu, W. A. Matthews, N. Toriyama, and M. Hirota, Tropospheric ozone and oxides of nitrogen over the north-western Pacific in summer, *J. Atmos. Chem.*, *6*, 235–250, 1988a.

Kondo, Y., W. A. Matthews, P. Aimedieu, and D. E. Robbins, Diurnal variation of nitric oxide at 32 km: measurements and interpretation, *J. Geophys. Res.*, *93*, 2451–2460, 1988b.

Leighton, P. A., *Photochemistry of Air Pollution*, Academic, San Diego, Calif., 1961.

Levy II, H., Normal atmosphere: large radical and formaldehyde concentrations predicted, *Science*, *173*, 141–143, 1971.

Levy II, H., J. D. Mahlman, and W. J. Moxim, A Stratospheric Source of Reactive Nitrogen in the Unpolluted Troposphere, *Geophys. Res. Lett.*, *7*, 441-444, 1980.

Levy II, H., and W. J. Moxim, Simulated global distribution and deposition of reactive nitrogen emitted by fossil fuel combustion, *Tellus*, *41B*, 256–271, 1989.

Li, S.-H. and J. W. Winchester, Geochemistry of organic and inorganic ions of late winter arctic aerosols, *Atm. Env.*, *23*, 2401–2415, 1989.

Lightman, P., A. S. Kallend, A. R. W. Marsh, B. M. R. Jones, and S. A. Penkett, Seasonal variation of hydrocarbons in the free troposphere at mid-latitudes, *Tellus*, *42B*, 408–422, 1990.

Lin, X., M. Trainer, and S. C. Liu, On the nonlinearity of the tropospheric ozone production, *J. Geophys. Res.*, *93*, 15,879–15,888, 1988.

Liu, S. C., M. Trainer, F. C. Fehsenfeld, D. D. Parrish, E. J. Williams, D. W. Fahey, G. Hübler, and P. C. Murphy, Ozone production in the rural troposphere and implications for regional and global ozone distributions, *J. Geophys. Res.*, *92*, 4191–4207, 1987.

Logan, J. A., M. J. Prather, S. C. Wofsy, and M. B. McElroy, Tropospheric chemistry: a global perspective, *J. Geophys. Res.*, *86*, 7210–7254, 1981.

Logan, J. A., Nitrogen oxides in the troposphere: Global and regional budgets, *J. Geophys. Res.*, *88*, 6641–6661, 1983.

Luther, F. M., and R. J. Gelinas, Effect of molecular multiple scattering and surface albedo on atmospheric photodissociation rates, *J. Geophys. Res.*, *81*, 1125–1132, 1976.

Madronich, S., D. R. Hastie, B. A. Ridley, and H. I. Schiff, Measurement of the photodissociation coefficient of NO_2 in the atmosphere, I, Method and surface measurements, *J. Atmos. Chem.*, *1*, 3–25, 1983.

Malmstadt, H. V., M. L. Franklin, and G. Horlick, Photon counting for spectrophotometry, *Anal. Chem.*, *44*, 63A–76A, 1972.

Mayewski, P.A., W. B. Lyons, M. J., M. Twickler, W. Dansgaard, B. Koci, C. I. Davidson, and R. E. Honrath, Sulfate and nitrate concentrations from a South Greenland ice core, *Science*, *232*, 975–977, 1986.

McFarland, D. Kley, J. W. Drummond, A. L. Schmeltekopf, and R. H. Winkler, Nitric oxide measurements in the equatorial Pacific region, *Geophys. Res. Lett.*, *6*, 605–608, 1979.

McFarland, M., B. A. Ridley, M. H. Proffitt, D. L. Albritton, T. L. Thompson, W. J. Harrop, R. H. Winkler, and A. L. Schmeltekopf, Simultaneous in situ measurements of nitrogen dioxide, nitric oxide, and ozone between 20 and 31 km, *J. Geophys. Res.*, *91*, 5421–5437, 1986.

Mickle, R. E., J. W. Bottenheim, W. R. Leaitch, and W. Evans, Boundary layer ozone depletion during AGASP-II, *Atm. Env.*, *23*, 2443–2449, 1989.

Montzka, D. D., M. A. Carroll, G. Hübler, C. Hahn, R. A. Ridley, J. G. Walega, P. Zimmerman, J. Greenberg, L. Heidt, E. Atlas, S. Schauffler, and B. Heikes, In-situ measurements of NO_x during the MLOPEX (spring 1988) program, Eos *Trans. AGU*, *70*, 1014, 1989.

Murphy, D. M. and D. W. Fahey, Mathematical treatment of the wall loss of a trace species in denuder and catalytic converter tubes, *Anal. Chem.*, *59*, 2753–2759, 1987.

National Oceanic and Atmospheric Administration, *Geophysical monitoring for climatic change, Summary rep. 17, 1988*, J. W. Elkins and R. M. Rosson (ed.), Boulder, Colo., 1989.

National Oceanic and Atmospheric Administration, *Climate Monitoring and Diagnostics Laboratory, Summary rep. 18, 1989*, W. D. Komhyr and R. M. Rosson (ed.), Boulder, Colo., 1990.

Nunnermacker, L. J., R. R. Dickerson, W. T. Luke, W. D. Dorko, and A. Fried, Detection of reactive nitrogen compounds by conversion to NO on stainless steel, molybdenum, and ferrous sulfate, Eos *Trans. AGU, 69*, 1060, 1988.

Oltmans, S. J., Surface ozone measurements in clean air, *J. Geophys. Res., 86*, 1174–1180, 1981.

Oltmans, S., and W. P. Komhyr, Surface ozone distributions and variations from 1973-1984: measurements at the NOAA Geophysical Monitoring for Climatic Change baseline observatories, *J. Geophys. Res., 91*, 5229–5236, 1986.

Parrish, D. D., M. Trainer, E. J. Williams, D. W. Fahey, G. Hübler, C. S. Eubank, S. C. Liu, P. C. Murphy, D. L. Albritton, and F. C. Fehsenfeld, Measurements of the NO_x-O_3 photostationary state at Niwot Ridge, Colorado, *J. Geophys. Res., 91*, 5361–5370, 1986.

Parrish, D. D., C. H. Hahn, D. W. Fahey, E. J. Williams, M. J. Bollinger, G. Hübler, M. P. Buhr, P. C. Murphy, M. Trainer, E. Y. Hsie, S. C. Liu, and F. C. Fehsenfeld, Systematic variations in the concentration of NO_x (NO plus NO_2) at Niwot Ridge, Colorado, *J. Geophys. Res., 95*, 1817–1836, 1990.

Patterson, D. E. and R. B. Husar, A direct simulation of hemispherical transport of pollutants, *Atm. Env., 15*, 1479–1482, 1981.

Radke, L. F., P. V. Hobbs, and J. E. Pinnons, Observations of cloud condensation nuclei, sodium-containing particles, ice nuclei and the light-scattering coefficient near Barrow, Alaska, *J. Appl. Meteorol., 15*, 982–995, 1976.

Rasmussen, R. A., M. A. K. Khalil, and R. J. Fox, Altitudinal and temporal variation of hydrocarbons and other gaseous tracers of arctic haze, *Geophys. Res. Lett., 10*, 144–147, 1983.

Ridley, B. A. and L. C. Howlett, An instrument for nitric oxide measurements in the stratosphere, *Rev. Sci. Instrum., 45*, 742–746, 1974.

Ridley, B. A., M. A. Carroll, and G. L. Gregory, Measurements of nitric oxide in the boundary layer and free troposphere over the Pacific Ocean, *J. Geophys. Res., 92*, 2025–2047, 1987.

Ridley, B. A., M. A. Carroll, G. L. Gregory, and G. W. Sachse, NO and NO_2 in the troposphere: technique and measurements in regions of a folded tropopause, *J. Geophys. Res., 93*, 15,813–15,830, 1988.

Ridley, B. A. and F. E. Grahek, A small, low flow, high sensitivity reaction vessel for NO

chemiluminescence detectors, *J. Atm. Oceanic Tech.*, *7*, 307–311, 1990.

Schiff, H. I., D. Pepper, and B. A. Ridley, Tropospheric NO Measurements up to 7 km, *J. Geophys. Res.*, *84*, 7895–7897, 1979.

Seinfeld, J. H., *Air Pollution. Physical and Chemical Fundamentals*, McGraw-Hill, New York, New York, 1975.

Shaw, G. E., Evidence for a central Eurasian source of arctic haze in Alaska, *Nature*, *299*, 815–818, 1982.

Singh, H. B., and P. L. Hanst, Peroxyacetyl nitrate (PAN) in the unpolluted atmosphere: an important reservoir for nitrogen oxides, *Geophys. Res. Lett.*, *8*, 941–944, 1981.

Singh, H. B., L. J. Salas, B. A. Ridley, J. Shetter, N. M. Donahue, F. C. Fehsenfeld, D. W. Fahey, D. D. Parrish, E. J. Williams, S. C. Liu, G. Hübler, and P. C. Murphy, Relationship between peroxyacetyl nitrate (PAN) and nitrogen oxides in the clean troposphere, *Nature*, *318*, 347–349, 1985.

Singh, H. B., L. J. Salas, and W. Viezee, Global distribution of peroxyacetyl nitrate, *Nature*, *321*, 588–591, 1986.

Singh, H. B., Reactive nitrogen in the troposphere, *Env. Sci. Tech.*, *21*, 320–327, 1987.

Singh, H. B., D. O'Hara, D. Herith, J. D. Bradshaw, S. T. Sandholm, G. L. Gregory, G. W. Sachse, D. R. Blake, P. J. Crutzen, and M. A. Kanakidou, Atmospheric Measurements of PAN and other organic nitrates at high latitudes: possible sources and sinks, *J. Geophys. Res.*, (in press) 1991a.

Singh, H. B., D. Herith, D. O'Hara, K. Zahnie, J. D. Bradshaw, S. T. Sandholm, R. Talbot, P. J. Crutzen, and M. A. Kanakidou, Relationship of PAN to active and total odd nitrogen at northern high latitudes: influence of reservoir species on NO_x and O_3, *J. Geophys. Res.*, (in press) 1991b.

Stamnes, K., and S.-C. Tsay, Optimum spectral resolution for computing atmospheric heating and photodissociation rates, *Planet. Space Sci.*, *38*, 807–820, 1990.

Stedman, D. H. and M. J. McEwan, Oxides of Nitrogen at Two Sites in New Zealand, *Geophys. Res. Lett.*, *10*, 168-171, 1983.

Stephens, E. G., The formation, reactions, and properties of peroxyacetyl nitrates (PANs) in photochemical air pollution, *Advances in Env. Sci*, *1*, 119–146, 1969.

Stevens, R. K., and J. A. Hodgeson, Applications of chemiluminescent reactions to the measurement of air pollutants, *Anal. Chem.*, *45*, 443A–449A, 1973.

Torres, A. L., Nitric oxide measurements at a nonurban eastern United States site: Wallops instrument results from July 1983 GTE/CITE Mission, *J. Geophys. Res.*, *90*, 12,875–12880, 1985.

Torres, A. L., and H. Buchan, Tropospheric nitric oxide measurements over the Amazon Basin, *J. Geophys. Res.*, *93*, 1396–1406, 1988.

Wesely, M. L., Parameterization of surface resistances to gaseous dry deposition in

regional-scale numerical models, *Atm. Env.*, *23*, 1293–1304, 1989.

Williams, E. J., D. D. Parrish, and F. C. Fehsenfeld, Determination of Nitrogen Oxide Emissions From Soils: Results From a Grassland Site in Colorado, United States, *J. Geophys. Res.*, *92*, 2173-2179, 1987.

Winer, A. M., J. W. Peters, J. P. Smith, and J. N. Pitts, Jr., Response of commercial chemiluminescence NO-NO_2 analyzers to other nitrogen-containing compounds, *Env. Sci. Tech.*, *8*, 1118–1121, 1974.

Appendix A

Labtech Notebook Setup Used During the 1990 Measurements

As described in section 2.2.8.1, the NO/NO_y detector was controlled using Labtech Notebook software. Operation of the Labtech Notebook program is controlled through the "Channels" setup file, which determines the data input and output and calculation channels used data acquisition/control. The Notebook setup is displayed below in Figure A.1, in the format of the Notebook VERIFY command. The setup refers to two input files: NONOY.MOD, used by channel number 4, and NONOY.SOL, used by channel number 5. One value was read from the file NONOY.MOD each 10 s. The value read determined the mode of the instrument (modes values 0.1 through 45.1 were used for the 46 instrument modes (Figure 2.26).). The value read from file NONOY.MOD each 10 s was used by the other setup channels to determine the settings of the instrument solenoid valves and to determine when to make measurements for each mode. The second file, NONOY.SOL, contained 46 values which each determined the settings (on or off) of the 3 solenoid valves and the calibration ultraviolet lamp during each of the modes. These values determined the state of the digital output channel (channel number 5), which

controlled the solenoid valves and the calibration ultraviolet lamp.

LABTECH NOTEBOOK Global Setup Checking MODE: Normal

Ch. No.	Channel Name	Intfc Dev	Intfc Ch	Channel Function	Channel Info.	Scale Factor	Offset	Iter	S t g	Stage Information Duration (sec)	Stage Information Rate (sec)	Stage Information Start State	Stage Information Tr. Ch.	Stage Information Trigger Level	File Name (first)	Wd #
1	cps	1	0	Counter	Increm.			1	1	3.10E+07	1.000	Normal	1	0.000		
2	Time			Time	Elapsed			1	1	3.10E+07	1.000	Normal	1	0.000		4
3	cps-5s			Blk Av(1)	5.000	1.000	0.000	1	1	3.10E+07	5.000	Normal	1	0.000	c:\nb\data\M*	1
4	MODE			Replay	MONOY.M*	1.000	0.000	9000	1	3.10E+07	10.000	Normal	1	0.000		4
5	Sol Ctl	1	0	Digital Out	MONOY.S*			9000	1	10.000	10.000	Normal	4	0.000		
									2	10.000	10.000	On Edge	4	1.000		
									3	10.000	10.000	On Edge	4	2.000		
									4	10.000	10.000	On Edge	4	3.000		
									5	10.000	10.000	On Edge	4	4.000		
									6	10.000	10.000	On Edge	4	5.000		
									7	10.000	10.000	On Edge	4	6.000		
									8	10.000	10.000	On Edge	4	7.000		
									9	10.000	10.000	On Edge	4	8.000		
									*	10.000	10.000	On Edge	4	9.000		
									*	10.000	10.000	On Edge	4	10.000		
									*	10.000	10.000	On Edge	4	11.000		
									*	10.000	10.000	On Edge	4	12.000		
									*	10.000	10.000	On Edge	4	13.000		
									*	10.000	10.000	On Edge	4	14.000		
									*	10.000	10.000	On Edge	4	15.000		
									*	10.000	10.000	On Edge	4	16.000		
									*	10.000	10.000	On Edge	4	17.000		
									*	10.000	10.000	On Edge	4	18.000		
									*	10.000	10.000	On Edge	4	19.000		
									*	10.000	10.000	On Edge	4	20.000		
									*	10.000	10.000	On Edge	4	21.000		
									*	10.000	10.000	On Edge	4	22.000		
									*	10.000	10.000	On Edge	4	23.000		
									*	10.000	10.000	On Edge	4	24.000		
									*	10.000	10.000	On Edge	4	25.000		
									*	10.000	10.000	On Edge	4	26.000		
									*	10.000	10.000	On Edge	4	27.000		
									*	10.000	10.000	On Edge	4	28.000		
									*	10.000	10.000	On Edge	4	29.000		
									*	10.000	10.000	On Edge	4	30.000		
									*	10.000	10.000	On Edge	4	31.000		
									*	10.000	10.000	On Edge	4	32.000		
									*	10.000	10.000	On Edge	4	33.000		
									*	10.000	10.000	On Edge	4	34.000		

Figure A.1 Labtech Notebook setup used during 1990.

										*	10.000	10.000	On Edge	4	35.000		
										*	10.000	10.000	On Edge	4	36.000		
										*	10.000	10.000	On Edge	4	37.000		
										*	10.000	10.000	On Edge	4	38.000		
										*	10.000	10.000	On Edge	4	39.000		
										*	10.000	10.000	On Edge	4	40.000		
										*	10.000	10.000	On Edge	4	41.000		
										*	10.000	10.000	On Edge	4	42.000		
										*	10.000	10.000	On Edge	4	43.000		
										*	10.000	10.000	On Edge	4	44.000		
										*	10.000	10.000	On Edge	4	45.000		
										*	10.000	10.000	On Edge	4	1.000		
6	NOy/C/O3			Blk Av(1)	40.000	1.000	0.000	9000	1	0.000	10.000	Normal	4	0.000	c:\nb\data\N*	
									2	10.000	10.000	On Edge	4	1.000		
7	NOy/C/O3 SD			Blk SD(1)	40.000	1.000	0.000	9000	1	0.000	10.000	Normal	1	0.000	c:\nb\data\N*	
									2	10.000	10.000	On Edge	4	1.000		
8	NOy/C/O3 Time			Blk Av(2)	40.000	1.000	0.000	9000	1	0.000	10.000	Normal	1	0.000	c:\nb\data\N*	3
									2	10.000	10.000	On Edge	4	1.000		
9	NO/C/O3			Blk Av(1)	15.000	1.000	0.000	9000	1	0.000	10.000	Normal	1	0.000	c:\nb\data\N*	
									2	10.000	10.000	On Edge	4	2.000		
10	NO/C/O3 SD			Blk SD(1)	15.000	1.000	0.000	9000	1	0.000	10.000	Normal	1	0.000	c:\nb\data\N*	
									2	10.000	10.000	On Edge	4	2.000		
11	NO/C/O3 Time			Blk Av(2)	15.000	1.000	0.000	9000	1	0.000	10.000	Normal	1	0.000	c:\nb\data\N*	
									2	10.000	10.000	On Edge	4	2.000		
12	NO (c)			Blk Av(1)	15.000	1.000	0.000	9000	1	0.000	10.000	Normal	1	0.000	c:\nb\data\N*	
									2	10.000	10.000	On Edge	4	3.000		
13	NO (c) SD			Blk SD(1)	15.000	1.000	0.000	9000	1	0.000	10.000	Normal	1	0.000	c:\nb\data\N*	
									2	10.000	10.000	On Edge	4	3.000		
14	NO (c) Time			Blk Av(2)	15.000	1.000	0.000	9000	1	0.000	10.000	Normal	1	0.000	c:\nb\data\N*	
									2	10.000	10.000	On Edge	4	3.000		
15	NO/C			Blk Av(1)	15.000	1.000	0.000	9000	1	0.000	10.000	Normal	1	0.000	c:\nb\data\N*	
									2	10.000	10.000	On Edge	4	4.000		
16	NO/C SD			Blk SD(1)	15.000	1.000	0.000	9000	1	0.000	10.000	Normal	1	0.000	c:\nb\data\N*	
									2	10.000	10.000	On Edge	4	4.000		
17	NO/C Time			Blk Av(2)	15.000	1.000	0.000	9000	1	0.000	10.000	Normal	1	0.000	c:\nb\data\N*	3
									2	10.000	10.000	On Edge	4	4.000		
18	NOy/C			Blk Av(1)	40.000	1.000	0.000	9000	1	0.000	10.000	Normal	1	0.000	c:\nb\data\N*	
									2	10.000	10.000	On Edge	4	5.000		
19	NOy/C SD			Blk SD(1)	40.000	1.000	0.000	9000	1	0.000	10.000	Normal	1	0.000	c:\nb\data\N*	
									2	10.000	10.000	On Edge	4	5.000		
20	NOy/C Time			Blk Av(2)	40.000	1.000	0.000	9000	1	0.000	10.000	Normal	1	0.000	c:\nb\data\N*	
									2	10.000	10.000	On Edge	4	5.000		
21	NO/C/Z			Blk Av(1)	20.000	1.000	0.000	9000	1	0.000	10.000	Normal	1	0.000	c:\nb\data\N*	
									2	10.000	10.000	On Edge	4	6.000		
22	NO/C/Z SD			Blk SD(1)	20.000	1.000	0.000	9000	1	0.000	10.000	Normal	1	0.000	c:\nb\data\N*	

Figure A.1 (continued) Labtech Notebook setup used during 1990.

										2	10.000	10.000	On Edge	4	6.000				
23	NO/C/Z Time			Blk Av(2)	20.000	1.000	0.000	9000	1	0.000	10.000	Normal	1	0.000	c:\nb\data\N*	3			
									2	10.000	10.000	On Edge	4	6.000					
24	Z-NO1a			Blk Av(1)	40.000	1.000	0.000	9000	1	0.000	10.000	Normal	1	0.000	c:\nb\data\N*				
									2	10.000	10.000	On Edge	4	7.000					
25	Z-NO1a SD			Blk SD(1)	40.000	1.000	0.000	9000	1	0.000	10.000	Normal	1	0.000	c:\nb\data\N*				
									2	10.000	10.000	On Edge	4	7.000					
26	Z-NO-1a Time			Blk Av(2)	40.000	1.000	0.000	9000	1	0.000	10.000	Normal	1	0.000	c:\nb\data\N*				
									2	10.000	10.000	On Edge	4	7.000					
27	NO-1			Blk Av(1)	40.000	1.000	0.000	9000	1	0.000	10.000	Normal	1	0.000	c:\nb\data\N*				
									2	10.000	10.000	On Edge	4	8.000					
28	NO-1 SD			Blk SD(1)	40.000	1.000	0.000	9000	1	0.000	10.000	Normal	1	0.000	c:\nb\data\N*				
									2	10.000	10.000	On Edge	4	8.000					
29	NO-1 Time			Blk Av(2)	40.000	1.000	0.000	9000	1	0.000	10.000	Normal	1	0.000	c:\nb\data\N*	2			
									2	10.000	10.000	On Edge	4	8.000					
30	Z-NO1b			Blk Av(1)	40.000	1.000	0.000	9000	1	0.000	10.000	Normal	1	0.000	c:\nb\data\N*				
									2	10.000	10.000	On Edge	4	9.000					
31	Z-NO1b SD			Blk SD(1)	40.000	1.000	0.000	9000	1	0.000	10.000	Normal	1	0.000	c:\nb\data\N*				
									2	10.000	10.000	On Edge	4	9.000					
32	Z-NO-1b Time			Blk Av(2)	40.000	1.000	0.000	9000	1	0.000	10.000	Normal	1	0.000	c:\nb\data\N*				
									2	10.000	10.000	On Edge	4	9.000					
33	NOy-1			Blk Av(1)	20.000	1.000	0.000	9000	1	0.000	10.000	Normal	1	0.000	c:\nb\data\N*				
									2	10.000	10.000	On Edge	4	10.000					
34	NOy-1 SD			Blk SD(1)	20.000	1.000	0.000	9000	1	0.000	10.000	Normal	1	0.000	c:\nb\data\N*				
									2	10.000	10.000	On Edge	4	10.000					
35	NOy-1 Time			Blk Av(2)	20.000	1.000	0.000	9000	1	0.000	10.000	Normal	1	0.000	c:\nb\data\N*				
									2	10.000	10.000	On Edge	4	10.000					
36	Z-NOy-1b			Blk Av(1)	20.000	1.000	0.000	9000	1	0.000	10.000	Normal	1	0.000	c:\nb\data\N*				
									2	10.000	10.000	On Edge	4	11.000					
37	Z-NOy-1b SD			Blk SD(1)	20.000	1.000	0.000	9000	1	0.000	10.000	Normal	1	0.000	c:\nb\data\N*				
									2	10.000	10.000	On Edge	4	11.000					
38	Z-NOy-1b Time			Blk Av(2)	20.000	1.000	0.000	9000	1	0.000	10.000	Normal	1	0.000	c:\nb\data\N*	2			
									2	10.000	10.000	On Edge	4	11.000					
39	Z-NO-2a			Blk Av(1)	40.000	1.000	0.000	9000	1	0.000	10.000	Normal	1	0.000	c:\nb\data\N*				
									2	10.000	10.000	On Edge	4	12.000					
40	Z-NO-2a SD			Blk SD(1)	40.000	1.000	0.000	9000	1	0.000	10.000	Normal	1	0.000	c:\nb\data\N*				
									2	10.000	10.000	On Edge	4	12.000					
41	Z-NO-2a Time			Blk Av(2)	40.000	1.000	0.000	9000	1	0.000	10.000	Normal	1	0.000	c:\nb\data\N*				
									2	10.000	10.000	On Edge	4	12.000					
42	NO-2			Blk Av(1)	40.000	1.000	0.000	9000	1	0.000	10.000	Normal	1	0.000	c:\nb\data\N*				
									2	10.000	10.000	On Edge	4	13.000					
43	NO-2 SD			Blk SD(1)	40.000	1.000	0.000	9000	1	0.000	10.000	Normal	1	0.000	c:\nb\data\N*				
									2	10.000	10.000	On Edge	4	13.000					
44	NO-2 Time			Blk Av(2)	40.000	1.000	0.000	9000	1	0.000	10.000	Normal	1	0.000	c:\nb\data\N*				
									2	10.000	10.000	On Edge	4	13.000					

Figure A.1 (continued) Labtech Notebook setup used during 1990.

45	Z-NO-2b			Blk Av(1)	40.000	1.000	0.000	9000	1	0.000	10.000	Normal	1	0.000 c:\nb\data\N*
									2	10.000	10.000	On Edge	4	14.000
46	Z-NO-2b SD			Blk SD(1)	40.000	1.000	0.000	9000	1	0.000	10.000	Normal	1	0.000 c:\nb\data\N*
									2	10.000	10.000	On Edge	4	14.000
47	Z-NO-2b Time			Blk Av(2)	40.000	1.000	0.000	9000	1	0.000	10.000	Normal	1	0.000 c:\nb\data\N*
									2	10.000	10.000	On Edge	4	14.000
48	NOy-2			Blk Av(1)	20.000	1.000	0.000	9000	1	0.000	10.000	Normal	1	0.000 c:\nb\data\N*
									2	10.000	10.000	On Edge	4	15.000
49	NOy-2 SD			Blk SD(1)	20.000	1.000	0.000	9000	1	0.000	10.000	Normal	1	0.000 c:\nb\data\N*
									2	10.000	10.000	On Edge	4	15.000
50	NOy-2 Time			Blk Av(2)	20.000	1.000	0.000	9000	1	0.000	10.000	Normal	1	0.000 c:\nb\data\N*
									2	10.000	10.000	On Edge	4	15.000
51	Z-NOy-2b			Blk Av(1)	20.000	1.000	0.000	9000	1	0.000	10.000	Normal	1	0.000 c:\nb\data\N*
									2	10.000	10.000	On Edge	4	16.000
52	Z-NOy-2b SD			Blk SD(1)	20.000	1.000	0.000	9000	1	0.000	10.000	Normal	1	0.000 c:\nb\data\N*
									2	10.000	10.000	On Edge	4	16.000
53	Z-NOy-2b Time			Blk Av(2)	20.000	1.000	0.000	9000	1	0.000	10.000	Normal	1	0.000 c:\nb\data\N*
									2	10.000	10.000	On Edge	4	16.000
54	Z-NO-3a			Blk Av(1)	40.000	1.000	0.000	9000	1	0.000	10.000	Normal	1	0.000 c:\nb\data\N*
									2	10.000	10.000	On Edge	4	17.000
55	Z-NO-3a SD			Blk SD(1)	40.000	1.000	0.000	9000	1	0.000	10.000	Normal	1	0.000 c:\nb\data\N*
									2	10.000	10.000	On Edge	4	17.000
56	Z-NO-3a Time			Blk Av(2)	40.000	1.000	0.000	9000	1	0.000	10.000	Normal	1	0.000 c:\nb\data\N*
									2	10.000	10.000	On Edge	4	17.000
57	NO-3			Blk Av(1)	40.000	1.000	0.000	9000	1	0.000	10.000	Normal	1	0.000 c:\nb\data\N*
									2	10.000	10.000	On Edge	4	18.000
58	NO-3 SD			Blk SD(1)	40.000	1.000	0.000	9000	1	0.000	10.000	Normal	1	0.000 c:\nb\data\N*
									2	10.000	10.000	On Edge	4	18.000
59	NO-3 Time			Blk Av(2)	40.000	1.000	0.000	9000	1	0.000	10.000	Normal	1	0.000 c:\nb\data\N*
									2	10.000	10.000	On Edge	4	18.000
60	Z-NO-3b			Blk Av(1)	40.000	1.000	0.000	9000	1	0.000	10.000	Normal	1	0.000 c:\nb\data\N*
									2	10.000	10.000	On Edge	4	19.000
61	Z-NO-3b SD			Blk SD(1)	40.000	1.000	0.000	9000	1	0.000	10.000	Normal	1	0.000 c:\nb\data\N*
									2	10.000	10.000	On Edge	4	19.000
62	Z-NO-3b Time			Blk Av(2)	40.000	1.000	0.000	9000	1	0.000	10.000	Normal	1	0.000 c:\nb\data\N*
									2	10.000	10.000	On Edge	4	19.000
63	NOy-3			Blk Av(1)	20.000	1.000	0.000	9000	1	0.000	10.000	Normal	1	0.000 c:\nb\data\N*
									2	10.000	10.000	On Edge	4	20.000
64	NOy-3 SD			Blk SD(1)	20.000	1.000	0.000	9000	1	0.000	10.000	Normal	1	0.000 c:\nb\data\N*
									2	10.000	10.000	On Edge	4	20.000
65	NOy-3 Time			Blk Av(2)	20.000	1.000	0.000	9000	1	0.000	10.000	Normal	1	0.000 c:\nb\data\N*
									2	10.000	10.000	On Edge	4	20.000
66	Z-NOy-3b			Blk Av(1)	20.000	1.000	0.000	9000	1	0.000	10.000	Normal	1	0.000 c:\nb\data\N*
									2	10.000	10.000	On Edge	4	21.000
67	Z-NOy-3b SD			Blk SD(1)	20.000	1.000	0.000	9000	1	0.000	10.000	Normal	1	0.000 c:\nb\data\N*

Figure A.1 (continued) Labtech Notebook setup used during 1990.

								2	10.000	10.000	On Edge	4	21.000		
68	Z-NOy-3b Time			Blk Av(2)	20.000	1.000	0.000	9000	1	0.000	10.000	Normal	1	0.000	c:\nb\data\N*
								2	10.000	10.000	On Edge	4	21.000		
69	Z-NO-4a			Blk Av(1)	40.000	1.000	0.000	9000	1	0.000	10.000	Normal	1	0.000	c:\nb\data\N*
								2	10.000	10.000	On Edge	4	22.000		
70	Z-NO-4a SD			Blk SD(1)	40.000	1.000	0.000	9000	1	0.000	10.000	Normal	1	0.000	c:\nb\data\N*
								2	10.000	10.000	On Edge	4	22.000		
71	Z-NO-4a Time			Blk Av(2)	40.000	1.000	0.000	9000	1	0.000	10.000	Normal	1	0.000	c:\nb\data\N*
								2	10.000	10.000	On Edge	4	22.000		
72	NO-4			Blk Av(1)	40.000	1.000	0.000	9000	1	0.000	10.000	Normal	1	0.000	c:\nb\data\N*
								2	10.000	10.000	On Edge	4	23.000		
73	NO-4 SD			Blk SD(1)	40.000	1.000	0.000	9000	1	0.000	10.000	Normal	1	0.000	c:\nb\data\N*
								2	10.000	10.000	On Edge	4	23.000		
74	NO-4 Time			Blk Av(2)	40.000	1.000	0.000	9000	1	0.000	10.000	Normal	1	0.000	c:\nb\data\N*
								2	10.000	10.000	On Edge	4	23.000		
75	Z-NO-4b			Blk Av(1)	40.000	1.000	0.000	9000	1	0.000	10.000	Normal	1	0.000	c:\nb\data\N*
								2	10.000	10.000	On Edge	4	24.000		
76	Z-NO-4b SD			Blk SD(1)	40.000	1.000	0.000	9000	1	0.000	10.000	Normal	1	0.000	c:\nb\data\N*
								2	10.000	10.000	On Edge	4	24.000		
77	Z-NO-4b Time			Blk Av(2)	40.000	1.000	0.000	9000	1	0.000	10.000	Normal	1	0.000	c:\nb\data\N*
								2	10.000	10.000	On Edge	4	24.000		
78	NOy-4			Blk Av(1)	20.000	1.000	0.000	9000	1	0.000	10.000	Normal	1	0.000	c:\nb\data\N*
								2	10.000	10.000	On Edge	4	25.000		
79	NOy-4 SD			Blk SD(1)	20.000	1.000	0.000	9000	1	0.000	10.000	Normal	1	0.000	c:\nb\data\N*
								2	10.000	10.000	On Edge	4	25.000		
80	NOy-4 Time			Blk Av(2)	20.000	1.000	0.000	9000	1	0.000	10.000	Normal	1	0.000	c:\nb\data\N*
								2	10.000	10.000	On Edge	4	25.000		
81	Z-NOy-4b			Blk Av(1)	20.000	1.000	0.000	9000	1	0.000	10.000	Normal	1	0.000	c:\nb\data\N*
								2	10.000	10.000	On Edge	4	26.000		
82	Z-NOy-4b SD			Blk SD(1)	20.000	1.000	0.000	9000	1	0.000	10.000	Normal	1	0.000	c:\nb\data\N*
								2	10.000	10.000	On Edge	4	26.000		
83	Z-NOy-4b Time			Blk Av(2)	20.000	1.000	0.000	9000	1	0.000	10.000	Normal	1	0.000	c:\nb\data\N*
								2	10.000	10.000	On Edge	4	26.000		
84	Z-NO-5a			Blk Av(1)	40.000	1.000	0.000	9000	1	0.000	10.000	Normal	1	0.000	c:\nb\data\N*
								2	10.000	10.000	On Edge	4	27.000		
85	Z-NO-5a SD			Blk SD(1)	40.000	1.000	0.000	9000	1	0.000	10.000	Normal	1	0.000	c:\nb\data\N*
								2	10.000	10.000	On Edge	4	27.000		
86	Z-NO-5a Time			Blk Av(2)	40.000	1.000	0.000	9000	1	0.000	10.000	Normal	1	0.000	c:\nb\data\N*
								2	10.000	10.000	On Edge	4	27.000		
87	NO-5			Blk Av(1)	40.000	1.000	0.000	9000	1	0.000	10.000	Normal	1	0.000	c:\nb\data\N*
								2	10.000	10.000	On Edge	4	28.000		
88	NO-5 SD			Blk SD(1)	40.000	1.000	0.000	9000	1	0.000	10.000	Normal	1	0.000	c:\nb\data\N*
								2	10.000	10.000	On Edge	4	28.000		
89	NO-5 Time			Blk Av(2)	40.000	1.000	0.000	9000	1	0.000	10.000	Normal	1	0.000	c:\nb\data\N*
								2	10.000	10.000	On Edge	4	28.000		

Figure A.1 (continued) Labtech Notebook setup used during 1990.

90	Z-NO-5b			Blk Av(1)	40.000	1.000	0.000	9000	1	0.000	10.000	Normal	1	0.000 c:\nb\data\N*
									2	10.000	10.000	On Edge	4	29.000
91	Z-NO-5b SD			Blk SD(1)	40.000	1.000	0.000	9000	1	0.000	10.000	Normal	1	0.000 c:\nb\data\N*
									2	10.000	10.000	On Edge	4	29.000
92	Z-NO-5b Time			Blk Av(2)	40.000	1.000	0.000	9000	1	0.000	10.000	Normal	1	0.000 c:\nb\data\N*
									2	10.000	10.000	On Edge	4	29.000
93	NOy-5			Blk Av(1)	20.000	1.000	0.000	9000	1	0.000	10.000	Normal	1	0.000 c:\nb\data\N*
									2	10.000	10.000	On Edge	4	30.000
94	NOy-5 SD			Blk SD(1)	20.000	1.000	0.000	9000	1	0.000	10.000	Normal	1	0.000 c:\nb\data\N*
									2	10.000	10.000	On Edge	4	30.000
95	NOy-5 Time			Blk Av(2)	20.000	1.000	0.000	9000	1	0.000	10.000	Normal	1	0.000 c:\nb\data\N*
									2	10.000	10.000	On Edge	4	30.000
96	Z-NOy-5b			Blk Av(1)	20.000	1.000	0.000	9000	1	0.000	10.000	Normal	1	0.000 c:\nb\data\N*
									2	10.000	10.000	On Edge	4	31.000
97	Z-NOy-5b SD			Blk SD(1)	20.000	1.000	0.000	9000	1	0.000	10.000	Normal	1	0.000 c:\nb\data\N*
									2	10.000	10.000	On Edge	4	31.000
98	Z-NOy-5b Time			Blk Av(2)	20.000	1.000	0.000	9000	1	0.000	10.000	Normal	1	0.000 c:\nb\data\N*
									2	10.000	10.000	On Edge	4	31.000
99	Z-NO-6a			Blk Av(1)	40.000	1.000	0.000	9000	1	0.000	10.000	Normal	1	0.000 c:\nb\data\N*
									2	10.000	10.000	On Edge	4	32.000
100	Z-NO-6a SD			Blk SD(1)	40.000	1.000	0.000	9000	1	0.000	10.000	Normal	1	0.000 c:\nb\data\N*
									2	10.000	10.000	On Edge	4	32.000
101	Z-NO-6a Time			Blk Av(2)	40.000	1.000	0.000	9000	1	0.000	10.000	Normal	1	0.000 c:\nb\data\N*
									2	10.000	10.000	On Edge	4	32.000
102	NO-6			Blk Av(1)	40.000	1.000	0.000	9000	1	0.000	10.000	Normal	1	0.000 c:\nb\data\N*
									2	10.000	10.000	On Edge	4	33.000
103	NO-6 SD			Blk SD(1)	40.000	1.000	0.000	9000	1	0.000	10.000	Normal	1	0.000 c:\nb\data\N*
									2	10.000	10.000	On Edge	4	33.000
104	NO-6 Time			Blk Av(2)	40.000	1.000	0.000	9000	1	0.000	10.000	Normal	1	0.000 c:\nb\data\N*
									2	10.000	10.000	On Edge	4	33.000
105	Z-NO-6b			Blk Av(1)	40.000	1.000	0.000	9000	1	0.000	10.000	Normal	1	0.000 c:\nb\data\N*
									2	10.000	10.000	On Edge	4	34.000
106	Z-NO-6b SD			Blk SD(1)	40.000	1.000	0.000	9000	1	0.000	10.000	Normal	1	0.000 c:\nb\data\N*
									2	10.000	10.000	On Edge	4	34.000
107	Z-NO-6b Time			Blk Av(2)	40.000	1.000	0.000	9000	1	0.000	10.000	Normal	1	0.000 c:\nb\data\N*
									2	10.000	10.000	On Edge	4	34.000
108	NOy-6			Blk Av(1)	20.000	1.000	0.000	9000	1	0.000	10.000	Normal	1	0.000 c:\nb\data\N*
									2	10.000	10.000	On Edge	4	35.000
109	NOy-6 SD			Blk SD(1)	20.000	1.000	0.000	9000	1	0.000	10.000	Normal	1	0.000 c:\nb\data\N*
									2	10.000	10.000	On Edge	4	35.000
110	NOy-6 Time			Blk Av(2)	20.000	1.000	0.000	9000	1	0.000	10.000	Normal	1	0.000 c:\nb\data\N*
									2	10.000	10.000	On Edge	4	35.000
111	Z-NOy-6b			Blk Av(1)	20.000	1.000	0.000	9000	1	0.000	10.000	Normal	1	0.000 c:\nb\data\N*
									2	10.000	10.000	On Edge	4	36.000
112	Z-NOy-6b SD			Blk SD(1)	20.000	1.000	0.000	9000	1	0.000	10.000	Normal	1	0.000 c;\nb\data\N*

Figure A.1 (continued) Labtech Notebook setup used during 1990.

113	Z-NOy-6b Time			Blk Av(2)	20.000	1.000
114	Z-NO-7a			Blk Av(1)	40.000	1.000
115	Z-NO-7a SD			Blk SD(1)	40.000	1.000
116	Z-NO-7a Time			Blk Av(2)	40.000	1.000
117	NO-7			Blk Av(1)	40.000	1.000
118	NO-7 SD			Blk SD(1)	40.000	1.000
119	NO-7 Time			Blk Av(2)	40.000	1.000
120	Z-NO-7b			Blk Av(1)	40.000	1.000
121	Z-NO-7b SD			Blk SD(1)	40.000	1.000
122	Z-NO-7b Time			Blk Av(2)	40.000	1.000
123	NOy-7			Blk Av(1)	20.000	1.000
124	NOy-7 SD			Blk SD(1)	20.000	1.000
125	NOy-7 Time			Blk Av(2)	20.000	1.000
126	Z-NOy-7b			Blk Av(1)	20.000	1.000
127	Z-NOy-7b SD			Blk SD(1)	20.000	1.000
128	Z-NOy-7b Time			Blk Av(2)	20.000	1.000
129	Z-NO-8a			Blk Av(1)	40.000	1.000
130	Z-NO-8a SD			Blk SD(1)	40.000	1.000
131	Z-NO-8a Time			Blk Av(2)	40.000	1.000
132	NO-8			Blk Av(1)	40.000	1.000
133	NO-8 SD			Blk SD(1)	40.000	1.000
134	NO-8 Time			Blk Av(2)	40.000	1.000

Figure A.1 (continued) Labtech Notebook setup used during 1990.

	2	10.000	10.000	On Edge	4	36.000	
0.000	9000	1	0.000	10.000	Normal	1	0.000	c:\nb\data\N*
	2	10.000	10.000	On Edge	4	36.000	
0.000	9000	1	0.000	10.000	Normal	1	0.000	c:\nb\data\N*
	2	10.000	10.000	On Edge	4	37.000	
0.000	9000	1	0.000	10.000	Normal	1	0.000	c:\nb\data\N*
	2	10.000	10.000	On Edge	4	37.000	
0.000	9000	1	0.000	10.000	Normal	1	0.000	c:\nb\data\N*
	2	10.000	10.000	On Edge	4	37.000	
0.000	9000	1	0.000	10.000	Normal	1	0.000	c:\nb\data\N*
	2	10.000	10.000	On Edge	4	38.000	
0.000	9000	1	0.000	10.000	Normal	1	0.000	c:\nb\data\N*
	2	10.000	10.000	On Edge	4	38.000	
0.000	9000	1	0.000	10.000	Normal	1	0.000	c:\nb\data\N*
	2	10.000	10.000	On Edge	4	38.000	
0.000	9000	1	0.000	10.000	Normal	1	0.000	c:\nb\data\N*
	2	10.000	10.000	On Edge	4	39.000	
0.000	9000	1	0.000	10.000	Normal	1	0.000	c:\nb\data\N*
	2	10.000	10.000	On Edge	4	39.000	
0.000	9000	1	0.000	10.000	Normal	1	0.000	c:\nb\data\N*
	2	10.000	10.000	On Edge	4	39.000	
0.000	9000	1	0.000	10.000	Normal	1	0.000	c:\nb\data\N*
	2	10.000	10.000	On Edge	4	40.000	
0.000	9000	1	0.000	10.000	Normal	1	0.000	c:\nb\data\N*
	2	10.000	10.000	On Edge	4	40.000	
0.000	9000	1	0.000	10.000	Normal	1	0.000	c:\nb\data\N*
	2	10.000	10.000	On Edge	4	40.000	
0.000	9000	1	0.000	10.000	Normal	1	0.000	c:\nb\data\N*
	2	10.000	10.000	On Edge	4	41.000	
0.000	9000	1	0.000	10.000	Normal	1	0.000	c:\nb\data\N*
	2	10.000	10.000	On Edge	4	41.000	
0.000	9000	1	0.000	10.000	Normal	1	0.000	c:\nb\data\N*
	2	10.000	10.000	On Edge	4	41.000	
0.000	9000	1	0.000	10.000	Normal	1	0.000	c:\nb\data\N*
	2	10.000	10.000	On Edge	4	42.000	
0.000	9000	1	0.000	10.000	Normal	1	0.000	c:\nb\data\N*
	2	10.000	10.000	On Edge	4	42.000	
0.000	9000	1	0.000	10.000	Normal	1	0.000	c:\nb\data\N*
	2	10.000	10.000	On Edge	4	42.000	
0.000	9000	1	0.000	10.000	Normal	1	0.000	c:\nb\data\N*
	2	10.000	10.000	On Edge	4	43.000	
0.000	9000	1	0.000	10.000	Normal	1	0.000	c:\nb\data\N*
	2	10.000	10.000	On Edge	4	43.000	
0.000	9000	1	0.000	10.000	Normal	1	0.000	c:\nb\data\N*
	2	10.000	10.000	On Edge	4	43.000	

135	Z-NO-8b			Blk Av(1)	40.000	1.000	0.000	9000	1	0.000	10.000	Normal	1	0.000	c:\nb\data\N*	
									2	10.000	10.000	On Edge	4	44.000		
136	Z-NO-8b SD			Blk SD(1)	40.000	1.000	0.000	9000	1	0.000	10.000	Normal	1	0.000	c:\nb\data\N*	
									2	10.000	10.000	On Edge	4	44.000		
137	Z-NO-8b Time			Blk Av(2)	40.000	1.000	0.000	9000	1	0.000	10.000	Normal	1	0.000	c:\nb\data\N*	
									2	10.000	10.000	On Edge	4	44.000		
138	NOy-8			Blk Av(1)	20.000	1.000	0.000	9000	1	0.000	10.000	Normal	1	0.000	c:\nb\data\N*	
									2	10.000	10.000	On Edge	4	45.000		
139	NOy-8 SD			Blk SD(1)	20.000	1.000	0.000	9000	1	0.000	10.000	Normal	1	0.000	c:\nb\data\N*	
									2	10.000	10.000	On Edge	4	45.000		
140	NOy-8 Time			Blk Av(2)	20.000	1.000	0.000	9000	1	0.000	10.000	Normal	1	0.000	c:\nb\data\N*	
									2	10.000	10.000	On Edge	4	45.000		
141	Z-NOy-8b			Blk Av(1)	20.000	1.000	0.000	9000	1	0.000	10.000	Normal	1	0.000	c:\nb\data\N*	
									2	10.000	10.000	On Edge	4	1.000		
142	Z-NOy-8b SD			Blk SD(1)	20.000	1.000	0.000	9000	1	0.000	10.000	Normal	1	0.000	c:\nb\data\N*	
									2	10.000	10.000	On Edge	4	1.000		
143	Z-NOy-8b Time			Blk Av(2)	20.000	1.000	0.000	9000	1	0.000	10.000	Normal	1	0.000	c:\nb\data\N*	
									2	10.000	10.000	On Edge	4	1.000		
144	Time (1/data)			(2)	1.000	1.000	0.000	9000	1	0.000	10.000	Normal	1	0.000		
									2	10.000	10.000	On Edge	4	1.000		
145	NO/C Delt cps			(15)-(12)	1.000	1.000	0.000	9000	1	0.000	10.000	Normal	1	0.000		
									2	10.000	10.000	On Edge	4	1.000		
146	NO/C/Z Delt cps			(21)-(24)	1.000	1.000	0.000	9000	1	0.000	10.000	Normal	1	0.000		
									2	10.000	10.000	On Edge	4	1.000		
147	NO2 Created			(15)-(9)	1.000	1.000	0.000	9000	1	0.000	10.000	Normal	1	0.000		
									2	10.000	10.000	On Edge	4	1.000		
148	NO2 not Found			(18)-(6)	1.000	1.000	0.000	9000	1	0.000	10.000	Normal	1	0.000		
									2	10.000	10.000	On Edge	4	1.000		
149	Sens.			(145)	10.000	4.17E-05	0.000	9000	1	0.000	10.000	Normal	1	0.000		3
									2	10.000	10.000	On Edge	4	1.000		
150	NO2 Conv. Eff.			(148)/(147)	1.000	-100.000	-1.000	9000	1	0.000	10.000	Normal	1	0.000		3
									2	10.000	10.000	On Edge	4	1.000		
151	Perc. Zeroed			(146)/(145)	1.000	-100.000	-1.000	9000	1	0.000	10.000	Normal	1	0.000		3
									2	10.000	10.000	On Edge	4	1.000		
152	NO-1 Delt. cps			(27)-(24)	1.000	1.000	0.000	9000	1	0.000	10.000	Normal	1	0.000		
									2	10.000	10.000	On Edge	4	1.000		
153	NOy-1 Delt. cps			(33)-(36)	1.000	1.000	0.000	9000	1	0.000	10.000	Normal	1	0.000		
									2	10.000	10.000	On Edge	4	1.000		
154	NO-1 ppt			(152)/(149)	1.000	1.000	0.000	9000	1	0.000	10.000	Normal	1	0.000		2
									2	10.000	10.000	On Edge	4	1.000		
155	NOy-1 ppt			(153)/(149)	1.000	1.000	0.000	9000	1	0.000	10.000	Normal	1	0.000		2
									2	10.000	10.000	On Edge	4	1.000		
156	Cal MFC	1	0	Analog In	0..1 V	10.000	0.000	9000	1	0.000	10.000	Normal	1	0.000		
									2	10.000	10.000	On Edge	4	1.000		
157	MFC-2 V	1	1	Analog In	0..1 V	2.000	0.000	9000	1	0.000	10.000	Normal	1	0.000		

Figure A.1 (continued) Labtech Notebook setup used during 1990.

```
   |              |  |   |           |        |        |        |  |2|  10.000|  10.000| On Edge|  4|   1.000|              |
 158|     GC Trigger| 1|  2|  Analog In|  0..1 V|   1.000|   0.000|  1|1|3.10E+07|   1.000|  Normal|  1|   0.000|              |
 159|       GC Volts| 1|  3|  Analog In|  0..1 V|   1.000|   0.000|  1|1|3.10E+07|   1.000|  Normal|  1|   0.000|              |
-------------------------------------------------------------------------------------------------------------------------------------

Setup OK
Interface Devices:
  0: DEMO BOARD
  1: Dash-16
```

Figure A.1 (continued) Labtech Notebook setup used during 1990.

Appendix B

Data Analysis Program Used With the 1990 Measurements

The FORTRAN program used to analyze the data obtained during the 1990 measurement period is listed beginning on the next page.

Data Analysis Program

```
************************************************************************
************************************************************************
************************ MODULE ANALYZE.FOR ************************
************************************************************************
      PROGRAM ANALYZE
************************************************************************
*                QUASI-INTERACTIVE NO/NOy DATA ANALYZER
*
* designed by              Richard Honrath      Jan. 1990
* written by               Randy Meitner and    January-March, 1990.
*                          Richard Honrath
*
* PURPOSE: To analyze data taken by the UAF NO/NOy monitor
*          running at Barrow during 1990 (+?).
*          The program allows calculation of calibration and concentration
*          info., plotting, and saving of ASCII calibration and conc. files.
*
* SUBROUTINES in this file:
*          SAVE,LOAD,CALC,PRGM,DISP,HELP,QUIT,
*          NITNO
*
* COMPILED                         NOTES
*   version 1.01  Mid March, 1990.          FIRST RUNNING VERSION
*           2.01  Mid March, 1990.      Included max/min mean checking in
*                                       RSDOK. The arrays needed to store
*                                       acceptable max/min created a little
*                                       incompatability w/ old .PGM files.
*                 Spring, 1990.         Added plotting routine.
*           2.02  June, 1990.           Added main routine to calculate
*                                       nighttime NO average values
*           3.01  October, 1990.        Added radmax value for maximum absolute
*                                       running average of conv. eff. for
*                                       data correction
*
*
*
*
*          PROGRAM COMMANDS: SAVE,LOAD,CALC,HELP,DISP,QUIT,PRGM,PLOT
* ASSOCIATED FILES CONTAIN VALUABLE SUBROUTINES AND INFORMATION:
*      GlobalVar.def   variables used time and again.
*      Parameters.def  indices and global parameters.
*      Flags.def       bookkeeping flags.
*      con'var.def     variables used for concentration calculations
*      cal'var.def     variables used for calibration calculations
*      cps'var.def     variables used for count-per-second display
*      ANAFILE         file gets and puts.
*      ANACONCEN       calculates concentrations
*      ANACALIB        calculates calibrations
*      ANALIB          misc. subroutine library
*      ANAUTIL         misc. subroutines for ASCII data output, etc.
*      ANAPLOT         plotting routines (not included in this printout)
************************************************************************
      include 'GlobalVar.def'
      include 'cal'var.def'
      include 'con'var.def'
      include 'Flags.def'
      character*60 header,time,date,fil,param,ArtFil
      logical BadCom,there
      character*4  comand,object
      call StartUp
10    BadCom=.true.                  !Get the command.  If no known
      call bell
      write(*,11)                    !command is entered in, call for help.
11    format('$Enter command: ')
      read 9,comand,object,param
9     format (a4,a4,a60)
      param=param(2:60)//' '
      if (comand.eq.'LOAD') then
        call load(Object,Param,Date,Time,Frczrd,Sens,CnvEff,NEWNO2,
     1    NoySen,Zero,ConNO,ConNOy,ConNit,fil,header,ArtFil)
        BadCom=.false.
        print *,' '
      elseif (comand.eq.'SAVE') then
        call save(Object,Param,Date,Time,Frczrd,Sens,CnvEff,NEWNO2,
     1      NoySen,Zero,ConNO,ConNOy,ConNit,fil,header,ArtFil)
        BadCom=.false.
        print *,' '
      elseif (comand.eq.'CALC') then
        call calc(object,param,date,time,ConNO,ConNOy,ConNit,
     1      FrcZrd,Sens,CnvEff,NOySen,NEWNO2,Zero,ArtFil)
        BadCom=.false.
        print *,' '
      elseif (comand.eq.'PLOT') then
        call plot(object,param,fil,Date,FrcZrd,Sens,CnvEff,NewNO2,
     1      NOySen,Zero,ConNO,ConNOy,ConNit)
        BadCom=.false.
        print *,' '
      elseif (comand.eq.'DISP') then
        call disp(object,fil,header,date,time,ConNO,ConNOy,ConNit,
     1 FrcZrd,Sens,CnvEff,NOySen,Zero,NEWNO2,ArtFil)
        BadCom=.false.
        print *,' '
      elseif (comand.eq.'SUMM') then
      call Summ(fil,header,date,time,conno,connoy,ConNit,
     1 FrcZrd,sens,cnveff,noysen,zero,newno2,ArtFil)
      badcom=.false.
      print*,' '
      elseif (comand.eq.'QUIT') then
        call quit
        BadCom=.false.
        print *,' '
      elseif (comand.eq.'PRGM') then
        call Prgm
        BadCom=.false.
        print *,' '
      else if (comand.eq.'UTIL') then
      call UTil(Date,Time,FrcZrd,Sens,CnvEff,NewNO2,
     1          NOySen,Zero,ConNO,ConNOy,ConNit,fil,header)
      BadCom=.false.
      print*,' '
      endif
** ANY NEW COMMANDS ADDED MUST GO BEFORE THIS POINT, OTHERWISE, THEY
** WILL GENERATE A HELP MESSAGE EACH TIME THEY ARE CALLED (BadCom must
** be set before the following if statement.).
      if ((comand.eq.'HELP').or.(BadCom)) then
        call help
      endif
      goto 10
      end
************************************************************************
** saves either .CAL, .CON, .PGM, or all of them, or .DAT.
** external calls PutCal, PutCon, PutPgm, PutRaw (analile).
** success will set the svd flags true so the program knows that
** the files have been saved.
** inputs
**   obj,param          tell the command
**   date,time,header,fil  hold misc. storage info.
**   FrcZrd,Sens,CnvEff,NewNO2,NOySen,Zero,ConNO,ConNOy
**                      the stuff stored in files
** outputs
**   calsvd,consvd,pgmsvd  flags to help the program remember what
**                         the heck it's doing.
** calls
**   PutPgm, PutRaw, PutCon, PutCal (external: ANAFILE)
************************************************************************
      subroutine save(Obj,Param,Date,Time,Frczrd,Sens,CnvEff,NEWNO2,
     1          NoySen,Zero,ConNO,ConNOy,ConNit,fil,header,ArtFil)
      include 'globalvar.def'
      include 'cal'var.def'
      include 'con'var.def'
      INCLUDE 'FLAGS.DEF'
      character*4, obj
      integer a
      character*60,param,fil,Header,Date,Time,ArtFil
      logical all,puttad,there
      all = (Obj.eq.' ALL')
      if (fil(1:8).eq.'        ') fil=param
       if ((obj.eq.' PGM').or.(all)) then
       print*,'Saving PGM for ',fil
         call PutPgm(fil,header)
         print *,'.PGM file saved.'
       endif
       if ((obj.eq.' CAL').or.(all)) then
         if (caldne) then
         print*,'Saving CAL for ',fil
           call PutCal(fil,header,date,time,frczrd,
     1               sens,cnveff,NEWNO2,noysen,zero)
         print *,'.CAL file saved.'
        else
         print *,'You need to CALC CAL before saving .CAL!'
        endif
       endif
       if ((obj.eq.' CON').or.(all)) then
        if (condne) then
        print*,'Saving CON for ',fil
          call PutCon(fil,header,date,time,ConNo,ConNoy,ArtFil)
          print *,'.CON file saved.'
        else
          print *,'You need to CALC CON before saving .CON!'
        endif
       endif
      if ((obj.eq.' NIT').or.(all)) then
       if (nitdne) then
          print*,'Saving NIT for ',fil
          Call PutNit(param,header,data,time,ConNit)
           print*,'.NIT file saved.'
            else
          print*,'You must CALC NIT first!'
          endif
        endif
      if (obj.eq.' RAW') then
       if (rawLdd) then
         print*,'Saving RAW for ',fil
         Call PutRaw(Header,Date,Time,lines,FIL)
         else
         print*,'You must LOAD RAW first!'
         endif
       endif
       if (all) print *,'We've all been saved! (** except RAW **)'
       if (.not.(all)) print *,'Done saving.'
      return
      end
************************************************************************
** Loads either .DAT, .CAL, .CON, .PGM, or all of them.
** A successful load will set the dne flags true, and analysis
** can continue as if raw had been loaded and the operations had already
** been done.  For example, a successful LOAD CAL will set caldne=.true.
** and CALC CON can be done immediately after.
** inputs
**   obj,param,fil        tells the procedure what to do and what
```

Data Analysis Program (continued: page 2)

```
**                    file to use
** outputs
**  date,time,frczrd,sens,cnveff,newno2,noysen,zero,conno,connoy
**                    these are the data returned
**  rawldd,caldne,condne  flags to help the program remember itself
**  fil                 if a different filename is loaded, this is it
**  date, time, hdr     misc. non-data file parameters
** calls
**  GetRaw,GetCon,GetCal,GetCon (external ANAFILE)
**
*************************************************************************
      subroutine load(Obj,Param,Date,Time,Frczrd,Sens,CnvEff,NEWNO2,
     1    NoySen,Zero,ConNO,ConNOy,ConNit,fil,header,ArtFil)
      include 'globalvar.def'
      include 'cal'var.def'
      include 'con'var.def'
      include 'cps'var.def'
      include 'flags.def'
      character*4, obj
      character*60,param,fil,fcps,date,time,header,ArtFil
      logical all
        print *,'Loading...'
        all = (obj.eq.' ALL')
        if (param.ne.' ') fil=param
        if ((obj.eq.' RAW').or.(all)) then
          call GetRaw(Header,date,time,lines,fil)
          print *,'Raw loaded.'
        if (RawLdd) THEN
            caldne=.FALSE.
            condne=.FALSE.
            calsvd=.FALSE.
            consvd=.FALSE.
            ELSE
            print*,'Error loading raw data.  Raw NOT LOADED.'
            ENDIF
          print 8,lines
8         format (' Done.',i4,' lines of data loaded.')
        endif
      IF (obj.eq.' CPS') then
        Call GetCPS(fil,fcps,cps5,Ndat)
        print*,' CPS file loaded.  ',
     1      'This is only for conversion to bin.'
        endif
        if ((obj.eq.' PGM').or.(all)) then
          call GetPgm(fil,header)
          print *,'.PGM loaded.'
          if (.not.(all)) then
            print *,'Calculations no longer valid.'
            print *,'You'll have to re-calculate.'
            caldne=.false.
            condne=.false.
          endif
        endif
        if ((obj.eq.' CAL').or.(all)) then
          call GetCal(fil,header,date,time,
     1    frczrd,sens,cnveff,NEWNO2,noysen,zero)
          if (caldne) print *,'.CAL loaded.'
        endif
        if ((obj.eq.' CON').or.(all)) then
          call GetCon(fil,header,date,time,ConNo,ConNoy,ArtFil)
          if (condne) print *,'.CON loaded.'
        endif
      IF (obj.eq.' NIT') THEN
        Call GetNit(Param,ConNit)
        if (NitDne) print*,'.NIT loaded.'
        endif
      return
      end
*************************************************************************
** calculates the data if the appriate flags are true:
** nothing can be done if RawLdd is false,
** CALC CON cannot be done if CalDne is false.
** Note that CALC ALL will work since calibrations are done before
** concentrations so that by the time concerations is reached,
** CalDne will be true.
** inputs
**  object,param   tell which calculations to do
** outputs
**  conNO,conNOy,FrcZrd,Sens,CnvEff,NOySen,newNO2,Zero,ConNIT
**                 the data calculated by various subroutines
**  CalDne,ConDne,NitDne  flags that say stuff has been calculated.
** calls
**  CalCal,CalCon,CalNit  let the program know it has done these.
*************************************************************************
      subroutine calc(object,param,date,time,ConNO,ConNOy,ConNit,
     1      FrcZrd,Sens,CnvEff,NOySen,NEWNO2,Zero,ArtFil)
        character*4,  object
        character*60, param,date,time,ArtFil
        logical all
        include 'GlobalVar.def'
      include 'cal'var.def'
      include 'con'var.def'
        include 'Flags.def'
        all = (object.eq.' ALL')
      if (all) then
        print*,'Calculating calibration ...'
          call CalCal(FrcZrd,Sens,CnvEff,NOySen,NEWNO2,Zero)
        CalDne=.true.
        print*,'Calculating concentrations ...'
          call CalCon(ConNO,ConNOy,Zero,FrcZrd,
     1    Sens,NOySen,CnvEff)
          condne=.true.
        ArtDne=.false.
        print',Calculating nighttime NO statistics ...'
        Call CalNit(date,time,ConNit,ConNO,Zero,Sens)
        NitDne=.true.
      else if (object.eq.' CAL') then
        if (rawldd) then
          print *,'Calculating calibration data...'
          call CalCal(FrcZrd,Sens,CnvEff,NOySen,NEWNO2,Zero)
          caldne =.true.
        else
          print *,'You need to load a raw file first!'
        endif
      else if (object.eq.' CON') then
        if ((rawldd).and.(caldne)) then
          print *,'Calculating concentration data...'
          call CalCon(ConNO,ConNOy,Zero,FrcZrd,
     1    Sens,NOySen,CnvEff)
          condne =.true.
        ArtDne =.false.
        else
          if (.not.rawldd) print *,'You need to load raw first!'
          if (.not.caldne) print *,'You need to calculate',
     +                    ' calibrations first!'
        endif
      else IF (object.eq.' NIT') then
        if ((caldne).and.(condne)) then
          print',Calculating nighttime NO statistics...'
          Call CalNit(date,time,ConNit,ConNO,Zero,Sens)
          nitdne=.true.
          else
          print*,'You must CALC CAL and CALC CON ',
     1          'or CALC ALL before CALC NITE!'
        ENDIF
      else if (object.eq.' ART') then
        if (condne) then
          Call CalArt(ConNO,ConNOy,ArtFil)
          else
          print*,'You must CALC CON first.'
          ENDIF
      else
      print*,'Use CALC CAL or CALC CON or CALC NIT or CALC ART or ',
     1    'CALC ALL.'
      endif
      return
      end
*************************************************************************
** Modify the programmable constants.
** This includes the following:
**  UseNOy, Navg, NumAve, Ccg, RSDMax
** Note that calling PRGM clears all the dne and svd flags since entering new
**  programmables implies the old data is no longer valid!
*************************************************************************
      subroutine Prgm
       include 'GlobalVar.def'
       include 'Flags.def'
       integer i,j,k,l,fstspc,sndspc
       character*60 s,param,lil,hdr
       logical all,there
         CalDne =.false.
         ConDne =.false.
         DisDne =.false.
         CalSvd =.false.
         ConSvd =.false.
         PgmSvd =.false.
       ArtDne =.false.
      print *,'The following things will be asked for:'
      print *,'  Whether to use NOy or NO sensitivity for [NOy] calc,'
      print *,'  The number how many values to use in various averages,'
      print *,'  Calibration gas constant,'
      print *,'  RSD maximums,'
      print *,'  acceptable ranges for using certain numbers,'
      print*,'  The maximum SD used for interpolated nighttime ',
     1    'NO satisfacts,'
      print *,'  and the number of counts used in each mode.'
        if (UseNoy) then
          print *,'Currently using NOy Sens to find [NOy].'
        else
          print *,'Currently using NO Sens to find [NOy].'
        endif
       IF (GetYN('Switch (NO -¿ NOy or NOy -¿ NO)? ','N')) THEN
          print *,'Now using '
          UseNOy=(.not.UseNOy)
          if (useNoy) then
            print *,'NOy.'
          else
            print *,'NO.'
          endif
        endif
        print 2,'Fraction zeroed',numave(ifzd)
        print 48,' '
        read *,NumAve(iFzd)
        print 2,'Conversion eff.',numave(icvef)
        print 48,' '
        read *,NumAve(iCvEf)
2       format (1x,a15,' uses ',i4,' values for each average.')
8       format (1x,a11,' used',i4,' values/running average.')
        print 18,ccg
        print 48,' '
```

Data Analysis Program (continued: page 3)

```
      read *,ccg
18    format (1x,'[Cal. Gas] (ppt) =',F8.2,'.')
      print 28,'Sens.',rsdmax(iSens)
      print 48,' '
      read *,rsdmax(iSens)
      print 28,'FrZd',rsdmax(iFzd)
      print 48,' '
      read *,rsdmax(iFzd)
      print 28,'NOySen',rsdmax(iySen)
      print 48,' '
      read *,rsdmax(iySen)
      print 28,'CnvEff',rsdmax(iCvEf)
      print 48,' '
      read *,rsdmax(iCvEf)
      print 28,'Zero',rsdmax(iZro)
      print 48,' '
      read *,rsdmax(iZro)
      print 28,'NO nighttime measurements for stat calcs',
     1    RSDMax(iCNit)
      print 48,' '
      read*,RsdMax(iCNit)
      print 28,'Avg NO nighttime conc. for artifact correction',
     1    RsdMax(iNit)
      print 48,' '
      read*,RsdMax(iNit)
      print*,'Enter maximum SD acceptable for running-avg conv.',
     1      'eff.: '
      print*,'Current value is ',rsdmax(iCvSd)
      read*,rsdmax(iCvSd)
      print *,'Now, the enter the mean ranges...'
      print 68,'Sens.',minmn(iSens)
      print 48,' '
      read *,minmn(iSens)
      print 58,'Sens.',maxmn(iSens)
      print 48,' '
      read *,maxmn(iSens)
      print 68,'FrZd',MinMn(iFzd)
      print 48,' '
      read *,MinMn(iFzd)
      print 58,'FrZd',MaxMn(iFzd)
      print 48,' '
      read *,MaxMn(iFzd)
      print 68,'NOySen',MinMn(iySen)
      print 48,' '
      read *,MinMn(iySen)
      print 58,'NOySen',MaxMn(iySen)
      print 48,' '
      read *,MaxMn(iySen)
      print 68,'CnvEff',MinMn(iCvEf)
      print 48,' '
      read *,MinMn(iCvEf)
      print 58,'CnvEff',MaxMn(iCvEf)
      print 48,' '
      read *,MaxMn(iCvEf)
      print 68,'Zero',MinMn(iZro)
      print 48,' '
      read *,MinMn(iZro)
      print 58,'Zero',MaxMn(iZro)
      print 48,' '
      read *,MaxMn(iZro)
28    format (1x,'Old RSD Max for ',a6,' was',F8.2,'.')
58    format (1x,'Old max mean for ',a6,' was',f8.2,'.')
68    format (1x,'Old min mean for ',a6,' was',f8.2,'.')
    write(*,69)
69    format('$Enter the minimum SD used for interp. art obs: ')
    read*,SArMin
      do 10,i=1,modes
        print 38,i,navg(i)
        print 48,' '
        read*,navg(i)
10    continue
38    format (1x,'Mode ',i4,' is set for ',i4,' counts.')
48    format (1x,'Enter new value.',a1)
** Have new values.  Now, need to save them in the default startup pgm file
**  if desired
    if (GetYN(
    1 'Enter Y to save the pgm constants in the default startup file ',
    1 'Y')) then
    hdr = ' DEFAULT PROGRAMMABLE CONSTANTS'
      inquire(file='START.CNF',exist=there)          !check to see if
      if (there) then                                !start.cnf and
        open(unit=15,file='START.CNF',status='OLD')   !startup .pgm files
        read(15,9),fil
9       format(a60)
        close(15)
      Call PutPgm(fil,pgmsvd,Hdr)
      else
      print*,'file START.CNF does not exist.  You must SAVE PGM!!'
      ENDIF
    endif
    return
     end
*****************************************************************************
** Subroutine Plot -- is contained in file ANAPLOT.FOR
*****************************************************************************
*****************************************************************************
**Dumps just about any kind of information to the screen.
** does not in any way affect anything.
*****************************************************************************
    subroutine disp(obj,fil,header,date,time,conNO,conNOy,ConNit,
    1 FrcZrd,Sens,CnvEff,NoySen,Zero,NEWNO2,ArtFil)
    include 'globalvar.def'
    include 'cal var.def'
    include 'con var.def'
    include 'flags.def'
    character*60 fil,ArtFil
    character*4 obj
    integer i,j
    real minNO2,maxNO2,mincon,maxcon,minNyS,maxNyS,minFrz,maxFrz,
    1     MinSen,MaxSen,minNO2,maxNO2,minCon,MaxCon,MinNys,
    1     MaxNys,MinFrz,MaxFrz,minSen,MaxSen
    character*60 fname,header,date,time
    logical all
      all=(obj.eq.' ALL')
      if ((all).or.(obj.eq.' FIL')) then
        print *,'Current filename is ',fil(1:filcat(fil)),'.'
      if ((all).or.(obj.eq.' VER')) then
        print 4,pgmver
4       format (' VERSION ',f4.2)
      endif
        if (rawldd) then
          print *,'Raw file loaded.'
        else
          print *,'Raw file NOT loaded.'
        endif
        if (pgmsvd) then
          print *,'.PGM is saved.'
        else
          print *,'.PGM is NOT saved.'
        endif
        if (calsvd) then
          print *,'.CAL is saved.'
        else
          print *,'.CAL is NOT saved.'
        endif
        if (consvd) then
          print *,'.CON is saved.'
        else
          print *,'.CON is NOT saved.'
        endif
      if (ArtDne) then
        print*,'Artifact correction done.'
        else
        print*,'Artifact correction NOT done.'
        endif
      endif
      if ((all).or.(obj.eq.' RAW')) then
      if (rawldd) then
        print *,' '
        print *,' Raw file is: ',fil
        print *,' Heaer line: ',header
        print *,' Date:       ',date
        print *,' Time:       ',time
        print 6,tstart
6       format (1X,'Julian time is ',f10.4' days.')
        print 8,lines
8       format (1x,'It contains:',i4,' lines of data.')
        print *,' '
        if (GetYN('List the data? ','N')) then
          do 10,i=1,lines
          print *,' '
          print *,' '
          do 10,j=1,modes,8
          print *,' '
          print*,'Line    Mode    Mode    Mode    Mode',
     1 '    Mode    Mode    Mode    Mode'
          if ((j+7).lt.modes) then
            print 38,i,(i1,i1=j,j+7)
            print 48,(raw(i,i1,1),i1=j,j+7)
            print 58,(raw(i,i1,2),i1=j,j+7)
            print 68,(raw(i,i1,3),i1=j,j+7)
          else
            print 38,i,(i1,i1=j,modes)
            print 48,(raw(i,i1,1),i1=j,modes)
            print 58,(raw(i,i1,2),i1=j,modes)
            print 68,(raw(i,i1,3),i1=j,modes)
          endif
38        format (1x,11(i4,5x))
48        format (1x,'MEAN:',8f9.1)
58        format (1x,'  SD:',8f9.1)
68        format (1x,'TIME:',8f9.1)
10        continue
        endif
        else
          print *,'Raw data must be loaded first!'
      endif
      endif
       if ((all).or.(obj.eq.' CAL')) then
       if (caldne) then
         print *,' '
*** Display ranges of cal values ...
***  Range of "real" values is currently set by MaxMn and MinMn
       mrsen=MinMn(iSens)
       marsen=MaxMn(iSens)
       mirfrz=MinMn(iFzd)
       marfrz=MaxMn(iFzd)
       mirnys=MinMn(iySen)
       marnys=MaxMn(iySen)
       mircon=MinMn(iCvEf)
       marcon=MaxMn(iCvEf)
```

Data Analysis Program (continued: page 4)

```
      mimo2=0.0
      mamo2=1.5*24000.
      Tmin=CnvEff(1,3)
      Tmax=FrcZrd(lines,3)
      minsen=marsen
      minfrz=marfrz
      minnys=marnys
      mincon=marcon
      minno2=marno2
      maxsen=mrsen
      maxfrz=mirfrz
      maxnys=mirnys
      maxcon=mircon
      maxno2=mirno2
      do 19 i=1,lines
        IF (sens(i,1).ge.mrsen)
     1        minsen=MIN(minsen,sens(i,1))
        if (sens(i,1).le.marsen)
     1        maxsen=MAX(maxsen,sens(i,1))
        if (FrcZrd(i,1).ge.mirfrz)
     1        minfrz=MIN(MINFRz,FrcZrd(i,1))
        if (FrcZrd(i,1).le.marfrz)
     1        maxfrz=MAX(maxfrz,frczrd(i,1))
        if (noysen(i,1).ge.mirnys)
     1        minnys=MIN(minnys,noysen(i,1))
        if (noysen(i,1).le.marnys)
     1        maxnys=MAX(maxnys,noysen(i,1))
        if (cnvelf(i,1).ge.mircon)
     1        mincon=MIN(mincon,cnvelf(i,1))
        if (cnvelf(i,1).le.marcon)
     1        maxcon=MAX(maxcon,cnvelf(i,1))
        if (newno2(i,1).ge.mirno2)
     1        minno2=MIN(minno2,newno2(i,1))
        if (newno2(i,1).le.marno2)
     1        maxno2=MAX(maxno2,newno2(i,1))
19      continue
      print 75, '..........',' MIN  ',' MAX  '
      print 76, 'Sens',minsen,maxsen
      print 76, '% Zero',minfrz,maxfrz
      print 76, 'NOy Sens',minnys,maxnys
      print 76, 'Conv Eff',mincon,maxcon
      print 76, 'NO2 Created',minno2,maxno2
      print 76,' Time    ',tmin,tmax
      print*,' '
      if (GetYN(
     2'Enter Y/N for display of individual values for each line. ',
     1'N')) then
75      format(A12,2A12)
76      format(A12,2F12.4)
        do 20,i=1,lines
          print 78,i
      print*,'      Frac. Zeroed   Sens.   NOy Sens.',
     1' Conv. Eff.  NO created'
          print 88,'MEAN',frczrd(i,1),sens(i,1),
     1 noysen(i,1),cnvelf(i,1),NEWNO2(i,1)
78      format (1x,'LINE: ',i4)
88      format (1x,a4,':',F10.2,4(3x,f10.2))
          print 88,'  SD',frczrd(i,2),sens(i,2),
     1 noysen(i,2),cnvelf(i,2),NEWNO2(i,2)
          print 88,'TIME',frczrd(i,3),sens(i,3),
     1 noysen(i,3),cnvelf(i,3),NEWNO2(i,3)
          print 88,'SCNT',frczrd(i,4),sens(i,4),
     1 noysen(i,4),cnvelf(i,4),NEWNO2(i,4)
          print*,' '
20      continue
      endif
      else
       print *,'Calibrations must be calculated first!'
      endif
      endif
      if ((all).or.(obj.eq.' PGM')) then
        if (useNOy) then
          print *,'Calculates [NOy] based on NOy Sens.'
        else
          print *,'Calculates [NOy] based on NO Sens.'
        endif
        print 98,'Fraction zeroed',numave(ifzd)
        print 98,'Conversion eff.',numave(icvef)
98        format (1x,a15,' uses ',i4,' values for each average.')
        print 108,ccg
108       format (1x,'Old [Cal. Gas] was',F8.2,'.')
        print 128,'Sens.',rsdmax(iSens)
        print 128,'FrZd',rsdmax(iFzd)
        print 128,'NOySen',rsdmax(iySen)
        print 128,'CnvEff',rsdmax(iCvEf)
        print 128,'Zero',rsdmax(iZro)
        print 128,'Zenith',rsdmax(iCNit)
        print 128,'Nighttime NO',rsdmax(iNit)
        print 128,'Max SD of Run. Avg. Cnv Eff',rsdmax(iCvSD)
        print 127,'Sens.',minmn(iSens),maxmn(isens)
        print 127,'FrZd',minmn(iFzd),maxmn(ifzd)
        print 127,'NOySen',minmn(iySen),maxmn(iysen)
        print 127,'CnvEff',minmn(iCvEf),maxmn(icvef)
        print 127,'Zero',minmn(iZro),maxmn(izro)
128       format (1x,'RSD Max for ',a5,' is',F8.2,'.')
127       format (1x,'Average range for ',a5,' is',f8.2,' (min) to ',
     1          f8.2,' (max).')
        print*,'Number of seconds averaged in each mode: '
        print 147, (i,j=1,6)
        print 138, (navg(i),i=1,6)
        do 30,j=7,modes,5
         print 148, (i+j,j=0,4)
         print 138, (navg(i+j),j=0,4)
30      continue
138     format(1x,i4,6(7x,i4))
147       FORMAT(1X,6('Mode',i3,4x))
148     format(1x,5('Mode',i3,4x))
      endif
** print [NO]
** note 1,2,3,4 are used here rather than imean,isd,itime,iscnt.
      if ((all).or.(obj.eq.' CON')) then
      if (ArtDne) then
       write(*,301)ArtFil
301         format(1x,'Artifact correction has been applied, using ',
     1    'data ',/,10x,'from file ',A60)
       else
       print*,'Artifact correcton NOT applied.'
       endif
      IF (GetYN('Enter Y to display all NO and NOy concns: ','N'))
     1   THEN
        do 300 i=1,lines
          print 158,i
          print *,'        Take 1   Take 2   Take 3',
     +'  Take 4   Take 5   Take 6   Take 7   Take 8'
          print 168,(conno(i,j,1),j=1,8)
          print 178,(conno(i,j,2),j=1,8)
          print 188,(conno(i,j,3),j=1,8)
          print 198,(conno(i,j,4),j=1,8)
** print [NOy]
          print 208,i
          print *,'        Take 1   Take 2   Take 3',
     +'  Take 4   Take 5   Take 6   Take 7   Take 8'
          print 168,(connoy(i,j,1),j=1,8)
          print 178,(connoy(i,j,2),j=1,8)
          print 188,(connoy(i,j,3),j=1,8)
          print 198,(connoy(i,j,4),j=1,8)
158       format(1x,'[NO] LINE:',i3)
168       format(1x,'Mean    ',8(f8.2,' '))
178       format(1x,'S.D.    ',8(f8.2,' '))
188       format(1x,'Time    ',8(f8.2,' '))
198       format(1x,'Scount  ',8(f8.2,' '))
208       format(1x,'[NOy] LINE',i4)
300     continue
      endif     ! end of if want to display all data.
      endif
      return
      end
*****************************************************************
** SUMM creates a summary (to screen and to a file) of the current data file.
** RAW must be loaded, and both CAL and CON calc'd.
** Summary to file is appended if the file specified currently exists,
** otherwise a new file is created.
*****************************************************************
      Subroutine SUMM(fil,header,fdate,ftime,conNO,conNOy,ConNt,
     1          FrcZrd,Sens,CnvEff,NOySen,Zero,NewNO2,ArtFil)
      INCLUDE 'GlobalVar.def'
      include 'cal_var.def'
      include 'con_var.def'
      INCLUDE 'Flags.def'
      character *60 fil,fname,header,fdate,ftime,fout,ArtFil
      character *80 line
      character *9 TodDat
      character *8 TodTim
      integer i,j
      real xmin,xmax
      REAL x(MaxZ,2)              ! mean, s/scnt.  for min/max tests.
      Logical ready,Exist,Append    ! True if all nec. data is in memory.
      ready = .TRUE.
      if (.not.(rawldd)) then
       ready=.FALSE.
       print*,'You must LOAD RAW prior to SUMM.'
       ENDIF
      IF (.not.(caldne)) THEN
       ready=.FALSE.
       print*,'You must CALC CAL prior to SUMM.'
       ENDIF
      IF (.not.(condne)) THEN
       ready=.FALSE.
       print*,'Your must CALC CON prior to SUMM.'
       ENDIF
      IF (.not.(ready)) RETURN
** Get file
      call bell
      write(*,101)
101     format('$Please enter the file (prefix only) for the summary: ')
      read(*,60)fout
60      format(A60)
      append=.FALSE.
      call Files(fout,Exist,SumExt)
      IF (Exist) THEN
       append=(GetYN(
      1'This file already exists.  Do you want to append to it? ',
      1'Y'))
       ENDIF
      Call Date(TodDat)
      call time(TodTim)
      IF (append) THEN
       open(unit=isumLb,file=fout,status='OLD',access='APPEND')
       write(isumlb,201)TodDat,TodTim
       ELSE
```

Data Analysis Program (continued: page 5)

```
      open(unit=isumLb,file=fout,status='NEW')
      write(isumlb,202)TodDat,TodTim
      ENDIF
201     format(1x,'File added to on ',A9,' ',A8)
202     format(1x,'File created on ',A9,' ',A8)
      write(isumlb,203)Fil
203     format(1x,'File name: ',A60)
      Fname=Fil
      Call Files(FName,exist,NotExt)
      IF (exist) THEN
       write(isumlb,204)
204     format(1x,'Note file contents: ')
       open(iNotLb,file=Fname,status='OLD')
20      continue
       read(iNotLb,80,end=991)line
       write(isumLb,81)line
80      format(a80)
81      format(1x,a80)
       goto 20
991     continue
      else
       write(isumlb,205)
205     format(1x,'Note file not found.')
      ENDIF
      write(isumLb,206)fdate,ftime
206     FORMAT(1x,'Start time: ',A,LenStr(Fdate,60),' ',
     1    A(LenStr(Ftime,60))
      write(isumlb,207)tstart,(tstart+raw(ines,modes,itime)/3600./24.)
207     format(1x,'Julian day range: ',F6.2,' to ',F6.2)
      write(isumlb,208)lines
208     format(1x,'Number of lines:',I4)
      write(iSumLb,*)
** If there's data in the file, summarize it
      IF (lines.gt.0) THEN
      write(isumLb,209)
209     format(1x,' Ranges:  ',' ',' Min ',' ',' Max ',
     1    ' ','with s/scnt |',' ','% Incl.',' ',
     1    '(within range)',/,1x,
     1    '**********',
     1    '**********')
210     format(1x,A12,'  ',F8.2,'  ',F8.2,'  ',4x,F5.1,4x,'  ',F5.1,
     1    ' ',F9.1,'  ',F9.1)
** Get ranges and print out
      DO i=1,lines
       x(i,1)=Sens(i,imean)
       x(i,2)=Sens(i,iscnt)
       enddo
      DO i=lines+1,Maxz
       x(i,1)=999.
       x(i,2)=999.
       enddo
      Call Range(x,RSDMAX(iSens),minmn(isens),maxmn(isens),
     1    xmin,xmax,frcn)
      frcn = frcn*100.0
      write(isumLb,210)'S-NO',xmin,xmax,Rsdmax(isens),frcn,minmn(isens),
     1    maxmn(isens)
      do i=1,lines
       x(i,1)=NOySen(i,imean)
       x(i,2)=NOySen(i,iscnt)
       enddo
      Call Range(x,RSDMAX(iSens),minmn(isens),maxmn(isens)
     1    ,xmin,xmax,frcn)
      frcn = frcn*100.0
      write(iSumLb,210)'S-NOy',xmin,xmax,Rsdmax(isens),frcn,
     1    minmn(isens),maxmn(isens)
      k=0
      do i=1,lines
       do j=1,takes
        k=k+1
        x(k,1)=zero(i,j,iNOa,imean)
        x(k,2)=zero(i,j,iNOa,iscnt)
        k=k+1
        x(k,1)=zero(i,j,iNOb,imean)
        x(k,2)=zero(i,j,iNOb,iscnt)
        enddo
       enddo
      Call Range(x,RSDMAX(iZro),minmn(izro),maxmn(izro),
     1    xmin,xmax,frcn)
      frcn = frcn*100.0
      write(iSumLb,210)'Z-NO',xmin,xmax,Rsdmax(iZro),frcn,
     1    minmn(izro),maxmn(izro)
      k=0
      do i=1,lines
       do j=1,takes
        k=k+1
        x(k,1)=zero(i,j,iNOy,imean)
        x(k,2)=zero(i,j,iNOy,iscnt)
        enddo
       enddo
      do i=k+1,MaxZ
       x(k,1)=999.
       x(k,2)=999.
       enddo
      Call Range(x,RSDMAX(iZro),Minmn(izro),maxmn(izro),
     1    xmin,xmax,frcn)
      frcn = frcn*100.0
      write(iSumLb,210)'Z-NOy',xmin,xmax,Rsdmax(iZro),frcn,
     1    minmn(izro),maxmn(izro)
      do i=1,lines
       x(i,1)=FrcZrd(i,imean)
       x(i,2)=FrcZrd(i,iscnt)
       enddo
      do i=lines+1,maxz
       x(i,1)=999.
       x(i,2)=999.
       enddo
      Call Range(x,rsdmax(iFzd),minmn(ifzd),maxmn(ifzd),
     1    xmin,xmax,frcn)
      frcn=frcn*100.0
      write(iSumLb,210)'Frcn Zeroed',xmin,xmax,rsdmax(ifzd),frcn,
     1    minmn(ifzd),maxmn(ifzd)
      do i=1,lines
       x(i,1)=CnvEff(i,imean)
       x(i,2)=CnvEff(i,iscnt)
       enddo
      Call Range(x,RSDMAX(iCvEf),minmn(icvef),maxmn(icvef),
     1    xmin,xmax,frcn)
      frcn = frcn*100.0
      write(iSumLb,210)'Conv. Eff.',xmin,xmax,Rsdmax(iCvEf),frcn,
     1    minmn(icvef),maxmn(icvef)
      do i=1,lines
       x(i,1)=NewNo2(i,imean)
       x(i,2)=NewNO2(i,iscnt)
       enddo
      Call Range(x,998.,0.0,5.E6,xmin,xmax,frcn)
      frcn = frcn*100.0
      write(iSumLb,210)'NO2 Created',xmin,xmax,998.,frcn,0.0,5.E06
      k=0
      DO i=1,lines
       do j=1,takes
        k=k+1
        x(k,1)=ConNO(i,j,imean)
        x(k,2)=ConNO(i,j,iscnt)
        enddo
       enddo
      Call Range(x,998.,-1000.,100000.,xmin,xmax,frcn)
      frcn = frcn*100.0
      write(iSumLb,210)'NO (ppt)',xmin,xmax,998.,frcn,-1000.,100000.
      k=0
      DO i=1,lines
       do j=1,takes
        k=k+1
        x(k,1)=ConNOy(i,j,imean)
        x(k,2)=ConNOy(i,j,iscnt)
        enddo
       enddo
      Call Range(x,998.,-1000.,100000.,xmin,xmax,frcn)
      frcn = frcn*100.0
      write(iSumLb,210)'NOy (ppt)',xmin,xmax,998.,frcn,-1000.,
     1    100000.
      endif     ! end of if (lines.gt.0)
** Done
      write(iSumLb,211)
211     format(1x,
     1    '**********',
     1    '**********')
      close(iSumLb)
      return
      end
*****************************************************************
** Another non-modification subroutine
**  Prints out available commands, syntax, and brief explainton of
**  their purpose.
*****************************************************************
      subroutine help
      print*,' '
      print*,'Commands must be in upper case.'
      print*,'Format of command is:'
      print*,'XXXX YYY [parameter list]'
      print*,'  XXXX stand for a command and YYY stands for an object.')
      print*,' '
      print*,'Currently available commands are:'
      print*,'  HELP -This message.'
      print*,'  QUIT -Exit the program.'
      print*,'  CALC -Calculate some of calibrations.'
      print*,'  LOAD -Loads a file (currently only raw).'
      print*,'  DISP -Dumps data to the screen (currently only raw).'
      print*,'  PLOT -Plot calibration or concentration data.'
      print*,'  PRGM -Modify programmable constants.'
      print*,' '
      print*,'Command formats are:'
      print*,'HELP'
      PRINT*,'QUIT'
      PRINT*,'PRGM'
      PRINT*,'CALC [CAL/CON/NIT/ALL/ART]'
      PRINT*,'LOAD [RAW/PGM/CAL/CON/ALL] filename'
      PRINT*,'SAVE [PGM/CAL/CON/ALL] filename'
      PRINT*,'PLOT [CAL/CON/NIT]'
      PRINT*,'DISP [FIL/VER/RAW/CAL/PGM/ALL]'
      PRINT*,'filename is an optional parameter.'
      return
      end
*****************************************************************
** Gracefully exit the program, if you've saved your work.
** If you haven't, then it'll let you know, and allow you the option
** of going back and doing the deed.
** doesn't affect anything, though.
*****************************************************************
      subroutine quit
      include 'GlobalVar.def'
```

Data Analysis Program (continued: page 6)

```
      INCLUDE 'FLAGS.DEF'
      character *1 inchr
      logical verify
      verify=.false.
       if ((caldne).and.(.not.calsvd)) then
          print*,'Warning! Calibrations not saved!'
          verify=.true.
          endif
       if ((condne).and.(.not.consvd)) then
          print *,'Warning! Concentrations not saved!'
          verify=.true.
          endif
       if (.not.pgmsvd) then
          print*,'Warning! Programmables not saved!'
          print*,'If you have modified the programmables OR '
          print*,'have created a new CAL or CON file, do not'
          print*,'exit until you SAVE PGM.'
          verify=.true.
          endif
      IF (verify) THEN
          call bell
          call bell
           write(*,110)
  110        format('$Enter capital Y to confirm exit: ')
          read(*,100)inchr
          if (inchr.ne.'Y') RETURN
          endif
        stop
  100   format(A1)
      end
*****************************************************************
*****************************************************************
************************ MODULE ANACALIB.FOR ************************
*****************************************************************
*****************************************************************
** This file includes all of the subroutines needed to calculated
** the calibration data for the program ANALYZE.
** Procedures in this file are
**    CalCal – Iteratively calls the number crunchers.
**    CalFzd – Calculates a fraction zeroed data line.
**    CalSen – Calculates a NO sensitivity line.
**    ClySen – Calculates a NOy sensitivity line.
**    CalNew – Calculates NO2 created line.
**    CalZro – Calculates the zeroes for a line.
**
** EXTERNAL CALLS:
**  globalvar.def, parameters.def
*****************************************************************
*****************************************************************
**    Calculate the calibration data.
**      Takes the first 6 modes (and part of 1st take) of raw as
**        c/NOy/O3, c/NOxO3, NO(c), c/NO, c/NOy, c/NO/z
**      to
**        FrcZrd,Sens,CnvEff,NewNO2,NOySen,Zro
**      through various calculations.
**
**
**    SUBROUTINE CALLS:
**      CalFzd, CalSen, CalCnv, ClySen, CalNew, CalZro
**    Inputs
**      /global/raw
**    Outputs
**      frczrd, sens, cnveff, noysen, newno2, zero
*****************************************************************
      subroutine CalCal(FrcZrd, Sens, CnvEff, NOySen, NewNO2, Zero)
      include 'GlobalVar.def'
      include 'cal'var.def'
      real x(4),y(3,4),z(4)
      integer i,j,k,l
       do 90,i=1,lines          !Compute all calib. one line at a time
         call CalFzd(x,i)       !Typical call. Uses dum-dum var.
         do 10 j=1,4            !x(j) to represent a single mode
          FrcZrd(i,j)=x(j)      !This one gets Fractions zeroed.
  10     continue
         call CalSen(x,i)       !Call for calibration sensitivity.
         do 20 j=1,4
          Sens(i,j)=x(j)
         Z(j)=x(j)              ! CalNew needs NO Sens for calculations
  20     continue
         call CalCnv(x,i)       !Calling conversion efficiency computation
         do 30 j=1,4
          CnvEff(i,j)=x(j)
  30     continue
         call ClySen(x,i)       !Get NOy sensitivity
         do 40 j=1,4
          NoySen(i,j)=x(j)
  40     continue
         call CalNew(x,i,z)     !Calculate NO2 created.
         do 50 j=1,4
          NewNO2(i,j)=x(j)
  50     continue
         do 60 j=1,takes        !This sloppiness iterates through
          call CalZro(y,i,j)    !a single line and finds the 3 zeros
          do 60 k=1,3           !–NOs, NOb, NOy–in each take.
           do 60 l=1,4
            Zero(i,j,k,l)=y(k,l)
  60      continue
  90    continue
        return
        end
*****************************************************************
** Liberties taken in the headers to follow:
** .def files not listed.
** array dimension of global stuff not retyped
*****************************************************************
*****************************************************************
**        Calculates an element of FrcZrd
**          –returns a 4-element array containing
**             mean, SD, time, Scount
**          from raw.
**    inputs
**      /global/raw
**      line
**    outputs
**      FrZd(4)
*****************************************************************
      subroutine CalFzd(FrZd,line)
      include 'GlobalVar.def'
      include 'cal'var.def'
      real   FrZd(4)
      integer line
      real   cNOz(3), cNO(3), NOc(3), CNO3(3), zNO(3), A, B
      integer j
        do 20 J=1,3                 !shorten typing for raw stuff
          cNOz(j)=raw(line,icNOz,j)
          cNO(j) =raw(line,icNO,j)
          NOc(j) =raw(line,iNOc,j)
          zNo(j) =raw(line,iNOz1,j)     ! iNOz1 is mode of Z/NO-1s
  20    continue
**ACTUAL NUMBER CRUNCHING STUFF.  A and B are dummy  variables.
       A=(cNOz(imean)-zNO(imean))/(cNO(imean)-NOc(imean))
       FrZd(imean)=1-A
       A = (cNOz(isd)**2)/Navg(icNOz)+(zNO(isd)**2)/Navg(iNOz1)
       A = A/(cNOz(imean)-zNO(imean))**2
       B = (cNO(isd)**2)/Navg(icNO)+(NOc(isd)**2)/Navg(iNOc)
       B = B/(cNO(imean)-NOc(imean))**2
       FrZd(isd)=sqrt(A+B)*FrZd(imean)
       FrZd(itime)=cNoz(itime)/24./3600.+tstart
       A = cNOz(imean)/Navg(icNOz) + zNO(imean)/Navg(iNOz1)
       A = A/(cNOz(imean) - zNO(imean))**2
       B = cNO(imean)/Navg(icNO) + NOc(imean)/Navg(iNOc)
       B = B/(cNO(imean) - NOc(imean))**2
       FrZd(iSCnt) = FrZd(isd)/(FrZd(imean)*sqrt(A+B))
      return
      end
*****************************************************************
** Calculates NO sensitivity.
** inputs
**   /global/raw
**   line
** Output
**   SEN(4) – sensitivity for the given line.
*****************************************************************
      subroutine CalSen(Sen,line)
      include 'GlobalVar.def'
      include 'cal'var.def'
      real Sen(4)
      integer line
        Sen(imean)=(raw(line,icNO,imean)-raw(line,iNOc,imean))/Ccg
        A=(raw(line,icNO,iSD)**2)/Navg(icNO)
        A=A+(raw(line,iNOc,iSD)**2)/Navg(iNOc)
        A=sqrt(A/(raw(line,icNO,imean)-raw(line,iNOc,imean))**2)
        Sen(isd)=A*Sen(imean)
        Sen(itime)=raw(line,icNO,itime)/24./3600. + tstart
        A=raw(line,icNO,iSD)**2/Navg(icNO)
        A=A+raw(line,iNOc,iSD)**2/Navg(iNOc)
        B=raw(line,icNO,imean)/Navg(icNO)
        B=B+raw(line,iNOc,imean)/Navg(iNOc)
        Sen(iScnt)=sqrt(A/B)
      return
      end
*****************************************************************
** Calculates the conversion efficieny for one calibration.
** inputs
**   /globa/raw
**   line
** Outputs
**   EFF(4) the conversion efficiency for the given line.
*****************************************************************
      subroutine CalCnv(Eff,line)
      include 'GlobalVar.def'
      include 'cal'var.def'
      real Eff(4),A,B
      integer line
        A=raw(line,icNOy,imean)-raw(line,icyO3,imean)
      IF (raw(line,icNO,imean)-raw(line,icO3,imean).ne.0) then
          A=A/(raw(line,icNO,imean)-raw(line,icO3,imean))
          Eff(imean)=1-A
        A=(raw(line,icNOy,iSd)**2)/Navg(icNOy)
        A=A+(raw(line,icyO3,isd)**2)/Navg(icyO3)
        A=A/(raw(line,icNOy,imean)-raw(line,icyO3,imean))**2
        B=(raw(line,icNO,isd)**2)/Navg(icNO)
        B=B+(raw(line,icO3,isd)**2)/Navg(icO3)
        B=B/(raw(line,icNO,imean)-raw(line,icO3,imean))**2
        Eff(isd)=sqrt(A+B)*eff(imean)
        A=raw(line,icNOy,imean)/Navg(icNOy)
        A=A+raw(line,icyO3,imean)/Navg(icyO3)
        A=A/(raw(line,icNOy,imean)-raw(line,icyO3,imean))**2
        B=raw(line,icNO,imean)/Navg(icNO)
        B=B+raw(line,icO3,imean)/Navg(icO3)
```

Data Analysis Program (continued: page 7)

```
      B=B/(raw(line,icNO,imean)-raw(line,icO3,imean))**2
      Eff(iScnt)=(Eff(isd)/(Eff(imean)*sqrt(A+B)))
      else
      eff(imean)=999.
      EFF(isd)=999.
      eff(iscnt)=999.
      endif
      Eff(itime)=raw(line,icyO3,itime)/24./3600.+tstart
     return
     end
*****************************************************************
** Calculates the NOy sensitivity of one calibration period.
**   NOTE THIS IS DIFFERENT FROM CALSEN WHICH FINDS NO SENSITIVITY
** Inputs
**     /global/raw
** Output
**   Sen(4) the NOy sensitivity for the given line.
*****************************************************************
     subroutine ClySen(Sen,line)
     include 'GlobalVar.def'
     include 'cal`var.def'
     real Sen(4),A,B
     integer line
      Sen(imean)=(raw(line,icNOy,imean)-raw(line,iNOy1,imean))/Ccg
      A=(raw(line,icNOy,iSd)**2)/Navg(icNOy)
      A=A+(raw(line,iNOy1,iSD)**2)/Navg(iNOy1)
      A=sqrt(A/(raw(line,icNOy,imean)-raw(line,iNOy1,imean))**2)
      Sen(isd)=A*Sen(imean)
      Sen(itime)=raw(line,icNOy,itime)/24./3600.+tstart
      A=raw(line,icNOy,isd)**2/Navg(icNOy)      ! A = Var of numerator
      A=A+raw(line,iNOy1,isd)**2/Navg(iNOy1)
      B=raw(line,icNOy,imean)/Navg(icNOy)       ! B = Var of numerator expected
      B=B+raw(line,iNOy1,imean)/Navg(iNOy1)     ! from counting statistics.
      Sen(iScnt)=sqrt(A/B)
     return
     end
*****************************************************************
** Calculates the NO2 created for a single calibration.
** Inputs are LINE, RAW, and SEN--the NO sensitivity
**   /global/raw
**   line
**   SEN(4)  (the NO sensitivity)
** Output
**   NEW(4) a typical 1:4 array that returns the NO2 created.
*****************************************************************
     subroutine CalNew(New,line,Sen)
     include 'GlobalVar.def'
     include 'cal`var.def'
     real New(4),Sen(4),A,B
     integer line
      A=raw(line,icNO,imean)-raw(line,icO3,imean)
      New(imean)=A/sen(imean)
      A=raw(line,icNO,iSD)**2/Navg(icNO)     ! Formula for SD assumes
     A=A+raw(line,icO3,iSD)**2/Navg(icO3)    ! RSD of Sens is negligible.
     IF (raw(line,icNO,imean)-raw(line,icO3,imean).ne.0) then
        A=A/(raw(line,icNO,imean)-raw(line,iCO3,imean))**2
        New(isd)=sqrt(A)*New(imean)
      else
      new(isd)=999.
      endif
      New(itime) = raw(line,icO3,itime)/24./3600. + tstart
     A=raw(line,icNO,isd)**2./Navg(icNO)
     A=A+raw(line,icO3,isd)**2./Navg(icO3)
     B=raw(line,icNO,imean)/Navg(icNO)
     B=B+raw(line,icO3,imean)/Navg(icO3)
     New(iscnt)=SQRT(A/B)
     return
     end
*****************************************************************
** Subroutine calculates all the zeros for a single take.
** inputs
**  /global/line
**  line
**  take
** output
**  Zro(3,4) zeroes for the 3 zeros/take (NO-a, NO-b, NOy)
*****************************************************************
     subroutine CalZro(Zro,line,take)
     include 'GlobalVar.def'
     include 'cal`var.def'
     real Zro(3,4),A,B
     integer line,take,m
     integer mde,mode,tke,offset
     real x,s,t,sc
** NOTE THAT THE FOLLOWING 5 LINES (and 1 extension) ARE LOCAL FUNCTIONS!!!
     mde(tke,offset)=6+(offset*2-1)+5*(tke-1)    ! Formula corrected 3/17/90
     x(mode)=raw(line,mode,imean)
     s(mode)=raw(line,mode,isd)/sqrt(float(Navg(mode)))
     t(mode)=raw(line,mode,itime)/24./3600.+tstart
     sc(mode)=raw(line,mode,isd)/sqrt(raw(line,mode,imean))
** END OF FUNCTIONS
**   mode gives the mode (from 1) in raw that a line,take,offset is at
**   example: zNO-1 is at mode 8: 6 + 1 + (1-1)*5 = 7
**    since zNO-1 is the second entry in take 1.
**   x is the mean, s the standard deviation, t the time, and c the Scount
     m = mde(take,iNOa)          !blocks of code like this simply
     Zro(iNOa,imean)=x(m)        !call functions that compute
     Zro(iNOa, isd)  =s(m)       !the required goober number.
     Zro(iNOa,itime)=t(m)        !functions are defined above.
     Zro(iNOa,iScnt)=sc(m)
     m = mde(take,iNOb)
     Zro(iNOb,imean)=x(m)
     Zro(iNOb,isd)  =s(m)
     Zro(iNOb,itime)=t(m)
     Zro(iNOb,iScnt)=sc(m)
     m = mde(take,iNOy)
     Zro(iNOy,imean)=x(m)
     Zro(iNOy,isd)  =s(m)
     Zro(iNOy,itime)=t(m)
     Zro(iNOy,iScnt)=sc(m)
    return
    end
*****************************************************************
*****************************************************************
********************* MODULE ANACONCEN.FOR **********************
*****************************************************************
*****************************************************************
** contains most of the subroutines for finding the concentrations.
**EXTERNAL CALLS                          (ANALIB.FOR)
**          INTERP(INT,P1,P2,TIME,IAVE)
**          RSDOK(X(S),S,IAVE(S))
**          RUNAVE(AVE,LINE,MODE,LIST,IAVE)
**  CALCON calls various stuff to crunch numbers, it iterates
**       take by take, line by line through the data and zeroes
**       and calls NOCon and NOyCon each time to get [NO], [NOy]
**  NOCon calculates [NO] for a single line,take.
**  NOyCon  "       [NOy] " "  "  "
**  IntNOz interpolates the NO zeros for a single take
**  IntNyz  "        " NOy "  "  "  "
*****************************************************************
*****************************************************************
** Calculates the concentrations for the whole data set.
** INPUTS:
**       Zero    these are explained in globalvar.def
**       FrcZrd
**       Sens
**       CnvEff
**       NOySen
** OUTPUTS:
**       ConNO
**       ConNOy
** CALLS
**       NOCon
**       NOyCon
*****************************************************************
     subroutine CalCon(ConNO,ConNOy,Zero,FrcZrd,
    1     Sens,NOySen,CnvEff)
     include 'GlobalVar.def'
    include 'cal`var.def'
    include 'con`var.def'
     real x(4)
     integer i,j,k
      do 40 i=1,lines
       do 30 j=1,takes
        call NoCon(x,i,j,Zero,FrcZrd,Sens)
        do 10, k=1,4
         ConNO(i,j,k)=x(k)
10       continue
30      continue                          ! correction.
40     continue
    do 50 I=1,LINES
     dO 60,J=1,TAKES
        call NOyCon(x,i,j,ConNo,Zero,Sens,NOySen,  ! NOyCon uses NOCon from
    1                FrcZrd,CnvEff)               ! current take to
        do 20, k=1,4                      ! estimate non-NO NOy
         ConNOy(i,j,k)=x(k)               ! for conversion
20       continue                         ! efficiency
60     CONTINUE
50    CONTINUE
     return
     end
*****************************************************************
** laid back attack for headers:
** global inputs don't have array dimensions retyped.
*****************************************************************
*****************************************************************
**  Calculates a single [NO] (one line,take)
** INPUTS:
**       /global/raw
**       line   line and take index the position in raw
**       take   the rest of these are explain in globalvar.def
**       zero
**       frczrd
**       sens
**  outputs:
**       con(4), a single [NO] point.
**  calls:
**       IntNOz
**       IntSen
**       RunAve   (external)
**       RSDOk    (external)
*****************************************************************
     Subroutine NOCon(Con,line,take,Zero,FrcZrd,Sens)
     include 'GlobalVar.def'
    include 'cal`var.def'
    include 'con`var.def'
     real Con(4),zro(4),sns(4),ave(4),A,B,x(3,4)
     integer y(4),line,mode,s,take
      mode=8+(take-1)*5      ! Mode 8 is first NO-measure mode.
      call IntNOz(zro,line,TAKE,zero,raw(line,mode,itime),
```

Data Analysis Program (continued: page 8)

```
     1          Raw(line,mode,imean))
          call IntSen(sns,line,sens,raw(line,mode,itime),isens)
          CALL RunAve(ave,line,FrcZrd,iFzd)
           Con(itime)=raw(line,mode,itime)/24./3600.+tstart
           do 10 i=1,4
            x(1,j)=ave(i)
            x(2,j)=sns(i)
            x(3,j)=Zro(i)
 10        continue
           y(1)=iFzd
           y(2)=iSens
           y(3)=iZro
           e=rsdok(x,3,y)
           if (e.eq.999) THEN
            con(imean)=999
            con(isd)=999.
            con(iscnt)=999.
            return
            ENDIF
           call RunAve(ave,line,FrcZrd,iFzd)
           A=raw(line,mode,imean)-zro(imean)
           Con(imean)=A/(Sns(imean)*ave(imean))
           A=raw(line,mode,isd)**2/Navg(mode)+zro(isd)**2
          C=(raw(line,mode,imean)-zro(imean))**2
          IF (C.ne.0) THEN
            A=A/(raw(line,mode,imean)-zro(imean))**2
            B=(ave(isd)/ave(imean))**2
            B=B + (sns(isd)/sns(imean))**2
            Con(isd)=con(imean)*sqrt(A+b)
          ELSE
          Con(isd)=Con(imean)*raw(line,mode,isd)/raw(kne,mode,jmean)
          ENDIF
          Con(iScnt)=raw(line,mode,isd)/sqrt(raw(ins,mode,imean))
          return
          end
*****************************************************************************
** Calculates [NOy] for a single mode,take.
** inputs:
**       /global/raw
**       line   line,take give posibon in raw.
**       take
**       ConNO   [NO] IS REQUIRED FOR [NOy]
**       Zero    rest of this is explained in globalvar.def.
**       FrcZrd
**       Sens
**       NoySen
**       CnvEff
** outputs:
**       Con(4) a single [NOy]
** calls
**       IntNyz
**       IntSen
**       RSDOK (external)
**       RunAve (external)
*****************************************************************************
          subroutine NOyCon(Con,line,take,ConNO,Zero,
     1                Sens,NOySen,FrcZrd,CnvEff)
          include 'GlobalVar.def'
          include 'cal'var.def'
          include 'con'var.def'
          real con(4),zro(4),ens(4),fzd(4),ave(4),x(4,4),e,b,c,
     1       NOint(4),P1(4),P2(4)
          integer y(4),line,take,mode
           mode=10+(take-1)*5      ! Mode 10 is 1st NOy-measure mode
           call IntNyz(zro,line,take,zero,raw(line,mode,itime),
     1           raw(line,mode,imean))
           if (useNOy) then
            call IntSen(ens,line,NoySen,raw(line,mode,itime),iySen)
           else
            call IntSen(ens,line,Sens,raw(line,mode,itime),iSens)
           endif
           call RunAve(fzd,line,FrcZrd,iFzd)
           call RunAve(ave,line,CnvEff,iCvEf)
          CON(ITIME)=RAW(LINE,mode,itime)/24./3600.0+tstart
          IF ((line.ne.lines)
     1      .OR.((line.eq.lines-1).and.(take.eq.takes))) THEN
           DO 5 i=1,4
            P1(i)=ConNO(line,take,i)
            IF (take.eq.takes) THEN
             P2(i)=ConNO(line+1,1,i)
             ELSE
             P2(i)=ConNO(line,take+1,i)
             ENDIF
 5           CONTINUE
**          Interpolate between nearest 2 NO values.  Use both in all cases.
            Call Interp(NOint,P1,P2,
     1            (Raw(line,mode,itime)/3600./24.+TStart),999)
           ELSE
             DO 6 i=1,4
 6            NOint(i)=ConNO(line,take,i)
           ENDIF
           do 10,i=1,4
            x(1,j)=sns(i)
            x(2,j)=Fzd(i)
           x(3,j)=ave(i)
            x(4,j)=zro(i)
 10        continue
          y(1)=isens
           y(2)=iFzd
           y(3)=iCvEf
           y(4)=iZro
           e = rsdok(x,4,y)
          if (ave(isd).gt.rsdmax(iCvSD)) e=999.
           if ((e.eq.999).OR.(NOint(imean).eq.999.)) then
           con(isd)=999.
           con(iscnt)=999.
           con(imean)=999
           RETURN
           endif
            C=(Raw(line,mode,imean)-zro(imean))/(Sns(imean)*Fzd(imean))
            C=C-NOint(imean)
            B=C/ave(imean)
            con(imean)=B+NOint(imean)
           A=(raw(line,mode,imean)-zro(imean))/(sns(imean)*fzd(imean))
           B=raw(line,mode,isd)**2./Navg(mode)
           C=(B+Zro(isd)**2.)/(raw(line,mode,imean)-Zro(imean))**2.
           C=C+(sns(isd)/sns(imean))**2.
           C=C+(Fzd(isd)/fzd(imean))**2.
           C=A**2.*C      ! At this point, C=Std Dev**2 of A
           C=(C+NOint(isd)**2.)/(A-NOint(imean))**2.
           Con(isd)=(A-NOint(imean))/ave(imean)
          1        *SQRT((ave(isd)/ave(imean))**2.+C)+NOint(isd)**2.
           con(iscnt)=RAW(line,mode,isd)/SQRT(Raw(line,mode,imean))
           if (UseNOy) then
            y(1)=iySen
           else
            y(1)=iSens
           endif
          return
          end
*****************************************************************************
** CalNit calculates average and SD of NO concentrations each "night."
**   "night" is defined by solar zenith angle¿=ZenMin.  (ZenMin is a
**   main program parameter - see GlobalVar.DEF.)  Only points with
**   Scnt¡=RSDMAX(izen) (another parameter) are included in the statistics.
**   Subroutines STAT and SUNPOS are in ANALIB.FOR.
** Output is ConNit - avg, SDavg, Scnt, Time FOR EACH ¡=8 hr period each night.
*****************************************************************************
          Subroutine CalNit(date,time,ConNit,ConNO,Zero,Sens)
          include 'GlobalVar.Def'
          include 'con'var.def'
          include 'cal'var.def'
          character *4 obj,cyear
          character *60 param,fil,header,date,time,fname
          logical Exist,Loaded,rsdok,zok,NitOK
          real NitNO(200),NitTim(200),sns(4),zro(4),TimMax
          parameter (TimMax=8.0)      ! hours
          cyear=date(8:11)
          year=1000.0*ic(cyear(1:1))+100.0*ic(cyear(2:2))
          1    +10.0*ic(cyear(3:3))+ic(cyear(4:4))
          rmin=1.e10
          rmax=-1.e10
          il=1
          it=1
             dy=int(conno(il,it,itime))
             hr=24.0*(conno(il,it,itime)-dy)
             call sunpos(dy,YEAR,hr,0.0,0.0,71.3233,
          2     156.6067,Zenith)
          zprev=zenith
          Do il=1,lines
           Do it=1,takes
            dy=int(conno(il,it,itime))
            hr=24.0*(conno(il,it,itime)-dy)
            call sunpos(dy,YEAR,hr,0.0,0.0,71.3233,
          2     156.6067,Zenith)
            zprev=zenith
            if (zenith.lt.rmin)rmin=zenith
            if (zenith.gt.rmax)rmax=zenith
           enddo
          enddo
          print*,'Range of zenith angles in this file is ',Rmin,' to ',Rmax
          if (Rmax.LT.90.) then
              znmin=85.
             else
              znmin=90.
             endif
          print*,'Using all data with zenith angle ¿= ',znmin
**                      ! Now, calculate for each night.
          Dayp=int(ConNO(1,1,itime))
          Timp=(ConNO(1,1,itime)-dayp)*24.0
          iinit=0
          Nnit=0
          Do il=1,lines
           Do it=1,takes
            dy=int(conno(il,it,itime))
            hr=24.0*(conno(il,it,itime)-dy)
            call sunpos(dy,YEAR,hr,0.0,0.0,71.3233,
          2     156.6067,Zenith)      ! hour,min,sec = 0; it's all in ConNO.
            ZOK=.FALSE.
            IF (zenith.gt.Znmin) Zok=.TRUE.
            RSDOK=.FALSE.
            IF (ConNO(il,it,iscnt).LE.RSDMAX(iCNit)) RSDOK=.TRUE.
            IF (((Zok).AND.(RsdOk)).AND.(ConNO(il,it,imean).NE.999)) THEN
             Day=int(ConNO(il,it,itime))
             TimC=(ConNO(il,it,itime)-Day)*24.
             IF ((Day.eq.Dayp).and.((TimC-TimP).le.TimMax)) THEN
**                 ! One more datum for current day
              iinit=iinit+1
              NitNO(iinit)=ConNO(il,it,imean)
              NitTim(iinit)=ConNO(il,it,itime)
```

Data Analysis Program (continued: page 9)

```
          ELSE                    ! Previous day is over.
         NitOK=.true.
         IF (iinit.gt.0) THEN
           Nnit=Nnit+1
           Call EndNit(NitNO,NitTim,iinit,Sens,Zero,il,ConNit)
           ENDIF
         Dayp=Day                ! Start the next day.
         Timp=TimC
         iinit=1
         NitNO(1)=ConNO(il,it,imean)
         NitTim(1)=ConNO(il,it,itime)
         ENDIF                   ! If day.eq.dayp
       ENDIF                     ! IF rsdok.and.zok
      ENDDO
      ENDDO                      ! Loops over it,il
     IF (iinit.ne.0) THEN
**                               ! Output for last day.
      Nnit=Nnit+1
      Call EndNit(NitNO,NitTim,iinit,Sens,Zero,il,ConNit)
      NitOk=.TRUE.
      endif
    IF (.not.(nitok)) THEN
     print*,'No valid nighttime data in this file.'
     print*
     endif
    print*,'Nighttime NO statistics calculated.'
    RETURN
    END
*****************************************************************************
*****************************************************************************
    Subroutine EndNit(NitNO,NitTim,iinit,Sens,Zero,il,ConNit)
    include 'globalvar.def'
    include 'con'var.def'
    include 'cal'var.def'
    real NitNO(200),NitTim(200)
    Call STAT(NitNO,200,iinit,avg,SD,rmin,rmax)
    Call STAT(NitTim,200,iinit,Tavg,Tsd,tmin,tmax)
    ConNit(Nnit,imean)=avg
    ConNit(Nnit,isd)=SD/SQRT(float(iiNit))
    ConNit(NNit,itime)=tavg
** Calculate expected (counting stats) SD = SD expected for [NO]=0.
** Estimate based on previous Sens and 1st Z for the line of tavg
    ilprev=il
10    continue
     if ((sens(ilprev,itime).lt.tavg).AND.(ilprev.LE.lines))
    1   goto 20
     ilprev=ilprev-1
     goto 10
20    continue
    Z1=zero(ilprev,1,iNOa,imean)
    Z2=zero(ilprev,1,iNOb,imean)
    Z3=zero(ilprev,2,iNOa,imean)
    if (z1.ne.999) then
      z=z1
     else if (z2.ne.999) then
       z=z2
      else if (z3.ne.999) then
       z=z3
      else
       do 30 i=1,4
30        ConNit(Nnit,i)=999.
       return
      endif
    SDexp = SQRT(2.0*Z/Navg(8))/Sens(ilprev,imean)
**                    ! Mode 8 is the 1st NO-measure mode
    ConNit(Nnit,iScnt)=SD/SDexp
    RETURN
    END
*****************************************************************************
** interpolates the [NO] zeroes.
** inputs
**      /global/raw
**      line  index to position in raw
**      mode
**      zero  zero array
**      time  time to be interpolated at
**      mcps  cps value during NO measure mode.  Used for comparison
**          with the difference between the adjacent zeros.
** outputs
**      int(4) interpolated zero.  bad if 999.
** calls
**      InterZ
*****************************************************************************
     subroutine IntNOz(int,line,take,zero,time,mcps)
     include 'globalvar.def'
    include 'cal'var.def'
     real int(4),z1(4),z2(4),time,TLoc,mcps
     integer line,take,i
      do 10,i=1,4
       z1(i)=zero(line,take,iNOa,i)          ! Always have prior and
       z2(i)=zero(line,take,iNOb,i)          ! succeeding NO Zero modes
10     continue
     TLoc=time/3600./24.+tstart              ! Convert time from seconds
**                          ! to Julian days
      call InterZ(int,Z1,Z2,tLoc,iZro,mcps,1)     ! 1=¿ NO, not NOy
     return
     end
*****************************************************************************
**Interpolates zero value between p1 and p2.  Int is returned.
**inputs
**      p1    first point.
**      p2    second point.
**      time  time of interpolation
**      iave  the index in RSDMAX to use to check validity of p1,p2.
**      mcps  Measure mode cps for comparison to diff between adjacent Zeros.
**      iNO   1 if this is for NO zero, 2 if for NOy zero.
**
**outputs
**      int(4) interpolated value.
** if p1 is bad, returns p2.  if p2 is bad, returns p1.
** if both bad, returns 999.
** otherwise, returns value as follows:
**
** Mean  = time*((mean2-mean1)/(time2-time1))  + timet
**  SD  = calculated by error propagation.
** Time  = time
**Scount = max(Scount1,Scount2)
*****************************************************************************
     subroutine InterZ(int,p1,p2,time,iave,mcps,iNO)
     include 'globalvar.def'
     real int(4),p1(4),p2(4),time,t(2),M,mcps,DcpsMx(2),DCpsRl(2)
     integer i,iave,iNO
     logical oka,okb
**                 ! Maximum values of delta-Z/delta-cps
     DcpsRl(1)=0.15     ! Cutoff values approximately the relative accuracy of
     DcpsRl(2)=0.20     ! the NO (1) and NOy (2) measurements.
     DcpsMx(1)=15.0     !Maximum delta-cps values when the relative constraint
     DcpsMx(2)=30.0     ! is not met.
     if (iave.eq.999) then
      oka=((P1(imean).ne.999.).and.(P1(iscnt).ne.999.))
      okb=((P2(imean).ne.999.).and.(P2(iscnt).ne.999.))
      else
      okb=( (p2(iscnt).le.rsdmax(iave))          ! Points are OK if they
     1     .AND.( (p2(imean).ge.minmn(iave))     ! satisfy the Scnt
     1          .AND.(p2(imean).le.maxmn(iave))))     ! and mean range
      oka=( (p1(iscnt).le.rsdmax(iave))          ! constraints
     1     .AND.( (p1(imean).ge.minmn(iave))
     1          .AND.(p1(imean).le.maxmn(iave))))
      endif
     if (.not.oka) then                    !if p1 is bad, use p2
      do 10,i=1,4
       int(i)=p2(i)
10     continue
     endif
     if (.not.okb) then                    !if p2 is bad, use p1
      do 20,i=1,4
       int(i)=p1(i)
20    continue
     endif
     if ((.not.(oka)).and.(.not.(okb))) then   !if both p1,p2 bad, return
      do 30,i=1,4
       int(i)=999
       return
30     continue
     endif
     if ((.not.(okb)).or.(.not.(oka))) return   !if either bad, leave.
     if ((oka).and.(okb)) then                  !otherwise, interpolate.
      A = 1.0 - (time-P1(itime))/(P2(itime)-P1(itime))
      B = (time-P1(itime))/(P2(itime)-P1(itime))
       M=(p2(imean)-p1(imean))/(p2(itime)-p1(itime))
       int(imean)=M*(time-p1(itime))+p1(imean)
      int(isd) = sqrt( (A*P1(isd))**2. + (B*P2(isd))**2.)
      DelZ=ABS(p1(imean)-p2(imean))
      Delcps=mcps-int(imean)
      IF (Delcps.LT.0) Delcps=0     ! This is necessary to ensure
**                     ! that for the occasional outlier
**                     ! with Delcps|-20cps, the relative
**                     ! constraint is not satisfied.
     IF ( (DelZ.GT.DcpsMx(iNO)).AND.
    1     (DelZ.GT.DCpsRl(iNO)*Delcps) ) THEN
*** Throw out the NO data point if the difference between two OK zeros
*** is ¿ DcpsMx and this difference contributes more than DcpsRl to
*** the relative uncertainty of the data point.  By flaging int(iscnt)
*** the data point will be dumped back in NOcon, NOycon.
          int(imean)=999.
          int(isd)=999.
          int(iscnt)=999.
          ELSE
          int(iscnt)=0.      ! temporary for checking in a few lines.
          ENDIF
        int(itime)=time
       if (int(iscnt).ne.999.) int(iscnt)=max(p1(iscnt),p2(iscnt))
     endif
    return
    end
*****************************************************************************
** interpolats NOy zeroes.
** inputs
**      /global/raw
**      line  line,mode in raw.
**      mode
**      zero  zero array
**      time  time to be interpolated at
**      mcps  measure mode cps value.
** outputs
**      int(4) single interpolated zero.
** calls
**      interZ
*****************************************************************
     subroutine IntNyz(int,line,take,zero,time,mcps)
```

Data Analysis Program (continued: page 10)

```
      include 'globalvar.def'
      include 'cal'var.def'
      real int(4),z1(4),z2(4),time,TIoc
      integer line,take
      tLoc=time/3600./24.+tstart      ! convert s to days
      if (take.eq.takes) then
        if (line.eq.lines) then
          do 10, i=1,4
           int(i)=zero(line,take,iNOy,i)
10        continue
        else
          do 20, i=1,4
           z1(i)=zero(line,take,iNOy,i)
           z2(i)=zero(line+1,1,iNOy,i)
20        continue
          call InterZ(int,z1,z2,tLoc,iZro,mcps,2)
        endif
      else
        do 30, i=1,4
          z1(i)=zero(line,take,iNOy,i)
          z2(i)=zero(line,take+1,iNOy,i)
30        continue
        call InterZ(int,z1,z2,TLoc,iZro,mcps,2)
      endif
      return
      end
*****************************************************************************
** interpolates between current sensitivity and sensitivity of next
** line. if last line of file, uses sens of current line.
**
** inputs sens = list of sensitivities.
**       line = current line.
**       iave = radmax index
**       time = interpolation time
** output sns  = interpolated value.
**
** calls  interp (external)
*****************************************************************************
      subroutine IntSen(sns,line,sens,time,iave)
      include 'globalvar.def'
      include 'cal'var.def'
      real sns(4),x(4),y(4),time,iave,TLoc
      integer line,i
      TLoc=time/3600./24.+tstart    ! Convert sec. to days
       if (.not.line.eq.lines) then  !if not last line of data then
         do 10,i=1,4                 !we know line+1 will contain info.
          x(i)=sens(line,i)
          y(i)=sens(line+1,i)
10       continue
         call interp(sns,x,y,tLoc,iave)
       else                          !if last line, use current line's
         do 20,i=1,4                 !sens.
          sns(i)=sens(line,i)
20       continue
       endif
      return
      end
*****************************************************************************
** Subroutine CalArt(ConNO,ConNOy,ArtFil)
** Input:
**     ConNO,ConNOy: UnCorrected NO and NOy concentrations
** Output:
**     ArtFil: File name of artifact (nighttime NO averages) data
**     ConNO,ConNOy: Corrected concentrations.
**     ArtDne: Flag indicating artifact correction
      Subroutine CalArt(ConNo,ConNOy,ArtFil)
      include 'GlobalVar.def'
      include 'Con'Var.def'
      include 'Flags.def'
      character *60 ArtFil
      Real Nit1(4),Nit2(4),IntNit(4)
      IF (ArtDne) THEN
        print*,'********** E R R O R *****************'
        print*,'***  Artifact correction already completed ***'
        print*,
     1'**** To change correction, you must restart with raw data'
        print*,' '
        return
        endif
      print*,
     1'Nighttime NO artifact averages must be previously saved in a'
      IF (.NOT.(GetYN('file.  Enter Y to continue. ','Y'))) THEN
        return
        else
        write(*,10)
10        format('$Enter nighttime NO artifact data file name: ')
        read(*,60)ArtFil
60        format(A60)
        print*,'Loading artifact data file ...'
        Call GetNit(ArtFil,ConNit)
        print*,'Correcting NO and NOy data ...'
        do 100 il=1,lines
          do 100 it=1,TAKES
*** First, NO
**                    ! Find previous and next nit value.
**                      ! Assign 999 to values too far away.
          Call FndNit(ConNit,ConNo(il,it,itime),Nit1,Nit2)
**                    ! Interp.  Use pts with scnt|=RSDMAX(init) and
**                    !  not = 999.
          Call Interp(IntNit,Nit1,Nit2,ConNO(il,it,itime),iNit)
**                    ! If SD of interpolated value ¡ SArMin, increase
**                    !  SD to SArMin (global variable)
          IF (IntNit(isd).lt.SArMin) IntNit(isd)=SArMin
**                    ! Flag bad data
          IF ( (IntNit(iscnt).eq.999.) .OR.
     1         (ConNO(il,it,imean).eq.999.) )then
            ConNO(il,it,iscnt)=999.
            ConNO(il,it,imean)=999.
          else
**                    ! Correct the data
           ConNO(il,it,imean)=ConNO(il,it,imean)-IntNit(imean)
           ConNO(il,it,isd)=SQRT(ConNO(il,it,isd)**2.0+
     1          IntNit(isd)**2.0)
          endif
*** Repeat for NOy
**                    ! Find previous and next nit value.
**                      ! Assign 999 to values too far away.
          Call FndNit(ConNit,ConNOy(il,it,itime),Nit1,Nit2)
**                    ! Interp.  Use pts with scnt|=RSDMAX(init) and
**                    !  not = 999.
          Call Interp(IntNit,Nit1,Nit2,ConNOy(il,it,itime),iNit)
**                    ! If SD of interpolated value ¡ SArMin, increase
**                    !  SD to SArMin (global variable)
          IF (IntNit(isd).lt.SArMin) IntNit(isd)=SArMin
**                    ! Flag bad data
          IF ( (IntNit(iscnt).eq.999.) .or.
     1         (ConNOy(il,it,imean).eq.999.) ) then
            ConNOy(il,it,iscnt)=999.
            ConNOy(il,it,imean)=999.
            else
**                    ! Correct the data
             ConNOy(il,it,imean)=ConNOy(il,it,imean)-IntNit(imean)
             ConNOy(il,it,isd)=SQRT(ConNOy(il,it,isd)**2.0+IntNit(isd)**2.0)
            endif
100       Continue          ! End of loop over lines,takes
        ArtDne=.true.
        RETURN
        ENDIF               ! End of IF user wants to abort
      END     ! end of subroutine
*****************************************************************************
**    Subroutine FndNit called by CalArt above
      Subroutine FndNit(ConNit,time,Nit1,Nit2)
      include 'globalvar.def'
      include 'Con'Var.def'
      REAL Nit1(4),Nit2(4)
      parameter (TMax=48.0/24.0)     ! hours maximum distance from time to
**                                   !  valid Nit NO
      DO i=1,4
       Nit1(i)=999.
       Nit2(i)=999.
       enddo
      if (time.lt.ConNit(1,itime)) THEN
        DO 100 i=1,4
100       Nit1(i)=ConNit(1,i)
       if (ConNit(1,itime)-time .GT. Tmax) then
        print*,'Using first Nighttime point.  DT = ',
     1     (ConNit(1,itime)-time)
        endif
       return
       endif
      DO 1000 iinit=2,NNit
       dt1=time-ConNit(iinit-1,itime)
       dt2=-ConNit(iinit,itime)+time
       if ( (dt1.gt.0).and.(dt2.gt.0) ) then     ! between these two values
        if ( (dt1.le.tmax).and.(dt2.le.tmax) ) then
          do 200 i=1,4
           Nit1(i)=ConNit(iinit-1,i)
200         Nit2(i)=ConNit(iinit,i)
          return
          else                  ! 1 or both beyond tmax
          if (dt1.le.tmax) then     ! # 2 bad
            do 300 i=1,4
300           Nit1(i)=ConNit(iinit-1,i)
            return
            else if (dt2.le.tmax) then     ! # 1 bad
            DO 400 i=1,4
400           Nit1(i)=ConNit(iinit,i)
            return
           else                 ! Both data points are beyond Tmax
*                               ! Use closest
            if (dt1.le.dt2) THEN
              do 500 i=1,4
500             Nit1(i)=ConNit(iinit-1,i)
             return
             else
             do 600 i=1,4
600             Nit1(i)=ConNit(iinit,i)
             return
             endif          ! end of finding which one closest
           endif            ! End of if (dt1.le.tmax) etc.
         endif              ! End of both OK
       endif          ! End of if time between dt1 and dt2
1000   continue
**                    ! Only reach here if time¿ConNit(NNit,itime)
      do 700 i=1,4
700     Nit1(i)=ConNit(NNit,i)
      DT = time-ConNit(NNit,itime)
      if (DT.gt.tmax) then
        print*,'Using last Nighttime observation. Del-T = ',DT
        endif
```

Data Analysis Program (continued: page 11)

```
      return
      end
*****************************************************************************
*****************************************************************************
************************** MODULE ANAFILE.FOR ******************************
*****************************************************************************
*****************************************************************************
**  CONTAINS DATA LOADING/SAVING FILES.  This unit contains
**        GetRaw -- Loads a raw data file, returns info.
**        GetCal -- Loads a calibration file, returns info.
**        PutCal -- Saves a calibration file, requires info.
**        GetCon -- Loads a concentration file, returns info.
**        PutCon -- Saves a concentration file, requires info.
**        GetPgm -- Loads a programmable constant file. Returns little info.
**        PutPgm -- Saves a programmable constant file. Requires little info.
**        GetCPS -- Loads a cps file
**        PutCPS -- Saves a cps file in binary format.
**
**  Some routines read/save in either binary or ascii format.  Format choice
**    for reading ie automatic.  For writing, format choice is by user
**    input.  Binary files must have an initial character (*1), 'b'.
**    This paragraph applies to all routines except GetPgm and PutPgm, which
**    only use ascii files.
**
**  EXTERNAL CALLS (ANALIB)
**    Filels,FilCat,GetTime,BinFil
**    All the subroutines except getpgm return a flag to tell if they are
**    sucessful.  GetPgm does not because if it isn't in memory always,
**    the program won't work (everything else assumes it's been loaded.
**    when the program boots up, it will load or ask for this data.
**    Comments: global stuff doesn't
**    have the array dimensions retyped!
*****************************************************************************
*****************************************************************************
**  GetRaw loads a raw data file.
**  It's input is FN, the file asked for.
**  Before loading the raw data file, it checks for existance of a
**  note file.  If it exists, the note file is printed out.  This
**  allows easy cross-checking of the time and info. in the note
**  file and that in the raw data file.
**  It's outputs are
**          Header : the header of the raw file.
**                   this is saved w/ all files but Pgm files
**          loaded : flag to tell if a file is loaded
**          date   : date from raw file
**          time   : time from raw file
**          Size   : the number of lines in the file
**          fn     : the file actually loaded, if "loaded" is true.
**    /global/ Raw   : the actual numbers.
**
**
**  EXTERNAL CALLS (ANALIB): Filels,FilCat,GetTime
*****************************************************************************
      subroutine GetRaw(Header,Date,Time,Size,FN)
      include 'globalvar.def'
      include 'flags.def'
      character*60   fn,fname,header,date,time,junk,fnNOT
      character*80   NotLin
      integer        i,j,k,size
      logical        Exist, Loaded,NewTim,NExist,BinRaw
      character*1 yesno
       exist =.false.
      NExist=.false.
       loaded=.false.
       i=FilCat(fn)                        !this little mess is in all
       FName=fn(1:i)//rawext               !the Get's and Put's
       call Filels(FName,exist,rawext)     !All it does is add the
       i=filcat(fname)                     !file extensions onto the file
       fn=fname(1:i)                       !names.
      BinRaw=BinFil(FName)
**  Allow user to change the date and time in the file if it is in its
**  original (ASCII) format
**
       If ((.not.(BinRaw)).and.(exist) then
**                 ! First, print .NOT file, if it exists
      FnNot=fn(1:FilCat(fn))//NotExt
      Call Filels(FnNot,NExist,NotExt)
      if (NExist) then
          print*
          print*,'A Note file exists.  Here it is:'
          print*
          open(unit=10,file=FnNot,status='OLD')
6           continue
           read(10,7,end=8)notlin
           print*,notlin
           goto 6
8          continue
7          format(A80)
          print*,'*** End of Note file ***'
          close(10)
          Endif
       open(unit=10,file=FName,status='OLD')
       read(10,9),header
       read(10,9),date
       read(10,9),time
       read(10,9),junk
9       format(a60)
      print*,'Date and time from the file are:'
      print*,date
      print*,time
      if (GetYN('Do you wish to change the date/time? ','N')) THEN
          NewTim=.true.
          print*,'Enter new date:'
           read 9, date
          print*,'Enter new time'
            read 9, time
          print*,'New Date and Time are:'
          print*,date
          print*,time
          IF (.NOT.(GetYN('Enter Y to continue. ','Y'))) return
          print*,
     1'Please rename the old version so it will not be PURGED!'
**    Load the file prior to rewriting it with new date and time
          i=1
10         continue
             read(10,*,end=999),((raw(i,j,k),k=1,3),j=1,modes)
             i=i+1
             goto 10
999          continue
           size=i-1
           IF (SIZE.GT.MaxLin) then
            print*,'ERROR LOADING RAW DATA FILE ',FNAME
           print*,'Number of lines ie ¿ maximum.'
           print*,'Number of lines in file = ',size
           print*,'Number of lines allowed = ',MaxLin
           print*,'You must split the file or revise the program.'
           return
           endif
          CLOSE(10)
          Call PutRaw(Header,Date,Time,size,FNAME)
         ENDIF  ! End of IF want to reset the file date and time.
          IF (.NOT.(NEWTIM)) close(10)
      ENDIF  ! End of IF raw file exists and is ASCII.
**
**  Now, really load the file.
       BinRaw=BinFil(Fname)
       IF (BinRaw) THEN
        print*,' Loading binary file...'
        OPEN(UNIT=10,FILE=FNAME,STATUS='OLD',FORM='UNFORMATTED')
        READ(10)HEADER
        READ(10)DATE
        read(10)time
        read(10)junk
        read(10)size
            IF (SIZE.GT.MaxLin) then
             print*,'ERROR LOADING RAW DATA FILE ',FNAME
            print*,'Number of lines is ¿ maximum.'
            print*,'Number of lines in file = ',size
            print*,'Number of lines allowed = ',MaxLin
            print*,'You must split the file or revise the program.'
            return
            endif
        do i=1,size
           read(10)((raw(i,j,k),k=1,3),j=1,modes)
           enddo
        loaded=.true.
        close(10)
        ELSE      ! file is ASCII
        print*,'Loading ASCII file...'
        open(unit=10,file=FName,status='OLD')
        read(10,9)header
        read(10,9)date
        read(10,9)time
        read(10,9)junk
        i=1
11      CONTINUE
          read(10,*,end=1999)((raw(i,j,k),k=1,3),j=1,modes)
          i=i+1
          GOTO 11
1999      continue
        size=i-1
        close(10)
            IF (SIZE.GT.MaxLin) then
             print*,'ERROR LOADING RAW DATA FILE ',FNAME
            print*,'Number of lines is ¿ maximum.'
            print*,'Number of lines in file = ',size
            print*,'Number of lines allowed = ',MaxLin
            print*,'You must split the file or revise the program.'
            return
            endif
        loaded=.true.
        ENDIF      ! End of IF file is binary
        call GetTime(tstart,date,time)
       rawldd=loaded
       return
       end
*****************************************************************************
**  PutRaw saves raw data in either binary or ASCII format.
      Subroutine PutRaw(Header,date,time,size,fn)
      include 'globalvar.def'
      include 'flags.def'
      character *60 fname,fn,header,date,time,junk,fnnot
      integer i,j,k,size
      i=filcat(fn)
      fname=fn(1:i)//rawext
      IF (GetYN('Do you want to save in binary format? ','Y')) THEN
**  Save in binary format
          open(unit=10,file=fname,status='NEW',form='UNFORMATTED')
          WRITE(10)header
          write(10)date
```

Data Analysis Program (continued: page 12)

```
      write(10)time
      write(10)junk
      write(10)size
      do i=1,size
        write(10)((raw(i,j,k),k=1,3),j=1,modes)
        enddo
      close(10)
      ELSE
        open(unit=10,file=FName,status='NEW')
        write(10,9)header
        write(10,9)date
        write(10,9)time
        write(10,9)junk
       do i=1,size
         write(10,*)((raw(i,j,k),k=1,3),j=1,modes)
         enddo
       CLOSE(10)
       ENDIF
9     FORMAT(A60)
      END
*****************************************************************
**  PutCal saves a calibration data file.
**  It's inputs are:
**          fn     : the file actually loaded, if "loaded" is true.
**          Hdr    : the header of the raw file.
**                   this is saved w/ all files but Pgm files
**          date   : date from raw file
**          time   : time from raw file
**          FrcZrd,Sens,CnvEff,NewNO2,NOySen,Zero: the data saved.
**
**  Its output is Putted, a flag to tell that the file has been saved.
**
**  EXTERNAL CALLS (ANALIB): FileIs,FilCat
*****************************************************************
      subroutine PutCal(FN,Hdr,Date,Time,
     1                  FrcZrd,Sens,CnvEff,NewNO2,NOySen,Zero)
      include 'GlobalVar.def'
      include 'cal_var.def'
      include 'flags.def'
      character*60, FN,FName,Hdr,Date,Time
      integer i,j,k,l
      logical exist,putted
      exist=.false.
      i=filcat(fn)
      FName=fn(1:i)//calext
      IF (GetYN('Do you want to save in binary format? ','Y')) THEN
*  I save in binary format
      open(unit=iCalLb,file=fname,status='NEW',form='UNFORMATTED')
       write(iCalLb),hdr
       write(iCalLb),date
       write(iCalLb),time
       write(iCalLb),lines
       do 710 i=1,lines
         write(iCalLb),(FrcZrd(i,k),k=1,4)
710    continue
       do 720,i=1,lines
         write(iCalLb),(Sens(i,k),k=1,4)
720    continue
       do 730,i=1,lines
         write(iCalLb),(CnvEff(i,k),k=1,4)
730    continue
       do 740,i=1,lines
         write(iCalLb),(NewNO2(i,k),k=1,4)
740    continue
       do 750,i=1,lines
         write(iCalLb),(NOySen(i,K),k=1,4)
750    continue
       do 760,i=1,lines
      do 760 j=1,takes
        do 760 k=1,3          ! Z/NO-a, Z/NO-b, Z/NOy
760         write(iCalLb),(Zero(i,j,k,l),l=1,4)
      putted=.true.
      close(iCalLb)
      ELSE      ! Save in ASCII format
       open(unit=iCalLb,file=fname,status='NEW')
       write(iCalLb,9),hdr
       write(iCalLb,9),date
       write(iCalLb,9),time
9      format (a60)
       write(iCalLb,*),lines
       do 10 i=1,lines
         write(iCalLb,*),(FrcZrd(i,k),k=1,4)
10     continue
       do 20,i=1,lines
         write(iCalLb,*),(Sens(i,k),k=1,4)
20     continue
       do 30,i=1,lines
         write(iCalLb,*),(CnvEff(i,k),k=1,4)
30     continue
       do 40,i=1,lines
         write(iCalLb,*),(NewNO2(i,k),k=1,4)
40     continue
       do 50,i=1,lines
         write(iCalLb,*),(NOySen(i,K),k=1,4)
50     continue
       do 60,i=1,lines
      do 60 j=1,takes
        do 60 k=1,3          ! Z/NO-a, Z/NO-b, Z/NOy
60         write(iCalLb,*),(Zero(i,j,k,l),l=1,4)
      putted=.true.
      close(iCalLb)
      ENDIF
      calsvd=putted
      return
      end
*****************************************************************
**  GetCal loads a calibration data file.
**  Its outputs are:
**          fn     : the file actually loaded, if "loaded" is true.
**          gotten : a flag that tells if a file has been loaded.
**          Hdr    : the header of the raw file.
**                   this is saved w/ all files but Pgm files
**          date   : date from raw file
**          time   : time from raw file
**          FrcZrd,Sens,CnvEff,NewNO2,NOySen,Zero: the data loaded.
**
**  Its input is FN, the file to be loaded.
**
**  EXTERNAL CALLS (ANALIB): FileIs,FilCat
*****************************************************************
      subroutine GetCal(FN,Hdr,Date,Time,
     1                  FrcZrd,Sens,CnvEff,NewNO2,NOySen,Zero)
      include 'GlobalVar.def'
      include 'cal_var.def'
      include 'flags.def'
      character*60, FN,FName,Hdr,Date,Time
      CHARACTER *80 LINE
      integer i,j,k,calin
      logical exist,gotten
      exist=.false.
      i=filcat(fn)
      fname=fn(1:i)//calext
      call FileIs(FName,Exist,calext)
      i=filcat(fname)
      fn=fname(1:i)
      if (exist) then
      IF (BinFil(Fname)) THEN          ! File was saved in binary
      open(unit=calib,file=fname,status='OLD',form='UNFORMATTED')
       read(iCalLb),hdr
       read(iCalLb),date
       read(iCalLb),time
       read (iCalLb),calin          ! CALLIN is the value of LINES when
       do 710 i=1,calin
         read(iCalLb)(FrcZrd(i,k),k=1,4)
710      continue
       do 720,i=1,calin
         read(iCalLb)(Sens(i,k),k=1,4)
720      continue
       do 730,i=1,calin
         read(iCalLb)(CnvEff(i,k),k=1,4)
730      continue
       do 740,i=1,calin
         read(iCalLb)(NewNO2(i,k),k=1,4)
740      continue
       do 750,i=1,calin
         read(iCalLb)(NOySen(i,k),k=1,4)
750      continue
      do 760,i=1,calin
     do 760 j=1,takes
       do 760 k=1,3          ! Z/NO-a, Z/NO-b, Z/NOy
760         read(iCalLb),(Zero(i,j,k,l),l=1,4)
       gotten=.true.
       close(iCalLb)
      ELSE
       open(unit=iCalLb,file=fname,status='OLD')
       read(iCalLb,9),hdr
       read(iCalLb,9),date
       read(iCalLb,9),time
9      format (a60)
       read (iCalLb,*),calin          ! CALLIN is the value of LINES when
       do 10 i=1,calin
         read(iCalLb,*)(FrcZrd(i,k),k=1,4)
10     continue
       do 20,i=1,calin
         read(iCalLb,*)(Sens(i,k),k=1,4)
20     continue
       do 30,i=1,calin
         read(iCalLb,*)(CnvEff(i,k),k=1,4)
30     continue
       do 40,i=1,calin
         read(iCalLb,*)(NewNO2(i,k),k=1,4)
40     continue
       do 50,i=1,calin
         read(iCalLb,*)(NOySen(i,k),k=1,4)
50     continue
      do 60,i=1,calin
     do 60 j=1,takes
       do 60 k=1,3          ! Z/NO-a, Z/NO-b, Z/NOy
60         read(iCalLb,*),(Zero(i,j,k,l),l=1,4)
       gotten=.true.
       close(iCalLb)
     endif          ! end of if exist
      endif      ! end of if binary
     if ((lines.ne.0).and.(calin.ne.lines)) THEN      ! this file was saved.
         print*,
     1'Inconsistent number of lines.  Current LINES = ',lines
         print*,'New value (from .CAL file) LINES = ',calin
         print*,
     1'This should not happen with the same file prefixes!'
         if (condne) then
```

Data Analysis Program (continued: page 13)

```
        print*,
     1'Previously calculated concentrations are no longer valid.'
          condne=.false.
          endif
        if (rawldd) then
          print*,'Raw data previously loaded no longer valid.'
          rawldd=.false.
          endif
        ENDIF
          lines=callin
     caldne=gotten
     return
     end
*****************************************************************
**  PutCon saves a concentration data file.
**  Its inputs are:
**          fn    : the file actually saved, if "putted" is true.
**
**          Hdr   : the header of the raw file.
**                  this is saved w/ all files but Pgm files
**          date  : date from raw file
**          time  : time from raw file
**          ConNO,ConNOy: the data saved.
**
**  Its output is putted, flag to tell that the file has been saved.
**
**  EXTERNAL CALLS (ANALIB): Fileis,FilCat
*****************************************************************
      subroutine PutCon(FN,Hdr,Date,Time,ConNO,ConNOy,ArtFil)
      include 'GlobalVar.def'
      include 'con`var.def'
      include 'flags.def'
      character*60, FN,FName,Hdr,date,time,artfil
      integer i,j,k
      logical exist,putted
        i=flicat(fn)
        fname=fn(1:i)//conext
      IF (GetYN('Do you want to save in binary format? ','Y')) THEN
**      I SAVE in binary format
      open(unit=iconlb,file=fname,status='NEW',form='UNFORMATTED')
        write(iConLb)hdr
        write(iConLb)date
        write(iConLb)time
      write(iConLb)ArtDne
      write(iConLb)ArtFil
        write(iConLb),lines
        do 710, i=1,lines
        do 710, j=1,takes
          write(iConLb)(ConNO(i,j,k),k=1,4)
710       continue
        do 720, i=1,lines
        do 720 j=1,takes
          write(iConLb)(ConNOy(i,j,k), k=1,4)
720       continue
        putted=.true.
        close(iConLb)
      else
        open(unit=iConLb,file=fname,status='NEW')
        write(iConLb,9)hdr
        write(iConLb,9)date
        write(iConLb,9)time
      write(iConLb,*)ArtDne
      write(iconlb,9)ArtFil
 9      format (a60)
        write(iConLb,*),lines
        do 10, i=1,lines
        do 10, j=1,takes
          write(iConLb,*)(ConNO(i,j,k),k=1,4)
10      continue
        do 20, i=1,lines
        do 20 j=1,takes
          write(iConLb,*)(ConNOy(i,j,k), k=1,4)
20      continue
        putted=.true.
        close(iConLb)
      endif ! end of if binary
      consvd=putted
      return
      end
*****************************************************************
**  GetCon loads a concentration data file.
**  Its outputs are:
**          fn    : the file actually loaded, if "loaded" is true.
**          gotten : flag tells if file has been loaded.
**          Hdr   : the header of the raw file.
**                  this is saved w/ all files but Pgm files
**          date  : date from raw file
**          time  : time from raw file
**          ConNO,ConNOy: the data saved.
**
**  Its input is FN, the file to try to load.
**
**  EXTERNAL CALLS (ANALIB): Fileis,FilCat
*****************************************************************
      subroutine GetCon(FN,Hdr,Date,Time,ConNO,ConNOy,ArtFil)
      include 'GlobalVar.def'
      include 'con`var.def'
      include 'flags.def'
      character*60, fn,fname,Hdr,date,time,ArtFil
      integer i,j,k,conlin
      logical exist,gotten
        i=flicat(fn)
        fname=fn(1:i)//conext
        call Fileis(Fname,exat,conext)
        i=flicat(fname)
        fn=fname(1:i)
        if (exist) then
      IF (BinFil(Fname)) THEN      ! file was saved in binary
        open(unit=iconlb,file=fname,status='OLD',form='UNFORMATTED')
          read(iConLb)hdr
          read(iConLb)date
          read(iConLb)time
        read(iconlb)ArtDne
        read(iconlb)ArtFil
          read(iConLb) conlin              ! Value of LINES when
          do 710, i=1,conlin
            do 710 j=1,takes
            read(iConLb)(ConNO(i,j,k),k=1,4)
710       continue
          do 720, i=1,conlin
            do 720 j=1,takes
            read(iConLb)(ConNOy(i,j,k),k=1,4)
720       continue
          gotten=.true.
          close(iConLb)
        else
          open(unit=iConLb,file=fname,status='OLD')
          read(iConLb,9)hdr
          read(iConLb,9)date
          read(iConLb,9)time
        read(iconlb,*)ArtDne
        read(iconlb,9)ArtFil
 9        format (a60)
          read(iConLb,*),conlin            ! Value of LINES when
          do 10, i=1,conlin
            do 10 j=1,takes
            read(iConLb,*)(ConNO(i,j,k),k=1,4)
10        continue
          do 20, i=1,conlin
            do 20 j=1,takes
            read(iConLb,*)(ConNOy(i,j,k),k=1,4)
20        continue
          gotten=.true.
          close(iConLb)
        endif ! End of if binary
        else
          gotten=.false.
        endif      ! end of if exist
      if ((lines.ne.0).and.(conlin.ne.lines)) THEN      ! this file was saved.
          print*,
     1'Inconsistent number of lines.  Current LINES = ',lines
          print*,'New value (from .CON file) LINES = ',conlin
          print*,
     1'This should not happen with the same file prefixes!'
          if (caldne) then
            print*,
     1'Previously calculated CAL data are no longer valid.'
            caldne=.false.
            endif
          if (rawldd) then
            print*,'Raw data previously loaded no longer valid.'
            rawldd=.false.
            endif
        ENDIF
      lines=conlin
      condne=gotten
      return
      end
*****************************************************************
**  PutNit saves ConNit data.  (Nightime NO statistics).
**  NOTE! This Put routine is different from the others because it
**  appends all night data stats to the same file, to be used later for
**  correcting NO concentrations for artifacts.
**  NOTE! The user is responsible for ensuring that the order in which
**  info. is SAVEd is correct.  Otherwise, an error will occur when
**  artifact correction is attempted.
*****************************************************************
      Subroutine PutNit(fn,header,date,time,ConNit)
      include 'globalvar.def'
      include 'con`var.def'
      include 'flags.def'
      character *60 fn,fname,header,date,time
      integer i,j,k
      logical exist,saved,bincut
5     continue
      IF (fn(1:4).eq.'    ') THEN
        IF (GetYN('Do you want to save/append to the file NITE.NIT? ',
     1      'Y')) THEN
          fname='Nite.NIT'
          ELSE
          write(*,200)
200           format('$Enter file name: ')
          read(*,60)fname
60          format(A60)
        ENDIF
      ELSE
      fname=fn(1:flicat(fn))//NitExt
      ENDIF
      inquire(file=fname,exist=exist)
      if (.not.(exist) THEN
```

Data Analysis Program (continued: page 14)

```
      write(*,202)fname
202     format('$File ',A,LenStr(fname),' does not exist  ')
        IF (.not.(GetYN('Create it? ',
     1    'N'))) GOTO 5
        ENDIF
        IF (exist) THEN
        BinOut=BinFil(fname)
        else
        BinOut=GetYN('Do you want to create a binary file? ','Y')
        endif
        IF (BinOut) THEN
          IF (exist) THEN
          print*,'Appending to binary file ...'
          open(unit=iNitLb,file=fname,status='OLD',
     1         access='APPEND',form='UNFORMATTED')
          ELSE
          print*,'Writing to binary file ...'
          open(unit=iNitLb,file=fname,status='NEW',
     1         form='UNFORMATTED')
            ENDIF
            write(iNitLb)NNit
            do 10 i=1,Nnit
            write(iNitLb)(ConNit(i,j),j=1,4)
10            continue
          saved=.true.
          close(iNitLb)
            else
          IF (exist) THEN
          print*,'Appending to ASCII file ...'
          open(unit=iNitLb,file=fname,status='OLD',
     1         access='APPEND')
          ELSE
          print*,'Writing to ASCII file ...'
          open(unit=iNitLb,file=fname,status='NEW')
          ENDIF
            write(iNitLb,*)NNit
            do 20 i=1,Nnit
            write(iNitLb,100)(ConNit(i,j),j=1,4)
20            continue
            close(iNitLb)
          saved=.true.
          ENDIF     ! End of IF binout
      nitsvd=saved
      return
100     format(4(1x,F9.2))
      end
*****************************************************************
** GetNit retrieves nighttime NO statistics
*****************************************************************
      Subroutine GetNit(fn,ConNit)
      include 'globalvar.def'
      include 'con var.def'
      include 'flags.def'
      character *60 fn,fname,header,date,time
      integer i,j,k
      logical exist,gotten
      IF (fn(1:4).ne.'    ') THEN
        fname=fn(1:filcat(fn))//NitExt
        else
        fname='NITE.NIT'
        print*,'Looking for file NITE.NIT.'
        endif
      inquire(file=fname,exist=exist)
      if (exist) then
        if (BinFil(Fname)) THEN
          OPEN(UNIT=iNitLb,file=fname,
     1         status='OLD',form='UNFORMATTED')
          Nnit=0
900         continue
          read(iNitLb,end=991)Nnit1
          do 10 i=NNit+1,Nnit+Nnit1
            read(iNitLb)(ConNit(i,j),j=1,4)
10          continue
          Nnit=Nnit+NNit1
           goto 900
991         continue
          close(iNitLb)
          gotten=.true.
          else
          open(iNitLb,file=fname,status='OLD')
          Nnit=0
910         continue
          read(iNitLb,*,end=992)Nnit1
          do 20 i=NNit+1,NNit+NNit1
            read(iNitLb,*)(ConNit(i,j),j=1,4)
20          continue
          NNit=NNit+NNit1
          goto 910
992         continue
          close(iNitLb)
          gotten=.true.
          endif
        else
        print*,'File does not exist.'
        gotten=.false.
        endif
      NitDne=.true.
      return
60    format(A60)
      end
*****************************************************************
** PutPgm saves a programmable constant data file.
** Its inputs are:
**          fname  : the file actually saved, if "putted" is true.
**          gotten : flag tells if file has been loaded.
**          Hdr    : the header of the raw file.
**                   this is saved w/ all files but Pgm files
**      /global/usenoy,ccg,numave,rsdmax,navg,maxmn,minmn
**                 : the stuff to be saved.
** Its output is putted, flag that says file has been saved.
**
** EXTERNAL CALLS (ANALIB): FileIs,FilCat
*****************************************************************
      subroutine PutPgm(FN,Hdr)
      include 'GlobalVar.def'
      include 'flags.def'
      integer i,j,k
      character*60 fn,fname,hdr
      logical exist,putted
       i=filcat(fn)
       fname=fn(1:i)//pgmext
       open(unit=iPgmLb,status='NEW',file=fname)
      write (iPgmLb,8),PgmVer          ! PgmVer is the version of the current
       write (iPgmLb,9),hdr            ! version of ANALYZE.
8     format (F10.4,' Version Number of ANALYZE.')
9      format (a60)
       write (iPgmLb,*),UseNOy
       write (iPgmLb,*),ccg
       write (iPgmLb,*),NumAve
       write (iPgmLb,*),RSDMax
       write (iPgmLb,*),MaxMn
       write (iPgmLb,*),MinMn
      write (iPgmLb,*),SarMin
       write (iPgmLb,*),Navg
       putted=.true.
       close(iPgmLb)
      pgmsvd=putted
      return
      end
*****************************************************************
** GetPgm loads a programmable constant data file.
** Its outputs are:
**          fname  : the file actually loaded, if "loaded" is true.
**
**          Hdr    : the header of the raw file.
**                   this is saved w/ all files but Pgm files
**      /global/usenoy,ccg,numave,rsdmax,navg,maxmn,minmn
**                 : the stuff to be saved.
** Its input is FName, which returns the file actually loaded.
**
** EXTERNAL CALLS (ANALIB): FileIs,FilCat
*****************************************************************
      subroutine GetPgm(FN,hdr)
      include 'GlobalVar.def'
      include 'flags.def'
      integer i,j,k
      real VerNew
      character*60 FN,fname,hdr,junk
      logical exist,gotten
       i=filcat(fn)
       fname=fn(1:i)//pgmext
       call fileis(fname,exist,pgmext)
       i=filcat(fname)
       fn=fname(1:i)
       if (exist) then
         open(unit=iPgmLb,status='OLD',file=fname)
       read (iPgmLb,*),VerNew
       if (INT(VerNew).NE.INT(PgmVer)) then
           print*,
     1'You are trying to use incompatible versions of ANALYZE and'
           print*,'the PGM file.'
          print*,'Version in PGM file is ',VerNew
          print*,'Version of ANALYZE is ',PgmVer
          print*,'You must find an old version of ANALYZE.'
          stop
          endif
        read (iPgmLb,9),hdr
9       format (a60)
        read (iPgmLb,*),UseNOy
        read (iPgmLb,*),ccg
        read (iPgmLb,*),NumAve
        read (iPgmLb,*),RSDMax
        read (iPgmLb,*),MaxMn
        read (iPgmLb,*),MinMn
       read (iPgmLb,*),SArMin
         read (iPgmLb,*),Navg
       endif
       gotten =.true.
       close(iPgmLb)
      return
      end
*****************************************************************
      SUBROUTINE GetCPS (Fname,fcps,cps5,Ndat)
      include 'cps var.def'
      include 'globalvar.def'
      include 'flags.def'
      character *60 fcps,fname
      character *1 YesNo
      logical exist
10    continue
```

Data Analysis Program (continued: page 15)

```
      print*,'Current data file name is ',fname
      print*,'Enter full name of cps file:'
      read 60,fcps
60      FORMAT(A60)
      inquire(file=fcps,Exist=exist)
      if (.not.exist) then
       print*,'ERROR!  File does not exist.'
       goto 10
       endif
      IF (BinFil(fcps)) THEN          ! File was saved in binary format
       write(*,101)fcps
101       format(1x,'Reading file ',A¡LenStr(fcps,60)¿,
     1     ' in binary format.')
      print*,' '
      OPEN(unit=icpslb,file=fcps,form='UNFORMATTED',status='OLD')
      read(icpslb)Ndat
      Do i=1,Ndat
       ri = i
       if (ri/10000.0.eq.int(ri/10000.0)) write(*,22)i
       read(icpslb)cps5(i)
       enddo
      close(icpslb)
      ELSE
      write(*,102)fcps
102       format(1x,'Reading file ',A¡LenStr(fcps,60)¿,
     1     ' in ASCII format.')
      open(unit=icpslb,file=fcps,status='OLD')
      idat=0
      print*
20      continue
       idat=idat+1
       ri = idat
       if (ri/500.0.eq.int(ri/500.0)) write(*,22)idat
22        format('+','Reading line ',I8)
       if (idat.gt.maxpt) goto 999
       read(icpslb,*,end=999)cps5(idat)
       goto 20
999       continue
      if (idat.gt.maxpt) print*,'Stopped reading after ',
     1          maxpt,' lines.'
      Ndat=idat-1
      print*,'Loaded ',ndat,' lines.'
      close(icpslb)
300       continue
       IF (GetYN(
     1'Would you like to save the cps file in binary format? '.
     1'Y'))     THEN
           print*,'Saving in binary format ...'
          Call Putcps(fcps,cps5,Ndat)
          ENDIF
       ENDIF
      return
      end
*****************************************************************
** PutCps saves cps data in binary format.  This is used after reading cps
** data that was in ASCII format.
**
      SUBROUTINE PutCPS (fcps,cps5,Ndat)
      include 'cps'var.def'
      include 'flags.def'
      character *60 fcps,fname
      logical exist
      open(unit=icpslb,file=fcps,status='NEW',form='UNFORMATTED')
      write(icpslb)Ndat
      do i=1,ndat
       write(icpslb)cps5(i)
       enddo
      close(icpslb)
      return
      end
*****************************************************************
*****************************************************************
************************ MODULE ANALIB.FOR ************************
*****************************************************************
********************* A N A L I B . F O R *************************
*****************************************************************
* ANALIB.FOR contains general routines used by ANALYZE
* for the most part, these should be useful in other programs with
* minor modifications (except startup, which is pretty specific).
*
* SUBROUTINES:
*   Files  returns a file name and an existance flag.
*   BinFil  True if file FNAME is unformatted (binary). False if ascii.
*   Interp  interpolates (linearly) between 2 points.
*   RadOk   returns 999 if any of one of a list is greater than it should be
*   RunAve  takes a running average of S values of a list.
*   StartUp  is ANALYZE specific, the startup routine.
*   GetTime  returns Julian date from strings.
*   IC      turns a character digit into an integer digit.
*   FilCat  returns the first occurence of a space or . in a filename
*   SunPos  returns the solar zenith angle
*   Stat    returns avg,sd,min,max
* EXTERNAL CALLS
*   getpgm (analile)
*   putpgm (analile)
*   prgm   (analyze)
* EXTERNAL FILES parameters.def, globalvar.def, analile
*****************************************************************
*****************************************************************
***     Checks to see if FName exists.
***       If not, it asks for an alternate name until it gets a valid
***        answer, or no name is given.
***       If no name is given, it returns false.
***       If a valid name is given, it returns true.
***     input
***       fname  the file name to try (extension is ignored)
***       ext    the extension of the file name
***     output
***       fname  the file name used
***       exist  flag if file found
*****************************************************************
      subroutine Files(FName,Exist,ext)
      character*60 FName,fn
      character*4  Ext
      logical      Exist,there
      integer      i
      Exist=.false.
      if (FName.eq.'QUIT') then
       Exist=.false.
       FName='xxxx'
       RETURN
      endif
     i=FilCat(Fname)
     Fname=Fname(1:i)//Ext
10     Inquire(file=FName,Exist=there)
      if (.not.there) then
      call bell
      write(*,100)Fname
100       format(1x,'File ',A¡LenStr(Fname,60)¿,' does not exist.'/,
     1     '$Enter a new name (RETURN to cancel): ')
       read 9,Fn
9       format(a60)
       if (LenStr(FN,60).eq.0) then
        Exist=.false.
        RETURN
       endif
       i=index(fn,' ')-1
       fname=fn(1:i)//ext
      else
       Exist=.true.
       RETURN
      endif
      goto 10
     end
*****************************************************************
** LOGICAL FUNCTION BinFil(Fname).  Fname (character *60) = file name
** Tests file to determine whether it's in binary or ascii format
**
      LOGICAL FUNCTION BinFil(FNAME)
      CHARACTER *1 CHAR
      CHARACTER *60 Fname
      open(UNIT=99,file=FNAME,form='UNFORMATTED',status='OLD')
      read(99,err=10)char
** File is binary.
       BinFil=.TRUE.
       close(99)
       RETURN
10     continue
       BinFil=.FALSE.
       close(99)
        RETURN
      END
*****************************************************************
**interpolates at time between (p1,p2).  int is returned.
**inputs
**       p1    first point.
**       p2    second point.
**       time  time of interpolation
**       iave  the index in RSDMAX to use to check validity of p1,p2.
**
**outputs
**       int(4) interpolated value.
** if p1 is bad, returns p2.  if p2 is bad, returns p1.
** if both bad, returns 999.
** otherwise, returns value as follows:
**
** Mean  = time*((mean2-mean1)/(time2-time1))  + bmet
**  SD   = calculated by error propagation.
** Time  = time
**Scount = max(Scount1,Scount2)
*****************************************************************
      subroutine Interp(int,p1,p2,time,iave)
      include 'globalvar.def'
      real int(4),p1(4),p2(4),time,x(2),M
      integer i,iave
      logical oka,okb
      if (iave.eq.999) then
       oka=((P1(imean).ne.999.).and.(P1(iscnt).ne.999.))
       okb=((P2(imean).ne.999.).and.(P2(iscnt).ne.999.))
       else
       okb=( (p2(iscnt).le.rsdmax(iave))          ! Points are OK if they
     1      .AND.( (p2(imean).ge.minmn(iave))     ! satisfy the Scnt
     1           .AND.(p2(imean).le.maxmn(iave))))     ! and mean range
       oka=( (p1(iscnt).le.rsdmax(iave))          ! constraints
     1      .AND.( (p1(imean).ge.minmn(iave))
     1           .AND.(p1(imean).le.maxmn(iave))))
       endif
      if (.not.oka) then                  ! if p1 is bad, use p2
       do 10,i=1,4
        int(i)=p2(i)
```

Data Analysis Program (continued: page 17)

```
      write(*,101)
101     format('$Please type the default PGM file',
     1        ' name (with no extension): ')
        read 9,fil
        l=filcat(fil)
        fil=fil(1:l)//pgmext
        write(15,9),fil
        print*,'Thanks!'
        close(15)
        inquire(file=fil,exist=there)
        if (there) then                          !if new .pgm exists,
          call GetPgm(fil,hdr)                   !use it and leave.
        else                                     !otherwise, make a new
          print*,'ERROR! .CNS file does not exist'  !one.
          print*,'Please program the file now...'
        call bell
          call Prgm
          call PutPgm(fil,there,hdr)
          print*,'Thank you for you patience.',
     1          ' Now, on with the program!'
        endif
      endif
      return
      end
*****************************************************************************
** Converts time loaded from raw file into Julian time.  Accounts for
** leap year, even!  (but-not-every-other-hundred-year-leap-year-ingore)
**
** inputs
**   day   date taken from raw file...
**   time  time taken from same file.
** outputs
**    StDay Julian date.
** calls
**    IC
*****************************************************************************
      subroutine GetTime(StDay,date,time)
        real stday,dy,hr,mn,sc,yr,mon
        character*1,a
        character*60, date, time
        character*3,month,day,hour,min
        character*5,year,sec
          sec=time(6:12)
          sc=10.0*IC(sec(1:1))+1.0*IC(sec(2:2))+0.1*
     1      IC(sec(4:4))+0.01*IC(sec(5:5))
          min=time(5:6)
          mn=10.0*IC(min(1:1))+1.0*IC(min(2:2))
          hour=time(2:3)
          hr=10.0*IC(hour(1:1))+1.0*IC(hour(2:2))
          day=date(5:6)
          dy=10.0*IC(day(1:1))+1.0*IC(day(2:2))
          month=date(2:3)
        mon = 10.0*IC(month(1:1))+1.0*IC(month(2:2))
          year=date(8:11)
          yr=1000.0*IC(year(1:1))+100.0*IC(year(2:2))
     1      +10.0*IC(year(3:3))+1.0*IC(year(4:4))
          StDay=0
          if (mon.ne.1) then
            StDay=StDay+31
          else
            goto 10
          endif
          if (mon.ne.02) then
            StDay=StDay+28
            if (amod(yr,4.0).eq.0) StDay=StDay+1
          else
            goto 10
          endif
          if (mon.ne.03) then
            StDay=StDay+31
          else
            goto 10
          endif
          if (mon.ne.04) then
            StDay=StDay+30
          else
            goto 10
          endif
          if (moN.ne.05) then
            StDay=StDay+31
          else
            goto 10
          endif
          if (mon.ne.06) then
            StDay=StDay+30
          else
            goto 10
          endif
          if (mon.ne.07) then
            StDay=StDay+31
          else
            goto 10
          endif
          if (mon.ne.08) then
            StDay=StDay+31
          else
            goto 10
          endif
          if (mon.ne.09) then
            StDay=StDay+30
          else
            goto 10
          endif
          if (Mon.ne.10) then
            StDay=StDay+31
          else
            goto 10
          endif
          if (mon.ne.11) then
            StDay=StDay+30
          else
            goto 10
          endif
          if (mon.ne.12) then
            StDay=StDay+31
          else
            goto 10
          endif
10        continue
          StDay=StDay+dy+(hr+(mn+sc/60.0)/60.0)/24.0
        return
        end
*****************************************************************************
** inputs a character (a) and returns it's value ('0' -¿ 0).  Non-numeric
** characters are treated as zero.
*****************************************************************************
        function IC(a)
        character*1 a
          if ((ichar(a).le.58).and.(ichar(a).ge.48)) then
            IC=IChar(a)-48
          else
            IC=0
          endif
        return
        end
*****************************************************************************
** Finds the first of the first . or the first ' (space)
** in fil
**
** input is fil     : a 60 char str
** ouptut is FilCat : a postion
*****************************************************************************
        function FilCat(fil)
        integer e,b
        character*60,fil
          a=index(fil,' ')-1  !finds first occurences
          b=index(fil,'.')-1
          if (a.lt.0) a=61    !if no occurence, ignore
          if (b.lt.0) b=61
          FilCat=min(a,b)
        return
        end
*****************************************************************************
** Returns solar zenith angle
*****************************************************************************
        SUBROUTINE SUNPOS (DAY,YEAR,HouR,MIN,SEC,LAT,Long,
     1                     Zenith)
C*
C  Calculates solar zenith angle for use in photolysis calcs.
C*
C*  MODIFIED VERSION
C*  USES LONGITUDE TO CALC LOCAL SOLAR TIME FOR WESTERN HEMISPHERE
C*
        IMPLICIT REAL (A-H,O-Z)
        REAL MIN, LATITUDE,LAT,LONG
        REAL PTEMP
        PARAMETER (pi=3.14159265358979323846264338327 9)
        PARAMETER (TWOPI=2*PI,RAD=PI/180.,RIGHT=PI/2.)
C  ** - SIGN IN NEXT LINE INSERTED 4/4 **
        LATITUDE = -RAD*LAT
C
C COMPUTE YEAR RELATIVE TO 1980 AND IF A LEAP YEAR
c*  Next line inserted 5/24/1989
        HR = HouR + LONG/350.0*24.0      ! Correct UT -¿ Local Solar Time
        DELYR=YEAR-1980.
        PTEMP=DELYR
        LEAP=IFIX(PTEMP/4.)
C COMPUTE DECLINATION FROM DATE
        T=HR+(MIN+SEC/60.)/60.
        TIME=DELYR*365.+LEAP+DAY-1.+T/24.
        IF ((DELYR.EQ.LEAP*4.).AND.(YEAR.GT.1980.))TIME=TIME-1.
        IF (YEAR.GT.1980.)TIME=TIME+1
        IF (YEAR.GT.2000.)TIME=TIME-1
        THETA=TWOPI*TIME/365.25
        G=-0.06564993-4.541864E-7*TIME+THETA
        EL=4.866563352+3.67658E-7*TIME+(0.0334339-2.288E-9*TIME)
     1             *SIN(G)+3.439303E-4*SIN(2.*G)+THETA
        EPS=0.409138-6.2149E-9*TIME
        DECLINATION=ASIN(SIN(EL)*SIN(EPS))
C
C  compute zenith angle
C COMPUTE AZIMUTH AND ELEVATION
        H=T*TWOPI/24.
        ELEVATION=ASIN(SIN(LATITUDE)*SIN(DECLINATION)
     1                +COS(LATITUDE)*COS(DECLINATION)*COS(H))
        X=-COS(DECLINATION)*SIN(H)/COS(ELEVATION)
        IF (X.GT.1.) X=1.
        IF (X.LT.-1.) X=-1.
        AZIMUTH=ASIN(X)
C
```

Data Analysis Program (continued: page 16)

```
10      continue
      endif
      if (.not.okb) then                    !if p2 is bad, use p1
        do 20,i=1,4
          int(i)=p1(i)
20      continue
      endif
      if ((.not.(oka)).and.(.not.(okb))) then   !if both p1,p2 bad, return
        do 30,i=1,4
          int(i)=999
          return
30      continue
      endif
      if ((.not.(okb)).or.(.not.(oka))) return  !if either bad, leave.
      if ((oka).and.(okb)) then                 !otherwise, interpolate.
        A = 1.0 - (time-P1(itime))/(P2(itime)-P1(itime))
        B = (time-P1(itime))/(P2(itime)-P1(itime))
          M=(p2(imean)-p1(imean))/(p2(itime)-p1(itime))
        int(imean)=M*(time-p1(itime))+p1(imean)
        int(isd) = sqrt( (A*P1(isd))**2. + (B*P2(isd))**2.)
          int(itime)=time
          int(iscnt)=max(p1(iscnt),p2(iscnt))
      endif
      return
      end
*****************************************************************************
**  checks all s of x(s,iscnt) to see if each is less than rsdmax(y(s,iScnt)).
**  checks all s of x(s,imean) to see if each is less than maxmn(y(s,iscnt)).
**  checks all s of x(s,imean) to see if each is more than minmn(y(s,iscnt)).
**  Checks all s of x(s,imean) to see if any=999.
** NOTE THAT THE SD CHECKS ARE AGAINST THE ABSOLUTE VALUES OF X(i,j).
**  inputs
**          x(s)  list of values to check.
**          s     number of x's
**          y(s)  list of rsdmax indexes (one for each x)
**  outputs
**          returns 999 if point is out of range, otherwise returns -1.
*****************************************************************************
      function RSDOK(x,s,y)
      include 'globalvar.def'
      integer s,y(s)
      real    x(s,4)
        max=-1
        do 10,i=1,s                             !Check Scnt.
          if ( abs(x(i,iScnt)).gt.rsdmax(y(i)) ) max= 999
10      continue
        do 20,i=1,s                             !Check Max.
          if ( (x(i,iMean)).gt.maxmn(y(i)) ) max = 999
        if (x(i,imean).eq.999.) max=999
20      continue
        do 30,i=1,s                             !Check Min.
          if ( (x(i,iMean)).lt.minmn(y(i)) ) max = 999
30      continue
        rsdok=max
      return
      end
*****************************************************************************
**  takes an average of numave values centered around line in
**  list(line,-imean..iscnt)
**  if line is too close to one end or another of the array
**  then it shifts the center up or down until all of numave values are
**  within the bounds of the list.
**  The number of points in the average is governed by NUMAVE(iave).
**  However, if some of those points do not satisfy the range and RSDMAX
**  constraints, they are omitted and are not replaced.
**  inputs
**          line   line of center
**          list   list that average is taken from.
**          iave   index in RSDMAX, NUMAVE MAXMN and MINMN for values given.
**  outputs
**          ave(4) running average
**          SD of run. average is SD of observed values / sqrt(N)
*****************************************************************************
      subroutine RunAve(Ave,line,list,iave)
      include 'globalvar.def'
      real ave(4),list(maxlin,4),MaxSc
      REAL *8 x,sd,SS,svg8
      integer line,i,h,l,num,iave,Ntot
      logical OK
        if (lines.lt.numave(iave)) then     !not enough data lines for
          l=1                               !average, use max. available
          h=lines
          Num=lines
        else                                !otherwise, find the endpoints.
          num=numave(iave)
          l=LINE+int(num/2.0)
          h=LINE+int(num/2.0)-(1-mod(num,2))
        endif
10      continue                            !if lower limit is less than
        if (l.lt.1) then                    !1, move range up until it is
          l=l+1                             !one.
          h=h+1
          goto 10
        endif
20      continue
        if (h.gt.lines) then                !if upper limit is greater than
          l=l-1                             !then number of lines then
          h=h-1                             !shift the averageing range down
          goto 20                           !until it fits within the list.
        endif
** note the above will never shift the range back below the lower limit
** by the following reasoning.  If the number of averages is smaller than
** the length of the list (the value of lines), then there's no problem,
** it will always fit.  If the number of averages is larger, it will be
** cut to (0..lines) and no shifting will occur.
      Ntot=0
      MaxSc=0.0
      SS=0.0
      X=0.0
        do 30, i=l,h                        !only use point if it falls
        OK=((list(i,iscnt).LE.RSDMAX(iave))     !within the allowable RSDMAX's
     1    .AND. ((list(i,imean).ge.MinMn(iave))     ! and is within
     1          .AND.(list(i,imean).le.MaxMn(iave))))     ! [MinMn,MaxMn]
        if (OK) then
          x=x+list(i,imean)
          ss=ss+list(i,imean)**2.0
          Ntot=Ntot+1
          MaxSc=Max(MaxSc,list(i,iscnt))
          SD=list(i,isd)
          endif
30      continue
      if (ntot.eq.0) then
          do 31 i=1,4
31          ave(i)=999.
          else
          ave(imean)=x/ntot
          Avg8=x/Dfloat(ntot)
          ave(itime)=list(line,itime)
          ave(iscnt)=MaxSc
          if (Ntot.gt.1) then
            if (ss.GT.Dfloat(ntot)*Avg8**2.) THEN
              SD = SQRT((ss-Dfloat(ntot)*Avg8**2.)
     1              /(Dfloat(ntot)-1.))
            ave(isd)=SD/sqrt(float(ntot))
            else
            ave(isd)=SD
            endif
          else
          ave(isd)=sd
          endif
        endif
      return
      end
*****************************************************************************
** This horribly ugly pig pen hodge podge routine does the stuff needed
** to initialize ANALYZE.  There are no inputs and no outputs (other than
** then initialized variables: programmable constants.
** calls
**  filcat
**  getpgm (external anafile)
**  putpgm (external anafile)
**  prgm   (external analyze)
*****************************************************************************
      subroutine StartUp
      include 'parameters.def'
      logical there
      character*60,fil,hdr,fill
      integer l
      print *,' '
      print *,' '
      print *,'                 WELCOME TO [NO] ANALYZE'
      print *,' '
      print *,'                    written by'
      print *,' '
      print *,'                  Richard Honrath'
      print *,'                      and'
      print *,'                  Randy Meitner'
      print *,' '
      print *,'                     3/90'
      print *,'                  Updated 11/90'
      print 2,PgmVer
2     format(1x,'                  VERSION ',f4.2)
      print *,' '
      print *,' '
      print *,'All commands must be in CAPITAL LETTERS.',
     +'  Press CAP LOCK, please.'
      print *,'Type HELP for more information.'
        do 1 i=1,4
          print *,' '
1       continue
        hdr='DEFAULT PROGRAMMABLE CONSTANTS'
        inquire(file='START.CNF',exist=there)       !check to see if
        if (there) then                             !start.cnf and
          open(unit=15,file='START.CNF',status='OLD')   !startup .pgm files
          read(15,9,end=999),fil                    !exist.  if not, goto
9         format(a60)                               !999
          close(15)
          inquire(file=fil,exist=there) !checks for .pgm file.
          if (.not.there) goto 998
          open(unit=15,file=fil,status='OLD')
          read(15,9,end=999),hdr
          close(15)                                 !if .pgm exists,
          call GetPgm(fil,hdr)                      !load it and leave.
        else
998       print*,'ERROR! Startup file START.CNF missing.'
        call bell
999       print*,'ERROR! No startup file ',fil      !create new startup.
        call bell
          print*,'Creating new startup...'
          open(unit=15,file='START.CNF',status='NEW')
```

Data Analysis Program (continued: page 18)

```
      IF (SIN(ELEVATION).GE.
     &        (SIN(DECLINATION)/SIN(LATITUDE))) THEN
        IF (AZIMUTH.LT.0.0) AZIMUTH=AZIMUTH+TWOPI
        AZIMUTH=PI-AZIMUTH
      END IF
      AZIMUTH=(AZIMUTH+PI)/RAD
      ELEVATION=(-ELEVATION)/RAD
      Zenith = 90-ELEVATION
      RETURN
      END
*****************************************************************************
** Returns simple statistics: mean, sd, min, max
*****************************************************************************
      Subroutine Stat(x,Ndim,Ndat,avg,sd,rmin,rmax)
      dimension x(ndim)
      sum = 0.0
      ss = 0.0
      rmax=-1.E10
      rmin=1.E10
      do i=1,ndat
        sum=sum+x(i)
        ss = ss + x(i)**2.0
        if (x(i).lt.rmin) rmin=x(i)
        if (x(i).gt.rmax) rmax=x(i)
        enddo
      if (ndat.gt.0) then
        avg = sum/float(ndat)
        else
        avg=999.
        endif
      rnum = ss-ndat*avg**2.0
      if ( (rnum.gt.0).and.(ndat.gt.1)) then
        sd = sqrt( rnum/(float(ndat-1)))
        else
        sd = 999.
        endif
      return
      end
*****************************************************************************
** RANGE.  Returns min and max satisfying s/scntj=input and within
** allowable range (input).  Also returns
** fraction satisfying s/scntj=input.  (999s are not included in frcn
** calculation.)
*****************************************************************************
      Subroutine Range(x,xmax,MinNpos,maxpos,xmin,xmax,frcn)
      include 'parameters.def'
      dimension x(MaxZ,2)
      real minpos,maxpos
      xmin=1.e10
      xmax=-1.e10
      Ntot=0
      Ngood=0
      do i=1,MaxZ
        if ( (x(i,2).le.xmax).AND.
     1     ( (x(i,1).ge.minpos).and.(x(i,1).le.maxpos)) ) then
          Ngood=Ngood+1
          Ntot=Ntot+1
          if (x(i,1).gt.xmax) xmax=x(i,1)
            if (x(i,1).lt.xmin) xmin=x(i,1)
          else
          if ((x(i,1).ne.999).and.(x(i,2).ne.999)) Ntot=Ntot+1
          endif
        enddo
      IF (ntot.gt.0) then
          frcn = float(ngood)/float(ntot)
          else
          frcn = 0.0
           endif
      return
      end
*****************************************************************************
** GetYN.  Logical function.
** Returns true if user enters Y, False if user enters N.
** Input:      PrStr: Prompting string
**             Def  : Default ('Y' or 'N')
*****************************************************************************
      LOGICAL FUNCTION GetYN(PrStr,Def)
      character *(*) PrStr
      character *1 YesNo,Def
5     continue
      Call bell
      write(*,10)PrStr,Def
      read(*,11)YesNo
      if (LenStr(YesNo,1).eq.0) YesNo=Def     ! User hit return
      IF ((YesNo.ne.'Y').and.(YesNo.ne.'N')) THEN
          print*,'Please enter Y or N.'
          goto 5
          ENDIF
      IF (YesNo.eq.'Y') THEN
          GetYN=.true.
          ELSE
          GetYN=.false.
          ENDIF
      RETURN
10      format('$',A,LenStr(PrStr,80),¿,'[',A1,']: ')
11      format(A1)
      END
*****************************************************************************
** LenStr. Returns the length of a string
*****************************************************************************
      INTEGER FUNCTION LenStr(str,iSiz)
** Note: iSize is a relic and is not needed.
      character *(*) str
      do i=1,LEN(STR)
        if (ichar(str(i:i)).eq.32) then
          lenS=min(lenS,(i-1))
          else
          lenS=i
            endif
        enddo
      LENSTR = LENS
      return
      end
*****************************************************************************
** Bell - Beeps the terminal without adding a carriage return.
*****************************************************************************
      Subroutine Bell
      write(*,100)char(7)
100     format('+',A1)
      return
      end
*****************************************************************************
** Convert 1-2 digit integer to character*2.
**
      subroutine itoch(iday,day)
      character *2 day
      character *1 chfri
      if (iday.lt.10) then
          day(1:1)='0'
          day(2:2)=chfri(iday)
          else
          iten=int(iday/10)
          day(1:1)=chfri(iten)
          day(2:2)=chfri(iday-10*iten)
          endif
      return
      end
      function chfri(i)
      character *1 chfri
      chfri = char(i+48)
      return
      end
*****************************************************************************
*****************************************************************************
*************************** MODULE ANAUTIL.FOR ******************************
*****************************************************************************
************************** ANAUTIL.FOR **************************
*****************************************************************************
** ANAUTIL.FOR
** Contains UTIL subroutine and sub-subroutines: utility programs used
** with ANALYZE system.
**
*****************************************************************************
      SUBROUTINE UTIL(Date,Time,FrcZrd,Sens,CnvEff,NewNO2,
     1               NOySen,Zero,ConNO,ConNOy,ConNit,fil,header)
      INCLUDE 'globalvar.def'
      INCLUDE 'cal_var.def'
      INCLUDE 'con_var.def'
      INCLUDE 'flags.def'
      character *60 fil,header,date,time
      minch=1
      maxch=5
** Display menu
105     continue
      write(*,10)char(7)
10      format(1x,
     1'*************************************************',
     1/,
     1'****************** UTILITY SUBROUTINES ******************',
     1/,/,
     1 5x,'Choices: ',/,
     1 10x,
     1'1  Create SENS.CAL etc ASCII calibration summary files.',/,
     1 10x,'2  Convert between .CAL and .BCAL calibration files.',
     1 /,
     1 10x,'3  Write ASCII file of running-average CnvEff.',/,
     1 10x,'4  Write concentration ASCII file ',
     1 'for MINITAB etc. use.',/,
     1 10x,'5  EXIT',/,
     1 /,'$ Please enter your choice: ',A1)
      read*,ich
      if ((ich.lt.minch).or.(ich.gt.maxch)) goto 105
      if (ich.eq.1) call CalMtb(FrcZrd,Sens,CnvEff,NOySen,Zero)
      if (ich.eq.2) call CalBin
      if (ich.eq.3) call CnvOut(fil,CnvEff,NEWNO2)
      if (ich.eq.4) call ConMtb(fil,ConNO,ConNOy)
      if (ich.eq.5) return
      return
      end
*****************************************************************************
* Program to convert .CAL output from CALMTB into a smaller, faster binary
* file, OR vice versa.  NOTE THAT THIS IS NOT FOR THE NNOYD*.CAL FILES!
      SUBROUTINE CalBin
      dimension xmin(48000),xsd(48000),xscnt(48000),Perc(48000),Pbin(50)
      character *60 fname
      logical binfil
      write(*,55)
55      format('$Enter file name: ')
      call bell
      read(*,60)fname
```

Data Analysis Program (continued: page 19)

```
60    format(a60)
      if (binfil(fname)) THEN      ! file is already binary - convert to ASCII
        print*,'Will convert binary to ASCII'
        open(10,file=fname,status='OLD',FORM='UNFORMATTED')
        read(10)ndat
        do i=1,ndat
          read(10)xmn(i),xsd(i),xscnt(i)
          enddo
        close(10)
        print*,'Ndat = ',ndat
        print*,'Writing to ASCII file. ...'
        open(10,FILE=FNAME,STATUS='NEW')
        do i=1,ndat
          write(10,*)xmn(i),xsd(i),xscnt(i)
          enddo
        close(10)
        else
      print*,'Reading from ASCII file ',fname
      open(unit=10,file=fname,status='OLD')
      i=0
10      continue
          i=i+1
        read(10,*,end=999)xmn(i),xsd(i),xscnt(i)
        goto 10
999     continue
      ndat=i-1
      print*,'Ndat = ',ndat
      close(10)
      print*,'Writing binary file to new version of ',fname
      open(10,file=fname,status='NEW',form='UNFORMATTED')
      write(10)ndat
      do i=1,ndat
        write(10)xmn(i),xsd(i),xscnt(i)
        enddo
      close(10)
      endif
      print*,'Done.'
      return
      end
*****************************************************************
** cal data into ASCII file for MINITAB analysis.
** Input: FrcZrd,Sens,CnvEff,NoySen,Zero
** CalMtb is called via the command SAVE MTB
** Time is not saved (only mean, sd, scnt).
** Data are appended into the following files:
**   Sens.Cal
**   NOySen.Cal
**   FrcZrd.Cal
**   CnvEff.Cal
**   ZNO.Cal
**   ZNOy.Cal
** Within each file, data are ordered by time, with each row holding
**       mean   sd   scnt
*****************************************************************
      Subroutine CalMtb(FrcZrd,Sens,CnvEff,NOySen,Zero)
      include 'GlobalVar.def'
      include 'cal`var.def'
      integer i,j,k,l
      logical exist
      print*,'Saving to .CAL MINITAB summary files ...'
      open(unit=icalib,file='Sens.Cal',status='OLD',access='APPEND')
      do i=1,lines
        write(icalib,100)Sens(i,imean),sens(i,isd),sens(i,iscnt)
        enddo
      close(icalib)
      open(unit=icalib,file='NOySen.Cal',status='OLD',access='APPEND')
      Do i=1,lines
        write(icalib,100)NOySen(i,imean),NOySen(i,isd),noysen(i,iscnt),
     1     noysen(i,itime)
        enddo
      close(icalib)
      open(unit=icalib,file='FrcZrd.Cal',status='OLD',access='APPEND')
      do i=1,lines
        write(icalib,100)frczrd(i,imean),frczrd(i,isd),frczrd(i,iscnt),
     1     frczrd(i,itime)
        enddo
      close(icalib)
      open(unit=icalib,file='CnvEff.Cal',status='OLD',access='APPEND')
      do i=1,lines
        write(icalib,100)CnvEff(i,imean),cnveff(i,isd),cnveff(i,iscnt),
     1     cnveff(i,itime)
        enddo
      close(icalib)
      open(unit=icalib,file='ZNO.Cal',status='OLD',access='APPEND')
      do i=1,lines
        do j=1,takes
          write(icalib,110)zero(i,j,iNOa,imean),
     1          zero(i,j,iNOa,isd),zero(i,j,iNOa,iscnt),
     1          zero(i,j,iNOa,itime)
          write(icalib,110)zero(i,j,iNOb,imean),
     1          zero(i,j,iNOb,isd),zero(i,j,iNOb,iscnt),
     1          zero(i,j,iNOb,itime)
          enddo
        enddo
      close(icalib)
      open(unit=icalib,file='ZNOy.cal',status='OLD',access='APPEND')
      DO I=1,LINES
        DO J=1,TAKES
          WRITE(ICALLB,110)ZERO(I,J,Inoy,mean),
     1          zero(i,j,iNOy,isd),zero(i,j,iNOy,iscnt),
     1          zero(i,j,iNOy,itime)
          enddo
        enddo
      close(icalib)
      print*,'Done writing cal data.'
      return
100   format(1x,1P,E11.4,1x,E11.4,1x,E9.3,1X,0P,F9.4)
110   format(1x,1P,E10.3,1x,E10.3,1x,E9.3,1X,0P,F9.4)
      end
*****************************************************************
** CNVOUT -      Writes running-averaged conversion efficiency data to an ASCII
**          file for MINITAB or other analysis.  Parameters (max scnt,
**          ok range, number in average) are already in from startup file.
**          Output is to main file name.(cnvext)
**          Output is:
**               Mean-CnvEff  SD-CnvEff  NO2-Produced  Time(JDay of year)
*****************************************************************
      Subroutine CnvOut(fn,CnvEff,NewNO2)
      include 'globalvar.def'
      include 'cal`var.def'
      include 'flags.def'
      dimension ave(4),RCnvEf(maxlin,4)
      character *60 fn,fname
      if (.not.(caldne)) then
        print*,'You must CALC CAL first!'
        return
        endif
      do il=1,lines
        call RunAve(ave,il,CnvEff,iCvEf)
        DO i=1,4
          RCnvEf(il,i)=ave(i)
          enddo
        enddo
      IF (GetYN('Enter Y to append to an existing file: ','N')) THEN
          write(*,95)
95          format('$Enter file name: ')
          read(*,80)fname
80          format(A80)
          open(unit=icnvlb,file=fname,STATUS='OLD',
     1          ACCESS='APPEND')
        else
            fname=fn(1:filcat(fn))//cnvext
          open(unit=icnvlb,file=fname,status='NEW')
          endif
      do il=1,lines
        IF (RCnvEf(il,imean).ne.999) THEN
          write(icnvlb,100)RCnvEf(il,imean),RCnvEf(il,isd),
     1      NewNO2(il,imean),
     1      RCnvEf(il,itime)
          endif
        enddo
      close(icnvlb)
      return
100   format(1x,F7.4,1x,F7.4,1x,E9.3,1x,F7.2)
      end
*****************************************************************
*****************************************************************
** ConMTB.  Writes concentration data to .NODat and .NOyDat files for
** use by MINITAB etc.
** Only valid (not=999) values are written out, so Delta-T may be variable.
*****************************************************************
      Subroutine ConMtb(fn,ConNO,ConNOy)
      include 'globalvar.def'
      include 'con`var.def'
      include 'flags.def'
      character *60 fn,fname
      if (.not.condne) then
        print*,'You must CALC CON first!'
        return
        endif
      IF (GetYN('Write out NO data? ','Y')) THEN
        IF (GetYN('Write only nighttime data? ','N')) THEN
          nitonl=.true.
          fname=fn(1:filcat(fn))//'.NONIT'
          WRITE(*,920)
920           format('$Enter minimum zenith angle (85 or 90): ')
          read*,zminan
          else
          nitonl=.false.
            fname = fn(1:filcat(fn))//'.NODAT'
          endif
        IF (GetYN('Screen data by SDi10ppt or RSDi15%? ','N')) THEN
          do 90 i=1,lines
            do 90 j=1,takes
              if ( (conno(i,j,isd).gt.10.0) .and.
     1            (conno(i,j,isd)/conno(i,j,imean).gt.0.15)) THEN
                CONNO(i,j,imean)=999.
              conno(i,j,isd)=999.
              endif
90              continue
        ENDIF
        print*,'Writing NO data to ',fname
        open(unit=iConLb,file=fname,status='NEW')
        year=1990.
        Npt=0
        Ndo=0
        do 100 i=1,lines
          do 100 j=1,takes
            Npt=Npt+1
            dy=int(conno(i,J,itime))
```

Data Analysis Program (continued: page 20)

```
          hr=24.0*(cenno(i,j,itime)-dy)
          call sunpos(dy,YEAR,hr,0.0,0.0,71.3233,
     2      156.6067,Zenith)
          if ((zenith.gt.zminen).or.(.not.(nitonl))) then
           if (ConNo(i,j,1).ne.999.) then
            IF (((ABS(ConNO(i,j,1)).lt.100000).and.
     1        (ABS(ConNO(i,j,2)).lt.100000)).and.
     1        (ABS(ConNO(i,j,4)).lt.100000)) then
             write(iconlb,1001)(ConNO(i,j,k),k=1,4)
             else
             write(iconlb,1000)(ConNO(i,j,k),k=1,4)
             endif
            Ndo=Ndo+1
            ELSE
c            PRINT*,'Skipping data point = 999.'
            endif
           endif
100         continue
        close(iconlb)
        Print*,'Wrote out ',ndo,' of ',npt,' points.'
        ENDIF
      IF (GetYN('Write out NOy data? ','Y')) THEN
        lname=ln(1:ifcat(ln))//'.NOyDat'
        print*,'Writing NOy data to ',lname
        open(unit=iconlb,file=lname,status='NEW')
        Ndo=0
        Npt=0
        do 200 i=1,lines
         do 200 j=1,takes
          if (ConNOy(i,j,1).ne.999) then
           IF (((ABS(ConNOy(i,j,1))).lt.100000).and.
     1       (ABS(ConNOy(i,j,2)).lt.100000)).and.
     1       (ABS(ConNOy(i,j,4)).lt.100000)) then
            write(iconlb,1001)(ConNOy(i,j,k),k=1,4)
            else
            write(iconlb,1000)(ConNOy(i,j,k),k=1,4)
            endif
           Ndo=Ndo+1
           ELSE
c           PRINT*,'Skipping flagged data point.'
           endif
           Npt=Npt+1
200         continue
        close(iconlb)
       endif
      print*,'Wrote ',Ndo,' of ',Npt,' points.'
      return
1000    format(1x,1P,E10.3,E10.3,0P,F8.3,1P,E10.3)
1001    format(1x,F10.1,F10.1,F8.3,F10.1)
      end
*****************************************************************************
*****************************************************************************
************************* DEFINITION MODULES ********************************
*****************************************************************************
************************ MODULE PARAMETERS.DEF ******************************
*****************************************************************************
** All of the parameters for the program ANALYZE are contained
** in this file.  All changes at this level will be reflected
** throughout the entire program with little or (usually) no
** code modification.  However, arbitrary changes may cause
** funky errors: for example, setting iNOz1=iNOy1 would cause
** the program to try to store both pieces of data in the same
** place in an array, and give you weird results.
*****************************************************************************
      integer icyO3, icO3, iNOc, icNO, icNOy, icNOz,iNOz1,iNOy1
      integer iNOa,iNOb,iNOy
      integer iRawLb,iConlb,iCalLb,iPgmlb,iNitLb,iSumLb,
     1    icpslb,iCnvLb
      integer iSens,iFzd,iySen,iZro,iCvEf,iCNit,iNit
      integer imean, isd, itime, iscnt, MaxLin, Modes,Takes
      character*4, rawext,conext,calext,pgmext,notext,nitext,sumext,
     1        CnvExt
      real PgmVer
      parameter (PgmVer=3.01)
      parameter (iCyO3=1, iCO3=2, iNOc=3, icNO=4, icNOy=5, icNOz=6)
      parameter (iNOz1=7,iNOy1=10)
      parameter (imean=1,isd=2,itime=3,iscnt=4)
      parameter (iNOa=1, iNOb=2, iNOy=3)
      parameter (iRawLb=10,iConLb=11,iCalLb=12,iPgmLb=13,iNitLb=14,
     1      iSumLb=15,icpsLb=16,iCnvLb=17)
      parameter (rawext='.DAT',conext='.CON',calext='.CAL',
     1      notext='.NOT',nitext='.NIT',sumext='.SUM',
     1      CnvExt='.CNV')
      parameter (pgmext='.CSN')
      parameter (MaxLin=200, Modes=46,takes=8,MaxZ=2*MaxLin*Takes)
      parameter (iSens=1,iFzd=2,iySen=3,iCvEf=4,iZro=5,iCNit=6,iNit=7,
     1      iCvSD=8)
      parameter (ZenMin=85.0,ZenScn=1.5)
*** iCyO3 is index for calibration of NOy w/ cal. gas, cal O3
*** iCO3  *  *    *    *      * NO *  *  *  *  *
*** iNOc  *  *    *    *      * NO measure. for use in calib.
*** icNO  *  *    *    *      * NO w/ cal. gas
*** icNOy *  *    *    *      * Noy *  *  *
*** icNOz *  *    *    *      * NO w/ cal gas=zero mode
*** iNOz1 *  *    *    *      * first [NO] zero
*** iNOy1 *  *    *    *      *  *  [NOy] *
****** the above indices are modes in raw;
****** raw(line,icNO,imean) is the mean of line for NO w/ cal. gas.
***  imean is index for means
***  isd   is index for standard deviations
***  itime is index for times
***  iscnt is index for Scount
***** these indices are at the end of data arrays and represent
*****  the four (three for raw) different pieces of data needed
*****  for each point.
***** NOCon(line,take,imean) is the mean [NO] for the data point
***** at (line,take).  FrcZrd(line,itime) is the time that the
***** fraction zeroed for (line) was taken.
*** iNOa is index to first NO zero in Zero(line,mode,iNOa..iNOy,4)
*** iNOb  *  *  *  2nd  *  *  *  *
*** iNOy  *  *  *  NOy zero  *  *
***** for example, zero(4,6,iNOb,imean) holds the mean of the second NO zero
***** of line 4, take 6.
*** iRawLb is the file number used for raw data
*** iConLb *  *  *  *  *  *  *  concentration data
*** iCalLb *  *  *  *  *  *  *  calibration data
*** iPgmLb *  *  *  *  *  *  *  programmables
*** iNitLb *  *  *  *  *  *  *  nighttime NO summary
*****  these variables are used locally (in Get*** and Put*** and NITE) only.
*****  earlier program design required seperate numbering.  They are
*****  used as file numbers when files are opened.  Because this
*****  method of accessing data was phased out, the startup file
*****  open/close number is typed explicitly in where it is used,
*****  rather than having an index like the other files.
*** RawExt is the file extension for raw files
*** ConExt *  *  *  *  *  con files
*** CalExt *  *  *  *  *  cal files
*** PgmExt *  *  *  *  *  pgm files
*** NitExt *  *  *  *  *  nit file
***** These are added to the end of each file type.  this allows
***** simpler access to the data.
*** MaxLin is the maximum number of lines in a RAW file
*** Modes is the number of modes/line in a RAW file
*** Takes is the number of cycles (zNO,NO,zNO,NOy,zNOy) per line
***** Global array sizes. changing them here will change (after
***** recompilation) every array and statement that depends on
***** the size of the various arrays.  This includes do loops,
***** if statements, local array assignments and so on.
***** The final dimesion of data arrays (1:3 or 1:4), which represent
***** different pieces of information about the same dat point,
***** are not global.  Since these numbers are fundamental to the
***** program, changing them would require aproximately 90% of the
***** code to be modified anyway.
****** ONE PLACE WHERE THIS IS NOT TRUE IS IN Subroutine Disp in ANALYZE
****** THIS PROCEDURE USES THE INDICES 1..4 rather than imean..iscnt
****** and assumes there are 8 takes/line.
**_____________________________________
**                CHANGING THOSE WILL MESS UP
**                      DISP
**_____________________________________
*** iSens is index in RSDMAX and NumAve for sensitivity
*** iFzd is index in RSDMAX and NumAve for fraction zeroed
*** iySen is index in RSDMAX and NumAve for NOy Sen
*** iCvEf is index in RSDMAX and NumAve for Conv. Eff.
*** iZro is index in RSDMAX for NOy zero.
*** iCNit is index in RSDMAX for nighttime NO concns to include in stats.
*** iNit is index in RSDMAX for 2-hour avg nighttime NO concentrations.
***** These tell the maximum allowable counting statistic for
***** the point of data to be good for calculations.  Programs
***** that use say, fraction zeroed, for a calculation would check
***** the FrcZrd(line,iScnt) against RSDMAX(iFZd).  If FrcZrd is larger
***** the calculated mean is given a value of 999.
*** ZenMin is the minimum zenith angle to use for nighttime NO calculations.
*** ZenScn is the maximum S/Scnt for screening nighttime NO data for
***   for artifact calculations.
*** PgmVer is version number of the program ANALYZE.  It is used to
***   ensure that later versions that are inconsistent with earlier
***   versions are not used with old PGM and/or data files.
*** Minor modifications change the fractional part of PgmVer.
*** Major modifications (incompatible) change the integer part of PgmVer
*****************************************************************************
*****************************************************************************
************************ MODULE GLOBALVAR.DEF *******************************
*****************************************************************************
**** common block stuff for analyze.for and its subroutines
****  including this file will save the effort and unsightliness
****  of having to retype all this for each subroutine that uses it
*****************************************************************************
      include 'parameters.def'
*****************************************************************************
** Here are all the global variables and the /Global/ common block
** for the program ANALYZE and its subroutines.
** Array sizes are defined in the file parameters.def.
*****************************************************************************
**
**
** This file contains only the general declarations and all comments.
** Also the raw data declaration
** The other declarations are contained in the file:
**      cal'var.def
**      con'var.def
**      cps'var.def
**
** General stuff
      real Ccg,rsdmax(8),maxmn(8),minmn(8),tstart
      integer lines,NumAve(4),Navg(modes)
      logical RawLdd,Caldne,ConDne,DisDne,CalSvd,ConSvd,PgmSvd,NitDne
      logical GetYN
      logical UseNOy,BinFil
** raw
```

Data Analysis Program (continued: page 21)

```
      real raw(maxdin,modes,3)
*****************************************************************
*** Raw data is recieved as follows.  A data file contains a number
*** of LINES.  Each line consists of a number of MODES (parameters
*** defined in parameters.def).  Each line is also broken up into
*** the calibration information (the first 6 modes), and 8 TAKES (each
*** take consists of 5 modes).  Finally, each mode is broken up
*** into three records: MEAN, S.D., TIME.  Data that is calculated
*** has an additional record, Scount, a counting statistic.
*** The arrays raw, ConNO, and ConNOy are divided up in this order.
*** Thus the dimensions of the arrays.  ConNO(line,take,record)
*** The calibration information is taken only once/line.  Thus when
*** calculated it is stored in arrays (FrcZrd, Sens, CnvEff, NewNO2,
*** NOySen) of the form FrcZrd(line,record).  The other calculated
*** value array is ZERO.  There are 3 zeroes/take, so (sadly I might
*** add) it has to be a 4-dimensional array:
*** Zero(line,take,zero #,record).
*** There are three other kinds of data in ANALYZE.  The first are
*** calculation parameters (or programmable constants).
*** They are Ccg,RsdMax,tstart,NumAve,Navg,UseNOy,MaxMn,MinMn.
*** CCg is the device's calibration gas constant.  RsdMax is an
*** array which holds the maximum allowable Scount (counting statistic)
*** for several different numbers.  Doing a calculation with a messed
*** up Scount generates and error as follows: the mean of the final
*** result is set to 999.  MaxMn and MinMn are used in a similar way.
*** When RSDMax is checked, the max and min values of the mean are also
*** checked against the mean of the variable.  A discrpency has the same
*** effect as a bad RSD check.  Tstart is the initial time taken from the
*** raw data file.  It is added to each calculated time.  NumAve tells
*** how many values to include in a running average.  Navg gives the
*** number of points the machine uses to to generate the mean for a given
*** mode.  UseNOy tells the program whether to use NOy sensitivity
*** of the device as opposed to NO sens. for calculation of NOy.
*** The next kind of data is book keeping information.  This keeps
*** the program aware of what it is doing and what it has done.
*** It consists primarily of flags (RawLdd,CalDne,ConDne,DisDne,CalSvd,
*** ConSvd,PgmSvd).  Other things are object, parameter, comand (see
*** ANALYZE.FOR) which is not listed here.
*** BinFil is a logical function (in ANALIB), used by the file subroutines.
*** GetYN is a logical function (in ANALIB), that gets user Y/N input.
*** A lot of parameters are indices (anything that starts with an i,
*** iNOa for example).  These indices each connect with a specific
*** array (or group of arrays) and point to a specific location in
*** the array.  The are used to make what is being done a little
*** more comprehensible.  Parameters.def explains the value the
*** each index references.
*** The last kind of data is local data.
*** It is used for a variety of short lived tasks and is not covered
*** here (or anywhere).
*** Raw is the data imported directly from .dat files
*****************************************************************
***          (programmable constants)
*** Navg is the number of data points/mode
*** NumAve is the number of measurements averaged for a given mode.
*** Ccg is the calibration gas constant
*** RsdMax is the max. various Scounts can be (see parameters.def)
*** UseNOy flags to use NOy sens instead of NO sens for calculating
*** [NOy]
***          (calibration info.)
*** FrcZrd is the fraction zeroed
*** Sens is the sensitivity
*** CnvEff is conversion efficiencies
*** NewNO2 is the amount of [NO2] made
*** NoySen is the sensitivity to NOy
*** Zero contains the zeroes for each trial: Zero(line,take,izero,imean..iscnt)
***   where izero = iNOa,iNOb,iNOy (1,2,3)
***          (concentration info.)
*** ConNOy is the calculated [NOy]
*** ConNO is the calculated [NO]
***          (data info)
*** tstart is the starting time for the file
*** lines is the number of lines of data
***          (program bookkeeping)
*** RawLdd flags if a RAW file has been loaded
*** CalDne tells if calibrations have been loaded/calculated
*** ConDne does the same for concentrations
*** DisDne tells if a graph has been created
*** CalSvd tells if calibration data has been saved
*** ConSvd tells if concentrations have been saved
*** PgmSvd tells if programmable constants are saved
      common /Global/ Raw,Ccg,RsdMax,Navg,NumAve,tstart,lines,
     1     UseNOy,MaxMn,MinMn,Nnit
*** Note there is another common block defined in Flags.def that
*** is sometimes used.
***
*****************************************************************
*****************************************************************
********************* MODULE CAL'VAR.DEF *************************
*****************************************************************
** Calibration stuff
      real FrcZrd(maxlin,4),Sens(maxlin,4),CnvEff(maxlin,4)
      real NewNO2(maxlin,4),NOySen(maxlin,4),Zero(maxlin,takes,3,4)
*****************************************************************
*****************************************************************
********************* FILE CON'VAR.DEF ***************************
*****************************************************************
** Concentration stuff
      real ConNOy(maxlin,takes,4),ConNO(maxlin,takes,4)
      real ConNit(maxZ,4)
*****************************************************************
*****************************************************************
********************* FILE CPS'VAR.DEF ***************************
*****************************************************************
      integer maxpt
      parameter (maxpt=172800)
      real cps5(maxpt)
*****************************************************************
*****************************************************************
********************* FILE FLAGS.DEF *****************************
*****************************************************************
*****************************************************************
** flags for main program
** some procedures use flags as passed parameters, so these can't
** be included in globalvar.def.
** for flag explaination, see GlobalVar.def.
*****************************************************************
      common /flags/ RawLdd,CalDne,ConDne,DisDne,CalSvd,
     1 ConSvd,PgmSvd,NitDne,NitSvd
```